frontiers | Research Topics

# Protein homeostasis in growth, development and disease

**Edited by**
Francesco Fazi, Silvia Masciarelli and Linda M. Hendershot

**Published in**
Frontiers in Cell and Developmental Biology

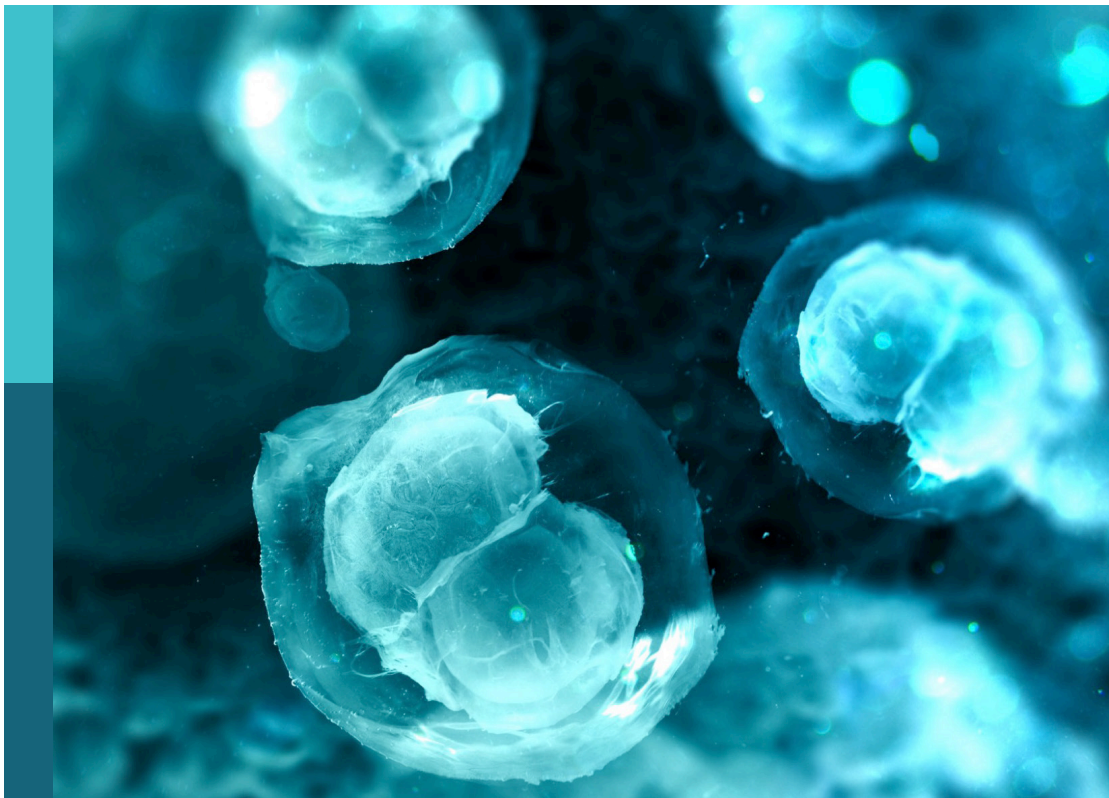

ISSN 1664-8714
ISBN 978-2-83251-706-2
DOI 10.3389/978-2-83251-706-2

## About Frontiers

Frontiers is more than just an open access publisher of scholarly articles: it is a pioneering approach to the world of academia, radically improving the way scholarly research is managed. The grand vision of Frontiers is a world where all people have an equal opportunity to seek, share and generate knowledge. Frontiers provides immediate and permanent online open access to all its publications, but this alone is not enough to realize our grand goals.

## Frontiers journal series

The Frontiers journal series is a multi-tier and interdisciplinary set of open-access, online journals, promising a paradigm shift from the current review, selection and dissemination processes in academic publishing. All Frontiers journals are driven by researchers for researchers; therefore, they constitute a service to the scholarly community. At the same time, the *Frontiers journal series* operates on a revolutionary invention, the tiered publishing system, initially addressing specific communities of scholars, and gradually climbing up to broader public understanding, thus serving the interests of the lay society, too.

## Dedication to quality

Each Frontiers article is a landmark of the highest quality, thanks to genuinely collaborative interactions between authors and review editors, who include some of the world's best academicians. Research must be certified by peers before entering a stream of knowledge that may eventually reach the public - and shape society; therefore, Frontiers only applies the most rigorous and unbiased reviews. Frontiers revolutionizes research publishing by freely delivering the most outstanding research, evaluated with no bias from both the academic and social point of view. By applying the most advanced information technologies, Frontiers is catapulting scholarly publishing into a new generation.

## What are Frontiers Research Topics?

Frontiers Research Topics are very popular trademarks of the *Frontiers journals series*: they are collections of at least ten articles, all centered on a particular subject. With their unique mix of varied contributions from Original Research to Review Articles, Frontiers Research Topics unify the most influential researchers, the latest key findings and historical advances in a hot research area.

Find out more on how to host your own Frontiers Research Topic or contribute to one as an author by contacting the Frontiers editorial office: frontiersin.org/about/contact

# Protein homeostasis in growth, development and disease

**Topic editors**

Francesco Fazi — Sapienza University of Rome, Italy

Silvia Masciarelli — Sapienza University of Rome, Italy

Linda M. Hendershot — St. Jude Children's Research Hospital, United States

**Citation**

Fazi, F., Masciarelli, S., Hendershot, L. M., eds. (2023). *Protein homeostasis in growth, development and disease*. Lausanne: Frontiers Media SA.

doi: 10.3389/978-2-83251-706-2

# Table of contents

frontiers | Frontiers in Cell and Developmental Biology

TYPE Editorial
PUBLISHED 06 February 2023
DOI 10.3389/fcell.2023.1150158



OPEN ACCESS

EDITED AND REVIEWED BY
Ana Cuenda,
Spanish National Research Council (CSIC), Spain

*CORRESPONDENCE
Silvia Masciarelli,
silvia.masciarelli@uniroma1.it
Francesco Fazi,
francesco.fazi@uniroma1.it
Linda M. Hendershot,
linda.hendershot@stjude.org

SPECIALTY SECTION
This article was submitted to Signaling, a section of the journal Frontiers in Cell and Developmental Biology

RECEIVED 23 January 2023
ACCEPTED 30 January 2023
PUBLISHED 06 February 2023

CITATION
Masciarelli S, Fazi F and Hendershot LM (2023), Editorial: Protein homeostasis in growth, development and disease. *Front. Cell Dev. Biol.* 11:1150158. doi: 10.3389/fcell.2023.1150158



# Editorial: Protein homeostasis in growth, development and disease

Silvia Masciarelli[1]*, Francesco Fazi[1]* and Linda M. Hendershot[2]*

[1]Department of Anatomical, Histological, Forensic and Orthopedic Sciences, Sapienza University of Rome, Rome, Italy, [2]Department of Tumor Cell Biology, St. Jude Children's Research Hospital, Memphis, TN, United States

KEYWORDS

**proteostasis, molecular chaperones and chaperonins, stress responses, homeostasis and differentiation, quality control in the endoplasmic reticulum**

Editorial on the Research Topic
Protein homeostasis in growth, development and disease

## Introduction

The transition of a linear polypeptide chain into a functional, 3-dimensional protein is fraught with dangers, but a successful outcome is critical to all aspects of life. To assist and monitor this process, all cells and organism are endowed with a cadre of molecular chaperones, their co-factors and folding enzymes (Balchin et al., 2016). The ability of the cell to rapidly regulate the availability of these chaperones and folding enzymes is necessary to maintain cellular and organellar homeostasis in response to changes in secretory capacity or alterations in the cellular environment that adversely affect protein folding (Richter et al., 2010; Walter and Ron, 2011). Imbalances in these can lead to disease. In addition to these ubiquitously expressed components of protein folding and quality control systems, tissue-specific factors exist that are more restrictive in their clients and are often important in developmental and differentiation processes. This Research Topic is comprised of a combination of original research articles and reviews that address cutting edge work in this field.

## Generalist chaperones

As polypeptide chains emerge from the ribosome, they can begin to fold co-translationally, which could inhibit appropriate interactions with more distal sequences needed to reach their native states. Chaperone families including Hsp70, Hsp90 and the cage-like chaperonins are found in all lineages of organisms (bacteria, archaea, and both plant and animal eukaryotes) and serve to protect reactive regions on nascent proteins. They are particularly non-selective and can recognize a vast number of sequence unrelated proteins and can therefore be considered generalists. Hsp70s recognize linear stretches of amino acids that are hydrophobic in nature and will ultimately be buried upon correct protein folding and/or assembly (Blond-Elguindi et al., 1993). They prevent misfolding by protecting these regions but do not directly contribute to folding. Conversely, the chaperonins are multi-subunit ring structures that provide a protective cavity that accommodates partially folded clients and drives their proper maturation through

nucleotide-dependent interactions between the various subunits and the incompletely folded client (Gestaut et al., 2019). One review in this series addresses recent findings that contribute to our understanding of how the mammalian chaperonin TRiC (Tailless complex polypeptide 1 (TCP-1) Ring Complex) is able to contribute to the folding of proteins too large to fit into its central cavity (Ghozlan et al.). Another review focuses on prefoldin, an adapter that conveys clients to TRiC to maintain protein homeostasis in physiological and pathological conditions (Tahmaz et al.). A third review summarizes studies revealing the role of generalist chaperones in protecting the proteome of the parasite and in renovating the host proteome to its own benefit (Blatch).

## Quality control in the endoplasmic reticulum

The endoplasmic reticulum (ER) is the gateway into the secretory pathway and is responsible for the biosynthesis of 1/3 of the proteins encoded in the mammalian genome, which includes proteins that are secreted, expressed on the cell surface, or that populate all organelles of the secretory pathway (Dancourt and Barlowe, 2010). Stringent quality control programs comprised of molecular chaperones and folding enzymes aid and monitor the maturation of nascent proteins entering this organelle (Wiseman et al., 2022). While bound to the chaperone, incompletely folded clients are prevented from moving further along the secretory pathway due to retention sequences on the chaperones. In the case of most soluble chaperones, the tetrapeptide sequence, KDEL, is encoded at their C-terminus. Should the chaperone exit the ER incorrectly it encounters a KDEL receptor in the intermediate compartment or *cis* Golgi, which returns it and any bound client to the ER (Lewis et al., 1990). A review in this Research Topic discusses variations in recycling rates that alter the concentration of individual soluble chaperones in specific proximal regions of the secretory pathway, as well as examples where capture and return fails allowing specific soluble chaperones to be secreted (Palazzo et al.). Equally important to maintaining the secretory proteome is the ability to identify proteins that ultimately fail to mature and/or assemble properly and target them for degradation. In most cases this involves extracting the protein from the ER for degradation by cytosolically localized proteasomes in a process referred to as ER-associated degradation (ERAD) (Vembar and Brodsky, 2008; Hwang and Qi, 2018). The presence of a single unfolded domain or region necessitates that the protein be degraded raising the question of how folded regions are accommodated for passage through an intermembrane channel. An original research study identifies the checkpoints in this process and the components that execute them (Mann et al.).

## Regulating chaperone levels to accommodate secretory loads during differentiation

An ER stress-sensing response termed the Unfolded Protein Response (UPR) transcriptionally adjusts chaperone levels to the secretory capacity of the cell (Walter and Ron, 2011). As such the UPR provides an essential function during the differentiation of highly secretory cells like plasma cells (Iwakoshi et al., 2003), and in response to environmental cues received by insulin-secreting β islet cells (Scheuner et al., 2005) to enhance and populate the secretory pathway. An original research paper in this Research Topic explores temporal changes in the proteostasis network and their triggers, which provide massive reshaping of the secretory pathway during the progesterone-stimulated differentiation of endometrial stromal cells allowing allows them to secrete large quantities of factors necessary for embryo implantation (Pittari et al.).

## Tissue-specific chaperones and differentiation

The chaperone system is extremely plastic. For example, generalist chaperones, like those of the Hsp70 family, can cooperate with different co-chaperones, changing their substrate specificity (Kampinga and Craig, 2010). Higher eukaryotes, composed of many different cell types, tissues, and organs, present different folding demands that must be specifically addressed. A recent systematic analysis of the basal chaperone network in a variety of human tissues experiencing normal physiological conditions showed that most chaperones have tissue-specific behaviors, and this organization is established during organ development, maintained through adulthood, and altered in aging (Shemesh et al., 2021). The same research group contributed to this Research Topic with two original papers focusing on tissue-specific regulation of chaperone expression. In one they identified a neural G protein coupled receptor as a key regulator of proteostasis in different somatic tissues, which is required to transfer resources to progeny production during the transition to adulthood in *Caenorhabditis elegans* (Kishner et al.). In the other they show that the *C. elegans* ortholog of the main muscle transcription factor MyoD, is essential to preserve proper expression of the muscle specific chaperone system not only during differentiation but also in adulthood (Nisaa and Ben-Zvi).

## Chemical manipulation of proteostasis for therapeutic interventions

Whereas the core proteostasis network consists of the mechanisms driving protein translation, folding and degradation, stress response pathways such as the UPR, the Heat Shock Response (HSR), the Integrated Stress Response (ISR) and the oxidative stress response add levels of regulation that allow the cell to cope with and survive situations that unbalance proteostasis (Brehme et al., 2019). Cancer cells are able to survive under prolonged conditions of proteotoxic stress that is due to an unfavorable environment, including hypoxic and insufficient nutrients, by activating pro-survival stress responses. When these mechanisms of adaptation are not sufficient to handle proteostasis alterations, cells undergo apoptosis. Thus, there is a growing interest in targeting proteostasis to induce death of cancer cells (Marciniak et al., 2022; Wolska-Washer and Smolewski, 2022; Śniegocka et al., 2022). In this context, a review article in this Research Topic discusses the potential of using ascorbic acid (Vitamin C) as an adjuvant therapy for acute myeloid leukemia

on the basis of its role in epigenetics and of its pro-oxidant properties (Travaglini et al.).

## Author contributions

SM, FF, and LH equally contributed as Guest Editors of this Research Topic and closely interacted throughout the editorial process, by defining the subjects to be treated and inviting leaders in specific research fields to contribute their work, and by acting as handling editors of the manuscripts submitted to the Research Topic and writing the Editorial. All authors contributed to the article and approved the submitted version.

## Funding

SM and FF were supported from research project grants from Sapienza University of Rome. LH was supported by NIH grant GM54068 and The American Lebanese Syrian Associated Charities of St. Jude Children's Research Hospital.

## Acknowledgments

We thank the Editorial Office of Frontiers in Cell and Developmental Biology for their assistance throughout the editorial process.

## Conflict of interest

The authors declare that the research was conducted in the absence of any commercial or financial relationships that could be construed as a potential conflict of interest.

## Publisher's note



## References

Balchin, D., Hayer-Hartl, M., and Hartl, F. U. (2016). *In vivo* aspects of protein folding and quality control. *Science* 353 (6294), aac4354. doi:10.1126/science.aac4354

Blond-Elguindi, S., Cwirla, S. E., Dower, W. J., Lipshutz, R. J., Sprang, S. R., Sambrook, J. F., et al. (1993). Affinity panning of a library of peptides displayed on bacteriophages reveals the binding specificity of BiP. *Cell* 75, 717–728. doi:10.1016/0092-8674(93)90492-9

Brehme, M., Sverchkova, A., and Voisine, C. (2019). Proteostasis network deregulation signatures as biomarkers for pharmacological disease intervention. *Curr. Opin. Syst. Biol.* 15, 74–81. doi:10.1016/j.coisb.2019.03.008

Dancourt, J., and Barlowe, C. (2010). Protein sorting receptors in the early secretory pathway. *Annu. Rev. Biochem.* 79, 777–802. doi:10.1146/annurev-biochem-061608-091319

Gestaut, D., Limatola, A., Joachimiak, L., and Frydman, J. (2019). The ATP-powered gymnastics of TRiC/CCT: An asymmetric protein folding machine with a symmetric origin story. *Curr. Opin. Struct. Biol.* 55, 50–58. doi:10.1016/j.sbi.2019.03.002

Hwang, J., and Qi, L. (2018). Quality control in the endoplasmic reticulum: Crosstalk between ERAD and UPR pathways. *Trends Biochem. Sci.* 43 (8), 593–605. doi:10.1016/j.tibs.2018.06.005

Iwakoshi, N. N., Lee, A. H., and Glimcher, L. H. (2003). The X-box binding protein-1 transcription factor is required for plasma cell differentiation and the unfolded protein response. *Immunol. Rev.* 194, 29–38. doi:10.1034/j.1600-065x.2003.00057.x

Kampinga, H. H., and Craig, E. A. (2010). The HSP70 chaperone machinery: J proteins as drivers of functional specificity. *Nat. Rev. Mol. Cell Biol.* 11 (8), 579–592. doi:10.1038/nrm2941

Lewis, M. J., Sweet, D. J., and Pelham, H. R. (1990). The ERD2 gene determines the specificity of the luminal ER protein retention system. *Cell* 61, 1359–1363. doi:10.1016/0092-8674(90)90699-f

Marciniak, S. J., Chambers, J. E., and Ron, D. (2022). Pharmacological targeting of endoplasmic reticulum stress in disease. *Nat. Rev. Drug Discov.* 21 (2), 115–140. doi:10.1038/s41573-021-00320-3

Richter, K., Haslbeck, M., and Buchner, J. (2010). The heat shock response: Life on the verge of death. *Mol. Cell* 40 (2), 253–266. doi:10.1016/j.molcel.2010.10.006

Scheuner, D., Mierde, D. V., Song, B., Flamez, D., Creemers, J. W., Tsukamoto, K., et al. (2005). Control of mRNA translation preserves endoplasmic reticulum function in beta cells and maintains glucose homeostasis. *Nat. Med.* 11, 757–764. doi:10.1038/nm1259

Shemesh, N., Jubran, J., Dror, S., Simonovsky, E., Basha, O., Argov, C., et al. (2021). The landscape of molecular chaperones across human tissues reveals a layered architecture of core and variable chaperones. *Nat. Commun.* 12 (1), 2180. doi:10.1038/s41467-021-22369-9

Śniegocka, M., Liccardo, F., Fazi, F., and Masciarelli, S. (2022). Understanding ER homeostasis and the UPR to enhance treatment efficacy of acute myeloid leukemia. *Drug Resist Updat* 64, 100853. doi:10.1016/j.drup.2022.100853

Vembar, S. S., and Brodsky, J. L. (2008). One step at a time: Endoplasmic reticulum-associated degradation. *Nat. Rev. Mol. Cell Biol.* 9 (12), 944–957. doi:10.1038/nrm2546

Walter, P., and Ron, D. (2011). The unfolded protein response: From stress pathway to homeostatic regulation. *Science* 334 (6059), 1081–1086. doi:10.1126/science.1209038

Wiseman, R. L., Mesgarzadeh, J. S., and Hendershot, L. M. (2022). Reshaping endoplasmic reticulum quality control through the unfolded protein response. *Mol. Cell* 82 (8), 1477–1491. doi:10.1016/j.molcel.2022.03.025

Wolska-Washer, A., and Smolewski, P. (2022). Targeting protein degradation pathways in tumors: Focusing on their role in hematological malignancies. *Cancers (Basel)* 14 (15), 3778. doi:10.3390/cancers14153778

frontiers in Cell and Developmental Biology

REVIEW
published: 17 January 2022
doi: 10.3389/fcell.2021.816214

# Prefoldin Function in Cellular Protein Homeostasis and Human Diseases

*Ismail Tahmaz†, Somayeh Shahmoradi Ghahe† and Ulrike Topf**

*Laboratory of Molecular Basis of Aging and Rejuvenation, Institute of Biochemistry and Biophysics, Polish Academy of Sciences, Warsaw, Poland*

Cellular functions are largely performed by proteins. Defects in the production, folding, or removal of proteins from the cell lead to perturbations in cellular functions that can result in pathological conditions for the organism. In cells, molecular chaperones are part of a network of surveillance mechanisms that maintains a functional proteome. Chaperones are involved in the folding of newly synthesized polypeptides and assist in refolding misfolded proteins and guiding proteins for degradation. The present review focuses on the molecular co-chaperone prefoldin. Its canonical function in eukaryotes involves the transfer of newly synthesized polypeptides of cytoskeletal proteins to the tailless complex polypeptide 1 ring complex (TRiC/CCT) chaperonin which assists folding of the polypeptide chain in an energy-dependent manner. The canonical function of prefoldin is well established, but recent research suggests its broader function in the maintenance of protein homeostasis under physiological and pathological conditions. Interestingly, non-canonical functions were identified for the prefoldin complex and also for its individual subunits. We discuss the latest findings on the prefoldin complex and its subunits in the regulation of transcription and proteasome-dependent protein degradation and its role in neurological diseases, cancer, viral infections and rare anomalies.

**Keywords: prefoldin, molecular chaperone, proteostasis, TRIC, PFDN, neurodegenerative diseases, cancer**

OPEN ACCESS

***Edited by:***
*Silvia Masciarelli, Catholic University of the Sacred Heart, Italy*

***Reviewed by:***
*Sandeep K. Sharma, Indian Institute of Toxicology Research (CSIR), India*
*Rahul S. Samant, Babraham Institute (BBSRC), United Kingdom*

****Correspondence:***
*Ulrike Topf*
*utopf@ibb.waw.pl*

*†These authors have contributed equally to this work*

***Specialty section:***
*This article was submitted to Signaling, a section of the journal Frontiers in Cell and Developmental Biology*

***Received:*** *16 November 2021*
***Accepted:*** *29 December 2021*
***Published:*** *17 January 2022*

***Citation:***
*Tahmaz I, Shahmoradi Ghahe S and Topf U (2022) Prefoldin Function in Cellular Protein Homeostasis and Human Diseases. Front. Cell Dev. Biol. 9:816214. doi: 10.3389/fcell.2021.816214*

## INTRODUCTION

Protein homeostasis (proteostasis) plays a vital role in various biological processes. Proteostasis is facilitated by the correct folding of proteins and removal of misfolded proteins to avoid protein aggregation, which can be toxic for the cell. To maintain proteostasis, cells contain various protein chaperones to check protein quality and conformation. A large family of chaperones, collectively called heat shock proteins (HSPs), are involved in the surveillance of misfolded and unfolded proteins in both the nucleus and cytosol (Hartl and Hayer-Hartl, 2002; Jones and Gardner, 2016). Non-native polypeptides must be sensed by chaperones and assisting proteins to assure correct folding. Disruption of the cooperation of chaperones and their assisting co-chaperones can result in protein misfolding and aggregation. Consequently, proteostasis can be impaired and drive the development of various pathologies (Hartl and Hayer-Hartl, 2002; Jones and Gardner, 2016).

Monomeric molecular chaperones are well established to assist in the folding of proteins into their native structure and responsible for the remodeling of proteins with erroneous conformations (Saibil, 2013). In addition to monomeric molecular chaperones, oligomeric chaperonins contribute to protein folding. Chaperonins can be divided into two groups. Group I chaperonins are found in bacteria and organelles of endosymbiotic origin (e.g., chloroplasts and mitochondria). Group II chaperonins exist in

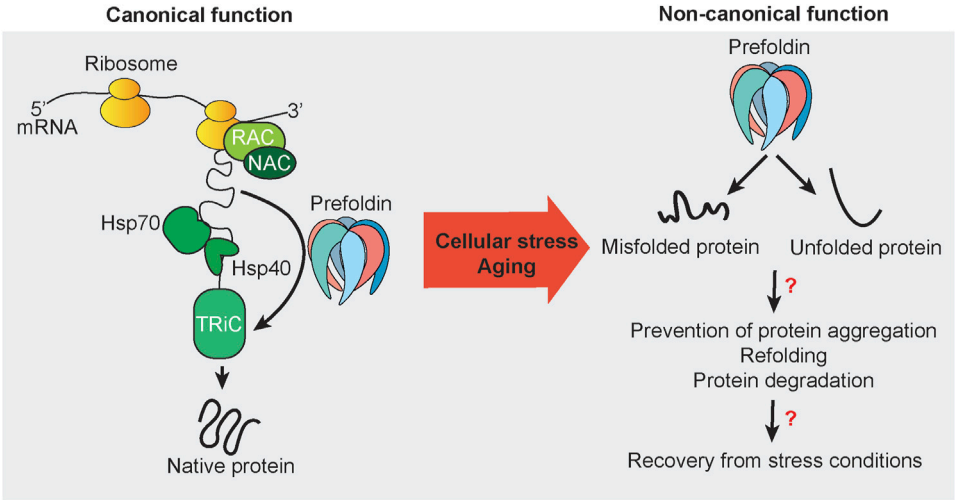


**FIGURE 1 |** Canonical and non-canonical functions of prefoldin. Nascent chains that emerge from actively translating ribosomes are subjected to protein folding that is mediated by the protein chaperones RAC, NAC, Hsp70, Hsp40, and TRiC. Some newly synthesized proteins utilize the co-chaperone prefoldin to guide substrates directly to its downstream folding chaperone TRiC. The canonical function of prefoldin results in substrate proteins with the native fold. Under stress conditions and potentially during aging, prefoldin is associated with misfolded and unfolded proteins. Mostly unknown are the nature of such cellular substrates *in vivo* and cellular consequences and mechanisms that may be necessary to recover from cellular stress conditions to restore cellular homeostasis.

eukaryotes and archaea (Russmann et al., 2012). One well-known member of Group II chaperonin is tailless complex polypeptide 1 ring complex (TRiC)/chaperonin containing tailless complex polypeptide 1 (CCT). TRiC/CCT localizes to both the nucleus and cytosol (Marracci et al., 2015).

Unlike prokaryotes, eukaryotes and archaea have another chaperone-assisted protein (Sahlan et al., 2018). Prefoldin is a co-chaperone of TRiC/CCT (Millan-Zambrano and Chavez, 2014; Zhang J. et al., 2020). It is a heterohexameric protein complex (Glover and Clark, 2015) that is composed of two α subunits (PFD3 and PFD5) and four β subunits [PFD1, PFD2, PFD4, and PFD6; (Siegert et al., 2000; Whitehead et al., 2007). All subunits differ in their amino acid sequence. In contrast, archaea prefoldin complex consists of six subunits composed of two identical α and four identical β subunits (Sahlan et al., 2018). Although prefoldin was not found in prokaryotes, its genetic origin is similar to chaperones that were found in prokaryotes (Bogumil et al., 2014). Likewise, the prefoldin complex is evolutionarily conserved in higher eukaryotes, including humans and plants (Siegert et al., 2000; Cao, 2016).

The prefoldin complex assists in the folding of newly synthesized polypeptides that are produced on ribosomes (**Figure 1**). In archaea, prefoldin exerts this function in combination with group II chaperonin. In eukaryotes, the canonical function of prefoldin is thought to be more specialized. In eukaryotes, prefoldin transfers mainly the cytoskeletal proteins actin and tubulin to TRiC/CCT (Abe et al., 2013; Povarova et al., 2014; Zhang et al., 2016). This transfer is also supported by cooperation with the monomeric chaperones HSP40 and HSP70 in a co-translational manner (Millan-Zambrano and Chavez, 2014; Gestaut et al., 2019) and required for accelerating the maturation of cytoskeletal proteins (Gestaut et al., 2019). During this process, nascent polypeptide chains bind to prefoldin in the initial phase (Kabir et al., 2011) and are transferred to TRiC/CCT in late stages of protein folding (Comyn et al., 2016; Gestaut et al., 2019). Binding of prefoldin subunits with TRiC/CCT subunits decreases the association of nascent chain with prefoldin (Gestaut et al., 2019; Liang et al., 2020). Thus, nascent chains are released from prefoldin and folded in an adenosine triphosphate (ATP)-dependent manner by TRiC/CCT. The holdase function of prefoldin is ATP-independent, similar to stress-inducible small HSPs (Webster et al., 2019). Its ATP independence raises the question of whether prefoldin has additional functions under conditions of low cellular energy levels such as mitochondrial dysfunction and metabolic disorders, aging, or chronic stress (Chaudhari and Kipreos, 2018; Andreasson et al., 2019; Fang et al., 2021).

Actin comprises 5–10% of cellular protein mass (Cooper, 2000). Thus, prefoldin is thought to be abundant with constitutive expression. However, the regulation of prefoldin expression has been scarcely addressed in the literature. The turnover of prefoldin subunits is regulated by ubiquitin-dependent degradation. However, prefoldin can become resistant to ubiquitination by forming a β-hairpin and coil-coil structure (Liang et al., 2020). Since the discovery of prefoldin in 1998 (Vainberg et al., 1998), much research has been performed to elucidate the prefoldin structure (Hansen et al., 1999) and describe its canonical functions as a co-chaperone (Sahlan et al., 2018). However, recent research has indicated involvement of the prefoldin complex and its subunits in withstanding cellular stress and maintaining protein homeostasis. Research on the non-canonical function of prefoldin is still scattered, consisting of the regulation of transcription, the regulation of protein aggregate formation, and protein degradation (**Figure 1**).

Alongside fundamental research describing various functions of prefoldin it is suggested that prefoldin is a potential biomarker and therapeutic target for human diseases that are associated with the disruption of protein homeostasis. The present review discusses non-

**TABLE 1 |** Interactions between prefoldin subunits and other proteins.

| Prefoldin subunit | Interactor | Organism | Function | References |
|---|---|---|---|---|
| PFDN1 | HLA-G | Human | Progression of pregnancy | Liu et al. (2013) |
| | cyclin A | Human | Cancer progression | Wang et al. (2017) |
| | RABV | Mouse | Upregulation in virus infection | Zhang et al. (2015) |
| | FILIP1L | Mouse and human | Progression of mucinous colon cancer | Kwon et al. (2021) |
| PFD2/PFDN2 | Irc15 | Yeast | Sister chromatid cohesion | Ming Sun et al. (2020) |
| | γ-synuclein | Mouse | Expression regulation in neurodegenerative disease | Chintalapudi and Jablonski, (2017) |
| | DELLA | Populus | Alteration of lignin content | Zhang W et al., (2020) |
| PFD3 | pVHL | Human | Tumor suppression | Kim et al. (2018) |
| | HDAC1 | Human | Delivery to CCT complex | Banks et al. (2018) |
| | hMSH4 | Human | Degradation | Xu and Her, (2013) |
| | DELLA | A. thaliana | Stress-dependent interaction | Locascio et al. (2013) |
| PFD4 | Irc15 | Yeast | Sister chromatid cohesion | Ming Sun et al. (2020) |
| | LSM8 | A. thaliana | Splicing | Esteve-Bruna et al. (2020) |
| PFDN5 | c-Myc | Human | Inhibitory effect on oncogenes | Satou et al. (2001) |
| | TIF1β | Human | Inhibitory effect on oncogenes | Hagio et al. (2006) |
| | Rabring7 | Human | c-Myc degradation | Narita et al. (2012) |
| | Egr1 | Human | c-Myc inhibition | Yoshida et al. (2008) |
| | ARFP/F | Human | c-Myc activation | Ma et al. (2008) |
| | p73α | Human | c-Myc inhibition | Watanabe et al. (2002) |
| | p63α | Human | c-Myc activation | Han et al. (2016) |
| | ΔNp63α | Human | Senescence | Chen et al. (2018) |
| | Fabp4 | Mouse | Regulation of sperm differentiation at transcription | Yamane et al. (2015) |
| | PLa2g3 | Mouse | Transcriptional regulation of sperm number and motility | Yamane et al. (2015) |
| | PLa2g10 | Mouse | Transcriptional regulation of sperm number and motility | Yamane et al. (2015) |
| | DELLA | A. thaliana | Stress-dependent interaction | Locascio et al. (2013) |
| PFD6/PFD-6 | DELLA | A. thaliana | Stress-dependent interaction | Locascio et al. (2013) |
| | FOXO | C. elegans | Transcriptional regulation of longevity | Son et al. (2018) |
| | Irc15 | Yeast | Sister chromatid cohesion | Ming Sun et al. (2020) |
| All subunits | mst | Drosophila | Assembly of spindle microtubules | Palumbo et al. (2015) |

canonical functions of prefoldin in eukaryotes and the involvement of prefoldin in human diseases.

## NON-CANONICAL FUNCTIONS OF THE PREFOLDIN COMPLEX

Apart from the canonical function of the cytosolic prefoldin complex as a co-chaperone for the co-translational folding of cytoskeletal proteins, all prefoldin subunits were found to have unique and specific interactors. These interactions presumably allow prefoldin subunits to engage in non-canonical cellular functions (Simons et al., 2004), but describing all of these interactions is beyond the scope of this review. **Table 1** summarizes the identified interactors with different prefoldin subunits. A recent review described links between interactors of prefoldin subunits and the progression of cancer (Liang et al., 2020; Herranz-Montoya et al., 2021). The sections below focus on the involvement of prefoldin subunits in transcription, protein aggregation, and degradation.

### Regulation of Transcription

Prefoldin was described to be a cytoplasmic protein complex (Geissler et al., 1998). The deletion of *PFD1* in yeast resulted in unexpected defects in transcription elongation (Millan-Zambrano et al., 2013), but these findings complemented other studies and suggested a role for prefoldin in the nucleus (Millan-Zambrano and Chavez, 2014; Mousnier et al., 2007; Watanabe et al., 2002) (**Figure 2**). All prefoldin subunits were found to exhibit nucleo-cytoplasmic localization in the yeast *Saccharomyces cerevisiae* (Millan-Zambrano et al., 2013). This newly identified transcriptional function of prefoldin subunits was independent of actin assembly in the cytoplasm and independent of the involvement of nuclear actin in transcription elongation. The deletion of *PFD1* decreased the RNA polymerase II occupancy of gene bodies (**Figure 2A**). This was explained by the role of prefoldin in the removal of histones from chromatin. These data were supported by numerous genetic interactions between prefoldin subunits and chromatin factors (Millan-Zambrano et al., 2013; Ming Sun et al., 2020). Genetic interactions between prefoldin and TRiC/CCT components and chromatin factors were similar and suggested a combined action of chaperonin and its co-chaperone in transcription regulation in the nucleus. Furthermore, the physical interaction between histone deacetylase 1 (HDAC1) and prefoldin and TRiC/CCT suggested the requirement for chaperone-mediated folding before its assembly into the active complex (Banks et al., 2018) (**Figure 2B**). This further strengthened the involvement of

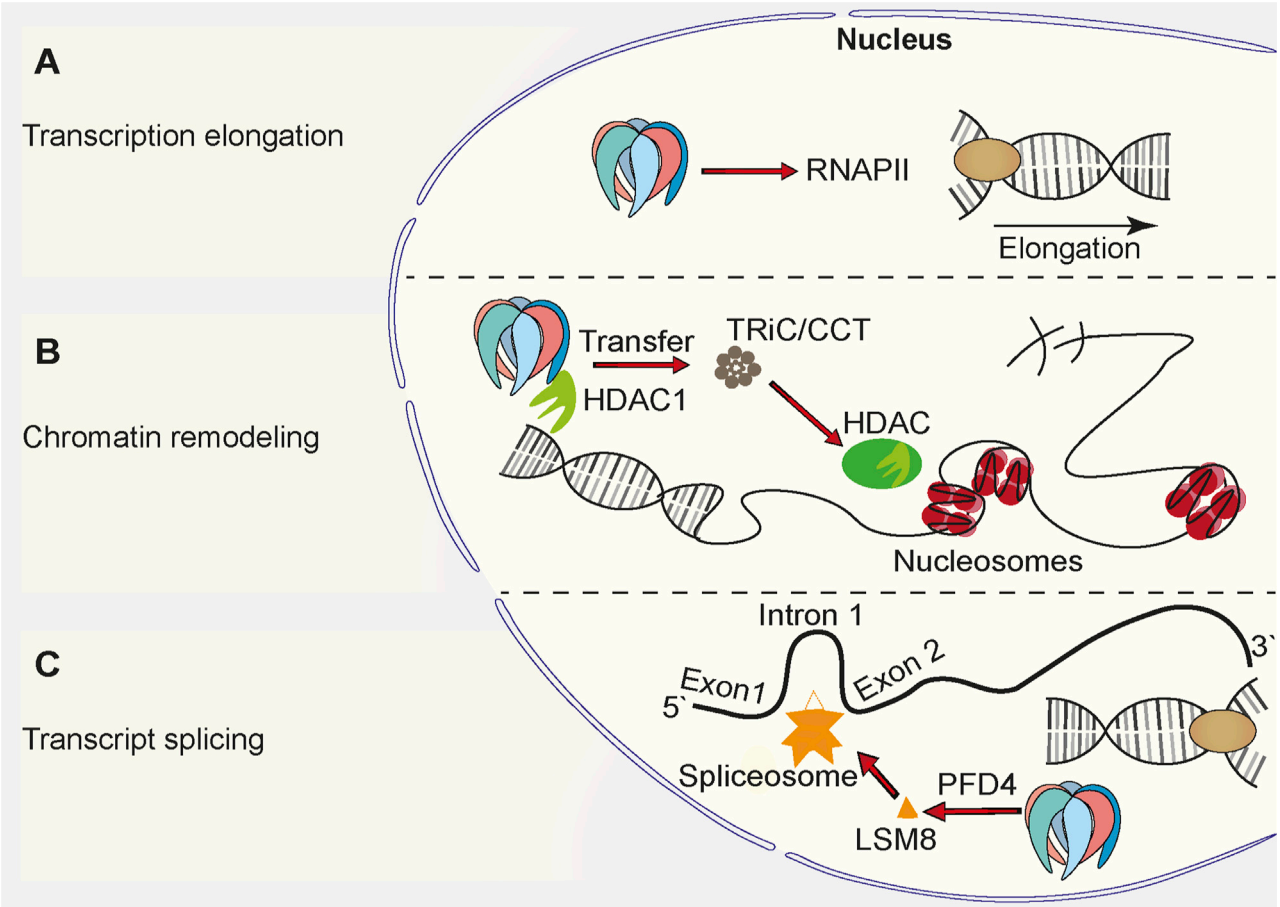


**FIGURE 2 |** Function of prefoldin complex in the cell nucleus. **(A)** Prefoldin stimulates transcription elongation by promoting binding of RNA Polymerase II (RNAPII) to euchromatin. **(B)** Prefoldin interacts with HDAC1 and supports incorporation of it into its active complex via TRiC/CCT complex. The interaction favors chromatin remodeling. **(C)** The PFD4 subunit is required for the incorporation of the spliceosome core complex subunit, LSM8, into the spliceosome.

prefoldin in the remodeling of chromatin and transcription regulation. A recent study in *Arabidopsis* showed that PFD4 mediates the chaperone-client interaction between Hsp90 and LSM8, a central component of the spliceosome core complex. Prefoldin was shown to be important for maintaining adequate levels of the spliceosome core complex (Esteve-Bruna et al., 2020) (**Figure 2C**). A strong genetic interaction between *pfd4*Δ (gim3 in yeast) and *lsm8*Δ in yeast (Costanzo et al., 2016) prompted Esteve-Bruna *et al* to the notion that the functional interaction between prefoldin and the spliceosome could be conserved. The implication of prefoldin in the regulation of co-translational splicing effects was also recently demonstrated for human prefoldin (Payán-Bravo et al., 2021). The binding of prefoldin to transcribed genes was detected genome-wide. The loss of prefoldin function led to a decrease in the phosphorylation of elongating polymerase II and decrease in the binding of splicing factors to chromatin. Links between prefoldin and cellular splicing machinery thus add another level of complexity to the ways in which prefoldin influences transcriptional processes in the nucleus.

## Role in Cellular Stress Defense

The importance of prefoldin-dependent regulation of gene expression became eminent under cellular stress conditions. The green fluorescent protein-tagged Pfd1 exhibited an increase in nuclear staining when cells were shifted to a restrictive growth temperature (Millan-Zambrano et al., 2013). This finding in yeast was consistent with studies in plants that investigated the regulated migration of prefoldin from the cytoplasm to the nucleus (Locascio et al., 2013). Here, the shuttling of plant prefoldin complex depended on the interaction of PFD3 and PFD5 with the transcriptional regulator DELLA under conditions of environmental and endogenous cue exposure (**Figure 3A**). A mutant of *Arabidopsis* that harbored deletions of all six prefoldin subunits was viable, and loss of the prefoldin complex did not significantly alter plant development under normal growth conditions. The prefoldin complex knockout mutant performed better than the wild type under osmotic stress conditions (Blanco-Touriñán et al., 2021). This indicates that

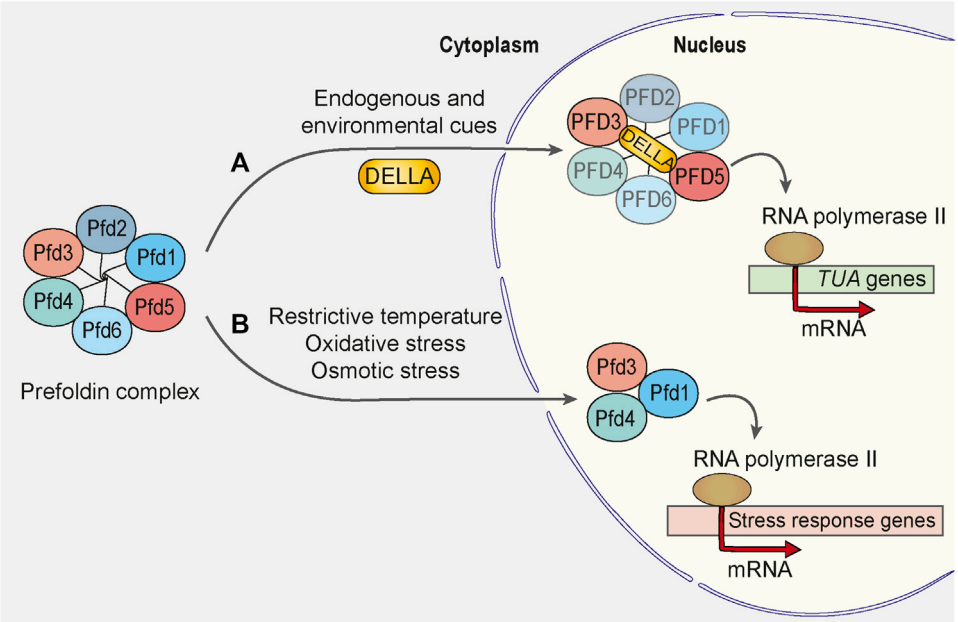


**FIGURE 3 |** Prefoldin complex is involved in transcriptional regulation upon cellular stress. **(A)** In *Arabidopsis*, endogenous and environmental stimulators control the growth rate of a plant by inducing the DELLA-mediated accumulation of prefoldin complex in the cell nucleus. PFD3 and PFD5 interact directly with DELLA, but integrity of the prefoldin complex during the translocation remains unaffected. In the nucleus, prefoldin complex or some of its subunits activate the transcription of α-tubulin encoding genes (*TUA*). **(B)** In response to exposure of yeast *Saccharomyces cerevisiae* to stress stimuli such as restrictive temperature, oxidative and osmotic stress, Pfd1, Pfd3 and Pfd4 subunits localize to the nucleus to facilitate the transcription elongation of some stress-response genes. Pfd1, Pfd3 and Pfd4 may form a distinct complex from the hexameric prefoldin complex because the absence of other prefoldin subunits and consequent disruption of the prefoldin complex does not suppress the stress response in *S. cerevisiae*.

prefoldin is needed to respond to stress conditions and/or environmental changes. Consistent with recent findings in plants are findings in yeast, in which Pfd3 (also called Gim2 or Pac10), Pfd4 (also called Gim3), and Pfd1 (also called Gim6) were shown to be involved in oxidative and osmotic stress-activated transcription (Amorim et al., 2017) (**Figure 3B**).

The deletion of prefoldin also affected yeast viability upon exposure to other exogenous stressors. A genome-wide screen of haploid deletion mutants found that subunits of the prefoldin complex were among the most sensitive mutants to arsenite treatment (Pan et al., 2010). Exposure to high temperatures decreased the growth of a *PFD5* deletion mutant in yeast (Gestaut et al., 2019). The induction of endoplasmic reticulum stress by thapsigargin treatment decreased cell viability in the absence of the prefoldin complex in mammalian cells (Abe et al., 2013). These stressors generally increase proteostatic stress in the cell, which might be an indication that prefoldin is required for the maintenance of protein homeostasis under conditions of high protein burden.

## Influence on Protein Turnover and Quality Control

Protein turnover defines the balance between protein production and protein degradation. Importantly, the correct folding of newly synthesized polypeptides is a limiting factor of both fundamental cellular processes (Rothman, 2010). Defects in the folding process can stall translation and require an increase in the removal of unfolded or misfolded proteins from the cell (Goldman et al., 2015). Nascent chains that emerge from the actively translating ribosome are passed to chaperones of the ribosome-associated complex (RAC) and nascent polypeptide-associated complex (NAC), which assist the folding of ~70% of polypeptides (Balchin et al., 2016). Downstream of ribosomes (i.e., the hub of the chaperone network), Hsp70, together with Hsp40s, folds ~20% of the proteome (Balchin et al., 2016). Ten percent of these proteins are passed further downstream to multi-domain cylindrical complexes, group II chaperonins [TRiC/CCT; Hsp60 chaperones in archaea and the eukaryotic cytosol (Thulasiraman et al., 1999; Yam et al., 2008);]. Some proteins bypass Hsp70 and are directly transferred to chaperonins via the prefoldin chaperone complex (Balchin et al., 2016) (see also **Figure 1**). The prefoldin structure was determined in archaea, revealing a jellyfish-shaped complex where the six subunits form six long coiled coils that are attached to a base of β barrels (Leroux et al., 1999; Fandrich et al., 2000; Siegert et al., 2000; Ohtaki et al., 2008). Biochemical experiments and low-resolution electron microscopy studies confirmed this structural arrangement for human prefoldin (Martin-Benito et al., 2002; Simons et al., 2004; Aikawa et al., 2015; Gestaut et al., 2019). In eukaryotes, charged residues in the distal end of coiled coils of certain prefoldin subunits bind to actin and tubulin, and defined residues in each of these substrates are necessary for this interaction. Thus, prefoldin

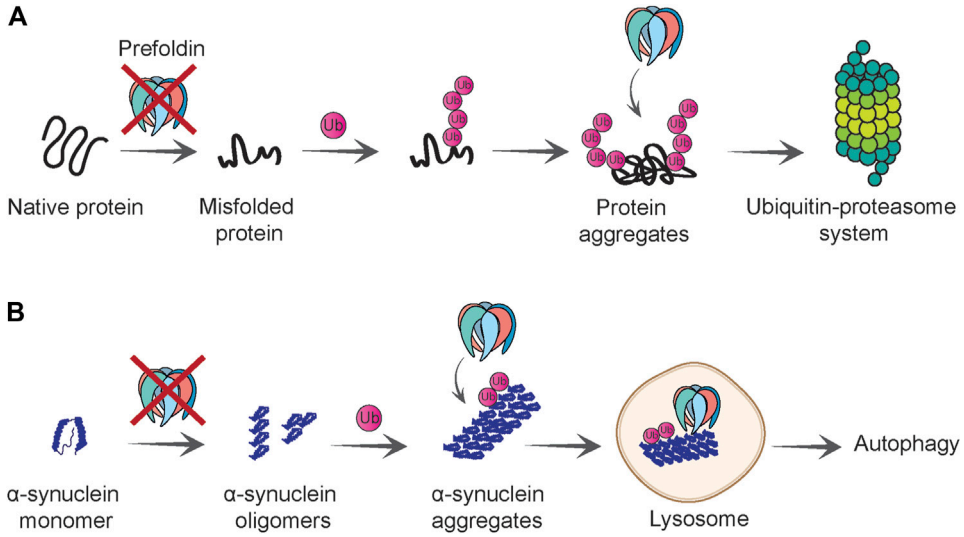


**FIGURE 4 |** Role of prefoldin complex in protein quality control and degradation. **(A)** Prefoldin is required for polypeptides to gain native fold and loss of prefoldin function causes protein misfolding. Misfolded proteins that cannot be refolded are polyubiquitinated. Prefoldin complex co-localizes with the polyubiquitinated proteins and presumably facilitates their degradation by the ubiquitin-proteasome system. **(B)** Prefoldin complex prevents aggregation of α-synuclein at initial steps of oligomerization. If α-synuclein oligomers form aggregates, they will be ubiquitinated and in proximity to prefoldin complex delivered to the lysosome in which aggregates can be degraded in an autophagy-dependent manner.

binding is specific and may involve the combinatorial binding of different subunits for different targets. However, in contrast to archaeal prefoldin, which was shown to interact with numerous non-native substrates (Arranz et al., 2018), knowledge of the substrate landscape in eukaryotic prefoldin is limited. Interestingly, genome-wide genetic interaction screens in yeast revealed a large variety of genes that when deleted in the background of deletions of single prefoldin subunits result in a synthetic lethal phenotype (Goehring et al., 2003; Krogan et al., 2003; Tong et al., 2004; Friesen et al., 2006; Mitchell et al., 2008). This might indicate that prefoldin has a broader cellular function than previously anticipated.

A few findings suggest a link between the prefoldin complex and the removal of proteins that are targeted to the proteasome (Abe et al., 2013; Comyn et al., 2016) (**Figure 4A**). In a mammalian cell culture model, the prefoldin complex co-localized with ubiquitinated proteins that were found in aggregates upon proteasome inhibition. Intriguingly, lower levels of the prefoldin complex resulted in the higher accumulation of poly-ubiquitinated proteins that were resistant to detergent. This effect depended on concomitant inhibition of the proteasome. A decrease in prefoldin function that was associated with an insufficient protein degradation system most likely overwhelmed the cellular proteostasis system, consequently leading to an increase in cell death (Abe et al., 2013).

Overexpression of the prefoldin complex lowered levels of detergent-insoluble ubiquitinated protein species upon proteasome inhibition, but this conferred only a minimal beneficial effect on cell viability. A mouse model that expressed PFDN5 with a point mutation (MM-1α/PFDN5) showed normal PFDN5 expression and no detectable differences in expression of the prefoldin complex (Lee et al., 2011). However, cells that were derived from this MM-1α/PFDN5 mouse model accumulated more poly-ubiquitinated proteins and were more sensitive to proteasome inhibition. Superficially, no defect in the prefoldin complex was observed, but amino acid substitution in PFDN5 changed the structure of the subunit and altered its affinity for substrates (Abe et al., 2013). These findings demonstrated that the prefoldin complex is an important component of the protein quality control system and performs functions beyond simply acting as a co-translational holdase of newly synthesized polypeptides of cytoskeletal proteins. However, the mechanistic role of the prefoldin complex with regard to the proteasome remained unclear.

Revealing the extended landscape of prefoldin substrates in eukaryotes could shed light on the function of prefoldin during stress conditions, such as limited availability of the protein degradation system. To identify factors that promote the proteasomal degradation of misfolded proteins in yeast, the function of Pfd4 was characterized (Comyn et al., 2016). In the absence of *PFD4*, the model protein Guk1-7, which is thermally unstable and is a substrate of the proteasome, were partially protected from degradation. The inhibition of Guk1-7 turnover occurred independently of functionality of the proteasome complex and its ubiquitination levels. Importantly, Pfd4 was shown to interact with the mutant form of Guk1 but not the wildtype version. Thus, Pfd4 acts as a holdase for Guk1-7 to ensure its solubility. In the absence of *PFD4*, Guk1-7 localized in distinctive foci that were also positive for the aggregation markers Hsp42 and Hsp104. Other thermosensitive alleles were also tested. Different prefoldin subunits stabilized various model proteins to different extents. This indicates that each prefoldin subunit has differential affinity for their substrates (Comyn et al., 2016). This work opens the field for further exploration of a wider

range of substrates. Much more work is needed to decipher interactions between single prefoldin subunits and specific substrates and substrate classes. Moreover, remaining unclear are whether the function of this holdase depends on a functional prefoldin complex or whether individual subunits act independently from their incorporation in the complex.

The involvement of the prefoldin complex and individual prefoldin subunits in protein quality control seems convincing, but unclear are how its function changes from being a canonical co-translational holdase to a translation-independent chaperone with holdase and disaggregase activity and whether this non-canonical function is independent of TRiC/CCT. Inhibition of the proteasome results in lower levels of amino acids, which in turn activates the integrated stress response. This universal response to unfavorable environmental conditions results in the attenuation of global translation by phosphorylation of eukaryotic initiation factor 2α (eIF2α) (Suraweera et al., 2012). Under such cellular conditions, co-translational chaperones might be free to perform other cellular tasks. Such a scenario was described for the ribosome-associated NAC and RAC-Ssb chaperone systems (Olzscha et al., 2011; von Plehwe et al., 2009; Wang et al., 2009).

## Implication in the Amelioration of Disease-Associated Protein Aggregation

Given the emerging role of prefoldin as a factor in maintaining protein solubility under physiological and cellular stress conditions, consistent observations have been made in model systems in which prefoldin can protect from toxic aggregates that are linked to human diseases.

The knockdown of PFDN2 in undifferentiated neuronal cells increased the formation of aggregates of polyQ stretches and polyQ-expanded huntingtin (HTT), gene defects that are related to the neurodegenerative Huntington's disease (Tashiro et al., 2013). The knockdown of PFDN5 also affected aggregation but to a much lesser extent. Importantly, only the aggregation of pathogenic forms was enhanced and not healthy forms. The knockdown of PFDN2 or PFDN5 did not influence the expression of other chaperones, such as HSP70, HSC70, HSP40, and CCTα, suggesting that prefoldin could be a limiting factor to prevent aggregate formation. The overexpression of prefoldin reduced the aggregated form of pathogenic huntingtin. *In vitro* single-molecule observation by total internal reflection fluorescence microscopy showed that prefoldin suppressed the dimer-to-tetramer stage of HTT aggregation. This indicates that prefoldin inhibits the elongation stage of large oligomers of pathogenic HTT rather than inclusion formation *per se* (Tashiro et al., 2013).

Similar to HTT aggregation, the formation of α-synuclein aggregates increased upon the knockdown of prefoldin expression in a neuronal cell culture model (Takano et al., 2014). Moreover, ubiquitinated forms of fluorescently tagged wildtype and mutant α-synuclein co-localized with prefoldin (**Figure 4B**). This observation is consistent with the finding that prefoldin co-localizes with poly-ubiquitinated protein species (Abe et al., 2013). The co-localization of α-synuclein with prefoldin was detected in the lysosome, an organelle that can mediate α-synuclein clearance under normal conditions but also under conditions of high protein burden (Mak et al., 2010). Notably, only a small percentage of prefoldin was detected in the lysosome, whereas most remained in the cytoplasm. One unanswered question is whether the effect of prefoldin knockdown on α-synuclein aggregation and toxicity is a direct effect or a consequence of exhaustion of overall folding capacity of the cell. In either case, this work demonstrates that prefoldin might assist with the transfer of misfolded proteins to the autophagy-dependent degradation pathway (Takano et al., 2014) (**Figure 4B**).

The effect of prefoldin on the oligomerization of amyloid-β (Aβ) peptides was also investigated. The fibrillation of Aβ was inhibited in the presence of archaeal prefoldin (Sakono et al., 2008). A similar observation was made in an *in vitro* model (Sorgjerd et al., 2013). Deposits of Aβ are found in the brain cortex and hippocampus. Prefoldin was detected in both brain regions, but its expression was elevated in a mouse model that exhibited an increase in Aβ deposition. Amyloid-β cytotoxicity was reduced in a cell culture model when Aβ oligomers were formed in the presence of human prefoldin. However, the addition of recombinant human prefoldin did not prevent the toxic effect of preformed toxic Aβ oligomers lending further weight to the hypothesis that prefoldin acts on pre-oligomeric misfolded species (Sorgjerd et al., 2013).

In contrast to higher prefoldin expression in brain regions that exhibit an increase in Aβ deposition, a mouse model that expressed a mutant version of Tau exhibited a decrease in PFDN5 expression, which was age-dependent (Kadoyama et al., 2019).

Little is known about prefoldin function during biological aging. However, considering accumulating evidence that prefoldin function can have beneficial effects on the aggregation and toxicity of proteins that are linked to age-associated diseases, further efforts need to be made to elucidate the potential role of prefoldin during aging. The nematode *Caenorhabditis elegans* was proven to be a useful model organism for understanding the biology of aging. In *C. elegans*, prefoldin is essential in early development of the embryo because of the need for cytoskeletal structures (Lundin et al., 2008). The use of RNA interference (RNAi) technology allows the knockdown of genes in *C. elegans*. RNAi against prefoldin subunits is lethal when applied throughout development of the worm. RNAi targeting at later stages of development allows the observation of phenotypes in adult worms. The knockdown of *pfd-6* did not alter lifespan *per se*, but *pfd*-6 was partially necessary for the long-lived phenotype of a *daf-2* mutant of the insulin/insulin-like growth factor 1 (IGF-1) pathway (Son et al., 2018). Essentially, this effect was dependent on heat shock factor 1 (HSF-1) and forkhead box O (FOXO/DAF-16) transcription factors, which mediate lifespan extension in *daf-2* mutant animals. Moreover, the action of HSF-1 increased the expression of PFD-6 protein levels, possibly by activating the expression of *hsp-70* and *hsp-90*, which in turn bind and stabilize PFD-6. PFD-6 expression in the *daf-2* mutant was necessary for the upregulation of a subset of DAF-16 target genes in *daf-2* mutants. The role of PFD-6-dependent lifespan extension in *daf-*

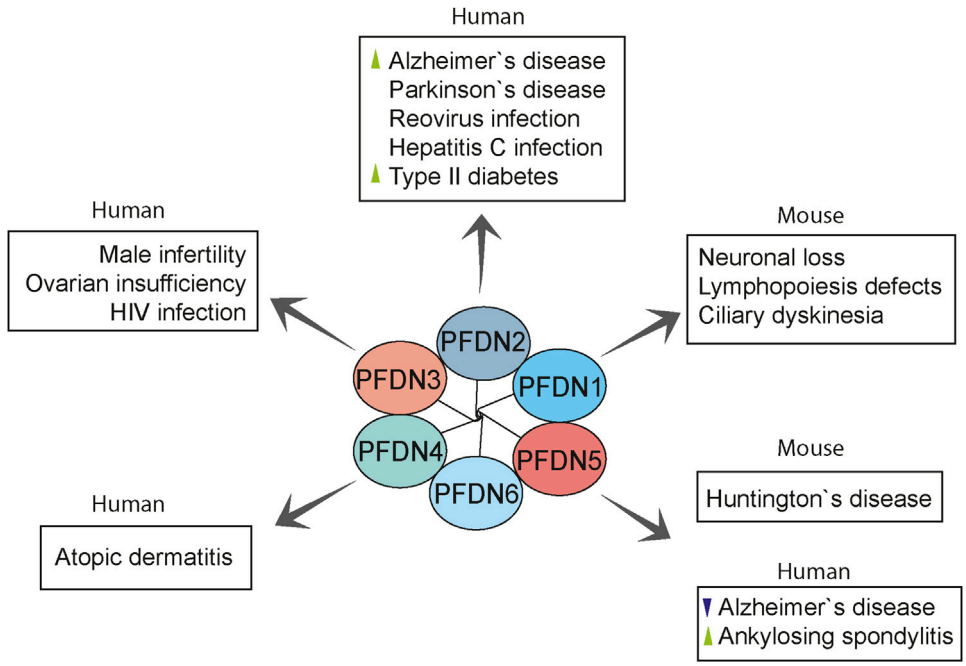


**FIGURE 5 |** Overview of prefoldin-mediated diseases in humans and mouse models. Prefoldin subunits are involved in various pathologies other than cancer. PFDN2 and PFDN5 were linked with neurodegenerative diseases. PFDN2 and PFDN3 mediate some virus infections. Moreover, prefoldin subunits have distinct roles in the progression of rare anomalies. Changes in prefoldin subunit regulation in human diseases are indicated with arrowhead (green, upregulation; violet, downregulation).

**TABLE 2 |** Altered expression of prefoldin subunits in human cancer.

| Subunit | Pathogenic alteration | Type of cancer | References |
|---|---|---|---|
| All subunits | Upregulation | Gastric cancer | Yesseyeva et al. (2020) |
| PFDN1 | Upregulation | Gastric cancer | Yesseyeva et al. (2020), Zhou et al. (2020) |
| | Upregulation | Lung cancer | Wang et al. (2017) |
| | Upregulation | Non-small-cell lung cancer | Peñate et al. (2020) |
| | Upregulation | Colorectal cancers | Wang P et al. (2015); Kwon et al. (2021) |
| PFDN2 | Upregulation (gain of copy number) | Urothelial carcinoma | López et al. (2013), Riester et al. (2014) |
| | | Bladder cancer | López et al. (2013) |
| | | Gastric cancer | Yesseyeva et al. (2020) |
| | Genetic alterations | Breast tumors | Nami and Wang, (2018) |
| | Gain or loss of interaction with pathogenic or altered cellular proteins | Liver cancer | Chang et al., (2006); Dash et al., (2020); El-Serag, (2012); Farooq et al., (2013) |
| PFDN3 in intact PFDN complex | Downregulation | Von Hippel-Lindau syndrome (various types of cancers) | Chesnel et al., (2020); Kim et al., (2018); Tsuchiya et al., (1996) |
| PFDN4 | Upregulation | Gastric cancer | Feng et al. (2009) |
| | Upregulation | Breast cancer | Collins et al. (2001) |
| | Upregulation | Hepatocellular carcinoma | Wang D et al., (2015) |
| | Downregulation | Colorectal cancer | Miyoshi et al. (2010) |
| PFDN5 | Downregulation | Human leukemia, lymphoma, and tongue cancer | Fujioka et al. (2001) |
| | Upregulation of spliced variants | Thyroid neoplasms | Guimarães et al. (2006) |
| | Upregulation | Non-small cell lung cancer | Peñate et al. (2020) |
| | Downregulation | Parathyroid hyperplasia | Santamaría et al. (2005) |
| PFDN6 | Downregulation | Pediatric acute lymphoblastic leukemia | Dehghan-Nayeri et al. (2017) |

*2* mutants is likely related to its non-canonical function in the R2TP (Rvb1-Rvb2-Tah1-Pih1)/prefoldin-like complex rather than the canonical prefoldin complex (Son et al., 2018). This single study in *C. elegans* demonstrates that we are only in the incipient stages of understanding prefoldin function within a stress-loaded milieu, such as during aging. Much more work needs to be dedicated to unravelling stress-dependent functions of prefoldin.

## IMPLICATIONS OF PREFOLDIN IN PATHOLOGICAL CONDITIONS

Cytoskeletal proteins, such as actin and tubulin, are fundamental to some cellular processes, such as signal transduction, macromolecular trafficking, cell migration, and cell division (Small et al., 1999). Given the role of the prefoldin complex in the biogenesis of cytoskeletal proteins and its additional roles in the cell nucleus (Millan-Zambrano and Chavez, 2014), the prefoldin complex has been speculated to contribute to various disorders. The abnormal expression and function of the prefoldin complex are linked with various disorders, including neurodegenerative diseases, cancer, and viral infections (**Figure 5** and **Table 2**).

### Neurodegenerative Diseases

Neurodegenerative diseases are characterized by the progressive dysfunction of specific neurons and loss of their connections, mainly through the formation of long-insoluble protein fibrils and aggregates (Vaquer-Alicea and Diamond, 2019). Alzheimer's disease is a major neurodegenerative disease that is characterized by progressive memory failure and age-related dementia, which are mainly caused by the aggregation of Aβ protein and formation of amyloid plaques in brain cells (Guo et al., 2020). Autopsies of human brain tissues and cDNA microarray analysis revealed the upregulation of PFDN2 transcript in Alzheimer's disease brains compared with controls (Loring et al., 2001). The association between the prefoldin complex and Alzheimer's disease was also confirmed by single-nucleotide polymorphism analysis and pathway assays (Broer et al., 2011). Interestingly, a study analyzing human whole blood mRNA expression data revealed downregulation of *PFDN5* in samples of Alzheimer's patients, which could suggest a link to increased toxicity of Aβ (Tao et al., 2020). The prefoldin complex has also been shown to exert a protective effect against the pathogenesis of Huntington's disease, a progressive neurodegenerative disorder, among a large family of proteopathies. Repeats of the CAG codon (which encodes glutamine) that are greater than 40 in exon 1 of the huntingtin gene elevate the risk of Huntington's disease at age 65 (Langbehn et al., 2004; Langbehn et al., 2019). The extension of polyglutamine regions alters the length and oligomerization of pathogenic huntingtin that subsequently form β-sheet-rich fibrils and large toxic aggregates (Davies et al., 1997; DiFiglia et al., 1997). Unexpectedly, transgenic mice that carried an integrated human *HTT* gene with 300 CAG repeats (Q300) had a prolonged lifespan and longer disease onset compared with their parental mice with shorter CAG repeats (Q150). Transcription studies revealed that phenotype amelioration in Q300 mice was associated with the overexpression of *Pfdn5* and other genes that are involved in protein folding and localization (Tang et al., 2011). These genes could be therapeutic targets for improving symptoms of Huntington's disease.

PFDN2 has been suggested to be involved in the pathogenesis of the most common neurodegenerative disease, Parkinson's disease. miR-153–3 p microRNA downregulated α-synuclein, one protein that is associated with Parkinson's disease, and decreased the abundance of PFDN2 in neuronal SH-SY5Y cells (Patil et al., 2015), suggesting a possible link between Parkinson's disease and the prefoldin complex.

### Cancer

Cancer refers to a group of disorders that are caused by the uncontrolled division of cells that may start in every organ of the body and, in severe cases, spread to other organs (Hausman, 2019). Several studies reported the contribution of the prefoldin complex and its subunits to the onset and progression of some cancers (**Table 2**) (Liang et al., 2020; Herranz-Montoya et al., 2021). Higher prefoldin expression was observed in cancer cell lines compared with non-cancerous cells (Boudiaf-Benmammar et al., 2013). Additionally, all prefoldin subunits were found to be involved in the development of gastric cancer (Yesseyeva et al., 2020).

The role of cytoskeleton remodeling in cancer metastasis has been confirmed by numerous studies (Aseervatham, 2020). Therefore, one can speculate that prefoldin mediates cancer progression through its role in cytoskeletal proteostasis. Much evidence confirmed that high PFDN1 expression is associated with the metastasis and poor prognosis of gastric cancer, lung cancer, and colorectal cancer (Wang P. et al., 2015; Wang et al., 2017; Zhou et al., 2020; Kwon et al., 2021). High levels of PFDN1 activates the epithelial-mesenchymal transition (EMT), which is necessary for the initiation of metastasis. The mechanism by which PFDN1 initiates activation of the EMT is different in various tumors. For example, in gastric cancer cells, PFDN1 activates alterations of the EMT through Wnt/β-catenin signaling (Zhou et al., 2020). In lung tumors, PFDN1 contributes to growth and metastasis by suppressing the transcription of cyclin A. PFDN1 directly interacts with the cyclin A promoter at the transcription initiation site and inhibits cyclin A expression, which eventually activates the EMT and facilitates the migration of lung cancer cells (Wang et al., 2017). A study of PFDN1 mRNA and protein levels in clinical specimens from patients with colorectal cancer showed higher levels of PFDN1 in colorectal cancer samples, particularly the invasive form of the disease, compared with healthy tissues. PFDN1 promotes the proliferation and metastasis of colorectal cancer by maintaining cytoskeletal proteins, particularly F-actin and α-tubulin (Wang P. et al., 2015). Clinical specimens of non-small cell lung cancer revealed that the overexpression of PFDN1, PFDN3, and PFDN5 are significantly associated with higher mortality and metastasis in non-small cell lung cancer (Peñate et al., 2020). In contrast, microarray data revealed that *PFDN1* had stable expression levels in nasopharyngeal carcinoma

samples, making it a suitable reference gene for expression studies (Guo et al., 2010).

PFDN1 functions as a tumor promoter, and its inhibition has a favorable effect in controlling the progression of some cancers. PFDN1 has been proposed as a target for the treatment of lung cancer (Wang et al., 2017). The silencing of PFDN1 decreased the expression of downstream proteins of Wnt/β-catenin signaling, suggesting that PFDN1 may be a specific target to attenuate the development of gastric cancer (Zhou et al., 2020). PFDN1 may also be a diagnostic biomarker and potential candidate for the treatment of colorectal cancer (Wang P. et al., 2015).

*PFDN2* is located on chromosome 1q23.3, and increases in its copy number are associated with a poor prognosis and treatment outcome of urothelial carcinoma (López et al., 2013; Riester et al., 2014). The amplification and overexpression of *PFDN2* were detected in high-grade tumors of the bladder. Additionally, high levels of PFDN2 were detected in urinary specimens from bladder cancer patients, suggesting that it may be a biomarker for prognosis, tumor staging, and clinical outcome (López et al., 2013). PFDN2 has been shown to interact with most α-tubulin and β-tubulin isoforms, and its genetic alterations are detected in 20% of breast tumors (Nami and Wang, 2018). Several studies indicated an association between PFDN2 and liver cancer. The alteration of one actin isoform, κ-actin, was discovered in some hepatocellular carcinoma tissues, with a decrease in its interaction with PFDN2. κ-Actin rearranges the actin cytoskeleton by replacing β-actin and becoming a dominant component of the actin cytoskeleton in cancerous hepatoma tissues (Chang et al., 2006). Interactions between F protein in hepatitis C virus with PFDN2 promote chronic infection (Tsao et al., 2006), which is known as a predominant risk factor for hepatocellular carcinoma (El-Serag, 2012; Dash et al., 2020). Additionally, alterations of histone deacetylase 1 protein expression were found in hepatocellular carcinoma, and this protein was shown to interact with prefoldin subunits in HepG2 human liver cancer cells (Farooq et al., 2013).

Low levels of the prefoldin complex, particularly the PFDN3 subunit, are associated with the severe phenotype of von Hippel-Lindau (VHL) syndrome (Chesnel et al., 2020). von Hippel-Lindau syndrome is a dominant cancer syndrome that predisposes to various familial or sporadic neoplasms of the central nervous system, adrenal glands, pancreas, retina, and kidney, including clear cell renal cell carcinoma. VHL syndrome is reviewed elsewhere (Varshney et al., 2017). von Hippel-Lindau syndrome is caused by mutations of the *VHL* tumor suppressor gene and the subsequent loss of its native protein product, pVHL. Tsuchiya and colleagues initially isolated PFDN3, also called von Hippel-Lindau binding protein 1 (VBP1), as a C-terminal binding partner of pVHL (Tsuchiya et al., 1996). PFDN3 was shown to stabilize pVHL and contribute to the pVHL-mediated degradation of hypoxia-inducible factor-1α, ultimately leading to the suppression of cancer metastasis (Kim et al., 2018). Although the main focus of the study by Kim and colleagues was on the PFDN3 subunit, recent research confirmed that the whole prefoldin complex is required to protect pVHL against aggregation. Lower levels of PFDN3 reduce stabilization of the whole prefoldin complex, eventually leading to the poor survival of clear cell renal cell carcinoma patients who harbor *VHL* missense mutations (Chesnel et al., 2020).

PFDN4, also known as protein C-1, was initially described as a transcription factor that regulates the cell cycle (Iijima et al., 1996). The expression of *PFDN4* is regulated by TWIST transcription factor, which plays an important role in the tumorigenesis and metastasis of gastric cancer. The silencing of TWIST increased *PFDN4* gene expression levels in gastric cancer cell lines, indicating that *PFDN4* might be related to gastric cancer (Feng et al., 2009). Accumulating evidence shows that the genetic locus of *PFDN4* confers potential susceptibility to breast cancer. The *PFDN4* gene is located on chromosome 20q13.2. A human genome sequence analysis of the 1.2 Mb amplified region of chromosome 20q13.2 showed that the *PFDN4* gene is located in the breast cancer amplicon. Amplification of this chromosome region increased *PFDN4* expression, suggesting that *PFDN4* is an oncogene that is associated with the development of breast cancer (Collins et al., 2001). However, quantitative polymerase chain reaction analysis of archival tissue samples from 54 patients with invasive ductal carcinoma of the breast did not show the significant overexpression of *PFDN4* in breast tumors (Born et al., 2005). These disparate results indicate the need for further studies to elucidate the role of *PFDN4* in the development of breast cancer.

The gain of whole chromosome 20q or specific regions therein also plays a role in progressive hepatocellular carcinoma. Analyses of copy number variations of chromosome 20q in hepatocellular carcinoma tumor samples and expression studies revealed that 20q13.12–13.33 gain correlates with the invasiveness of hepatocellular carcinoma. Moreover, *PFDN4* is among the genes whose higher expression is associated with a greater risk of extrahepatic metastasis and poor survival (Wang D. et al., 2015). Surgical specimens from 129 patients with colorectal cancer were assessed by Miyoshi et al. (2010) to determine *PFDN4* expression and its correlation with clinicopathological futures of colorectal cancer. Higher *PFDN4* expression was associated with better survival in colorectal cancer patients. This suggests that in the context of colorectal cancer, *PFDN4* functions as a tumor suppressor and may serve as a marker of favorable prognosis (Miyoshi et al., 2010). In breast and liver cancers, high *PFDN4* expression promoted carcinogenesis, suggesting that it is an oncogene (Collins et al., 2001; Wang D. et al., 2015). These findings indicate that the impact of *PFDN4* in the development of various cancers is tissue-specific.

PFDN5, also known as Myc modulator 1 (Mm-1), was shown to inhibit the transcriptional activity of c-MYC through various mechanisms (Mori et al., 1998; Yoshida et al., 2008). PFDN5 has been suggested to have a tumor-suppressing function. PFDN5 deficiency was shown to be associated with leukemia, lymphoma, and tongue cancer in humans and mammary cancer in canines (Fujioka et al., 2001; Hennecke et al., 2015).

The results of a cDNA microarray analysis of clinical colorectal cancer samples suggested that *PFDN5* may be a useful tumor histology and prognosis marker (Tsunoda et al., 2003). The high expression of an alternative splicing variant of *PFDN5* was detected in malignant thyroid neoplasms compared

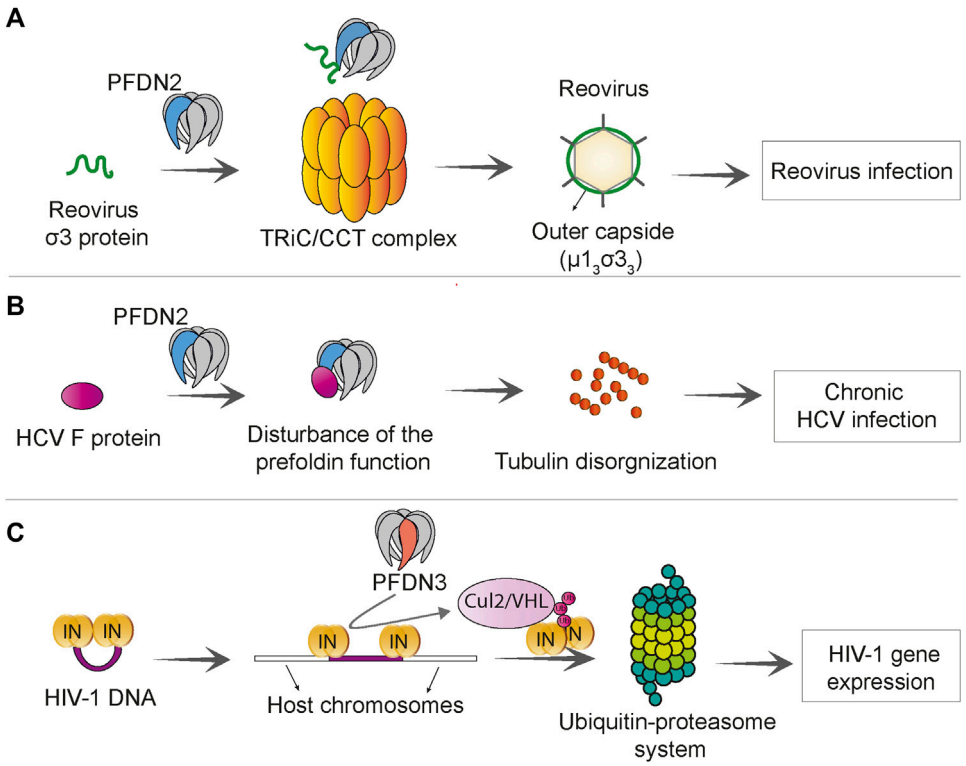


**FIGURE 6 |** Prefoldin is linked to viral infections. **(A)** PFDN2 subunit of the prefoldin complex interacts with reovirus σ3 protein and increases the efficiency of TRiC/CCT -mediated $\mu1_3\sigma3_3$ assembly, which promotes reovirus infection. **(B)** The Hepatitis C virus (HCV) F protein interacts with PFDN2 and disturbs the normal function of prefoldin complex in microtubule organization. This leads to persistence of virus in chronic HCV infection. **(C)** PFDN3 specifically interacts with HIV-1 integrase (IN) and mediates its interaction with cullin 2/VHL (Cul2/VHL) ubiquitin ligase, which subsequently leads to integrase "polyubiquitination" and proteasome-dependent degradation. This process promotes HIV-1 gene expression at a post-integration step.

with benign lesions and normal thyroid tissues (Guimarães et al., 2006). Moreover, low *PFDN5* expression was found to correlate with advanced parathyroid hyperplasia (Santamaría et al., 2005).

The low protein and mRNA expression of PFDN6 was reported to be associated with resistance to the chemotherapy drug dexamethasone in pediatric acute lymphoblastic leukemia. Additionally, low mRNA levels of PFDN6 were detected in bone marrow samples from high-risk cases of pediatric acute lymphoblastic leukemia compared with the low risk and control healthy groups, suggesting that PFDN6 may be a predictive and treatment biomarker of pediatric acute lymphoblastic leukemia (Dehghan-Nayeri et al., 2017).

## Viral Infections

Prefoldin subunits were found to promote some viral infections. The co-chaperone function of the prefoldin complex can be utilized to accelerate the folding of reovirus capsid protein (Knowlton et al., 2021). Reoviruses are rarely pathogenic in early human life but are associated with infection of the respiratory system (Jackson and Muldoon, 1973) and central nervous system (Tyler, 1998), gastroenteritis (Giordano et al., 2002), and celiac disease (Bouziat et al., 2017). The prefoldin complex was shown to augment the TRiC-mediated folding of σ3 reovirus capsid protein and enhance efficiency of σ3/μ1 assembly to form a heterohexameric proteinic capsid ($\mu1_3\sigma3_3$). In this process, PFDN2 directly interacts with reovirus σ3 protein (Knowlton et al., 2021) (**Figure 6A**). Frameshift protein (F protein) of hepatitis C virus has been shown to bind to PFDN2 and impair function of the prefoldin complex. The F protein-PFDN2 interaction disturbs organization of the tubulin cytoskeleton, subsequently leading to the attenuation of hepatitis C virus replication and onset of chronic infection (Tsao et al., 2006) (**Figure 6B**).

PFDN3 has been shown to play a role in human immunodeficiency virus (HIV) infection. HIV-1 viral integrase is required for the integration of proviral DNA into the host genome, but after integration it remains bound to proviral DNA. PFDN3 was shown to bind to the viral integrase (Rain et al., 2009) and mediate its degradation through the ubiquitin-proteasome pathway, which facilitates the transcription of a viral gene. The prefoldin complex and cullin2/VHL ubiquitin ligase are required for appropriate expression of the HIV-1 gene and its post-integration replication (Mousnier et al., 2007) (**Figure 6C**).

## Autoimmune Response and Other Diseases

Clinical research has focused on the implications of prefoldin in tumor progression and as a diagnostic biomarker, but other medical conditions have also been related to prefoldin. Results

of a mouse study showed that the loss of PFDN1 caused severe phenotypes that were related to cytoskeletal deficiencies, such as lymphopoiesis defects, neuronal loss, and ciliary dyskinesia (Cao et al., 2008). High plasma levels of PFDN2 antibody were reported in patients with type 2 diabetes, especially young adults, suggesting that it may be a clinical biomarker for this disease (Chang et al., 2017). PFDN3 is known to control the level of MutS homologue 4 (MSH4) protein by promoting its poly-ubiquitination in mitotic cells and subsequent degradation (Xu and Her, 2013). MSH4 is essential for meiotic recombination and proper gametogenesis. Lower expression levels of MSH4 were reported to be linked with human male infertility and primary ovarian insufficiency in women (Carlosama et al., 2017; Tang et al., 2020). A genome-wide association study found that the PFDN4 gene was a novel disease-susceptibility locus for atopic dermatitis, an inflammatory skin disorder, in the Japanese population (Hirota et al., 2012). To identify a diagnostic biomarker for uveitis in ankylosing spondylitis, an inflammatory disorder that usually affects the axial spine, Kwon *et al.* found higher serum levels of anti-PFDN5 antibody in ankylosing spondylitis patients with uveitis. The upregulation of PFDN5 was also confirmed in ocular lesions in a mouse model of this disorder, which was associated with high serum levels of anti-PFDN5 autoantibody. In uveitis, PFDN5 upregulation might be involved in protecting retinal cells against cell death. These observations indicate that serum levels of anti-PFDN5 antibody could be a predictive marker of the development of uveitis in ankylosing spondylitis patients (Kwon et al., 2019).

The PFD6 subunit of *Plasmodium falciparum* (*Pf*), a eukaryotic parasite that causes malaria, promotes its pathogenesis. Merozoite surface protein-1 (MSP-1) of *Pf* plays an essential role in the binding of merozoites to human erythrocytes and infecting erythrocytes. *Pf* PFD6 was shown to interact with MSP-1 suggesting that *Pf* PFD6 might stabilize and assist the trafficking of MSP-1, which indirectly promotes erythrocyte invasion and pathogenicity of malaria (Kumar et al., 2020).

## PREFOLDIN AS A PROMISING CANDIDATE IN NANOMEDICINE

Several studies investigated the ability of the prefoldin complex to serve as a nanorobot for the intelligent delivery of nano cargo, such as nano drugs. The special structure of prefoldin, which consists of six long coiled-coil tentacles with a flexible central cavity, and the fact that it does not need to utilize ATP to capture and deliver substrates make it an attractive candidate for designing a nano actuator. By introducing amino acid substitutions, a novel prefoldin nano actuator (PNA) was designed that could manipulate hydrophobic nano cargo and inhibit the formation of pathogenic Aβ oligomers. The latter ability suggests that the designed PNA can be effective for the treatment of Alzheimer's disease (Sacks et al., 2018). The binding and release of nano cargo to the PNA cavity can be controlled by pH and temperature. High temperature decreases the area of the central cavity without affecting the overall conformation of prefoldin. The central cavity of PNA is able to capture a positively charged nano cargo at neutral pH and release it at acidic pH (Ghaffari et al., 2012; Shokuhfar et al., 2012). Given the higher temperature and lower pH of the tumor microenvironment compared with normal tissues (Zhang W. et al., 2020), utilization of the PNA may be a site-specific therapeutic strategy whereby an anti-tumor drug is released only at the tumor site while other normal tissues remain unaffected.

## PERSPECTIVES

The molecular co-chaperone prefoldin is a multifaceted protein complex, but the molecular pathways to which it is linked remain poorly described. The diverse involvement of prefoldin in various interconnected cellular functions, ranging from transcriptional regulation to co-translational holdase and post-translational degradation processes, hamper rapid progress in this research field. One future research direction will be to elucidate the cellular and environmental conditions that allow the prefoldin complex to switch between its various functions. Understanding the involvement and regulation of prefoldin under both acute and chronic stress conditions requires further effort. Accumulating evidence suggests that specific prefoldin subunits have functions that are separate from the canonical complex. It is unclear how the balance between formation of the complex and functions of single subunits is regulated. Proteomics approaches that compare landscapes of prefoldin subunit interactions with each other could shed light on independent subunit functions. Pleiotropic positive and negative genetic interactions that are revealed in large-scale screens, mostly in yeast, suggest the existence of extended prefoldin interactors. More efforts should be made to determine whether prefoldin can fulfil its functions without its downstream chaperone TRiC/CCT. Other chaperones could also function together with prefoldin or direct the role of prefoldin under certain cellular conditions.

Finally, the prefoldin complex and its subunits appear to be promising for the discovery of biomarkers for human diseases, including various cancers. More basic research is needed to understand the cause of alterations of prefoldin regulation under pathological conditions to verify whether prefoldin can be a target for treating these diseases.

## AUTHOR CONTRIBUTIONS

IT, SSG, and UT wrote and edited the manuscript. IT and SSG prepared the figures and tables. All authors read and approved the final manuscript.

## FUNDING

This research was funded by the National Science Centre (Grant No. 2018/31/B/NZ1/02401).

## REFERENCES


Abe, A., Takahashi-Niki, K., Takekoshi, Y., Shimizu, T., Kitaura, H., Maita, H., et al. (2013). Prefoldin Plays a Role as a Clearance Factor in Preventing Proteasome Inhibitor-Induced Protein Aggregation. *J. Biol. Chem.* 288, 27764–27776. doi:10.1074/jbc.m113.476358

Aikawa, Y., Kida, H., Nishitani, Y., and Miki, K. (2015). Expression, Purification, Crystallization and X-ray Diffraction Studies of the Molecular Chaperone Prefoldin fromHomo Sapiens. *Acta Cryst. Sect F* 71, 1189–1193. doi:10.1107/s2053230x15013990

Amorim, A. F., Pinto, D., Kuras, L., and Fernandes, L. (2017). Absence of Gim Proteins, but Not GimC Complex, Alters Stress-Induced Transcription. *Biochim. Biophys. Acta (Bba) - Gene Regul. Mech.* 1860, 773–781. doi:10.1016/j.bbagrm.2017.04.005

Andréasson, C., Ott, M., and Büttner, S. (2019). Mitochondria Orchestrate Proteostatic and Metabolic Stress Responses. *EMBO Rep.* 20, e47865. doi:10.15252/embr.201947865

Arranz, R., Martín-Benito, J., and Valpuesta, J. M. (2018). Structure and Function of the Cochaperone Prefoldin. *Adv. Exp. Med. Biol.* 1106, 119–131. doi:10.1007/978-3-030-00737-9_9

Aseervatham, J. (2020). Cytoskeletal Remodeling in Cancer. *Biology (Basel)* 9. doi:10.3390/biology9110385

Balchin, D., Hayer-Hartl, M., and Hartl, F. U. (2016). *In Vivo* aspects of Protein Folding and Quality Control. *Science* 353, aac4354. doi:10.1126/science.aac4354

Banks, C. A. S., Miah, S., Adams, M. K., Eubanks, C. G., Thornton, J. L., Florens, L., et al. (2018). Differential HDAC1/2 Network Analysis Reveals a Role for Prefoldin/CCT in HDAC1/2 Complex Assembly. *Sci. Rep.* 8, 13712. doi:10.1038/s41598-018-32009-w

Blanco-Touriñán, N., Esteve-Bruna, D., and Serrano-Mislata, A., (2021). A Genetic Approach Reveals Different Modes of Action of Prefoldins. *Plant Physiol.* 187, 1534–1550.

Bogumil, D., Alvarez-Ponce, D., Landan, G., McInerney, J. O., and Dagan, T. (2014). Integration of Two Ancestral Chaperone Systems into One: the Evolution of Eukaryotic Molecular Chaperones in Light of Eukaryogenesis. *Mol. Biol. Evol.* 31, 410–418. doi:10.1093/molbev/mst212

Born, M., Quintanilla-Fend, L., Braselmann, H., Reich, U., Richter, M., Hutzler, P., et al. (2005). Simultaneous Over-expression of theHer2/neu andPTK6 Tyrosine Kinases in Archival Invasive Ductal Breast Carcinomas. *J. Pathol.* 205, 592–596. doi:10.1002/path.1720

Boudiaf-Benmammar, C., Cresteil, T., and Melki, R. (2013). The Cytosolic Chaperonin CCT/TRiC and Cancer Cell Proliferation. *PLoS One* 8, e60895. doi:10.1371/journal.pone.0060895

Bouziat, R., Hinterleitner, R., Brown, J. J., Stencel-Baerenwald, J. E., Ikizler, M., Mayassi, T., et al. (2017). Reovirus Infection Triggers Inflammatory Responses to Dietary Antigens and Development of Celiac Disease. *Science* 356, 44–50. doi:10.1126/science.aah5298

Broer, L., Ikram, M. A., Schuur, M., DeStefano, A. L., Bis, J. C., Liu, F., et al. (2011). Association of HSP70 and its Co-chaperones with Alzheimer's Disease. *Jad* 25, 93–102. doi:10.3233/jad-2011-101560

Cao, J. (2016). Analysis of the Prefoldin Gene Family in 14 Plant Species. *Front. Plant Sci.* 7, 317. doi:10.3389/fpls.2016.00317

Cao, S., Carlesso, G., Osipovich, A. B., Llanes, J., Lin, Q., Hoek, K. L., et al. (2008). Subunit 1 of the Prefoldin Chaperone Complex Is Required for Lymphocyte Development and Function. *J. Immunol.* 181, 476–484. doi:10.4049/jimmunol.181.1.476

Carlosama, C., Elzaiat, M., Patiño, L. C., Mateus, H. E., Veitia, R. A., and Laissue, P. (2017). A Homozygous Donor Splice-Site Mutation in the Meiotic Gene MSH4 Causes Primary Ovarian Insufficiency. *Hum. Mol. Genet.* 26, 3161–3166. doi:10.1093/hmg/ddx199

Chang, D. C., Piaggi, P., Hanson, R. L., Knowler, W. C., Bogardus, C., and Krakoff, J. (2017). Autoantibodies against PFDN2 Are Associated with an Increased Risk of Type 2 Diabetes: A Case-Control Study. *Diabetes Metab. Res. Rev.* 33. doi:10.1002/dmrr.2922

Chang, K., Yang, P., Lai, H., Yeh, T., Chen, T., and Yeh, C. (2006). Identification of a Novel Actin Isoform in Hepatocellular Carcinoma. *Hepatol. Res.* 36, 33–39. doi:10.1016/j.hepres.2006.05.003

Chaudhari, S. N., and Kipreos, E. T. (2018). The Energy Maintenance Theory of Aging: Maintaining Energy Metabolism to Allow Longevity. *Bioessays* 40, e1800005. doi:10.1002/bies.201800005

Chen, Y., Li, Y., Peng, Y., Zheng, X., Fan, S., Yi, Y., et al. (2018). ΔNp63α Down-Regulates C-Myc Modulator MM1 via E3 Ligase HERC3 in the Regulation of Cell Senescence. *Cell Death Differ* 25, 2118–2129. doi:10.1038/s41418-018-0132-5

Chesnel, F., Couturier, A., Alusse, A., Gagné, J.-P., Poirier, G. G., Jean, D., et al. (2020). The prefoldin complex stabilizes the von Hippel-Lindau protein against aggregation and degradation. *Plos Genet.* 16, e1009183. doi:10.1371/journal.pgen.1009183

Chintalapudi, S. R., and Jablonski, M. M. (2017). Systems Genetics Analysis to Identify the Genetic Modulation of a Glaucoma-Associated Gene. *Methods Mol. Biol.* 1488, 391–417. doi:10.1007/978-1-4939-6427-7_18

Collins, C., Volik, S., and Kowbel, D., (2001). Comprehensive Genome Sequence Analysis of a Breast Cancer Amplicon. *Genome Res.* 11, 1034–1042. doi:10.1101/gr.gr1743r

Comyn, S. A., Young, B. P., Loewen, C. J., and Mayor, T. (2016). Prefoldin Promotes Proteasomal Degradation of Cytosolic Proteins with Missense Mutations by Maintaining Substrate Solubility. *Plos Genet.* 12, e1006184. doi:10.1371/journal.pgen.1006184

Cooper, G. M. (2000). *The Cell: A Molecular Approach*. 2nd edition. Sunderland, Massachusetts: Sinauer Associates.

Costanzo, M., VanderSluis, B., Koch, E. N., Baryshnikova, A., Pons, C., Tan, G., et al. (2016). A Global Genetic Interaction Network Maps a Wiring Diagram of Cellular Function. *Science* 353. aaf1420. doi:10.1126/science.aaf1420

Dash, S., Aydin, Y., Widmer, K. E., and Nayak, L. (2020). Hepatocellular Carcinoma Mechanisms Associated with Chronic HCV Infection and the Impact of Direct-Acting Antiviral Treatment. *Jhc* Vol. 7, 45–76. doi:10.2147/jhc.s221187

Dehghan-Nayeri, N., Rezaei-Tavirani, M., Omrani, M. D., Gharehbaghian, A., Goudarzi Pour, K., and Eshghi, P. (2017). Identification of Potential Predictive Markers of Dexamethasone Resistance in Childhood Acute Lymphoblastic Leukemia. *J. Cel Commun. Signal.* 11, 137–145. doi:10.1007/s12079-016-0357-3

El-Serag, H. B. (2012). Epidemiology of Viral Hepatitis and Hepatocellular Carcinoma. *Gastroenterology* 142, 1264–1273. e1261. doi:10.1053/j.gastro.2011.12.061

Esteve-Bruna, D., Carrasco-López, C., Blanco-Touriñán, N., Iserte, J., Calleja-Cabrera, J., Perea-Resa, C., et al. (2020). Prefoldins Contribute to Maintaining the Levels of the Spliceosome LSM2-8 Complex through Hsp90 in Arabidopsis. *Nucleic Acids Res.* 48, 6280–6293. doi:10.1093/nar/gkaa354

Fandrich, M., Tito, M. A., Leroux, M. R., Rostom, A. A., Hartl, F. U., Dobson, C. M., et al. (2000). Observation of the Noncovalent Assembly and Disassembly Pathways of the Chaperone Complex MtGimC by Mass Spectrometry. *Proc. Natl. Acad. Sci.* 97, 14151–14155. doi:10.1073/pnas.240326597

Fang, Y., Wang, X., Yang, D., Lu, Y., Wei, G., Yu, W., et al. (2021). Relieving Cellular Energy Stress in Aging, Neurodegenerative, and Metabolic Diseases, SIRT1 as a Therapeutic and Promising Node. *Front. Aging Neurosci.* 13, 738686. doi:10.3389/fnagi.2021.738686

Farooq, M., Hozzein, W. N., Elsayed, E. A., Taha, N. A., and Wadaan, M. A. M. (2013). Identification of Histone Deacetylase 1 Protein Complexes in Liver Cancer Cells. *Asian Pac. J. Cancer Prev.* 14, 915–921. doi:10.7314/apjcp.2013.14.2.915

Feng, M.-Y., Wang, K., Shi, Q.-T., Yu, X.-W., and Geng, J.-S. (2009). Gene Expression Profiling in TWIST-Depleted Gastric Cancer Cells. *Anat. Rec.* 292, 262–270. doi:10.1002/ar.20802

Friesen, H., Humphries, C., Ho, Y., Schub, O., Colwill, K., and Andrews, B. (2006). Characterization of the Yeast Amphiphysins Rvs161p and Rvs167p Reveals Roles for the Rvs Heterodimer *In Vivo*. *MBoC* 17, 1306–1321. doi:10.1091/mbc.e05-06-0476

Fujioka, Y., Taira, T., Maeda, Y., Tanaka, S., Nishihara, H., Iguchi-Ariga, S. M. M., et al. (2001). MM-1, a C-Myc-Binding Protein, Is a Candidate for a Tumor Suppressor in Leukemia/lymphoma and Tongue Cancer. *J. Biol. Chem.* 276, 45137–45144. doi:10.1074/jbc.m106127200

Geissler, S., Siegers, K., and Schiebel, E. (1998). A Novel Protein Complex Promoting Formation of Functional Alpha - and Gamma -tubulin. *EMBO J.* 17, 952–966. doi:10.1093/emboj/17.4.952

Gestaut, D., Roh, S. H., Ma, B., Pintilie, G., Joachimiak, L. A., Leitner, A., et al. (2019). The Chaperonin TRiC/CCT Associates with Prefoldin through a Conserved Electrostatic Interface Essential for Cellular Proteostasis. *Cell* 177, 751–765. e715. doi:10.1016/j.cell.2019.03.012

Ghaffari, A., Shokuhfar, A., and Ghasemi, R. H. (2012). Capturing and Releasing a Nano Cargo by Prefoldin Nano Actuator. *Sensors Actuators B: Chem.* 171-172, 1199–1206. doi:10.1016/j.snb.2012.06.077

Giordano, M. O., Martínez, L. C., Isa, M. B., Ferreyra, L. J., Canna, F., Paván, J. V., et al. (2002). Twenty Year Study of the Occurrence of Reovirus Infection in Hospitalized Children with Acute Gastroenteritis in Argentina. *Pediatr. Infect. Dis. J.* 21, 880–882. doi:10.1097/00006454-200209000-00021

Glover, D. J., and Clark, D. S. (2015). Oligomeric Assembly Is Required for Chaperone Activity of the Filamentous γ-prefoldin. *FEBS J.* 282, 2985–2997. doi:10.1111/febs.13341

Goehring, A. S., Mitchell, D. A., Tong, A. H. Y., Keniry, M. E., Boone, C., and Sprague, G. F. (2003). Synthetic Lethal Analysis Implicates Ste20p, a P21-Activated Protein Kinase, in Polarisome Activation. *MBoC* 14, 1501–1516. doi:10.1091/mbc.e02-06-0348

Goldman, D. H., Kaiser, C. M., Milin, A., Righini, M., Tinoco, I., and Bustamante, C. (2015). Mechanical Force Releases Nascent Chain-Mediated Ribosome Arrest *In Vitro* and *In Vivo*. *Science* 348, 457–460. doi:10.1126/science.1261909

Guimarães, G. S., Latini, F. R., and Camacho, C. P. (2006). Identification of Candidates for Tumor-specific Alternative Splicing in the Thyroid. *Genes Chromosomes Cancer* 45, 540–553.

Guo, T., Zhang, D., Zeng, Y., Huang, T. Y., Xu, H., and Zhao, Y. (2020). Molecular and Cellular Mechanisms Underlying the Pathogenesis of Alzheimer's Disease. *Mol. Neurodegeneration* 15, 40. doi:10.1186/s13024-020-00391-7

Guo, Y., Chen, J.-x., Yang, S., Fu, X.-p., Zhang, Z., Chen, K.-h., et al. (2010). Selection of Reliable Reference Genes for Gene Expression Study in Nasopharyngeal Carcinoma. *Acta Pharmacol. Sin* 31, 1487–1494. doi:10.1038/aps.2010.115

Hagio, Y., Kimura, Y., Taira, T., Fujioka, Y., Iguchi-Ariga, S. M. M., and Ariga, H. (2006). Distinct Localizations and Repression Activities of MM-1 Isoforms toward C-Myc. *J. Cel. Biochem.* 97, 145–155. doi:10.1002/jcb.20619

Han, A., Li, J., Li, Y., Wang, Y., Bergholz, J., Zhang, Y., et al. (2016). p63α Modulates C-Myc Activity via Direct Interaction and Regulation of MM1 Protein Stability. *Oncotarget* 7, 44277–44287. doi:10.18632/oncotarget.10187

Hansen, W. J., Cowan, N. J., and Welch, W. J. (1999). Prefoldin-nascent Chain Complexes in the Folding of Cytoskeletal Proteins. *J. Cel Biol* 145, 265–277. doi:10.1083/jcb.145.2.265

Hartl, F. U., and Hayer-Hartl, M. (2002). Molecular Chaperones in the Cytosol: from Nascent Chain to Folded Protein. *Science* 295, 1852–1858. doi:10.1126/science.1068408

Hausman, D. M. (2019). What Is Cancer? *Perspect. Biol. Med.* 62, 778–784. doi:10.1353/pbm.2019.0046

Hennecke, S., Beck, J., Bornemann-Kolatzki, K., Neumann, S., Escobar, H. M., Nolte, I., et al. (2015). Prevalence of the Prefoldin Subunit 5 Gene Deletion in Canine Mammary Tumors. *PLoS One* 10, e0131280. doi:10.1371/journal.pone.0131280

Herranz-Montoya, I., Park, S., and Djouder, N. (2021). A Comprehensive Analysis of Prefoldins and Their Implication in Cancer. *iScience* 24, 103273. doi:10.1016/j.isci.2021.103273

Hirota, T., Takahashi, A., Kubo, M., Tsunoda, T., Tomita, K., Sakashita, M., et al. (2012). Genome-wide Association Study Identifies Eight New Susceptibility Loci for Atopic Dermatitis in the Japanese Population. *Nat. Genet.* 44, 1222–1226. doi:10.1038/ng.2438

Iijima, M., Kano, Y., Nohno, T., and Namba, M. (1996). Cloning of cDNA with Possible Transcription Factor Activity at the G1-S Phase Transition in Human Fibroblast Cell Lines. *Acta Med. Okayama* 50, 73–77. doi:10.18926/AMO/30489

Jackson, G. G., and Muldoon, R. L. (1973). Viruses Causing Common Respiratory Infection in Man. IV. Reoviruses and Adenoviruses. *J. Infect. Dis.* 128, 811–866. doi:10.1093/infdis/128.6.811

Jones, R. D., and Gardner, R. G. (2016). Protein Quality Control in the Nucleus. *Curr. Opin. Cel Biol.* 40, 81–89. doi:10.1016/j.ceb.2016.03.002

Kabir, M. A., Uddin, W., Narayanan, A., Reddy, P. K., Jairajpuri, M. A., Sherman, F., et al. (20112011). Functional Subunits of Eukaryotic Chaperonin CCT/TRiC in Protein Folding. *J. Amino Acids* 2011, 843206. doi:10.4061/2011/843206

Kadoyama, K., Matsuura, K., Takano, M., Maekura, K., Inoue, Y., and Matsuyama, S. (2019). Changes in the Expression of Prefoldin Subunit 5 Depending on Synaptic Plasticity in the Mouse hippocampus. *Neurosci. Lett.* 712, 134484. doi:10.1016/j.neulet.2019.134484

Kim, J. A., Choi, D. K., Min, J. S., Kang, I., Kim, J. C., Kim, S., et al. (2018). VBP 1 Represses Cancer Metastasis by Enhancing HIF -1α Degradation Induced by pVHL. *Febs j* 285, 115–126. doi:10.1111/febs.14322

Knowlton, J. J., Gestaut, D., Ma, B., Taylor, G., Seven, A. B., Leitner, A., et al. (2021). Structural and Functional Dissection of Reovirus Capsid Folding and Assembly by the Prefoldin-TRiC/CCT Chaperone Network. *Proc. Natl. Acad. Sci. U S A.* 118, e2018127118. doi:10.1073/pnas.2018127118

Krogan, N. J., Kim, M., Tong, A., Golshani, A., Cagney, G., Canadien, V., et al. (2003). Methylation of Histone H3 by Set2 in *Saccharomyces cerevisiae* Is Linked to Transcriptional Elongation by RNA Polymerase II. *Mol. Cel Biol* 23, 4207–4218. doi:10.1128/mcb.23.12.4207-4218.2003

Kumar, V., Rumaishaand Behl, A. (2020). Prefoldin Subunit 6 of Plasmodium Falciparum Binds Merozoite Surface Protein-1 (MSP-1). *FEBS Open Bio* 3. doi:10.1002/2211-5463.13022

Kwon, M., Rubio, G., Nolan, N., Auteri, P., Volmar, J. A., Adem, A., et al. (2021). FILIP1L Loss Is a Driver of Aggressive Mucinous Colorectal Adenocarcinoma and Mediates Cytokinesis Defects through PFDN1. *Cancer Res.* 81, 5523–5539. doi:10.1158/0008-5472.can-21-0897

Kwon, O. C., Lee, E.-J., Lee, J. Y., Youn, J., Kim, T.-H., Hong, S., et al. (2019). Prefoldin 5 and Anti-prefoldin 5 Antibodies as Biomarkers for Uveitis in Ankylosing Spondylitis. *Front. Immunol.* 10, 384. doi:10.3389/fimmu.2019.00384

Langbehn, D., Brinkman, R., Falush, D., Paulsen, J., and Hayden, M. (2004). A New Model for Prediction of the Age of Onset and Penetrance for Huntington's Disease Based on CAG Length. *Clin. Genet.* 65, 267–277. doi:10.1111/j.1399-0004.2004.00241.x

Langbehn, D. R., Stout, J. C., Gregory, S., Mills, J. A., Durr, A., Leavitt, B. R., et al. (2019). Association of CAG Repeats with Long-Term Progression in Huntington Disease. *JAMA Neurol.* 76, 1375–1385. doi:10.1001/jamaneurol.2019.2368

Lee, Y., Smith, R. S., Jordan, W., King, B. L., Won, J., Valpuesta, J. M., et al. (2011). Prefoldin 5 Is Required for normal Sensory and Neuronal Development in a Murine Model. *J. Biol. Chem.* 286, 726–736. doi:10.1074/jbc.m110.177352

Leroux, M. R., Fandrich, M., and Klunker, D. (1999). MtGimC, a Novel Archaeal Chaperone Related to the Eukaryotic Chaperonin Cofactor GimC/prefoldin. *EMBO J.* 18, 6730–6743. doi:10.1093/emboj/18.23.6730

Liang, J., Xia, L., Oyang, L., Lin, J., Tan, S., Yi, P., et al. (2020). The Functions and Mechanisms of Prefoldin Complex and Prefoldin-Subunits. *Cell Biosci* 10, 87. doi:10.1186/s13578-020-00446-8

Liu, H., Liu, X., Jin, H., Yang, F., Gu, W., and Li, X. (2013). Proteomic Analysis of Knock-Down HLA-G in Invasion of Human Trophoblast Cell Line JEG-3. *Int. J. Clin. Exp. Pathol.* 6, 2451–2459.

Locascio, A., Blázquez, M. A., and Alabadí, D. (2013). Dynamic Regulation of Cortical Microtubule Organization through Prefoldin-DELLA Interaction. *Curr. Biol.* 23, 804–809. doi:10.1016/j.cub.2013.03.053

López, V., González-Peramato, P., and Suela, J., (2013). Identification of Prefoldin Amplification (1q23.3-q24.1) in Bladder Cancer Using Comparative Genomic Hybridization (CGH) Arrays of Urinary DNA. *J. Transl Med.* 11, 182.

Loring, J. F., Wen, X., Lee, J. M., Seilhamer, J., and Somogyi, R. (2001). A Gene Expression Profile of Alzheimer's Disease. *DNA Cel Biol.* 20, 683–695. doi:10.1089/10445490152717541

Lundin, V. F., Srayko, M., Hyman, A. A., and Leroux, M. R. (2008). Efficient Chaperone-Mediated Tubulin Biogenesis Is Essential for Cell Division and Cell Migration in *C. elegans*. *Develop. Biol.* 313, 320–334. doi:10.1016/j.ydbio.2007.10.022

Ma, H.-C., Lin, T.-W., Li, H., Iguchi-Ariga, S. M. M., Ariga, H., Chuang, Y.-L., et al. (2008). Hepatitis C Virus ARFP/F Protein Interacts with Cellular MM-1 Protein and Enhances the Gene Trans-activation Activity of C-Myc. *J. Biomed. Sci.* 15, 417–425. doi:10.1007/s11373-008-9248-9

Mak, S. K., McCormack, A. L., Manning-Boğ, A. B., Cuervo, A. M., and Di Monte, D. A. (2010). Lysosomal Degradation of α-Synuclein *In Vivo*. *J. Biol. Chem.* 285, 13621–13629. doi:10.1074/jbc.m109.074617

Marracci, S., Martini, D., Giannaccini, M., Giudetti, G., Dente, L., and Andreazzoli, M. (2015). Comparative Expression Analysis of Pfdn6a and Tcp1? during

Xenopus Development. *Int. J. Dev. Biol.* 59, 235–240. doi:10.1387/ijdb.140275ma

Martin-Benito, J., Boskovic, J., and Gomez-Puertas, P., (2002). Structure of Eukaryotic Prefoldin and of its Complexes with Unfolded Actin and the Cytosolic Chaperonin CCT. *EMBO J.* 21, 6377–6386. doi:10.1093/emboj/cdf640

Millán-Zambrano, G., and Chávez, S. (2014). Nuclear Functions of Prefoldin. *Open Biol.* 4. doi:10.1098/rsob.140085

Millán-Zambrano, G., Rodríguez-Gil, A., Peñate, X., de Miguel-Jiménez, L., Morillo-Huesca, M., Krogan, N., et al. (2013). The Prefoldin Complex Regulates Chromatin Dynamics during Transcription Elongation. *Plos Genet.* 9, e1003776. doi:10.1371/journal.pgen.1003776

Ming Sun, S., Batté, A., Elmer, M., van der Horst, S. C., van Welsem, T., Bean, G., et al. (2020). A Genetic Interaction Map Centered on Cohesin Reveals Auxiliary Factors Involved in Sister Chromatid Cohesion in *S. cerevisiae*. *J. Cel Sci* 133. doi:10.1242/jcs.237628

Mitchell, L., Lambert, J.-P., Gerdes, M., Al-Madhoun, A. S., Skerjanc, I. S., Figeys, D., et al. (2008). Functional Dissection of the NuA4 Histone Acetyltransferase Reveals its Role as a Genetic Hub and that Eaf1 Is Essential for Complex Integrity. *Mol. Cel Biol* 28, 2244–2256. doi:10.1128/mcb.01653-07

Miyoshi, N., Ishii, H., Mimori, K., Nishida, N., Tokuoka, M., Akita, H., et al. (2010). Abnormal Expression of PFDN4 in Colorectal Cancer: a Novel Marker for Prognosis. *Ann. Surg. Oncol.* 17, 3030–3036. doi:10.1245/s10434-010-1138-5

Mori, K., Maeda, Y., Kitaura, H., Taira, T., Iguchi-Ariga, S. M. M., and Ariga, H. (1998). MM-1, a Novel C-Myc-Associating Protein that Represses Transcriptional Activity of C-Myc. *J. Biol. Chem.* 273, 29794–29800. doi:10.1074/jbc.273.45.29794

Mousnier, A., Kubat, N., Massias-Simon, A., Segeral, E., Rain, J.-C., Benarous, R., et al. (2007). von Hippel Lindau binding protein 1-mediated degradation of integrase affects HIV-1 gene expression at a postintegration step. *Proc. Natl. Acad. Sci.* 104, 13615–13620. doi:10.1073/pnas.0705162104

Nami, B., and Wang, Z. (2018). Genetics and Expression Profile of the Tubulin Gene Superfamily in Breast Cancer Subtypes and its Relation to Taxane Resistance, 10.274 doi:10.3390/cancers10080274*Cancers (Basel)*

Narita, R., Kitaura, H., Torii, A., Tashiro, E., Miyazawa, M., Ariga, H., et al. (2012). Rabring7 Degrades C-Myc through Complex Formation with MM-1. *PLoS One* 7, e41891. doi:10.1371/journal.pone.0041891

Ohtaki, A., Kida, H., Miyata, Y., Ide, N., Yonezawa, A., Arakawa, T., et al. (2008). Structure and Molecular Dynamics Simulation of Archaeal Prefoldin: the Molecular Mechanism for Binding and Recognition of Nonnative Substrate Proteins. *J. Mol. Biol.* 376, 1130–1141. doi:10.1016/j.jmb.2007.12.010

Olzscha, H., Schermann, S. M., Woerner, A. C., Pinkert, S., Hecht, M. H., Tartaglia, G. G., et al. (2011). Amyloid-like Aggregates Sequester Numerous Metastable Proteins with Essential Cellular Functions. *Cell* 144, 67–78. doi:10.1016/j.cell.2010.11.050

Palumbo, V., Pellacani, C., Heesom, K. J., Rogala, K. B., Deane, C. M., Mottier-Pavie, V., et al. (2015). Misato Controls Mitotic Microtubule Generation by Stabilizing the TCP-1 Tubulin Chaperone Complex. *Curr. Biol.* 25, 1777–1783. doi:10.1016/j.cub.2015.05.033

Pan, X., Reissman, S., Douglas, N. R., Huang, Z., Yuan, D. S., Wang, X., et al. (2010). Trivalent Arsenic Inhibits the Functions of Chaperonin Complex. *Genetics* 186, 725–734. doi:10.1534/genetics.110.117655

Patil, K. S., Basak, I., Pal, R., Ho, H.-P., Alves, G., Chang, E. J., et al. (2015). A Proteomics Approach to Investigate miR-153-3p and miR-205-5p Targets in Neuroblastoma Cells. *PLoS One* 10, e0143969. doi:10.1371/journal.pone.0143969

Payán-Bravo, L., Fontalva, S., and Peñate, X., (2021). Human Prefoldin Modulates Co-transcriptional Pre-mRNA Splicing. *Nucleic Acids Res.* 49, 6267–6280.

Peñate, X., Praena-Fernández, J.M, and Romero Pareja, P. (2020). Overexpression of Canonical Prefoldin Associates with the Risk of Mortality and Metastasis in Non-Small Cell Lung Cancer.*Cancers (Basel)*, 12 (4):1052. doi:10.3390/cancers12041052

Povarova, O. I., Uversky, V. N., Kuznetsova, I. M., and Turoverov, K. K. (2014). Actinous enigma or Enigmatic Actin. *Intrinsically Disordered Proteins* 2, e34500. doi:10.4161/idp.34500

Rain, J.-C., Cribier, A., Gérard, A., Emiliani, S., and Benarous, R. (2009). Yeast Two-Hybrid Detection of Integrase-Host Factor Interactions. *Methods* 47, 291–297. doi:10.1016/j.ymeth.2009.02.002

Riester, M., Werner, L., Bellmunt, J., Selvarajah, S., Guancial, E. A., Weir, B. A., et al. (2014). Integrative Analysis of 1q23.3 Copy-Number Gain in Metastatic Urothelial Carcinoma. *Clin. Cancer Res.* 20, 1873–1883. doi:10.1158/1078-0432.ccr-13-0759

Rothman, S. (2010). How Is the Balance between Protein Synthesis and Degradation Achieved? *Theor. Biol. Med. Model.* 7, 25. doi:10.1186/1742-4682-7-25

Russmann, F., Stemp, M. J., Monkemeyer, L., Etchells, S. A., Bracher, A., and Hartl, F. U. (2012). Folding of Large Multidomain Proteins by Partial Encapsulation in the Chaperonin TRiC/CCT. *Proc. Natl. Acad. Sci.* 109, 21208–21215. doi:10.1073/pnas.1218836109

Sacks, D., Sacks, D., Baxter, B., Campbell, B. C. V., Carpenter, J. S., Cognard, C., et al. (2018). Multisociety Consensus Quality Improvement Revised Consensus Statement for Endovascular Therapy of Acute Ischemic Stroke. *AJNR Am. J. Neuroradiol* 39, E61–E632. doi:10.3174/ajnr.A5638

Sahlan, M., Zako, T., and Yohda, M. (2018). Prefoldin, a Jellyfish-like Molecular Chaperone: Functional Cooperation with a Group II Chaperonin and beyond. *Biophys. Rev.* 10, 339–345. doi:10.1007/s12551-018-0400-0

Saibil, H. (2013). Chaperone Machines for Protein Folding, Unfolding and Disaggregation. *Nat. Rev. Mol. Cel Biol* 14, 630–642. doi:10.1038/nrm3658

Sakono, M., Zako, T., Ueda, H., Yohda, M., and Maeda, M. (2008). Formation of Highly Toxic Soluble Amyloid Beta Oligomers by the Molecular Chaperone Prefoldin. *FEBS J.* 275, 5982–5993. doi:10.1111/j.1742-4658.2008.06727.x

Santamaría, I., Alvarez-Hernández, D., and Jofré, R. (2005). Progression of Secondary Hyperparathyroidism Involves Deregulation of Genes Related to DNA and RNA Stability. *Kidney Int.* 67, 2267–2279. doi:10.1111/j.1523-1755.2005.00330

Satou, A., Taira, T., Iguchi-Ariga, S. M. M., and Ariga, H. (2001). A Novel Transrepression Pathway of C-Myc. *J. Biol. Chem.* 276, 46562–46567. doi:10.1074/jbc.m104937200

Shokuhfar, A., Ghaffari, A., and Ghasemi, R. H. (2012). Cavity Control of Prefoldin Nano Actuator (PNA) by Temperature and pH. *Nano-micro Lett.* 4, 110–117. doi:10.1007/bf03353701

Siegert, R., Leroux, M. R., Scheufler, C., Hartl, F. U., and Moarefi, I. (2000). Structure of the Molecular Chaperone Prefoldin. *Cell* 103, 621–632. doi:10.1016/s0092-8674(00)00165-3

Simons, C. T., Staes, A., Rommelaere, H., Ampe, C., Lewis, S. A., and Cowan, N. J. (2004). Selective Contribution of Eukaryotic Prefoldin Subunits to Actin and Tubulin Binding. *J. Biol. Chem.* 279, 4196–4203. doi:10.1074/jbc.m306053200

Small, J. V., Rottner, K., and Kaverina, I. (1999). Functional Design in the Actin Cytoskeleton. *Curr. Opin. Cel Biol.* 11, 54–60. doi:10.1016/s0955-0674(99)80007-6

Son, H. G., Seo, K., Seo, M., Park, S., Ham, S., An, S. W. A., et al. (2018). Prefoldin 6 Mediates Longevity Response from Heat Shock Factor 1 to FOXO in *C. elegans*. *Genes Dev.* 32, 1562–1575. doi:10.1101/gad.317362.118

Sörgjerd, K. M., Zako, T., Sakono, M., Stirling, P. C., Leroux, M. R., Saito, T., et al. (2013). Human Prefoldin Inhibits Amyloid-β (Aβ) Fibrillation and Contributes to Formation of Nontoxic Aβ Aggregates. *Biochemistry* 52, 3532–3542. doi:10.1021/bi301705c

Suraweera, A., Münch, C., Hanssum, A., and Bertolotti, A. (2012). Failure of Amino Acid Homeostasis Causes Cell Death Following Proteasome Inhibition. *Mol. Cel* 48, 242–253. doi:10.1016/j.molcel.2012.08.003

Takano, M., Tashiro, E., Kitamura, A., Maita, H., Iguchi-Ariga, S. M. M., Kinjo, M., et al. (2014). Prefoldin Prevents Aggregation of α-synuclein. *Brain Res.* 1542, 186–194. doi:10.1016/j.brainres.2013.10.034

Tang, B., Seredenina, T., Coppola, G., Kuhn, A., Geschwind, D. H., Luthi-Carter, R., et al. (2011). Gene Expression Profiling of R6/2 Transgenic Mice with Different CAG Repeat Lengths Reveals Genes Associated with Disease Onset and Progression in Huntington's Disease. *Neurobiol. Dis.* 42, 459–467. doi:10.1016/j.nbd.2011.02.008

Tang, D., Xu, C., Geng, H., Gao, Y., Cheng, H., Ni, X., et al. (2020). A Novel Homozygous Mutation in the Meiotic Gene MSH4 Leading to Male Infertility Due to Non-obstructive Azoospermia. *Am. J. Transl Res.* 12, 8185–8191.

Tao, Y., Han, Y., Yu, L., Wang, Q., Leng, S. X., and Zhang, H. (2020). The Predicted Key Molecules, Functions, and Pathways that Bridge Mild Cognitive Impairment (MCI) and Alzheimer's Disease (AD). *Front. Neurol.* 11, 233. doi:10.3389/fneur.2020.00233

Tashiro, E., Zako, T., Muto, H., Itoo, Y., Sörgjerd, K., Terada, N., et al. (2013). Prefoldin Protects Neuronal Cells from Polyglutamine Toxicity by Preventing Aggregation Formation. *J. Biol. Chem.* 288, 19958–19972. doi:10.1074/jbc.m113.477984

Thulasiraman, V., Yang, C. F., and Frydman, J. (1999). *In Vivo* newly Translated Polypeptides Are Sequestered in a Protected Folding Environment. *EMBO J.* 18, 85–95. doi:10.1093/emboj/18.1.85

Tong, A. H. Y., Lesage, G., Bader, G. D., Ding, H., Xu, H., Xin, X., et al. (2004). Global Mapping of the Yeast Genetic Interaction Network. *Science* 303, 808–813. doi:10.1126/science.1091317

Tsao, M.-L., Chao, C.-H., and Yeh, C.-T. (2006). Interaction of Hepatitis C Virus F Protein with Prefoldin 2 Perturbs Tubulin Cytoskeleton Organization. *Biochem. Biophysical Res. Commun.* 348, 271–277. doi:10.1016/j.bbrc.2006.07.062

Tsuchiya, H., Iseda, T., and Hino, O. (1996). Identification of a novel protein (VBP-1) binding to the von Hippel-Lindau (VHL) tumor suppressor gene product. *Cancer Res.* 56, 2881–2885.

Tsunoda, T., Koh, Y., Koizumi, F., Tsukiyama, S., Ueda, H., Taguchi, F., et al. (2003). Differential Gene Expression Profiles and Identification of the Genes Relevant to Clinicopathologic Factors in Colorectal Cancer Selected by cDNA Array Method in Combination with Principal Component Analysis. *Int. J. Oncol.* 23, 49–59. doi:10.3892/ijo.23.1.49

Tyler, K. L. (1998). Pathogenesis of Reovirus Infections of the central Nervous System. *Curr. Top. Microbiol. Immunol.* 233, 93–124. doi:10.1007/978-3-642-72095-6_6

Vainberg, I. E., Lewis, S. A., Rommelaere, H., Ampe, C., Vandekerckhove, J., Klein, H. L., et al. (1998). Prefoldin, a Chaperone that Delivers Unfolded Proteins to Cytosolic Chaperonin. *Cell* 93, 863–873. doi:10.1016/s0092-8674(00)81446-4

Vaquer-Alicea, J., and Diamond, M. I. (2019). Propagation of Protein Aggregation in Neurodegenerative Diseases. *Annu. Rev. Biochem.* 88, 785–810. doi:10.1146/annurev-biochem-061516-045049

Varshney, N., Kebede, A. A., Owusu-Dapaah, H., Lather, J., Kaushik, M., and Bhullar, J. S. (2017). A Review of Von Hippel-Lindau Syndrome. *jkcvhl* 4, 20–29. doi:10.15586/jkcvhl.2017.88

von Plehwe, U., Berndt, U., Conz, C., Chiabudini, M., Fitzke, E., Sickmann, A., et al. (2009). The Hsp70 Homolog Ssb Is Essential for Glucose Sensing via the SNF1 Kinase Network. *Genes Dev.* 23, 2102–2115. doi:10.1101/gad.529409

Wang, D., Shi, W., Tang, Y., Liu, Y., He, K., Hu, Y., et al. (2017). Prefoldin 1 Promotes EMT and Lung Cancer Progression by Suppressing Cyclin A Expression. *Oncogene* 36, 885–898. doi:10.1038/onc.2016.257

Wang, D., Zhu, Z.-Z., Jiang, H., Zhu, J., Cong, W.-M., Wen, B.-J., et al. (2015). Multiple Genes Identified as Targets for 20q13.12-13.33 Gain Contributing to Unfavorable Clinical Outcomes in Patients with Hepatocellular Carcinoma. *Hepatol. Int.* 9, 438–446. doi:10.1007/s12072-015-9642-0

Wang, P., Zhao, J., Yang, X., Guan, S., Feng, H., Han, D., et al. (2015). PFDN1, an Indicator for Colorectal Cancer Prognosis, Enhances Tumor Cell Proliferation and Motility through Cytoskeletal Reorganization. *Med. Oncol.* 32, 264. doi:10.1007/s12032-015-0710-z

Wang, Y., Meriin, A. B., Zaarur, N., Romanova, N. V., Chernoff, Y. O., Costello, C. E., et al. (2009). Abnormal Proteins Can Form Aggresome in Yeast: Aggresome-targeting Signals and Components of the Machinery. *FASEB j.* 23, 451–463. doi:10.1096/fj.08-117614

Watanabe, K.-i., Ozaki, T., Nakagawa, T., Miyazaki, K., Takahashi, M., Hosoda, M., et al. (2002). Physical Interaction of P73 with C-Myc and MM1, a C-Myc-Binding Protein, and Modulation of the P73 Function. *J. Biol. Chem.* 277, 15113–15123. doi:10.1074/jbc.m111281200

Webster, J. M., Darling, A. L., Uversky, V. N., and Blair, L. J. (2019). Small Heat Shock Proteins, Big Impact on Protein Aggregation in Neurodegenerative Disease. *Front. Pharmacol.* 10, 1047. doi:10.3389/fphar.2019.01047

Whitehead, T. A., Boonyaratanakornkit, B. B., Hollrigl, V., and Clark, D. S. (2007). A Filamentous Molecular Chaperone of the Prefoldin Family from the Deep-Sea Hyperthermophile Methanocaldococcus Jannaschii. *Protein Sci.* 16, 626–634. doi:10.1110/ps.062599907

Xu, Y., and Her, C. (2013). VBP1 Facilitates Proteasome and Autophagy-mediated Degradation of MutS Homologue hMSH4. *FASEB j.* 27, 4799–4810. doi:10.1096/fj.13-235127

Yam, A. Y., Xia, Y., Lin, H.-T. J., Burlingame, A., Gerstein, M., and Frydman, J. (2008). Defining the TRiC/CCT Interactome Links Chaperonin Function to Stabilization of Newly Made Proteins with Complex Topologies. *Nat. Struct. Mol. Biol.* 15, 1255–1262. doi:10.1038/nsmb.1515

Yamane, T., Shimizu, T., Takahashi-Niki, K., Takekoshi, Y., Iguchi-Ariga, S. M. M., and Ariga, H. (2015). Deficiency of Spermatogenesis and Reduced Expression of Spermatogenesis-Related Genes in Prefoldin 5-mutant Mice. *Biochem. Biophys. Rep.* 1, 52–61. doi:10.1016/j.bbrep.2015.03.005

Yesseyeva, G., Aikemu, B., Hong, H., Yu, C., Dong, F., Sun, J., et al. (2020). Prefoldin Subunits (PFDN1-6) Serve as Poor Prognostic Markers in Gastric Cancer. *Biosci. Rep.* 40. doi:10.1042/BSR20192712

Yoshida, T., Kitaura, H., Hagio, Y., Sato, T., Iguchi-Ariga, S. M. M., and Ariga, H. (2008). Negative Regulation of the Wnt Signal by MM-1 through Inhibiting Expression of the Wnt4 Gene. *Exp. Cel Res.* 314, 1217–1228. doi:10.1016/j.yexcr.2008.01.002

Zhang, J., Han, Q., Song, Y., Chen, Q., and Xia, X. (2015). Analysis of Subcellular Prefoldin 1 Redistribution during Rabies Virus Infection. *Jundishapur J. Microbiol.* 8, e24757. doi:10.5812/jjm.24757v2

Zhang, J., Xie, M., Li, M., Ding, J., Pu, Y., Bryan, A. C., et al. (2020). Overexpression of a Prefoldin β Subunit Gene Reduces Biomass Recalcitrance in the Bioenergy Crop Populus. *Plant Biotechnol. J.* 18, 859–871. doi:10.1111/pbi.13254

Zhang, W., Yu, L., Ji, T., and Wang, C. (2020). Tumor Microenvironment-Responsive Peptide-Based Supramolecular Drug Delivery System. *Front. Chem.* 8, 549. doi:10.3389/fchem.2020.00549

Zhang, Y., Rai, M., Wang, C., Gonzalez, C., and Wang, H. (2016). Prefoldin and Pins Synergistically Regulate Asymmetric Division and Suppress Dedifferentiation. *Sci. Rep.* 6, 23735. doi:10.1038/srep23735

Zhou, C., Guo, Z., Xu, L., Jiang, H., Sun, P., Zhu, X., et al. (2020). PFND1 Predicts Poor Prognosis of Gastric Cancer and Promotes Cell Metastasis by Activating the Wnt/β-Catenin Pathway. *Ott* 13, 3177–3186. doi:10.2147/ott.s236929

**Conflict of Interest:** The authors declare that the research was conducted in the absence of any commercial or financial relationships that could be construed as a potential conflict of interest.

**Publisher's Note:** All claims expressed in this article are solely those of the authors and do not necessarily represent those of their affiliated organizations, or those of the publisher, the editors, and the reviewers. Any product that may be evaluated in this article, or claim that may be made by its manufacturer, is not guaranteed or endorsed by the publisher.

frontiers | Frontiers in Cell and Developmental Biology

REVIEW
published: 05 May 2022
doi: 10.3389/fcell.2022.906530

# The TRiCky Business of Protein Folding in Health and Disease

*Heba Ghozlan*[1,2], *Amanda Cox*[1], *Daniel Nierenberg*[1], *Stephen King*[3] *and Annette R. Khaled*[1]*

[1]*Division of Cancer Research, Burnett School of Biomedical Sciences, College of Medicine, University of Central Florida, Orlando, FL, United States,* [2]*Department of Physiology and Biochemistry, Jordan University of Science and Technology, Irbid, Jordan,* [3]*Division of Neuroscience, Burnett School of Biomedical Sciences, College of Medicine, University of Central Florida, Orlando, FL, United States*

Maintenance of the cellular proteome or proteostasis is an essential process that when deregulated leads to diseases like neurological disorders and cancer. Central to proteostasis are the molecular chaperones that fold proteins into functional 3-dimensional (3D) shapes and prevent protein aggregation. Chaperonins, a family of chaperones found in all lineages of organisms, are efficient machines that fold proteins within central cavities. The eukaryotic Chaperonin Containing TCP1 (CCT), also known as Tailless complex polypeptide 1 (TCP-1) Ring Complex (TRiC), is a multi-subunit molecular complex that folds the obligate substrates, actin, and tubulin. But more than folding cytoskeletal proteins, CCT differs from most chaperones in its ability to fold proteins larger than its central folding chamber and in a sequential manner that enables it to tackle proteins with complex topologies or very large proteins and complexes. Unique features of CCT include an asymmetry of charges and ATP affinities across the eight subunits that form the hetero-oligomeric complex. Variable substrate binding capacities endow CCT with a plasticity that developed as the chaperonin evolved with eukaryotes and acquired functional capacity in the densely packed intracellular environment. Given the decades of discovery on the structure and function of CCT, much remains unknown such as the scope of its interactome. New findings on the role of CCT in disease, and potential for diagnostic and therapeutic uses, heighten the need to better understand the function of this essential molecular chaperone. Clues as to how CCT causes cancer or neurological disorders lie in the early studies of the chaperonin that form a foundational knowledgebase. In this review, we span the decades of CCT discoveries to provide critical context to the continued research on the diverse capacities in health and disease of this essential protein-folding complex.

**Keywords: cytoskeleton, cell cycle, cancer, neurological disorder, chaperonin, proteostasis**

OPEN ACCESS

***Edited by:***
*Silvia Masciarelli,*
*Sapienza University of Rome, Italy*

***Reviewed by:***
*Jorge Cuéllar,*
*National Center for Biotechnology (CSIC), Spain*
*Andrew Truman,*
*University of North Carolina at Charlotte, United States*

***Correspondence:**
*Annette R. Khaled*
*annette.khaled@ucf.edu*

***Specialty section:***
*This article was submitted to Signaling, a section of the journal Frontiers in Cell and Developmental Biology*

***Received:*** *28 March 2022*
***Accepted:*** *20 April 2022*
***Published:*** *05 May 2022*

***Citation:***
*Ghozlan H, Cox A, Nierenberg D, King S and Khaled AR (2022) The TRiCky Business of Protein Folding in Health and Disease. Front. Cell Dev. Biol. 10:906530. doi: 10.3389/fcell.2022.906530*

## INTRODUCTION

Keeping proteins in the correct shape and properly folded depends on balanced protein homeostasis that is essential for the growth and survival of cells. Failure of the quality control mechanisms that maintain the cellular proteome and regulate the synthesis, folding, trafficking, and degradation of proteins is a hallmark of disease. Neurodegenerative disorders may be a consequence of proteostasis deficiency, while cancer could result from enhanced proteostasis capacity (Powers et al., 2009). Key structural studies of molecular chaperones in the 1990s (Marco et al., 1993) revealed these as essential components of the network governing protein homeostasis. Though *in vitro* studies revealed much

on the basic principles of protein folding, how proteins fold in the crowded *in vivo* cellular environment remains to be fully understood. Most small proteins spontaneously fold (Anfinsen, 1973), while large proteins that represent the majority of a cellular proteome depend on molecular chaperones to reach their native state (Bartlett and Radford, 2009).

Chaperome refers to the collective cellular folding machinery that includes chaperone, co-chaperone, and chaperonin (Wang et al., 2006). Often chaperones are activated by stress; for example, heat shock proteins (HSPs) are chaperones first described in response to heat shock (Lindquist and Craig, 1988). Major chaperone classes are categorized by their molecular weight, like HSP40, HSP70, or HSP90, and have functions, such as *de novo* protein folding, that support proteostasis (Hartl et al., 2011). Chaperonins are multi-component complexes [~800–900 kilodalton (kDa)] that couple protein folding with adenosine 5′-triphosphate (ATP) hydrolysis or partner with co-factors like small HSPs and also prevent protein aggregation. Two major groups of chaperonins, group I and group II, are found in all lineages of organisms (bacteria, archaea, eukaryotes). The best studied group I chaperonin is GroEL-Gro-ES found in *Escherichia coli* (*E. coli*). The group II chaperonins include the archetypal *Thermoplasma acidophilim* α/β-thermosome and *Methanococcus maripaludis* chaperonin (Mm-Cpn) and the eukaryotic chaperonin, CCT, also known as TRiC. CCT, as is referred to herein, is a hetero-oligomeric chaperonin with a cylindrical structure composed of two stacked rings of eight subunits. While initial studies suggested that CCT folds 9–15% of the cellular proteome (Thulasiraman et al., 1999), other studies report that 7% or as little as 1% of the proteins in cells are CCT substrates (Yam et al., 2008; Willison, 2018). Indicative of its importance, deregulation of CCT is observed in cancer (Boudiaf-Benmammar et al., 2013; Roh et al., 2015; Vallin and Grantham, 2019), infectious diseases (Inoue et al., 2011; Bugnon Valdano et al., 2021) and neurodegenerative disorders (Pavel et al., 2016; Sot et al., 2017; Chen, 2019), suggesting a central role in the pathogenesis of these conditions. The early decades of CCT discoveries were focused on understanding CCT function, expression, and evolution. Obligate substrates, like actin and tubulin, were reported to interact with CCT along with a few non-cytoskeletal proteins. In the last decade, however, advances in proteomics and investigations into the role of CCT in disease prompted the discovery of new substrates and new activities. In this review, we will bridge discoveries from different eras to better understand the role of CCT in health and disease, addressing how CCT is formed and regulated, and in turn, modulates cellular processes through its distinctive structure and function.

## The Evolution of Chaperonin Containing TCP1 in the Crowded Cellular Environment

### The Structure of Chaperonin Containing TCP1 and Subunit Arrangement

CCT is a multi-oligomeric, double torus complex composed of eight subunits, termed CCT1-8 (yeast) or CCTα-θ (mammals) (Rommelaere et al., 1993; Kubota et al., 1994) (**Figure 1A**). Evolution of the eukaryotic chaperonin is the result of gene duplication and gene loss events that remain ongoing processes. The eight paralogous CCT subunits share high amino acid similarity (27–39% sequence identity) (Archibald et al., 2001), whereas CCT orthologues are conserved across species. Phylogenetic analysis suggested that different CCT subunit genes resulted from duplication events that happened early in the evolution of eukaryotes, then independently diverged to have a unique function that is maintained in most eukaryotes. CCTδ (CCT4), CCTε (CCT5), CCTα (TCP-1/CCT1), CCTβ (CCT2), and CCTη (CCT7) are the most recent results of gene duplication events (Kubota et al., 1994; Archibald et al., 2000; Archibald et al., 2001; Fares and Wolfe, 2003). CCT polypeptides vary in length from 531 to 556 residues, and in molecular weights from 52 to 65 kDa (Kubota et al., 1994). The ATP-binding domain is the most conserved across CCT subunits, while the substrate-binding domain varies across subunits (Kim et al., 1994; Kubota et al., 1994; Archibald et al., 2000).

Each CCT subunit assembles in a precise ring arrangement to form a cylindrical barrel with an enclosed chamber that supports a hydrophobic environment where substrate folding takes place. Each CCT subunit has three different domains: an apical domain that encloses the chamber and forms the substrate-binding site, an equatorial domain that forms the wall of the folding chamber, is involved in ring-ring interactions, and contains the ATP binding site, and an intermediate domain that connects the apical and equatorial domains (**Figure 1B**). Reports using a combination of methods (chemical cross-linking, mass spectrometry, and combinatorial modeling) revealed that CCT subunits are arranged in the ring in the following order: CCT4-2-5-7-8-6-3-1 (Leitner et al., 2012). The double ring complex displays a two-fold symmetry in which subunits CCT2 and CCT6 form a homotypic interface while the other subunits contact points on the heterotypic form (**Figure 1C**) (Leitner et al., 2012). The N-and C-termini of CCT subunits are buried inside the barrel to form a septum between the two chambers (Dekker et al., 2011b; Kalisman et al., 2013), with the exception of the N-terminus of CCT4 that protrudes towards the outside of the complex. This structural arrangement is evolutionally conserved as CCT4 is the only subunit with a conserved proline residue in the outward pointing N-terminus. The inner walls of the CCT folding chamber are hydrophilic, with a bipolar surface-charge distribution that is conserved as well, with the CCT5-2-4 side being positively charged while the CCT3-6-8 side is negatively charged (Leitner et al., 2012). The asymmetry of charge is among the features of CCT that may have evolved to provide specific solutions to the folding of proteins with complex topologies and assembly of large multi-protein structures.

### The Assembly, Disassembly, and Degradation of Chaperonin Containing TCP1

The specific order of subunit assembly could be critical in achieving the desired function of a multi-component complex. An example is the Biedel Bradet Syndrome (BBS) subunits forming the BBSsome that is involved in ciliary membrane biogenesis. Assembly of BBS some is dictated by specific protein-protein interactions involving CCT subunits, and

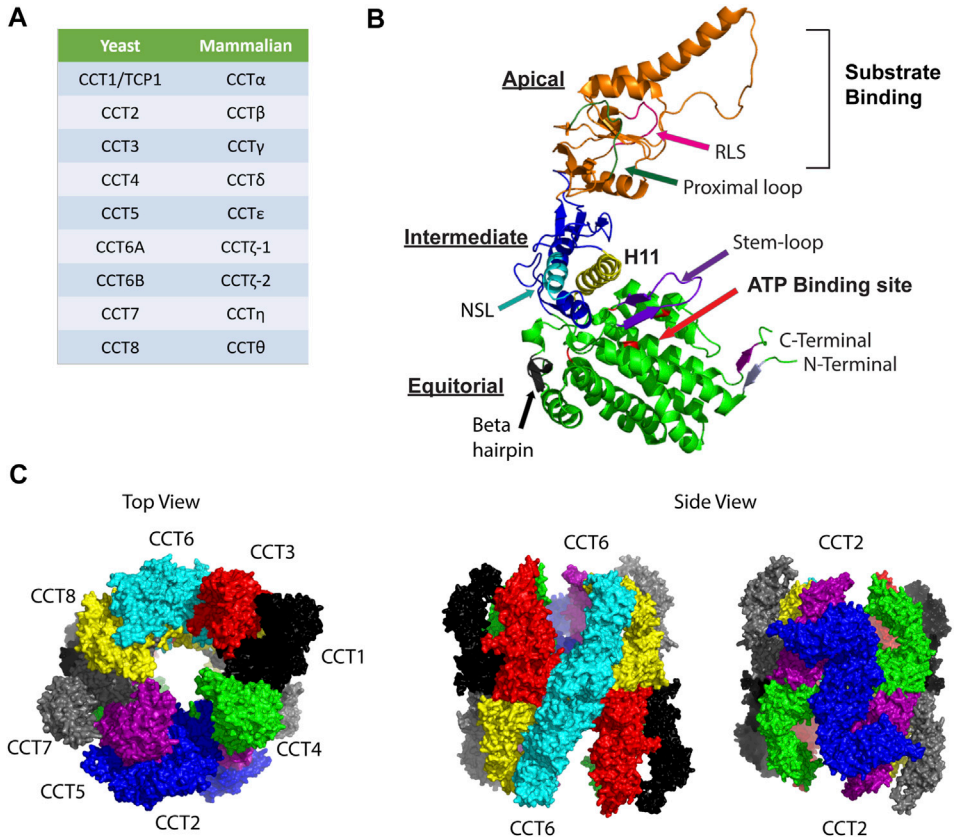


**FIGURE 1 |** Organization of the CCT complex. **(A)** Nomenclature for CCT subunits based on yeast and mammalian studies. **(B)** Model for structure of a CCT subunit with the major structural elements indicated in the apical, intermediate, and equatorial domains. NSL, nucleotide sensing loop; RSL: release loop for substrate. The model was made based on PDB:3KTT [atomic model of bovine CCT2 (Cong et al., 2010)]. **(C)** Ring structure organization of CCT subunits is shown based on PDB 5GW4 [Structure of Yeast NPP-TRiC (Zang et al., 2016)]. Top view shows the open ring conformation with subunits indicated as follows: CCT1 (black), CCT2 (blue), CCT3 (red), CCT4 (green), CCT5 (purple), CCT6 (cyan), CCT7 (grey), and CCT8 (yellow). Side views highlight the homotypic interactions between CCT2-CCT2 (blue) and CCT6-CCT6 (cyan).

regulation could be at the level of the BBS-chaperonin complex formation (Zhang et al., 2012). Whether CCT assembles in a similar manner is unknown. Early studies involving the purification of CCT from yeast (Dekker et al., 2011a), bovine tissue (Ferreyra and Frydman, 2000), or mouse testes (Knee et al., 2013) advanced understanding of the structure and function of the chaperonin but provided few insights on assembly of the complex. The presence of CCT micro-complexes, ranging from 120 to 250 kDa, were detected in cells along with the intact hetero-oligomer, but were minor species and their importance was unclear (Liou and Willison, 1997). Subsequently, single CCT subunits were expressed in *E. coli* and sedimentation of CCT subunits by a sucrose gradient revealed that two of the CCT subunit proteins, CCT4 and CCT5, formed functional homo-oligomeric rings, while other subunits, CCT2, CCT3, CCT7, and CCT8, were observed as slowly sedimenting species suggestive of monomers, and CCT1 was bound to the ribosome (Sergeeva et al., 2013). Data from structural studies showing that CCT complexes usually contained all eight subunits, even when reconstituted from eight plasmids (Machida et al., 2012), indicated that CCT4 and CCT5 homo-oligomers may not have activities similar to hetero-oligomer, but could have intermediate functions, for example in the assembly process.

Expression data from early studies of CCT suggested that there was equal stoichiometry of CCT at the mRNA and protein level (Rommelaere et al., 1993; Kubota et al., 1999b). However, a body of evidence later suggested that some CCT subunits could be overexpressed under certain conditions, such as cancer cell proliferation (Boudiaf-Benmammar et al., 2013) or cell cycling (Yokota et al., 2001b). Hence, it is possible that transient populations of CCT-complexes composed of select subunits could exist. CCT4 and CCT5 subunits formed functional homo-oligomers in *E. coli* (Sergeeva et al., 2013), and CCT5 homo-oligomers had a similar structure as the hetero-oligomeric CCT complex (Pereira et al., 2017). The existence of monomeric CCT subunits in cells was reported in multiple studies, and these subunits may interact with other proteins. Hence, monomeric CCT subunits could incorporate into CCT4 or CCT5 homo-oligomers as an initiating step of complex assembly. This was tested in an *E. coli* model system in which CCT subunits were individually expressed with either CCT4 or CCT5 homo-oligomers to determine which CCT subunits were

more likely to hetero-oligomerize with CCT4 or CCT5-based complexes (Sergeeva et al., 2019). With the exemption of CCT6, all CCT subunits were present in complexes when co-expressed with the CCT5 homo-oligomer, while the CCT4 homo-oligomer was the least effective in complex interactions, binding only CCT5 and CCT8. Based on these subunit-subunit interactions, sedimentation patterns, and previous structural data, a model for CCT complex assembly was proposed starting from the CCT5 homo-oligomer as a template or intermediate form. CCT subunits assemble onto the CCT5 homo-oligomeric ring in the order of CCT2 first, followed by CCT4, CCT1, CCT3, CCT7, CCT8, and lastly CCT6 (Sergeeva et al., 2019). This idea is supported by mass spectrometry analysis of human CCT purified from insect cells, in which CCT5 was the most stable subunit observed under chemical destabilization conditions, hence, the most likely to self-assemble or co-assemble with other subunits. Importantly, CCT5 formed dimers with all subunits except for CCT8 (Collier et al., 2021). However, since CCT subunits are independently transcribed in the crowded cellular environment, bringing together all the subunits for assembly could be challenging. Post-translational modifications (PTMs) that sequester CCT subunits in subcellular compartments would be a solution. S-palmitoylation is a PTM in which palmitic acid is attached to cysteines of proteins through a thioester bond, resulting in increased local hydrophobicity that drives associations with membranes and well as protein-protein interactions. Interestingly, most of the CCT subunits were found to be S-palmitoylated, with S-palmitoylation of CCT1, CCT2, CCT3, CCT4, and CCT5 experimentally proven (Blanc et al., 2015). Since S-palmitoylation is dynamic and reversible, it is intriguing to speculate that this PTM may help localize CCT subunits to membranes, like the endoplasmic reticulum, and facilitate the ordered assembly of CCT subunits onto a CCT5 template to form the hetero-oligomeric complex (Sergeeva et al., 2019).

Disassembly and degradation of the CCT complex are processes less well understood than assembly. Early studies performing *in vitro* translation reactions for the eight CCT subunits suggested that ring disassembly may not be a global process but rather occurs in one ring at a time during each protein-folding cycle to yield micro-complexes and monomers (Liou et al., 1998). Kinetics of the process further suggested that in the absence of a pre-existing template, assembly of the CCT complex would be too slow. Hence, a semiconservative model based on the disassembly of a single ring is likely to be thermodynamically favorable (Liou et al., 1998). Dissociation of CCT complexes into smaller micro-complexes and monomers was also observed under conditions of physiological levels of potassium (K+) and ATP (Roobol et al., 1999a). Implications are that CCT turnover may actively occur during the ATP-driven folding cycle. Performing immunoprecipitation of CCT using the neuroblastoma/rat dorsal ganglion hybrid cell line (ND7/23) revealed that ATP/K+ caused precipitation of monomeric CCT subunits, while CCT precipitated as the intact hetero-oligomeric complex in the absence of ATP. Interestingly, the addition of the non-hydrolyzable ATP analog, AMP-PNP, was not effective in precipitating free CCT subunits; therefore, ATP hydrolysis was important for the observed effect of subunit dissociation. The disassembly of subunits from the CCT complex occurred most readily with CCT2 and CCT8, followed by CCT1, CCT4, CCT6, and CCT5, with CCT3 being last. Homology analysis revealed that the length of the loop connecting the equatorial and intermediate domain for each CCT subunit correlated with the CCT precipitation profile in the presence of ATP. The longest loops were found in CCT3 and the shortest in CCT2 (Roobol et al., 1999a), which could control how CCT subunits exit the chaperonin complex. N-terminal modifications may also affect the formation of the CCT complex since the N-termini of subunit apical domains mediate inter-ring cooperativity. Truncation of N-termini through methionine loss or acetylation could lead to degradation of CCT subunits (Collier et al., 2021). Evident from these experiments is that assembly/disassembly of the CCT complex may be linked to the monomer/oligomer pool in a dynamic process that ultimately controls protein folding activity and critical cell functions.

Pulse-chase experiments with mammary carcinoma FM3A cells revealed that turnover rates of individual CCT subunits varied significantly, with CCT4 having the shortest half-life (~4 h) and CCT2 the longest half-life (~8 h) (Yokota et al., 2001b). A systematic analysis of protein half-lives in MCF-7 breast cancer cells found, in contrast, that CCT4 had the longest half-life (~10.6 h), followed by CCT8, CCT7 and CCT2, with half-lives between 7–8 h, and CCT5 and CCT3 with the shortest half-lives of 4.6 and 2.5 h, respectively (Tong et al., 2020). Such results suggest that, in addition to ATP hydrolysis controlling disassembly of the complex, variable turnover rates of CCT subunits could be cell type specific, limiting subunit availability and formation of the active chaperonin. Degradation of the CCT complex through the ubiquitin-proteasome system was shown using the proteasome inhibitor, lactacystin, as well as with temperature-sensitive mutations in the ubiquitin-activating enzyme E1 (Yokota et al., 2000a). CCT5 also associated with the 26S proteasome (Tokumoto et al., 2000). In MCF-7 cells treated with the proteasome inhibitor, bortezomib, the half-lives of CCT subunits doubled, with some, like CCT4, reaching a half-live of almost 20 h (Tong et al., 2020). Another quality control mechanism that could be triggered by CCT with unfolded actin is autophagy, a system for degradation and re-utilization of intracellular contents. Using a CCT1/TCP-1-RFP-GFP fusion protein as a readout, where GFP is pH sensitive, the degradation of CCT in lysosomes during autophagy was observed when actin dynamics were perturbed. While the mechanisms regulating the autophagic degradation of CCT remain to be determined, a link between CCT, actin homeostasis, and autophagy is possible and could be triggered by conditions that occur, for example, during cell cycle arrest (Date et al., 2022).

## The Chaperonin Containing TCP1 ATPase Cycle

In most chaperonins, ATP binding and hydrolysis are linked to substrate folding in an ordered process; however, in CCT the mechanism is more complex. Unlike Gro-EL in which the co-factor, Gro-ES, functions as a detachable lid, group II chaperonins have a built-in lid formed by protrusions in the apical domains of

each subunit. Subunit equatorial domains bind ATP through a conserved phosphate-binding or P-loop motif, while ATP hydrolysis is triggered by a catalytic aspartic acid residue located in the subunit intermediate domains. CCT can be in a lid open state, when substrate binding sites are accessible, or a lid closed state where the apical segments of the lid come together to form a beta-stranded iris (Llorca et al., 1999b; Gutsche et al., 2000; Cong et al., 2012; Zang et al., 2016). The transition between the open and closed states of CCT is referred to as the ATPase cycle. Insights on the chaperonin ATPase cycle first came from studies of Mm-Cpn that were later confirmed for CCT. In the nucleotide-free state, CCT is open, with subunit apical domains in different conformations. ATP binding alone is not enough to induce the closed state but does promote changes in the apical domains that generate a more compact open conformation called a tetramer of dimers that creates a pseudo four-fold symmetry first described in bovine CCT (Cong et al., 2012). Upon hydrolysis of ATP, triggered by the catalytic aspartic acid residue, a conformational change in the apical domains leads to closing of the lid and movement of the substrate into the central chamber where folding occurs. Subsequent release of phosphate and ADP end the cycle, re-opening the chamber to release substrate (Gestaut et al., 2019a).

High-resolution cryogenic electron microscopy (cryo-EM) revealed the structure of CCT in different states of nucleotide occupancy during the ATPase cycle. CCT structures reported in the decade between 1999–2010, using nucleotide analogs, showed possible models for arrangements of the eight subunits in a ring, with or without substrates (Llorca et al., 1999b; Llorca et al., 2001; Booth et al., 2008; Cong et al., 2010). But it was single particle cryo-EM studies of bovine CCT in the apo (nucleotide-free), ATP-bound, ADP-bound, and ATP-hydrolysis transition states that revealed mechanisms distinct from other group I or II chaperonins (Cong et al., 2012). The apical domains of CCT subunits in the apo, ATP- and ADP-bound states extended towards the central folding chamber at different angles but tilted upwards and open in the ATP-bound state, re-affirming that ATP binding did not close the lid. Moreover, in the open states, contacts between the apical domains created the open and more compact configuration termed the tetramer of dimers. The structure of CCT in these three states suggested that the ADP-bound state could be the substrate acceptor state. Some structures from the ATP transition states were of a hybrid or asymmetric conformation in which the *cis* ring was closed and the *trans* ring was open, suggestive of negative cooperativity and that CCT functioned like a two-stroke motor (Reissmann et al., 2007; Cong et al., 2012). However, recent cryo-EM structures of yeast CCT noted the synchronous hydrolysis of ATP that was indicative of positive inter-ring cooperativity in which both rings were closed (Jin et al., 2019), suggesting that nucleotide binding in both rings followed the same order.

Unlike the archaeal chaperonins, the ATPase cycle in CCT is highly asymmetric. Genetic studies and biochemical studies showed that CCT subunits have different ATP affinities—with four to five subunits strongly binding ATP (Reissmann et al., 2012; Zang et al., 2016). Hence a gradient of ATP affinities exists, with CCT5 and CCT4 having the highest affinities, followed by CCT2 and CCT1. The remaining subunits, especially CCT3, CCT6, and CCT8, have a low affinity for ATP. Using yeast as a model system to evaluate mutations introduced into the CCT subunits, mutations in the P-loop or the catalytic aspartic acid of the high ATP-affinity subunits (CCT7, 5, 4, 2) caused loss of growth. In contrast, the same mutations introduced into the low ATP affinity subunits (CCT8, 6, 3) did not cause loss of growth (Amit et al., 2010; Reissmann et al., 2012), with further work showing that these subunits may have very slow ADP off-rates (Zang et al., 2016). This suggests the existence of a staggered ATP-binding mechanism, which was shown by cryo-EM using single subunit eGFP tags. The subunits on the CCT2 side of the complex might initiate ATP binding, while the subunits on the CCT6 side might bind ATP later due to the delayed release of ADP (Zang et al., 2016) (**Figure 2**). Importantly, these studies indicate that the ATPase cycle of CCT is responsive to the concentration of ATP. Kinetics-based calculations inferred that the ATPase reaction in CCT reaches a plateau at 0.2 mM ATP with most subunits binding nucleotides (Shimon et al., 2008). It follows that at lower concentrations of ATP not all subunits will bind nucleotides. Resolution of the structure of yeast CCT at low concentrations of ATP (near cell starvation levels), revealed that CCT7, followed by CCT2, first reacted to nucleotide binding and may initiate ring closure, while the other subunits bound ATP as levels increased. CCT4 was the last subunit to bind ATP and could be an ATP sensor, triggering ATP hydrolysis only when the ATP concentration reaches cell sustainable levels (**Figure 2**). This is supported by previous studies showing the presence of a dynamic β-hairpin motif in the nucleotide-binding site of CCT4 (Zang et al., 2016) and the fact that loss of the ATP hydrolysis activity in CCT4 was lethal in yeast (Amit et al., 2010). CCT8 was also unique in that it remained bound to ADP longer than other subunits and may have a role independent of ATP hydrolysis, through its N-terminus, in CCT allosteric cooperativity (Jin et al., 2019) and complex assembly (Noormohammadi et al., 2016). Further, the dynamic CCT2 intra-ring interactions between the apical domains of CCT5 and CCT4 and the strong CCT2-CCT2 inter-ring interaction upon ATP binding also suggest an important role for CCT2 in CCT allosteric cooperativity (Zang et al., 2016).

The folding of substrate is dependent on the ATPase cycle. Structural studies revealed that the interface of substrate binding to the apical domain of chaperonin subunits involved a groove between Helix 11 (H11) and a proximal loop (PL) that contains a mix of charged, polar, and hydrophobic residues (Joachimiak et al., 2014) (**Figure 1B**). Shown in Mm-Cpn, ATP hydrolysis results in a conformational change that brings H11-PL into proximity of a loop in an adjacent subunit, with subsequent packing displacing the substrate and pushing it into the chamber for folding (Douglas et al., 2011). In studies with CCT, denatured actin (with some secondary and tertiary structure acquired) bound to the high ATP-affinity CCT2 side of the chaperonin, which kept the two lobes of actin extended and prevented misfolding. To achieve the native state of actin, ATP binding and subsequent hydrolysis triggered the segmental release of bound actin into the folding chamber (Balchin et al., 2018), bringing the actin lobes together. Hence, by controlling the

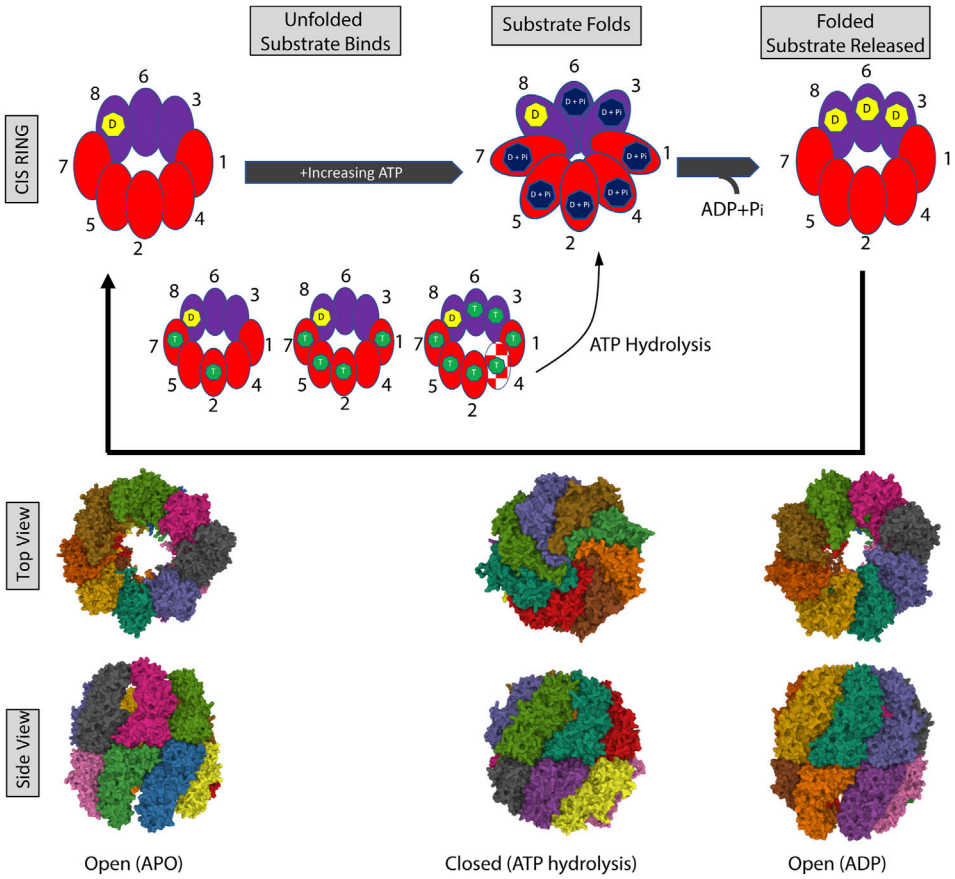


**FIGURE 2 |** The CCT ATPase cycle. (A) Schematic shows the sequential binding of ATP starting with subunits on the CCT2 side of the complex (red) followed by the CCT6 side of the complex (purple). CCT7 and CCT2 first react to and bind nucleotide, followed by the rest of the subunits with increasing ATP. CCT4 (red/white pattern) is the last to bind to ATP and this binding triggers ATP hydrolysis and closing of the ring. CCT3 and CCT6 may load with ATP later in the cycle (delayed release of ADP), while the ADP bound to CCT8 may be exchanged for ATP only under high nucleotide concentrations and/or not involved in ATP consumption. The processing of an unfolded and folded substrate is shown in the gray boxes. ADP (D) is indicated by the yellow heptagon, ATP by the green heptagon, and hydrolyzed ATP: ADP + phosphate (D + $P_i$) in the dark blue heptagon. The nucleotide-free open ring conformation is based on PDB 4A0O [nucleotide-free (apo) state (Cong et al., 2012)]. The closed ring conformation is based on PDB 6KS6 [Yeast CCT at 0.2 mM ADP-AlFx (Jin et al., 2019)]. The open ring conformation with ADP is based on PDB 4A13 [model refined against symmetry-free cryo-EM map of TRiC-ADP (Cong et al., 2012)].

order of folding through the ATPase cycle, CCT lowers the folding energy barrier for actin and similar proteins with complex topologies through the formation of high contact order interactions not possible with the simpler chaperonins. This sequential ATP-induced conformational change may also govern the cycles of protein folding and the subsequent release of multidomain proteins during the folding process (Rivenzon-Segal et al., 2005; Reissmann et al., 2012).

## Substrate Folding by Chaperonin Containing TCP1

Substrates folded by CCT are structurally and functionally diverse, driving the evolution of a complex chaperonin with diversification of subunits that can modulate substrate binding specificities. The apical domains of CCT subunits are the principal sites for substrate recognition, but exact structures or sequence rules that regulate substrate binding may depend on the conditions of protein synthesis and cooperation of co-chaperones. A comparison of substrates folded by CCT under *in vitro* compared to *in vivo* conditions revealed little overlap, other than actin and tubulin, between the two groups of proteins, suggesting that substrate binding to CCT depended on factors beyond specific amino acid sequences (Yam et al., 2008). As an example, patterns of polar and hydrophobic residues in the groove between H11 and PL in the apical domain of CCT subunits may govern substrate binding affinities through combinatorial interactions (Joachimiak et al., 2014). While the field is undecided on the size of the intracellular protein pool folded by CCT and the scope of the CCT interactome, early studies recognized the cytoskeletal proteins, actin and tubulin, as obligate substrates of the chaperonin complex (Sternlicht et al., 1993; Llorca et al., 1999a; Roobol et al., 1999b; Hynes and Willison, 2000; Llorca et al., 2000). Non-skeletal substrates include proteins from the 7-bladed WD40 propeller repeat family (Valpuesta et al., 2002; Kubota et al., 2006). WD40 proteins form the core of substrates conserved from yeast to human that are folded by CCT (Willison, 2018). Structural data

suggested that the size of the folding chamber in CCT was equivalent to GroEL-GroES (Cong et al., 2010; Cong et al., 2012) and would fold proteins up to ~70 kDa. However, CCT is known to fold proteins that are greater than 70 kDa. Studies using fusion proteins (e.g., actin-GFP) with *in vitro* translation systems found that CCT fully encapsulated substrates smaller than its folding chamber, like actin, and partially encapsulated large multidomain proteins like the 109-kDa spliceosomal U5 subunit, hSnu114; a beta-strand rich protein. CCT partially enclosed the C-terminal domain of this protein, while the N-terminal domain was CCT-independent (Rüßmann et al., 2012). CCT thus has the capacity to fold large multi-domain proteins in a sequential manner that is domain-specific, and this may explain its role in preventing aggregation of proteins with polyglutamine (polyQ) tracts (Nollen et al., 2004). The capacity of CCT to fold proteins with complex topologies is further supported by cooperative folding with co-chaperones, like HSP70 (Cuellar et al., 2008; Stein et al., 2019), phosducin-like proteins (PhLP) (Martin-Benito et al., 2004; Stirling et al., 2006), and prefoldin/GimC (PFD) (Siegers et al., 1999).

Actin ($\alpha$, $\beta$, and $\gamma$ isoforms) is a highly conserved protein among eukaryotes that exists as free G-actin monomers and F-actin polymers, depending on ionic concentrations and ATP. The actin monomer consists of two domains, originally called "large" and "small" domains. During folding, nascent actin binds two to three CCT subunits using a 1.4 geometrical configuration (numbering based on the position of the subunits in the ring) in an open conformation, starting with subunits opposite to CCT4 in the ring that are nucleotide-free or ADP-bound (Llorca et al., 1999b; Llorca et al., 2000). ATP binding then drives the power stroke movement that leads to actin folding. The folding kinetics of actin are biphasic, with the initial folding phase being the most efficient. The topology of the CCT-bound actin facilitates rapid folding during the first phase in concert with ATP binding and hydrolysis that triggers an asymmetric conformational change in the ring structure (Balchin et al., 2018). During the second phase, the assistance of the co-chaperone, PFD, may enhance the rate and yield of actin folding. PFD is a ~100 kDa chaperone consisting of two beta-subunits that assist actin and tubulin folding by CCT. Through a conserved electrostatic interaction, PFD interacts with CCT in the open state, aligning the substrate binding regions of the two chaperones and optimizing the substrate environment to facilitate actin folding and prevent aggregation (Gestaut et al., 2019b). In contrast, another co-chaperone, PhLP3, may inhibit CCT folding activity by forming a ternary complex with chaperonin along with actin or tubulin. The interaction of PhLP3 with CCT in the presence of substrate inhibited ATPase activity and affected the folding of nascent actin (and tubulin) *in vitro* (Stirling et al., 2006). Together, the antagonistic actions of PFD and PhLP3 may help modulate the activity of CCT to regulate the formation of the actin cytoskeleton and the biogenesis of tubulin in order to meet cellular demands.

The transcription of actin is regulated through the myocardin-related co-transcription factor-A (MRTF-A)/serum response factor (SRF) pathway. When cellular signaling receptors stimulate actin polymerization, G-actin levels decrease and disrupt the MRTF-A: actin interaction, allowing MRTF-A to move to the nucleus where it activates SRF to transcribe more actin. However, the impediment in producing actin is not at the level of transcription, but rather at the protein folding step through CCT. To regulate this, the monomeric form of CCT5 was reported to alter the nuclear accumulation of MRTF-A during serum stimulation, delaying the transcription of actin. Monomeric CCT5 accumulated when levels of the CCT hetero-oligomeric complex were low and decreased when levels of the oligomer were high (Elliott et al., 2015). Linking actin transcription and folding through CCT5 ensures that actin is synthesized only when enough CCT hetero-oligomeric complex is present to efficiently fold the cytoskeletal protein, else the presence of CCT5 monomers delays actin transcription. While free CCT monomers had been previously described (Liou and Willison, 1997; Brackley and Grantham, 2010), this report connects CCT5 monomer activity with the protein-folding function of the hetero-oligomeric chaperonin in the context of actin folding (Elliott et al., 2015).

Early studies, based on 3D reconstruction using cryo-EM, revealed that tubulin ($\alpha$, $\beta$, and $\gamma$ families) interacts with CCT differently from actin, with a mixture of shared and unique subunits used for binding (Llorca et al., 1999b). Tubulin binds up to five CCT subunits using a 1.5 geometrical configuration in a semi-closed conformation that spans the protein-folding chamber (Llorca et al., 2000). Tubulin binds to a cluster of high ATP-affinity and low ATP-affinity CCT subunits, engaging with electrostatic and polar side chains on residues (Pappenberger et al., 2002). Molecular dynamics simulations of single subunit interactions with substrate revealed that tubulin binds to CCT3 through an interface that spans the HL (helical region) and HP (helical protrusion) sites in the apical domain. This CCT3-tubulin interaction involved hydrophobic and electrostatic interactions on the HL site and a salt bridge network between charged amino acids on the HP. Generalizing this finding suggests that substrates interacting with CCT *via* hydrophobic interactions may use the HL binding sites, while substrates, like tubulin, that interact with CCT *via* electrostatic interactions, contact both HL and HP sites, with the salt bridge network being critical (Jayasinghe et al., 2010). Importantly, having obligate substrates bind to multiple CCT subunits based on geometric configurations may be advantageous in applying the mechanical force needed to fold substrates independently of having common features. Actin and tubulin are different proteins, yet both can be folded by CCT based on distinct geometric conformations (Vallin and Grantham, 2019). CCT may also fine-tune its protein-folding activity by interacting with partners. The binding of β-tubulin to CCT was modulated through interaction with Programmed cell death protein 5 (PDCD5). Cryo-EM studies showed that PDCD5 attached to the apical domain of CCT2, which sterically hindered β-tubulin binding to CCT. Hence, PDCD5 could interact with CCT to slow β-tubulin folding and disrupt microtubule formation, perhaps in response to apoptotic stimuli (Tracy et al., 2014).

WD40 repeats in proteins consist of multiple 40 amino acid repeats that form a blade of four anti-parallel β-sheets. Typically repeats end with a tryptophan-aspartic acid dipeptide (WD), from which its name is derived. WD40 repeats are widely variable among proteins in terms of sequence and number of repeats, with seven tandem repeats (WD1-7) forming a circular β-propeller being the most common. Early studies revealed that WD40 repeats have different folding kinetics, hence, different chaperone dependencies. CCT, when first identified as interacting with WD40 folds, had the needed shape and features to bind the propeller (Valpuesta et al., 2002). Screening WD40-repeat proteins for CCT interactions showed variable binding that was different from the ordered process of actin folding and suggested a role for CCT in the assembly, in addition to folding, of some WD40-containing proteins (Willison, 2018). One of the WD40 proteins that interact with CCT is the heterotrimeric G protein β subunit (Gβ), an essential component of G protein. Mutational analysis in a cell-free system showed that CCT binding to Gβ was reduced upon deletion of WD40 repeats, most especially upon loss of WD2. Specifically, the β-strand 3 (β3) region of WD2 was essential for CCT recognition, since this region has hydrophobic and polar residues aligned in a "φ-x-φ-x-φ-x" sequence (where φ is a hydrophobic residue) (Kubota et al., 2006). Thus, hydrophobic residues alongside β-strands are likely preferred recognition sites for CCT binding, and subsequent interactions with the chaperonin prevent aggregation and facilitate folding of the native WD40 repeat proteins. This was exemplified in a study of Gβγ dimer formation in which CCT not only folded Gβ subunits but also assisted Gβγ dimer assembly in an ATP-dependent manner (Wells et al., 2006). Cryo-EM studies further revealed that Gβ binds CCT in a near-native state, and subsequent binding with the co-chaperone, PhLP1, helps release Gβ for assembly with Gγ to form the dimer (Plimpton et al., 2015). Like G protein, the anaphase promoting complex/cyclosome (APC/C) is essential for biological activities. APC/C is a ubiquitin ligase that regulates cell cycle phases by targeted protein degradation using as co-activators, the WD repeat-containing proteins, Cdh1 and Cdc20. CCT is the only known chaperone to fold Cdh1 and Cdc20 and interacts directly with WD40 repeats of these proteins, like WD3-5 in Cdc20 (Camasses et al., 2003).

Early studies revealed that the von-Hippel-Lindau (VHL) tumor suppressor is an obligate substrate of CCT (Feldman et al., 1999). VHL is part of the ubiquitin ligase complex that targets proteins like HIF-1α, for degradation. CCT is needed not only for VHL folding but for complexing with partner proteins, elognin B and C. The interaction between VHL and CCT involved hydrophobic residues, with two regions, Box 1 and Box 2, identified as necessary for stable interactions with the chaperonin (Feldman et al., 2003). Crosslinking experiments between CCT and VHL showed that Box1 bound to CCT1 and CCT7 in the H11 of the apical domain region (Spiess et al., 2006). Interestingly, about 50% of the mutations occurring in tumor derived VHL are found in the CCT binding site (Feldman et al., 1999; Feldman et al., 2003). These results highlight the plasticity and specificity of substrate binding to CCT, involving specific configurations of polar and hydrophobic residues in the apical domains of each subunit to accommodate the binding of different substrates.

## Regulation of Chaperonin Containing TCP1 Subunit Gene Expression

The first CCT subunit discovered was CCT1/TCP-1 (CCTα) encoded by *Ccta*, which is highly expressed in mouse testicular germ cells (Silver et al., 1979). Subsequent studies identified an additional six CCT subunit genes: *Cctb, Cctg, Cctd, Ccte, Cctz*, and *Ccth*, encoding CCT2, CCT3, CCT4, CCT5, CCT6, and CCT7, followed by *Cctq* for CCT8 (Trent et al., 1991; Kubota et al., 1994; Kubota et al., 1995). A ninth subunit gene, *Cctz*-2 expressed in testis was discovered, which distinguished it from *Cctz-1* found in most tissues (Kubota et al., 1997). Current nomenclature for the subunit genes encoding the hetero-oligomeric complex found in most tissues is: *TCP1, CCT2, CCT3, CCT4, CCT5, CCT6a, CCT7, and CCT8.* CCT subunit genes have 11–16 exons and contain CpG dinucleotide-rich sequences and SP1 binding sites that are typically found in constitutive housekeeping genes (Kubota et al., 1999b). Using mouse tissues, initial studies of expression found that all eight CCT subunits were distributed across tissues tested, indicating that all eight subunits were required for the activity of the chaperonin. However, expression levels of CCT subunit genes among tissues varied, with the highest expression observed in testis and a mouse mammary tumor cell line. Since these are actively proliferating cells, findings were suggestive that CCT subunit expression correlated with the rate of cell division (Kubota et al., 1999b). CCT expression is also coupled with substrate synthesis Increased CCT expression was observed in testicular germ cells, neuronal cells, and other cells highly dependent on tubulin for synthesis of sperm tails, neurites, or cilia as examples (Kubota, 2002). CCT subunit protein also transiently increased during recovery from chemical stress induced by sodium arsenite, which causes accumulation of unfolded proteins (Yokota et al., 2000b). Searching the first intron of *Ccta* (*CCT1*), a potential binding sequence for heat shock transcription factors (HSF1 and HSF2) was found. Heat shock elements (HSE) for binding HSFs were subsequently located within the first intron or 5' coding regions of each CCT subunit gene (Kubota et al., 1999a). Since CCT evolved from a common ancestor with other HSPs, the *Cct* genes also have an HSE-HSF transcription system. However, unlike HSPs, upregulation of CCT in response to stress is not always observed. In HeLa cells during heat treatment, HSP70 increased, but not CCT, and a similar outcome was observed in mouse BALB/3T3 cells (Kubota et al., 1999a). CCT also did not increase in response to heat treatments in yeast (Ursic and Culbertson, 1992) or *Tetrahymena* (Soares et al., 1994). Moreover, reducing the levels of CCT did not induce a heat shock response (Grantham et al., 2006). *Cct* genes, having fewer HSEs compared to HSP70, may be less responsive to HSFs and more involved in *de novo* protein folding.

Other transcription factors that regulate the expression of CCT subunit genes include the Staf family members, ZNF143 and ZNF76, that were found in HeLa cells using reporter assays. These bind to two *cis*-acting elements, CAE1 and CAE2, in the promoter for *Ccta* (CCT1 or TCP1) (Kubota et al., 2000). Staf regulates the

transcription of small nuclear RNAs (snRNA), snRNA-type genes, and the promoter pol II mRNA (Myslinski et al., 1998); hence Staf family members are essential and their activity in most cells aligns with the fact that CCT1 (TCP-1) is detectable in most tissues. Because of the similarities in CCT subunit expression patterns, ZNF143 and ZNF76 may function as transcriptional regulators in the other seven CCT subunits as well. The transcription of *Cctq* (CCT8) is regulated by a *cis*-acting element comprising 8-base pair long element CCGGAAGT named CQE1 that is bound by the ternary complex factor (TCF): Elk-1, Sap-1a, and Net (Sap-2), which is a subfamily of the Ets domain transcription factors (Yamazaki et al., 2003). Recognition of CQE1 by TCF is independent of serum response factor (SRF). Instead, this transcriptional activity may be regulated by the Ras-mitogen-activated protein kinase (MAPK) pathway since inhibition of MEK (MAPK and ERK Kinase) 1/2 inhibited expression. The RAS/MAPK pathway may play a role in the upregulation of CCT8 after chemically induced stress through activation of the p38 or c-Jun N-terminal kinase/stress activated kinases. Interestingly, inhibition of MEK1/2 also reduced activity from the *Ccta* (CCT1) promoter, thus the MAPK pathway may be a common signaling mechanism to coordinate expression of the CCT subunit genes (Yamazaki et al., 2003).

## The Activity of Chaperonin Containing TCP1 During Cell Growth

Early observations of CCT expression in cells revealed that the activity of the chaperonin depended on the cell growth rate. Abundant CCT correlated with rapidly dividing cells and CCT decreased during growth arrest or nutrient loss. Re-addition of nutrients or growth factors resulted in recovery of CCT expression in a manner linked with the cell cycle. The cell cycle consists of an initial gap (G1) phase, during which a cell prepares for division, followed by the DNA synthesis (S) phase, a second short gap phase (G2) to assess for DNA damage, and the final phase of mitosis (M) when a cell separates the replicated chromosomes and performs the physical separation into daughter cells during cytokinesis. Initial studies noted that the highest levels of CCT were induced during the G1/S transition and early S phase (Yokota et al., 1999). Moreover, CCT from S-phase arrested cells had more protein-folding activity than CCT from M-phase arrested cells or asynchronously growing cells (Yokota et al., 2001b). In part, these findings could be explained by subunit preferences that correlated with cell cycle phases. For example, CCT1, 4, 6a were increased in S-phase cells compared to M-phase cells. Moreover, measurements of CCT subunit turnover suggested that the rates of synthesis were more variable than the rates of degradation during growth arrest, especially in S-phase arrested cells, enabling subunit levels to increase (Yokota et al., 2001b; Kubota, 2002).

One reason for the heightened need of CCT during the cell cycle is the critical role that both tubulin and actin play during cell division. During M phase, the formation of the mitotic spindle is essential for the segregation of replicated chromosomes. Microtubules formed by tubulin are the building blocks of the mitotic spindle. During cytokinesis, when dividing cells physically separate, the contractile ring that forms will contain F-actin along with myosin motors. Providing functional forms of these cytoskeletal proteins is a key function of CCT during the cell cycle. Early studies showed that high levels of tubulin were associated with S-phase CCT complexes, especially during the G1-S transition, but not in G1-arrested cells (Yokota et al., 1999). Targeting the apical domain of CCT5 with a microinjected antibody or using small interfering RNAs (siRNAs) to inhibit individual CCT subunits in 3T3 cells caused a delay of the G1-S transition and the accumulation of disordered microtubules (Grantham et al., 2006; Brackley and Grantham, 2010). Hence, the depletion of CCT subunits reduced tubulin levels and impacted actin folding, showing the important relationship between substrates like actin or tubulin and CCT during cell growth.

Control of the cell cycle in eukaryotic cells is driven by cyclins and cyclin-dependent kinases (CDKs). CDKs are inactive until bound by their cyclin partners, forming CDK-cyclin pairs that function in specific phases of the cell cycle. CDKs are subject to regulatory phosphorylations/dephosphorylations that fine tune their activity to drive cell cycle progression. The CDK2-cyclin E complex is active from late G1 through S-phase. Using yeast cells, in which overexpression of cyclin E and CDK2 is lethal, a genetic screen of negative regulators of cyclin E revealed that expression of human CCT2, CCT3, and CCT8 rescued the lethality caused by cyclin E expression, perhaps acting as dominant negative subunits in this mix of yeast and human proteins. Further work showed that CCT transiently associated with newly translated cyclin E, and that ATP was required for release from the chaperonin, which was confirmed by co-immunoprecipitation of CCT with cyclin E in the presence of EDTA to inhibit ATP and magnesium (Mg). Using HeLa cells arrested in S-phase, the ATP-dependent physical interaction between cyclin E and CCT was shown (Won et al., 1998). However, subsequent studies found that the folding of cyclin E by CCT was not required for CDK2 binding, and that the association of cyclin E with the chaperonin was processed distinctly from obligate substrates like actin, suggesting that the interaction of CCT with cyclin E may be indirect (Grantham et al., 2006). While early work found that CDK2 did not precipitate in complex with CCT (Won et al., 1998), a mass spectrometry study of the cellular processes involving CDK2 identified multiple CCT subunits as physical interactors of CDK2 (Neganova et al., 2011). In fact, data from the protein interactors database, BioGRID (https://thebiogrid.org), indicates that CCT subunits can interact with hundreds of proteins, suggesting that many proteins may occupy CCT complexes at a low abundance. As example, a proteomic screen for G1 phase proteins identified multiple CCT subunits as interactors of cyclin D1 (Jirawatnotai et al., 2011).

Progression through the cell cycle leads to M phase during which nuclear division takes place. M phase is highly coordinated to ensure that duplicated chromosomes are equally distributed into the pair of daughter cells. Sister chromatids attach to the mitotic spindle in early M phase and separation and segregation of sister chromatids to opposite ends of the cell occur in the later stages of M phase. Critical to the latter process is the degradation of the cell cycle regulator, securin, to unleash separase that triggers the separation of chromatids from the mitotic spindle.

Mitotic protein degradation is mediated by the APC/C complex that is activated by binding the co-activator, Cdc20. Checkpoint proteins, Mad1, 2, 3 and Bub1, 3 control the spindle checkpoint by inhibiting Cdc20 (and proteolysis) until all chromatids attach to the spindle. Layered onto this regulation is the role of CCT in folding the functional form of Cdc20. Studies in budding yeast showed that CCT subunits co-migrated with Cdc20 in a glycerol density gradient, and immunoprecipitants revealed stable interactions between CCT subunits and Cdc20, but no other components of the APC/C complex; hence, the binding between CCT and Cdc20 is specific. Mutations in CCT subunits abolished the interaction with Cdc20, suggesting that a functional chaperonin was required. Further, the interaction of CCT with Cdc20 was ATP-dependent, since non-hydrolyzable analogs of ATP inhibited binding. Cdc20 has three regions: the N-terminal domain that has the Mad2 binding sites, seven WD40 repeats, and a short C-terminal region. Deletion studies established that the WD40 repeats were the sites of interaction with CCT. Together this body of data indicates that CCT is required to produce a functional APC/C-Cdc20 complex needed to exit the spindle checkpoint in M phase. CCT is also required to produce functional Cdh1, the G1-specific co-activator of APC/C that ensures the completion of M phase and entry into G1 through destruction of mitotic cyclins (Camasses et al., 2003).

Polo-like kinases (Plk) are important components of the cell cycle, specifically active during the transition to M phase, the regulation of mitotic exit, and cytokinesis. Plk1 supports the maturation of the centrosome and spindle assembly, phosphorylating among its targets the Cdc25 family of phosphatases that remove inhibitory phosphorylations from CDK-cyclins. Using a yeast two-hybrid screen, Plk1 was identified as a possible interactor of CCT, which was confirmed *in vitro* using a rabbit reticulocyte lysate (RRL) system by co-immunoprecipitating Plk1 with CCT1, and *in vivo* using mouse mammary gland carcinoma FT210 cells. Depleting CCT1 by RNA interference (RNAi) in HeLa cells caused an arrest in G2/M phase, preventing mitotic entry. Continued depletion of CCT1 later resulted in apoptotic cell death, which could be prevented by inducing a G1 arrest to keep cells from entering M phase. Decreasing CCT1 also reduced levels of active Plk1 and resulted in low CDK activity that prevented progression through M phase. The addition of active Plk1 or cdc20 reversed the effects of CCT1 loss. Depletion of Plk1 recapitulated the G2-M arrest phenotype observed with depletion of CCT1 (Liu et al., 2005). Hence, Plk1 is likely a substrate of CCT. HSP90 was also found to regulate the stability of Plk1 (Simizu and Osada, 2000). Nascent Plk1 may associate with CCT co-translationally and then reach its functional form with the help of HSP90.

A novel function of CCT in the eukaryotic cell cycle is its role in the disassembly of the mitotic checkpoint complexes (MCC), which is distinct from the protein folding activity described for Cdc20 or Plk1. The MCC is formed by the checkpoint proteins: Mad2, BubR1, Bub3, and Cdc20. Studying the pathways of MCC disassembly led to the discovery of an ATP-dependent factor that enabled the release of Cdc20 from the MCC. This factor was identified as CCT and confirmed by generating CCT5 oligomers that could release Cdc20 (and Mad2) from the MCC, albeit with reduced activity compared to purified hetero-oligomeric CCT. Like its protein-folding activity, MCC disassembly by CCT was dependent on ATP hydrolysis (Kaisari et al., 2017). How this mechanism differs from the chaperonin's protein-folding activity, especially since CCT also folds Cdc20, is unknown, but could involve interactions with the WD40 repeats of Cdc20 and employ the chaperonin's capacity to sequentially bind domains of complex proteins in its central chamber.

Regulation of CCT protein-folding capacity could be achieved through PTMs as described for HSP70 and HSP90. For example, HSP70s are highly phosphorylated, especially during cell cycle progression, and their activity can be regulated by the MAPK pathway [reviewed in (Nitika et al., 2020)]. Likewise, in a study of CCT activity during growth factor signaling, CCT2 was phosphorylated by p90 ribosomal S6 kinase (RSK) and p70 ribosomal S6 kinase (S6K), serine/threonine kinases that are activated by the MAPK pathway and/or the phosphoinositide 3-kinase (PI3K)-mammalian target of rapamycin (mTOR) pathway, respectively. Importantly, depletion of CCT2 by RNAi inhibited cell proliferation, and complementation with an ectopically expressed CCT2 S260D mutant (phosphomimetic) restored cell growth, but not with a CCT2 S260A mutant that was phosphodeficient, indicating that Ser-260 phosphorylation may modulate the protein-folding activity of CCT during cell growth and possibly in the context of oncogenic stimulation (Abe et al., 2009).

## Chaperonin Containing TCP1 as a Preventive or Causative Factor in Disease

### Chaperonin Containing TCP1 in Neurological Disorders: Defects in Protein Folding and Aggregation

Aberrant protein folding and protein aggregation often underlie the development of neurological disorders. The onset of Parkinson's disease, Alzheimer's disease, or polyQ expansion diseases is associated with the accumulation of misfolded proteins in cells. In Huntington's disease, the expansion of polyQ tracts in huntingtin (Htt) protein is a hallmark of disease (DiFiglia et al., 1995). Mutant Htt (mHtt) containing greater than 40 polyQ tracts can misfold and aggregate, causing toxicity and neural damage through mechanisms still being studied. In a genome wide screen for genes that could regulate polyQ aggregation, a number of genes involved in protein folding were identified, including HSP70, CCT5, and five other CCT subunits (Nollen et al., 2004). Subsequent work in a yeast model with an aggregating form of Htt, Htt53Q, showed that the CCT hetero-oligomer could reduce fibril elongation and function cooperatively with HSP70 to inhibit the fibrillar aggregation of polyQ expansion proteins and suppress toxicity (Behrends et al., 2006). Disruption of CCT in HEK293 cells expressing polyQ-EYFP or Htt-fusion constructs, by depleting CCT6 using RNAi, caused polyQ-expansion-related cell death and a twofold increase in the aggregation of polyQ proteins; while overexpression of all eight CCT subunits (but not single subunits) in Htt-expressing Neuro2a cells reduced polyQ aggregation (Kitamura et al., 2006). In a subsequent study, overexpressing CCT1 or CCT4, or just the

**TABLE 1 |** CCT involvement in Neurological Disorders and other diseases.

| Neurological diseases | CCT subunits | Mechanism of action | Citations |
|---|---|---|---|
| Alzheimer's Disease | CCT2 | Downregulated in patients | Liu et al. (2020) |
| Axonal transport | CCT3, CCT1 (apical) | Individual subunits normalized axonal transport and lysosomal transport | Zhao et al. (2016) |
| | CCT5 | Regulated CDK5/p35 to increase phospho-Tau | Chen et al. (2018) |
| Huntington's disease | CCT1 | Single subunit reduced Htt-induced toxicity | Tam et al. (2006) |
| | CCT complex, CCT1 | Suppressed mHtt aggregation | Tam et al. (2009) |
| | CCT1 (apical domain) | Inhibited aggregation of mHtt and reduced mHtt-toxicity | Sontag et al. (2013) |
| | CCT complex | Capped mHtt fibril tips and encapsulated smaller mHtt oligomers | Shahmoradian et al. (2013) |
| | CCT5 | Homo-oligomer inhibited mHtt aggregation | Darrow et al. (2015) |
| | CCT3, CCT1 (apical) | Individual subunits reduced mHtt | Zhao et al. (2016) |
| Neuropathy | CCT5 | Missense A492G mutation causing His147Arg described | Bouhouche et al. (2006) |
| | CCT5 | His147Arg mutation examined in archaeal homolog | Min et al. (2014) |
| | CCT5 | Biochemical analysis of His147Arg mutants | Sergeeva et al. (2014) |
| | CCT5 | Structure of His147Arg mutation resolved | Pereira et al. (2017) |
| | CCT5 | Leu224Val mutation described | Antona et al. (2020) |
| Parkinson's disease | CCT2 | Subunit upregulated in MPP + -treated SH-SY5Y cells | Xie et al. (2016a) |
| | CCT7 | Oxidative stress-induced neuronal apoptosis | Anantharam et al. (2007) |
| | CCT complex, CCT3/6 | Interfered with amyloid fibril assembly | Sot et al. (2017) |
| PolyQ expansion proteins | CCT complex, CCT5 | Genome-wide RNA interference screen for PolyQ aggregation suppressors | Nollen et al. (2004) |
| | CCT complex | Synergistic function with HSP70 suppressed polyQ toxicity | Behrends et al. (2006) |
| | CCT complex | CCT6 knockdown and CCT1-8 overexpression modulated polyQ folding | Kitamura et al. (2006) |
| | CCT1 | Single subunit reduced Htt-induced toxicity | Tam et al. (2006) |
| | CCT complex, CCT4 | VRK2-mediated downregulation of CCT4 and polyQ aggregation | Kim et al. (2014) |
| | Targeted CCT2/5/7 | Loss of function inhibited autophagy, causing protein aggregation | Pavel et al. (2016) |
| Protein aggregates | CCT complex, CCT4 | USP25 catalyzed the de-ubiquitination of CCT reducing polyQ aggregation | Kim et al. (2015) |
| **Other diseases** | **CCT Subunits** | **Mechanism of action** | **Citations** |
| Amyotrophic lateral sclerosis | CCT5, CCT7, CCT8 | Overexpressed in cytoplasm of mutant cells | Kim et al. (2017) |
| Primary biliary cirrhosis | CCT5 | Upregulated compared to normal tissue, decreased with treatment | Chen et al. (2008) |
| Diabetes | CCT8 | Increased in insulin-resistant vs. insulin- sensitive | Xie et al. (2016b) |
| | Complex, CCT8, CCT4 | Increased in insulin resistance | Hwang et al. (2010) |
| Down syndrome | CCT5 | Decreased in parietal cortex | Yoo et al. (2001) |
| Epilepsy | CCT1 | Altered protein in hippocampi | Yang et al. (2006) |
| Atrial fibrillation | CCT5 | Elevated protein in atrial tissue | Goudarzi et al. (2011) |
| Coronary artery disease | CCT6A | Upregulated gene expression based on microarray data | Balashanmugam et al. (2019) |
| Hepatitis C virus | CCCT complex, CCT5 | Role in virus replication | Inoue et al. (2011) |
| Rabies virus | TCP1 | Role in virus replication | Zhang et al. (2014) |
| *Clostridium difficile* Toxins | CCT4/5 | Directly interacted with toxins | Steinemann et al. (2018) |
| Pain | CCT5 | Increased expression levels in pain models | Peters et al. (2013) |

apical domain of CCT1 (ApiCCT1) in Htt-expressing yeast cells or mammalian cells was sufficient to change the morphology of Htt aggregates, indicative of a possible mechanism for the suppressive behavior of CCT that was distinct from the protein-folding activity of the hetero-oligomer (Tam et al., 2006; Tam et al., 2009; Sontag et al., 2013) (**Table 1**).

Structural studies showed that the CCT hetero-oligomer can sequester a short Htt sequence responsible for aggregation and in this manner reduce mHtt aggregation (Tam et al., 2009). Using cryo-EM microscopy and cryo-electron tomography, the 3D structure of CCT with mHtt containing an expanded polyQ tract with 51 residues (mHtt51) was resolved. CCT capped the

fibril tips of mHttQ51 through the apical domains of its subunits as well as encapsulated smaller mHtt oligomers within its central cavity. Together these mechanisms are proposed to inhibit the *in vitro* aggregation of mHtt (Shahmoradian et al., 2013). In addition, a homo-oligomer composed of CCT5 could also cap fibrils and encapsulate mHtt oligomers, as shown using cryo-EM tomography, suggesting a shared mechanism with the CCT hetero-oligomer (Darrow et al., 2015). While these studies explain why CCT depletion enhances polyQ aggregation, the actual mechanism may be more complicated. In addition to protein folding, CCT supports lysosomal activity, so its loss could impair the process of autophagy. CCT also modulates the assembly of the mechanistic target of the mTOR complex, which is a regulator of autophagy (Cuellar et al., 2019). Using HeLa cells and mouse cortical neurons, CCT2/5/7 subunits were depleted by RNAi, which reduced autophagosome formation due to the defective folding of actin and increased polyQ aggregation. Importantly, when CCT was depleted in autophagy-deficient HeLa cells, the aggregation of polyQ proteins did not change. Hence, CCT loss resulted in an autophagy deficiency that caused the accumulation and aggregation of disease-causing proteins like mHtt (Pavel et al., 2016). Hence both direct effects of CCT on polyQ expanded proteins and indirect effects through cellular processes, like autophagy, contribute to the activity of CCT in reducing protein aggregate formation.

To determine if CCT controls the aggregation of other proteins, the action of the chaperonin on the amyloid fibril assembly of α-synuclein (α-syn) with the A53T mutation was examined. α-syn is a key protein involved in the pathogenesis of Parkinson's disease. CCT interfered with fibril assembly through specific interactions of CCT3 and CCT6, as part of the hetero-oligomeric complex, with the α-syn A53T central hydrophobic region. Since CCT partially encapsulated the A53T oligomers, closure of the ring induced by ATP binding and hydrolysis did not occur; hence, incomplete encapsulation is suggestive of ATP-independent inhibition of fibril assembly (Sot et al., 2017). Since CCT also inhibits mHtt aggregation in a similar nucleotide-independent manner (ApiCCT1), this could be indicative of a passive mechanism that reduces neurotoxicity by sequestering toxic proteins, as well as improving axonal transport of brain-derived neurotrophic factor (BDNF) needed for neurons (Zhao et al., 2016). Alternatively, *in vivo*, the cooperation of co-chaperones, like HSP70, may be needed to help CCT fully resolve misfolded proteins that cause neurological disorders.

Mutations in CCT subunits are associated with neuropathies (**Table 1**). In a rare case of mutilating hereditary sensory neuropathy, a missense mutation on exon four of *cct5* resulted in the substitution of a conserved histidine for arginine at amino acid 147 (H147R) (Bouhouche et al., 2006). This mutation is in the equatorial domain of CCT5 near the region where ATP/ADP binds. Using an archaeal Cpn60 homolog that is similar to CCT5, the reduction in ATP activity and defective oligomerization capacity were attributed to the histidine to arginine mutation in CCT5, demonstrating for the first time how a gene defect in CCT can cause disease (Min et al., 2014). Folding assays using γD-crystallin and actin substrates demonstrated the reduced folding activity of the H147R protein, but complete folding activity was not lost (Sergeeva et al., 2014). The subsequent crystal structure of CCT5 H147R mutant revealed that the position of R147 in CCT5 should not impair ring interactions or prevent assembly of the complex, nor block ATP binding. However, contacts between the side chains of R147 with other residues could impact the flexibility of the equatorial domain, changing the cooperativity within the rings of the complex that could reduce activity (Pereira et al., 2017). The importance of the CCT5 subunit in preventing neurological disorders was further shown in a different case of early-onset demyelinating neuropathy in which a L224V mutation in the intermediate domain of CCT5 was described. Similar modeling of CCT5 L224V, with or without nucleotides, showed that the apical domain was the most changed, affecting the subunit's conformation (Antona et al., 2020). Aberrant expression of other CCT subunits, like CCT2, also correlated with Alzheimer's disease or Parkinson's disease and could be used as biomarkers to assist with neurological disease prognosis and management (Brehme et al., 2014; Xie H. et al., 2016; Liu et al., 2020).

## Chaperonin Containing TCP1 in Cancer: Increased Protein Folding Activity

Beginning with the first report of CCT in hepatocellular carcinoma (HCC) and colon cancer (Yokota et al., 2001a), the increased expression of individual CCT subunit RNA and protein in tumor tissues compared to normal tissues was shown (**Table 2**). Consistent with this body of data is that CCT expression increased with tumor grade—the more advanced the tumor the higher the levels of CCT—and correlated with poor patient outcomes or prognosis. In recent years, the increasing amount of patient data available in datasets (e.g., The Cancer Genome Atlas (TCGA), The Human Protein Atlas, Oncomine etc.), provide strong support for CCT as a driver of cancer and potentially an oncogene (Klimczak et al., 2019; Dong et al., 2020; Liu et al., 2020). In many cancers, the genes encoding CCT subunits are genomically amplified and found in chromosomal hotspots (e.g., *CCT2*). Unlike the neurological disorders, loss of function CCT gene mutations are rarely seen in cancer (Ghozlan et al., 2021). Depletion studies of individual CCT subunits demonstrated the essential role of the chaperonin in cancer cell proliferation, cancer cell invasion and migration, and cancer cell death, advancing research on the chaperonin as a potential prognostic marker and therapeutic target in the management of cancer (**Table 2**).

Early studies showed that CCT activity is necessary for cancer cell proliferation due to the need for the functional forms of cytoskeletal proteins as well as cell cycle regulators like Cdc20 and Cdh1 (Grantham et al., 2006). Cancer cell lines tend to express more CCT than non-cancer cells, although expression and activity may not always correlate (Boudiaf-Benmammar et al., 2013; Bassiouni et al., 2016). Depletion of CCT2 in triple-negative breast cancer (TNBC) cells prevented tumor growth in a murine syngeneic model (Showalter et al., 2020) and impaired the formation of tumor spheroids (Ghozlan et al., 2021). Knockdown of CCT3 in a mouse model of gastric cancer reduced tumor size (Li et al., 2017). Depletion of CCT3 in thyroid gland papillary carcinoma cells, TNBC cells, or gastric cancer cells decreased cell cycle

**TABLE 2 |** CCT subunits are highly expressed in different cancers.

| Cancers | CCT subunits | Mechanism of action | Citations |
|---|---|---|---|
| Adenocarcinomas | CCT2 | Positive expression in tumor tissue correlated with clinical behavior | Zou et al. (2013) |
| Breast cancer | CCT2, TCP1 | Genes identified as being recurrently altered and necessary for growth of cancer cells | Guest et al. (2015) |
| | CCT2 | Gene and protein expressed in tumor tissues that correlated with patient outcomes and identified as a targeted peptide therapeutic | Bassiouni et al. (2016) |
| | CCT6A | RNA and protein were increased in tumor tissues compared to non-tumor tissues and associated with poor patient survival | Huang et al. (2019) |
| | CCT1, CCT2, CCT6A | Bioinformatics analysis revealed overexpression correlated with unfavorable prognosis with implications for other cancers | Klimczak et al. (2019) |
| | CCT2 | Gene increased in patients and correlated with poor survival; depletion reduced tumor growth in mice | Showalter et al. (2020) |
| | CCT2, 3, 4, 5, 6A, and 7 | Extensive data mining revealed that subunits were increased in tumor tissue compared to nontumor tissue and correlated with immune cell markers | Xu et al. (2021) |
| | CCT2 | Genomically amplified in cancers that correlated with reduced patient survival and co-occurrence reported with genes that regulate the cell cycle | Ghozlan et al. (2021) |
| | CCT2 | Transcriptomic profiling found increased expression in multiple cancers; association with PR+, HER2-, and advanced tumor stage; had prognostic value for luminal A cancers | Liu et al. (2021b) |
| | CCT2 | Bioinformatics and patient data correlated increased expression with patient prognosis; developed as a biomarker for diagnostic assay to detect circulating tumor cells | Cox et al. (2022) |
| Colorectal cancer | CCT2, CCT5 | Protein detected in tumor tissues that correlated with advanced stage and poor patient survival | Coghlin et al. (2006) |
| | cirCCT3 | Circulating RNA was highly expressed in clinical tumors | Li et al. (2020) |
| | CCT2 | Tumor tissues showed higher expression than normal colon tissue that correlated with reduced patient survival | Park et al. (2020) |
| Esophageal squamous cell carcinoma | CCT8 | Protein expression was high in tissues from patients with lymph nodes metastasis and overall survival was poor | Yang et al. (2018) |
| Ewing sarcoma | CCT6A | Bioinformatics analysis correlated high expression with poor prognosis; possible biomarker | Jiang et al. (2021) |
| Gastric cancer | CCT3 | High levels detected in cancer tissue compared to adjacent healthy tissue and knockdown reduced growth of cancer cells *in vitro* and *in vivo* | Li et al. (2017) |
| Glioma | CCT8 | Protein detected in tumor tissue and cell lines correlated with tumor grade; knockdown reduced growth and migration | Qiu et al. (2015) |
| Glioblastoma | CCT6A (also: CCT2, 3, 5, TCP1) | Neurosurgical aspirates contained extracellular vesicles with detectable protein that negatively correlated with patient survival | Hallal et al. (2019) |
| Head and neck squamous cell | CCT complex, CCT4, CCT7 | Database mining showed that gene expression was higher in tumors than normal tissues and correlated with low patient survival and advanced stage | Dong et al. (2020) |
| Hepatocellular and colonic carcinoma | CCT Complex, CCT2 | Increased expression in tumor tissue compared to non-tumor tissue and correlated with cell growth indicators | Yokota et al. (2001a) |
| Hepatocellular carcinoma | CCT8 | High expression correlated with histological grade and tumor size; also associated with poor prognosis | Huang et al. (2014) |
| | CCT3 | Increased expression in cell lines and tissue | Qiu et al. (2015) |
| | CCT Complex | Using patient samples and database mining, increased expression correlated with poor prognosis and dysregulated oncogenes | Yao et al. (2019) |
| | CCT5, CCT complex | Dataset mining found that RNA and protein are upregulated in tumors and associated with advanced tumor grade and poor survival; depletion or overexpression altered growth, invasion | Liu et al. (2021a) |
| | CCT6A | RNA and protein were increased in tumor tissues and associated with poor survival; depletion in cells reduced proliferation | Zeng et al. (2019) |
| | CCT1 (TCP1) | High levels observed in poorly differentiated tissue that was increased over normal adjacent tissues, which correlated with shorter survival and worse prognosis | Tang et al. (2020) |
| | CCT7 | Dataset mining showed that gene was higher in cancer tissue compared to normal and RNA and protein were independent risk factors for poor prognosis | Huang et al. (2022) |

(Continued on following page)

**TABLE 2 |** (*Continued*) CCT subunits are highly expressed in different cancers.

| Cancers | CCT subunits | Mechanism of action | Citations |
|---|---|---|---|
| Multiple myeloma | CCT3 | Database mining correlated expression with poor prognosis; potential role in diagnosis | Qian et al. (2020) |
| Non-small cell lung cancer | CCT5 | Proteomics analysis showed that protein was detectable in sera (autoantibody response) and was expressed in tissues | Gao et al. (2017) |
| | CCT6A | Increased expression in tumor tissues compared to tumor adjacent, associated with lymph node metastasis and negatively correlated with patient outcomes | Zhang et al. (2020) |
| Osteosarcoma | CCT complex, CCT4 | Database mining showed increased expression, with the highest among most cancers; expression correlated with metastasis and poor survival; small molecule inhibitor tested | Wang et al. (2022) |
| Pancreatic cancer | CCT8 | Mass spectrometry analysis detected protein in invasive cell line that could be secreted in exosomes; potential use in liquid biopsies | Liu et al. (2019a) |
| Prostate cancer | CCT2 | Protein increased in cell lines that were susceptible to targeted therapeutic | Flores et al. (2017) |
| Small cell lung cancer | CCT2 | Protein highly expressed in tumor compared to normal lung and correlated with increasing grade and poor survival; targeted therapeutic reduced growth in cell lines | Carr et al. (2017) |
| Thyroid cancer | CCT3 | Protein was increased in tumor tissues compared to matched controls and knockdown reduced cell proliferation | Shi et al. (2018) |

progression and caused cell cycle arrest, altering signal transduction pathways that drive cell cycling (Li et al., 2017; Shi et al., 2018; Xu et al., 2020). Similarly, pathway analysis positively correlated CCT6A with G2-M phase cyclins B and A in breast cancer (Huang et al., 2019). Knockdown of CCT8 in esophageal squamous cell carcinoma (ESCC) cells downregulated actin and tubulin and enhanced cell death upon treatment with cisplatin (Yang et al., 2018). CCT8 depletion in glioblastoma multiforme (GBM) cells affected the cytoskeleton and decreased proliferation and invasion, which was also observed in HCC cell lines (Huang et al., 2014; Qiu et al., 2015). While such studies provide additional evidence for an essential role of CCT in cancer cell growth, it is unclear from CCT subunit depletion experiments if effects are monomer specific, as was suggested for neurological disorders, or dependent on the depleted subunit for CCT complex assembly. In many of these studies, loss of cytoskeleton proteins was observed, suggestive of the latter idea—that the CCT hetero-oligomeric complex is needed to support cancer cell cycling. The consequence of depleting one CCT subunit on the rest of the subunits is not fully understood; yet evidence suggests that the remaining subunits may also decrease (Showalter et al., 2020). Hence, more work is needed to determine if there are unique activities for CCT subunit monomers in cancer cells.

Profiling more than 9,000 tumors from the TCGA revealed that most cancers have genetic alterations in 10 major signaling pathways (cell cycle, p53, MYC, PI-3 kinase/AKT, JAK-STAT, Hippo, Wnt, and TGF-beta among others) (Sanchez-Vega et al., 2018). Using the BioGRID database to search for protein interactions involving CCT revealed that there are potential CCT subunit interactors in all these signaling pathways that drive cancer (Ghozlan et al., 2021), supporting that CCT may promote oncogenesis through mechanisms that go beyond producing the functional forms of actin and tubulin.

The folding of the transcription factor, p53, is mediated by interactions with CCT. p53 is a tumor suppressor that prevents cancer development by activating pathways inducing cell cycle arrest or apoptosis when DNA damage is detected. In cancer, p53 is often mutated or ablated. Tumor-associated mutations can result in the generation of misfolded p53 that is unstable, which results in loss of the protective wild-type activity and a gain-of-function activity that promotes cancer invasiveness. CCT subunits were identified as part of the p53 interactome (Coffill et al., 2012) and immunoprecipitants of CCT1 (TCP-1) or CCT5 with wild-type or mutant forms of p53 were detected in cancer cells overexpressing the p53 constructs (Trinidad et al., 2013). Depletion of CCT subunits resulted in some loss of p53 binding to the chaperonin complex, but since other chaperones, including HSP70, can also fold p53, the existence of a cooperative mechanism for p53 folding cannot be ruled out. CCT binds to an N-terminal region of p53 that may involve hydrophobic interactions, since treatment with chaotropic salts disrupted binding. Depletion of CCT also decreased invasion in p53 mutant-expressing cancer cells, but since CCT folds other proteins (like actin) this effect may not solely be due to reduced folding of the p53 mutant proteins. However, depletion of both p53 and CCT decreased the invasive capacity of cancer cells (Trinidad et al., 2013). Interestingly, the negative regulator of p53, MDM2, may also be a CCT interacting protein, since it was identified in a mass spectrometry analysis of proteins in cancer cells captured by a FLAG-MDM2 construct (Yamauchi et al., 2014). MDM2 is also in the same chromosomal amplicon as CCT2 that is highly expressed in cancer cells (Ghozlan et al., 2021). While CCT may contribute to the correct folding of wild type p53, how its increased expression in cancer cells supports the mutant or unfolded forms of p53 remains to be determined but could involve interactions with other proteins like MDM2 or PTMs that modify CCT activity. As an example, functional enrichment analysis or treatments with inhibitors suggested that the function of CCT could be regulated through the PI3 kinase/AKT pathway (Guest et al., 2015; Dong et al., 2020). In fact, gene set enrichment analysis of mutant p53 identified a gene signature highly enriched in targets of the MYC transcription factor that were downregulated in head and neck squamous cell carcinoma (HNSCC) by treatment with a PI3 kinase inhibitor. Importantly, CCT2 was one of the MYC target genes, and mutant p53, MYC, and YAP bind to the promoter of CCT2, regulating its expression (Ganci et al., 2020). Whether CCT2 is part of a feedback

loop that could promote the invasiveness of mutant p53-expressing cancer cells is speculation that will require further investigation to determine.

A signaling pathway often perturbed in cancer cells is the Janus tyrosine kinase (JAK)-signal transducers and activators of transcription (STAT). Among JAK-STAT members, STAT3 is linked to the enhancement of cancer cell proliferation, migration, and suppression of anti-tumor immune responses (Yu et al., 2014). CCT was found to bind to STAT3. CCT2, and CCT5 were immunoprecipitated with newly transcribed STAT3 in RRLs and knockdown of CCT2 (which also reduced other subunits) decreased the levels of STAT3 in epithelial cell lines. Using a mixed RRLs approach in which STAT3 was co-expressed with single CCT subunits, STAT3 bound mainly to CCT3, likely through its DNA-binding domain (Kasembeli et al., 2014). Constitutively activated STAT3 promotes the oncogenic process through the expression of genes like *CCND1* (cyclin D1), a key driver of cell cycle progression when partnered with its cognate CDK (Leslie et al., 2006). CCT3 expression in multiple myeloma was associated with signaling pathways that included JAK-STAT3. The set of genes upregulated in the $CCT3^{high}$ group of patients correlated with those resulting from IL-6/JAK/STAT3 stimulation (Qian et al., 2020). CCT itself could activate genes that drive cell cycling, since overexpression of CCT2 in luminal A breast cancer cells increased the gene expression of *MYC* and *CCND1* that statistically correlated with *CCT2* (Ghozlan et al., 2021), while depletion of CCT6A in an HCC cell line decreased levels of cyclin D (Huang et al., 2019). Amplified CCT expression in cancer cells could, therefore, directly promote cell cycling by folding essential substrates like tubulin or cdc20 and indirectly through interactions with transcription factors like MYC, and promoting the expression of cell cycling factors like cyclin D.

Focusing on cancers in which CCT subunits were overexpressed revealed more ways that amplification of CCT could promote oncogenesis. Using two cancer cell lines [triple negative breast cancer (TNBC) and non-small cell lung cancer (NSCLC)] that highly expressed CCT2, depletion of this subunit decreased anti-apoptotic proteins like XIAP and inhibited phosphorylation of AKT and GSK3. Overexpression of CCT2 in CCT2-depleted cells restored the AKT-GSK3β-β-catenin and XIAP-survivin pathways, showing that the CCT complex may directly bind and stabilize XIAP and β-catenin (Chang et al., 2020). CCT3 supported breast cancer cell proliferation through the nuclear accumulation of β-catenin, perhaps directly since signals from CCT3 and β-catenin co-localized in the nucleus. A connection between CCT3 and microRNA (miR) MiR-223 further supports that CCT3 regulates the expression of β-catenin and therefore is involved in the competing endogenous RNA (ceRNA) network that regulates other genes like STAT5 through miR-223 (Qu et al., 2020). Depletion of CCT1 in HCC cells produced a similar outcome with reduction of Wnt signaling molecules Wnt7b and β-catenin (Tang et al., 2020), while in colorectal cancers (CRC), the presence of circulating RNA for CCT3 (circCCT3) was linked to advanced CRC and stimulated vascular growth endothelial factor A (VEGFA) and the Wnt signaling pathway (WNT3). CRC can also be promoted through hypoxia-driven signaling due to the loss of oxygen in these solid tumors. Hypoxic conditions activate the Hedgehog pathway. Gli-1, a Hedgehog signaling factor, interacted with CCT2, shown by mass spectrometry analysis of CRC cells. Depletion of CCT in CRC cells caused ubiquitination and degradation of Gli-1, likely through misfolding. Hence, in this model, the inhibition of CCT2 prevented tumor growth through decreases in Gli-1 levels (Park et al., 2020). In liver cancer, CCT3 was elevated and co-interacted with the transcriptional co-activator YAP, which is negatively regulated by the Hippo pathway, and transcription factor CP2 (TFCP2), a Hippo-independent oncoprotein in liver cancer. The pro-tumorigenic activity of CCT3 increased the half-lives of YAP and TFCP2 by preventing their interaction with the ubiquitination machinery (Liu Y. et al., 2019). CCT is also involved in TGF-β signaling. CCT6A bound SMAD2, a signal transducer of the TGF-β pathway, and suppressed SMAD2-mediated gene transcription in NSCLC cells, inducing metastasis in an animal model when overexpressed (Ying et al., 2017). While most of the known pro-cancer activity of CCT is in solid tumors, a role for CCT in acute myeloid leukemia was described. AML1-ETO is the result of a translocation in which two genes generate a fusion oncoprotein. The synthesis and folding of AML1-ETO are done by CCT, with the help of HSP70, by interacting with the fusion protein's β-strand rich, DNA-binding domain. Interestingly, the binding of AML1-ETO with CCT could occur under nucleotide-free conditions, which differs from the ATP-dependent folding model (Roh et al., 2016). This may be an example of a mechanism involving the apical domains of CCT subunits, in which CCT, like GroEL, could function as an "unfoldase" (Priya et al., 2013).

## Chaperonin Containing TCP1: Diagnostics and Therapeutics

One of the first CCT modulating compounds was Heat Shock Factor 1A (HSF1A), identified in a humanized yeast-based high-throughput screen for small molecule activators of HSF1. HSF1A reduced polyQ aggregation in neuronal precursor cells, which decreased cellular toxicity. But instead of binding to HSP90, HSF1A interacted with CCT1/TCP-1 and CCT8, shown in a biotin-based pull-down experiment, to regulate the activity of the chaperonin (Neef et al., 2010). A more specific interaction was targeted with the compound I-Trp, an iodomethyl ketone warhead that alkylates $Cys^{354}$ of β-tubulin. I-Trp disrupted protein-protein interactions between the CCT and tubulin, specifically targeting cancers that overexpress CCT2 (Lin et al., 2009; Liu et al., 2017). Specific interactions involving CCT4 were targeted with another small molecule compound called anticarin-β, which displayed more selectivity for cancer cells than normal cells. Anticarin-β is a natural coumarin compound from *Antiaris toxicaria* Lesch that inhibited the CCT4-mediated maturation of STAT3, among other effects, such as inhibiting the lysosomal-autophagy pathway. Anticarin-β reduced tumor growth in orthotopic and patient-derived xenograft models of osteosarcoma (Wang et al., 2022). A different approach to CCT inhibition was based on a peptide therapeutic derived from the apoptotic protein, Bax, called CT20p (Boohaker et al., 2012). CT20p displayed selective anti-cancer toxicity that was caspase-independent, and death involved disruption of the cytoskeleton (Lee et al., 2014). In a proteomics-based

pull-down experiment with biotinylated CT20p, seven of eight CCT subunits were identified as interactors of the peptide. CT20p directly bound to recombinant CCT2 in a cell-free system as well as to cytosolic CCT2 in an "in cell" pull-down assay. CCT2-depleted cancer cells were resistant to killing with CT20p, while cancer cells highly expressing CCT2 were sensitive (Bassiouni et al., 2016). Using polymeric nanoparticles to systemically deliver CT20p to cancer cells resulted in tumor growth inhibition in prostate and breast cancer animal models and small cell lung cancer cells (Lee et al., 2014; Carr et al., 2017; Flores et al., 2017). How CT20p inhibits CCT could be in line with the amphipathic nature of the peptide comprised of hydrophilic and hydrophobic amino acids (Boohaker et al., 2012).

Developing diagnostics targeting CCT subunits takes advantage of novel methodologies such as liquid biopsy using blood or serum (**Tables 1**, **2**). In Alzheimer's disease, CCT2 was part of a gene set used to develop a diagnostic profile (Liu et al., 2020). Likewise in breast cancer, CCT1 and CCT2 were part of HSP signature that could predict outcomes and help stratify patients for treatment (Klimczak et al., 2019). In pancreatic cancer, CCT8 was secreted from an invasive pancreatic cancer cell line, likely through the exosome pathway, and could serve as a liquid biopsy marker to monitor the progress of cancer patients (Liu P. et al., 2019). In CRC, circCCT3 was a potential biomarker of advanced disease (Li et al., 2020). CCT3 was also found to be a serum liver cancer biomarker. Seral-CCT3 was increased in liver cancer patients compared to normal patients and correlated with other serum markers like alpha-fetoprotein (AFP) (Liu Y. et al., 2019). A different approach found that NSCLC patients produced auto-antibodies to CCT5 at higher levels than healthy individuals; so, screening for these auto-autoantibodies in sera could be a novel diagnostic for cancer (Gao et al., 2017). CCT subunit proteins were found in extracellular vesicles or exosomes secreted by cancer cells. Exosomes from neurosurgical aspirates taken from patients with glioblastomas contained all eight CCT subunit proteins (Hallal et al., 2019). The capture and enumeration of circulating tumors cells from blood is another promising liquid biopsy approach, but is only approved by the FDA for breast, prostate, and colon cancer (Miller et al., 2010). Using CCT2 as a marker to identify circulating tumor cells in blood enhanced the ability to detect these cells from a broader range of cancers like small cell lung cancer (SCLC) that currently lack non-invasive diagnostics for patient management (Cox et al., 2022).

## SUMMARY AND OPEN QUESTIONS

The evolution of CCT in eukaryotes endowed the chaperonin with remarkable properties of plasticity to handle complex proteins along with the specificity required to produce essential cytoskeletal proteins. New research revealed novel substrates and functions that challenged the concept of CCT as only a protein folding complex for actin and tubulin. The work of many labs, beginning with the first structural studies in the 1990's, brought to light unique aspects of the chaperonin that are key to the etiology of diseases like cancer. However, gaps in knowledge need to be addressed to fully explore the therapeutic targeting of CCT. How large is the CCT interactome? *In silico* and affinity capture/mass spectrometry studies suggest that there are hundreds of proteins that could interact with CCT subunits. Demonstrating that these lower abundance interactors are directly bound by CCT requires further experimentation. Is ATP hydrolysis required for all the activities mediated by CCT? There are ATP-independent activities, such as those involving the apical domain of CCT1 (e.g., ApiCCT1) (Sontag et al., 2013) or the folding of AML1-ETO (Roh et al., 2016) that suggest otherwise. Different ATP-binding affinities for CCT subunits indicate that the chaperonin may function under a range of ATP concentrations, such as the nutrient-deprived tumor environment; however, findings on the role of CCT4 as an ATP sensor highlight the complex regulation of the ATPase cycle (Jin et al., 2019). Can non-folding activities of CCT be ascribed to subunit monomers or the hetero-oligomer? Nuclear CCT subunits were reported in early studies (Roobol and Carden, 1999), and unique monomer functions such as the interaction of the CCT5 monomer with MRTF-A are known (Elliott et al., 2015). The fact that CCT may interact with some substrates differently from actin or tubulin complicates the question of unique monomer/subunit activities. For example, CCT interacts differently with the actin filament severing and capping protein, gelosin, as compared to actin. Gelosin is not a classical folding substrate of chaperonin (Brackley and Grantham, 2011). In fact, CCT appears to sequester activated gelosin in the complex's central cavity to protect it from caspase-3 cleavage but does not fold gelosin (Cuellar et al., 2022). CCT may perform functions beyond protein folding that explain its activity in diseases like Huntington's or Alzheimer's or cancer. Do subunits like CCT2 or CCT5 have unique activities? The genes for these subunits are often amplified in cancers and correlate with poor patient prognosis. To answer this, new information on the transcriptional regulation of CCT subunits and the processes controlling assembly and disassembly of the complex may be needed. Unlike HSP70 and HSP90 (Backe et al., 2020; Nitika et al., 2020) in which proteomic-based investigations revealed the effects of PTMs on the chaperones' activities, much remains to be learned about how PTMs, like phosphorylation (Abe et al., 2009), acetylation, palmitoylation (Blanc et al., 2015), or others could modulate the function of CCT subunits. The activities of CCT go beyond neurological disorders and cancer and impact other diseases like diabetes, Down's Syndrome, hepatitis, and even pain syndrome (**Table 1**). As an example, targeting the malarial CCT complex with the antihistamine clemastine could be a new therapeutic approach for this parasitic disease (Lu et al., 2020), and CCT in T cells also promotes an immune response against helminths (Oftedal et al., 2021). Even though the gene encoding CCT was first reported in 1979, exploration of the complex activity of this eukaryotic chaperonin is just beginning. The initial work of researchers on the structure and function of CCT provided the foundation for the questions asked today on the role of chaperonins in disease, answers for which lie with current and future investigators working to understand the puzzle that is the CCT chaperonin.

## AUTHOR CONTRIBUTIONS

The manuscript was written through contributions of all authors. HG, AC, DN, SK, and AK.

## FUNDING

Funding was provided by the Live Like Bella Foundation grant # 21L11.

## REFERENCES


Abe, Y., Yoon, S.-O., Kubota, K., Mendoza, M. C., Gygi, S. P., and Blenis, J. (2009). p90 Ribosomal S6 Kinase and P70 Ribosomal S6 Kinase Link Phosphorylation of the Eukaryotic Chaperonin Containing TCP-1 to Growth Factor, Insulin, and Nutrient Signaling. *J. Biol. Chem.* 284 (22), 14939–14948. doi:10.1074/jbc.m900097200

Amit, M., Weisberg, S. J., Nadler-Holly, M., McCormack, E. A., Feldmesser, E., Kaganovich, D., et al. (2010). Equivalent Mutations in the Eight Subunits of the Chaperonin CCT Produce Dramatically Different Cellular and Gene Expression Phenotypes. *J. Mol. Biol.* 401 (3), 532–543. doi:10.1016/j.jmb.2010.06.037

Anantharam, V., Lehrmann, E., Kanthasamy, A., Yang, Y., Banerjee, P., Becker, K., et al. (2007). Microarray Analysis of Oxidative Stress Regulated Genes in Mesencephalic Dopaminergic Neuronal Cells: Relevance to Oxidative Damage in Parkinson's Disease. *Neurochem. Int.* 50 (6), 834–847. doi:10.1016/j.neuint.2007.02.003

Anfinsen, C. B. (1973). Principles that Govern the Folding of Protein Chains. *Science* 181 (4096), 223–230. doi:10.1126/science.181.4096.223

Antona, V., Scalia, F., Giorgio, E., Radio, F. C., Brusco, A., Oliveri, M., et al. (2020). A Novel CCT5 Missense Variant Associated with Early Onset Motor Neuropathy. *Ijms* 21 (20), 7631. doi:10.3390/ijms21207631

Archibald, J. M., Blouin, C., and Doolittle, W. F. (2001). Gene Duplication and the Evolution of Group II Chaperonins: Implications for Structure and Function. *J. Struct. Biol.* 135 (2), 157–169. doi:10.1006/jsbi.2001.4353

Archibald, J. M., Logsdon Jr., J. M., Jr., and Doolittle, W. F. (2000). Origin and Evolution of Eukaryotic Chaperonins: Phylogenetic Evidence for Ancient Duplications in CCT Genes. *Mol. Biol. Evol.* 17 (10), 1456–1466. doi:10.1093/oxfordjournals.molbev.a026246

Backe, S. J., Sager, R. A., Woodford, M. R., Makedon, A. M., and Mollapour, M. (2020). Post-translational Modifications of Hsp90 and Translating the Chaperone Code. *J. Biol. Chem.* 295 (32), 11099–11117. doi:10.1074/jbc.REV120.011833

Balashanmugam, M. V., Shivanandappa, T. B., Nagarethinam, S., Vastrad, B., and Vastrad, C. (2019). Analysis of Differentially Expressed Genes in Coronary Artery Disease by Integrated Microarray Analysis. *Biomolecules* 10 (1), 35. doi:10.3390/biom10010035

Balchin, D., Miličić, G., Strauss, M., Hayer-Hartl, M., and Hartl, F. U. (2018). Pathway of Actin Folding Directed by the Eukaryotic Chaperonin TRiC. *Cell* 174 (6), 1507–1521. e1516. doi:10.1016/j.cell.2018.07.006

Bartlett, A. I., and Radford, S. E. (2009). An Expanding Arsenal of Experimental Methods Yields an Explosion of Insights into Protein Folding Mechanisms. *Nat. Struct. Mol. Biol.* 16 (6), 582–588. doi:10.1038/nsmb.1592

Bassiouni, R., Nemec, K. N., Iketani, A., Flores, O., Showalter, A., Khaled, A. S., et al. (2016). Chaperonin Containing TCP-1 Protein Level in Breast Cancer Cells Predicts Therapeutic Application of a Cytotoxic Peptide. *Clin. Cancer Res.* 22 (17), 4366–4379. doi:10.1158/1078-0432.CCR-15-2502

Behrends, C., Langer, C. A., Boteva, R., Böttcher, U. M., Stemp, M. J., Schaffar, G., et al. (2006). Chaperonin TRiC Promotes the Assembly of polyQ Expansion Proteins into Nontoxic Oligomers. *Mol. Cell* 23 (6), 887–897. doi:10.1016/j.molcel.2006.08.017

Blanc, M., David, F., Abrami, L., Migliozzi, D., Armand, F., Bürgi, J., et al. (2015). SwissPalm: Protein Palmitoylation Database. *F1000Res* 4, 261. doi:10.12688/f1000research.6464.1

Boohaker, R. J., Zhang, G., Lee, M. W., Nemec, K. N., Santra, S., Perez, J. M., et al. (2012). Rational Development of a Cytotoxic Peptide to Trigger Cell Death. *Mol. Pharm.* 9 (7), 2080–2093. doi:10.1021/mp300167e

Booth, C. R., Meyer, A. S., Cong, Y., Topf, M., Sali, A., Ludtke, S. J., et al. (2008). Mechanism of Lid Closure in the Eukaryotic Chaperonin TRiC/CCT. *Nat. Struct. Mol. Biol.* 15 (7), 746–753. doi:10.1038/nsmb.1436

Boudiaf-Benmammar, C., Cresteil, T., and Melki, R. (2013). The Cytosolic Chaperonin CCT/TRiC and Cancer Cell Proliferation. *PLoS One* 8 (4), e60895. doi:10.1371/journal.pone.0060895

Bouhouche, A., Benomar, A., Bouslam, N., Chkili, T., and Yahyaoui, M. (2006). Mutation in the Epsilon Subunit of the Cytosolic Chaperonin-Containing T-Complex Peptide-1 (Cct5) Gene Causes Autosomal Recessive Mutilating Sensory Neuropathy with Spastic Paraplegia. *J. Med. Genet.* 43 (5), 441–443. doi:10.1136/jmg.2005.039230

Brackley, K. I., and Grantham, J. (2011). Interactions between the Actin Filament Capping and Severing Protein Gelsolin and the Molecular Chaperone CCT: Evidence for Nonclassical Substrate Interactions. *Cell Stress Chaperones* 16 (2), 173–179. doi:10.1007/s12192-010-0230-x

Brackley, K. I., and Grantham, J. (2010). Subunits of the Chaperonin CCT Interact with F-Actin and Influence Cell Shape and Cytoskeletal Assembly. *Exp. Cell Res.* 316 (4), 543–553. doi:10.1016/j.yexcr.2009.11.003

Brehme, M., Voisine, C., Rolland, T., Wachi, S., Soper, J. H., Zhu, Y., et al. (2014). A Chaperome Subnetwork Safeguards Proteostasis in Aging and Neurodegenerative Disease. *Cell Rep.* 9 (3), 1135–1150. doi:10.1016/j.celrep.2014.09.042

Bugnon Valdano, M., Massimi, P., Broniarczyk, J., Pim, D., Myers, M., Gardiol, D., et al. (2021). Human Papillomavirus Infection Requires the CCT Chaperonin Complex. *J. Virol.* 95. doi:10.1128/JVI.01943-20

Camasses, A., Bogdanova, A., Shevchenko, A., and Zachariae, W. (2003). The CCT Chaperonin Promotes Activation of the Anaphase-Promoting Complex through the Generation of Functional Cdc20. *Mol. Cell* 12 (1), 87–100. doi:10.1016/s1097-2765(03)00244-2

Carr, A. C., Khaled, A. S., Bassiouni, R., Flores, O., Nierenberg, D., Bhatti, H., et al. (2017). Targeting Chaperonin Containing TCP1 (CCT) as a Molecular Therapeutic for Small Cell Lung Cancer. *Oncotarget* 8 (66), 110273–110288. doi:10.18632/oncotarget.22681

Chang, Y.-X., Lin, Y.-F., Chen, C.-L., Huang, M.-S., Hsiao, M., and Liang, P.-H. (2020). Chaperonin-Containing TCP-1 Promotes Cancer Chemoresistance and Metastasis through the AKT-Gsk3β-β-Catenin and XIAP-Survivin Pathways. *Cancers* 12 (12), 3865. doi:10.3390/cancers12123865

Chen, L., Borozan, I., Milkiewicz, P., Sun, J., Meng, X., Coltescu, C., et al. (2008). Gene Expression Profiling of Early Primary Biliary Cirrhosis: Possible Insights into the Mechanism of Action of Ursodeoxycholic Acid. *Liver Int.* 28 (7), 997–1010. doi:10.1111/j.1478-3231.2008.01744.x

Chen, X.-Q., Fang, F., Florio, J. B., Rockenstein, E., Masliah, E., Mobley, W. C., et al. (2018). T-complex Protein 1-ring Complex Enhances Retrograde Axonal Transport by Modulating Tau Phosphorylation. *Traffic* 19 (11), 840–853. doi:10.1111/tra.12610

Chen, X.-Q. (2019). Involvement of T-Complex Protein 1-ring Complex/chaperonin Containing T-Complex Protein 1 (TRiC/CCT) in Retrograde Axonal Transport through Tau Phosphorylation. *Neural Regen. Res.* 14 (4), 588–590. doi:10.4103/1673-5374.247460

Coffill, C. R., Muller, P. A. J., Oh, H. K., Neo, S. P., Hogue, K. A., Cheok, C. F., et al. (2012). Mutant P53 Interactome Identifies Nardilysin as a p53R273H-specific Binding Partner that Promotes Invasion. *EMBO Rep.* 13 (7), 638–644. doi:10.1038/embor.2012.74

Coghlin, C., Carpenter, B., Dundas, S., Lawrie, L., Telfer, C., and Murray, G. (2006). Characterization and Over-expression of Chaperonin T-Complex Proteins in Colorectal Cancer. *J. Pathol.* 210 (3), 351–357. doi:10.1002/path.2056

Collier, M. P., Moreira, K. B., Li, K. H., Chen, Y.-C., Itzhak, D., Samant, R., et al. (2021). Native Mass Spectrometry Analyses of Chaperonin Complex TRiC/CCT Reveal Subunit N-Terminal Processing and Re-association Patterns. *Sci. Rep.* 11 (1), 13084. doi:10.1038/s41598-021-91086-6

Cong, Y., Baker, M. L., Jakana, J., Woolford, D., Miller, E. J., Reissmann, S., et al. (2010). 4.0-Å Resolution Cryo-EM Structure of the Mammalian Chaperonin TRiC/CCT Reveals its Unique Subunit Arrangement. *Proc. Natl. Acad. Sci. U.S.A.* 107 (11), 4967–4972. doi:10.1073/pnas.0913774107

Cong, Y., Schröder, G. F., Meyer, A. S., Jakana, J., Ma, B., Dougherty, M. T., et al. (2012). Symmetry-free Cryo-EM Structures of the Chaperonin TRiC along its ATPase-Driven Conformational Cycle. *EMBO J.* 31 (3), 720–730. doi:10.1038/emboj.2011.366

Cox, A., Martini, A. C., Ghozlan, H., Moroose, R., Zhu, X., Lee, E., et al. (2022). Chaperonin Containing TCP1 as a Marker for Identification of Circulating Tumor Cells in Blood. *PLoS One*. In press.

Cuéllar, J., Ludlam, W. G., Tensmeyer, N. C., Aoba, T., Dhavale, M., Santiago, C., et al. (2019). Structural and Functional Analysis of the Role of the Chaperonin CCT in mTOR Complex Assembly. *Nat. Commun.* 10 (1), 2865. doi:10.1038/s41467-019-10781-1

Cuéllar, J., Martín-Benito, J., Scheres, S. H. W., Sousa, R., Moro, F., López-Viñas, E., et al. (2008). The Structure of CCT-Hsc70NBD Suggests a Mechanism for Hsp70 Delivery of Substrates to the Chaperonin. *Nat. Struct. Mol. Biol.* 15 (8), 858–864. doi:10.1038/nsmb.1464

Cuéllar, J., Vallin, J., Svanström, A., Maestro-López, M., Bueno-Carrasco, M. T., Ludlam, W. G., et al. (2022). The Molecular Chaperone CCT Sequesters Gelsolin and Protects it from Cleavage by Caspase-3. *J. Mol. Biol.* 434 (5), 167399. doi:10.1016/j.jmb.2021.167399

Culbertson, M. R., and Culbertson, M. R. (1992). Is Yeast TCP1 a Chaperonin? *Nature* 356 (6368), 392. doi:10.1038/356392a0

Darrow, M. C., Sergeeva, O. A., Isas, J. M., Galaz-Montoya, J. G., King, J. A., Langen, R., et al. (2015). Structural Mechanisms of Mutant Huntingtin Aggregation Suppression by the Synthetic Chaperonin-like CCT5 Complex Explained by Cryoelectron Tomography. *J. Biol. Chem.* 290 (28), 17451–17461. doi:10.1074/jbc.M115.655373

Date, Y., Matsuura, A., and Itakura, E. (2022). Disruption of Actin Dynamics Induces Autophagy of the Eukaryotic Chaperonin TRiC/CCT. *Cell Death Discov.* 8 (1), 37. doi:10.1038/s41420-022-00828-6

Dekker, C., Roe, S. M., McCormack, E. A., Beuron, F., Pearl, L. H., and Willison, K. R. (2011a). The Crystal Structure of Yeast CCT Reveals Intrinsic Asymmetry of Eukaryotic Cytosolic Chaperonins. *Embo J.* 30 (15), 3078–3090. doi:10.1038/emboj.2011.208

Dekker, C., Willison, K. R., and Taylor, W. R. (2011b). On the Evolutionary Origin of the Chaperonins. *Proteins* 79 (4), 1172–1192. doi:10.1002/prot.22952

DiFiglia, M., Sapp, E., Chase, K., Schwarz, C., Meloni, A., Young, C., et al. (1995). Huntingtin Is a Cytoplasmic Protein Associated with Vesicles in Human and Rat Brain Neurons. *Neuron* 14 (5), 1075–1081. doi:10.1016/0896-6273(95)90346-1

Dong, Y., Lu, S., Wang, Z., and Liu, L. (2020). CCTs as New Biomarkers for the Prognosis of Head and Neck Squamous Cancer. *Open Med. (Wars)* 15 (1), 672–688. doi:10.1515/med-2020-0114

Douglas, N. R., Reissmann, S., Zhang, J., Chen, B., Jakana, J., Kumar, R., et al. (2011). Dual Action of ATP Hydrolysis Couples Lid Closure to Substrate Release into the Group II Chaperonin Chamber. *Cell* 144 (2), 240–252. doi:10.1016/j.cell.2010.12.017

Elliott, K. L., Svanström, A., Spiess, M., Karlsson, R., and Grantham, J. (2015). A Novel Function of the Monomeric CCTε Subunit Connects the Serum Response Factor Pathway to Chaperone-Mediated Actin Folding. *MBoC* 26 (15), 2801–2809. doi:10.1091/mbc.E15-01-0048

Fares, M. A., and Wolfe, K. H. (2003). Positive Selection and Subfunctionalization of Duplicated CCT Chaperonin Subunits. *Mol. Biol. Evol.* 20 (10), 1588–1597. doi:10.1093/molbev/msg160

Feldman, D. E., Spiess, C., Howard, D. E., and Frydman, J. (2003). Tumorigenic Mutations in VHL Disrupt Folding *In Vivo* by Interfering with Chaperonin Binding. *Mol. Cell* 12 (5), 1213–1224. doi:10.1016/s1097-2765(03)00423-4

Feldman, D. E., Thulasiraman, V., Ferreyra, R. G., and Frydman, J. (1999). Formation of the VHL-Elongin BC Tumor Suppressor Complex Is Mediated by the Chaperonin TRiC. *Mol. Cell* 4 (6), 1051–1061. doi:10.1016/s1097-2765(00)80233-6

Ferreyra, R. G., and Frydman, J. (2000). Purification of the Cytosolic Chaperonin TRiC from Bovine Testis. *Methods Mol. Biol.* 140, 153–160. doi:10.1385/1-59259-061-6:153

Flores, O., Santra, S., Kaittanis, C., Bassiouni, R., Khaled, A. S., Khaled, A. R., et al. (2017). PSMA-targeted Theranostic Nanocarrier for Prostate Cancer. *Theranostics* 7 (9), 2477–2494. doi:10.7150/thno.18879

Ganci, F., Pulito, C., Valsoni, S., Sacconi, A., Turco, C., Vahabi, M., et al. (2020). PI3K Inhibitors Curtail MYC-dependent Mutant P53 Gain-Of-Function in Head and Neck Squamous Cell Carcinoma. *Clin. Cancer Res.* 26 (12), 2956–2971. doi:10.1158/1078-0432.CCR-19-2485

Gao, H., Zheng, M., Sun, S., Wang, H., Yue, Z., Zhu, Y., et al. (2017). Chaperonin Containing TCP1 Subunit 5 Is a Tumor Associated Antigen of Non-small Cell Lung Cancer. *Oncotarget* 8 (38), 64170–64179. doi:10.18632/oncotarget.19369

Gestaut, D., Limatola, A., Joachimiak, L., and Frydman, J. (2019a). The ATP-Powered Gymnastics of TRiC/CCT: an Asymmetric Protein Folding Machine with a Symmetric Origin Story. *Curr. Opin. Struct. Biol.* 55, 50–58. doi:10.1016/j.sbi.2019.03.002

Gestaut, D., Roh, S. H., Ma, B., Pintilie, G., Joachimiak, L. A., Leitner, A., et al. (2019b). The Chaperonin TRiC/CCT Associates with Prefoldin through a Conserved Electrostatic Interface Essential for Cellular Proteostasis. *Cell* 177 (3), 751–765. e715. doi:10.1016/j.cell.2019.03.012

Ghozlan, H., Showalter, A., Lee, E., Zhu, X., and Khaled, A. R. (2021). Chaperonin-Containing TCP1 Complex (CCT) Promotes Breast Cancer Growth through Correlations with Key Cell Cycle Regulators. *Front. Oncol.* 11, 663877. doi:10.3389/fonc.2021.663877

Goudarzi, M., Ross, M. M., Zhou, W., Van Meter, A., Deng, J., Martin, L. M., et al. (2011). Development of a Novel Proteomic Approach for Mitochondrial Proteomics from Cardiac Tissue from Patients with Atrial Fibrillation. *J. Proteome Res.* 10 (8), 3484–3492. doi:10.1021/pr200108m

Grantham, J., Brackley, K. I., and Willison, K. R. (2006). Substantial CCT Activity Is Required for Cell Cycle Progression and Cytoskeletal Organization in Mammalian Cells. *Exp. Cell Res.* 312 (12), 2309–2324. doi:10.1016/j.yexcr.2006.03.028

Guest, S. T., Kratche, Z. R., Bollig-Fischer, A., Haddad, R., and Ethier, S. P. (2015). Two Members of the TRiC Chaperonin Complex, CCT2 and TCP1 Are Essential for Survival of Breast Cancer Cells and Are Linked to Driving Oncogenes. *Exp. Cell Res.* 332 (2), 223–235. doi:10.1016/j.yexcr.2015.02.005

Gutsche, I., Holzinger, J., Rößle, M., Heumann, H., Baumeister, W., and May, R. P. (2000). Conformational Rearrangements of an Archaeal Chaperonin upon ATPase Cycling. *Curr. Biol.* 10 (7), 405–408. doi:10.1016/s0960-9822(00)00421-8

Hallal, S., Russell, B. P., Wei, H., Lee, M. Y. T., Toon, C. W., Sy, J., et al. (2019). Extracellular Vesicles from Neurosurgical Aspirates Identifies Chaperonin Containing TCP1 Subunit 6A as a Potential Glioblastoma Biomarker with Prognostic Significance. *Proteomics* 19 (1-2), 1800157. doi:10.1002/pmic.201800157

Hartl, F. U., Bracher, A., and Hayer-Hartl, M. (2011). Molecular Chaperones in Protein Folding and Proteostasis. *Nature* 475 (7356), 324–332. doi:10.1038/nature10317

Huang, K., Zeng, Y., Xie, Y., Huang, L., and Wu, Y. (2019). Bioinformatics Analysis of the Prognostic Value of CCT6A and Associated Signalling Pathways in Breast Cancer. *Mol. Med. Rep.* 19 (5), 4344–4352. doi:10.3892/mmr.2019.10100

Huang, X., Wang, H., Xu, F., Lv, L., Wang, R., Jiang, B., et al. (2022). Overexpression of Chaperonin Containing TCP1 Subunit 7 Has Diagnostic and Prognostic Value for Hepatocellular Carcinoma. *Aging* 14 (2), 747–769. doi:10.18632/aging.203809

Huang, X., Wang, X., Cheng, C., Cai, J., He, S., Wang, H., et al. (2014). Chaperonin Containing TCP1, Subunit 8 (CCT8) Is Upregulated in Hepatocellular Carcinoma and Promotes HCC Proliferation. *APMIS* 122 (11), a–n. doi:10.1111/apm.12258

Hwang, H., Bowen, B. P., Lefort, N., Flynn, C. R., De Filippis, E. A., Roberts, C., et al. (2010). Proteomics Analysis of Human Skeletal Muscle Reveals Novel Abnormalities in Obesity and Type 2 Diabetes. *Diabetes* 59 (1), 33–42. doi:10.2337/db09-0214

Hynes, G. M., and Willison, K. R. (2000). Individual Subunits of the Eukaryotic Cytosolic Chaperonin Mediate Interactions with Binding Sites Located on Subdomains of β-Actin. *J. Biol. Chem.* 275 (25), 18985–18994. doi:10.1074/jbc.m910297199

Inoue, Y., Aizaki, H., Hara, H., Matsuda, M., Ando, T., Shimoji, T., et al. (2011). Chaperonin TRiC/CCT Participates in Replication of Hepatitis C Virus Genome via Interaction with the Viral NS5B Protein. *Virology* 410 (1), 38–47. doi:10.1016/j.virol.2010.10.026

Jayasinghe, M., Tewmey, C., and Stan, G. (2010). Versatile Substrate Protein Recognition Mechanism of the Eukaryotic Chaperonin CCT. *Proteins* 78 (5), 1254–1265. doi:10.1002/prot.22644

Jiang, J., Liu, C., Xu, G., Liang, T., Yu, C., Liao, S., et al. (2021). CCT6A, a Novel Prognostic Biomarker for Ewing Sarcoma. *Med. Baltim.* 100 (4), e24484. doi:10.1097/MD.0000000000024484

Jin, M., Han, W., Liu, C., Zang, Y., Li, J., Wang, F., et al. (2019). An Ensemble of Cryo-EM Structures of TRiC Reveal its Conformational Landscape and Subunit Specificity. *Proc. Natl. Acad. Sci. U.S.A.* 116 (39), 19513–19522. doi:10.1073/pnas.1903976116

Jirawatnotai, S., Hu, Y., Michowski, W., Elias, J. E., Becks, L., Bienvenu, F., et al. (2011). A Function for Cyclin D1 in DNA Repair Uncovered by Protein Interactome Analyses in Human Cancers. *Nature* 474 (7350), 230–234. doi:10.1038/nature10155

Joachimiak, L. A., Walzthoeni, T., Liu, C. W., Aebersold, R., and Frydman, J. (2014). The Structural Basis of Substrate Recognition by the Eukaryotic Chaperonin TRiC/CCT. *Cell* 159 (5), 1042–1055. doi:10.1016/j.cell.2014.10.042

Kaisari, S., Sitry-Shevah, D., Miniowitz-Shemtov, S., Teichner, A., and Hershko, A. (2017). Role of CCT Chaperonin in the Disassembly of Mitotic Checkpoint Complexes. *Proc. Natl. Acad. Sci. U.S.A.* 114 (5), 956–961. doi:10.1073/pnas.1620451114

Kalisman, N., Schröder, G. F., and Levitt, M. (2013). The Crystal Structures of the Eukaryotic Chaperonin CCT Reveal its Functional Partitioning. *Structure* 21 (4), 540–549. doi:10.1016/j.str.2013.01.017

Kasembeli, M., Lau, W. C. Y., Roh, S.-H., Eckols, T. K., Frydman, J., Chiu, W., et al. (2014). Modulation of STAT3 Folding and Function by TRiC/CCT Chaperonin. *PLoS Biol.* 12 (4), e1001844. doi:10.1371/journal.pbio.1001844

Kim, J.-E., Hong, Y. H., Kim, J. Y., Jeon, G. S., Jung, J. H., Yoon, B.-N., et al. (2017). Altered Nucleocytoplasmic Proteome and Transcriptome Distributions in an *In Vitro* Model of Amyotrophic Lateral Sclerosis. *PLoS One* 12 (4), e0176462. doi:10.1371/journal.pone.0176462

Kim, S., Lee, D., Lee, J., Song, H., Kim, H.-J., and Kim, K.-T. (2015). Vaccinia-Related Kinase 2 Controls the Stability of the Eukaryotic Chaperonin TRiC/CCT by Inhibiting the Deubiquitinating Enzyme USP25. *Mol. Cell Biol.* 35 (10), 1754–1762. doi:10.1128/MCB.01325-14

Kim, S., Park, D.-Y., Lee, D., Kim, W., Jeong, Y.-H., Lee, J., et al. (2014). Vaccinia-related Kinase 2 Mediates Accumulation of Polyglutamine Aggregates via Negative Regulation of the Chaperonin TRiC. *Mol. Cell Biol.* 34 (4), 643–652. doi:10.1128/MCB.00756-13

Kim, S., Willison, K. R., and Horwich, A. L. (1994). Cytosolic Chaperonin Subunits Have a Conserved ATPase Domain but Diverged Polypeptide-Binding Domains. *Trends Biochem. Sci.* 19 (12), 543–548. doi:10.1016/0968-0004(94)90058-2

Kitamura, A., Kubota, H., Pack, C.-G., Matsumoto, G., Hirayama, S., Takahashi, Y., et al. (2006). Cytosolic Chaperonin Prevents Polyglutamine Toxicity with Altering the Aggregation State. *Nat. Cell Biol.* 8 (10), 1163–1169. doi:10.1038/ncb1478

Klimczak, M., Biecek, P., Zylicz, A., and Zylicz, M. (2019). Heat Shock Proteins Create a Signature to Predict the Clinical Outcome in Breast Cancer. *Sci. Rep.* 9 (1), 7507. doi:10.1038/s41598-019-43556-1

Knee, K. M., Sergeeva, O. A., and King, J. A. (2013). Human TRiC Complex Purified from HeLa Cells Contains All Eight CCT Subunits and Is Active *In Vitro*. *Cell Stress Chaperones* 18 (2), 137–144. doi:10.1007/s12192-012-0357-z

Kubota, H., Matsumoto, S., Yokota, S., Yanagi, H., and Yura, T. (1999a). Transcriptional Activation of Mouse Cytosolic Chaperonin CCT Subunit Genes by Heat Shock Factors HSF1 and HSF2. *FEBS Lett.* 461 (1-2), 125–129. doi:10.1016/s0014-5793(99)01437-4

Kubota, H. (2002). Function and Regulation of Cytosolic Molecular Chaperone CCT. *Vitam. Horm.* 65, 313–331. doi:10.1016/s0083-6729(02)65069-1

Kubota, H., Hynes, G., Carne, A., Ashworth, A., and Willison, K. (1994). Identification of Six Tcp-1-Related Genes Encoding Divergent Subunits of the TCP-1-Containing Chaperonin. *Curr. Biol.* 4 (2), 89–99. doi:10.1016/s0960-9822(94)00024-2

Kubota, H., Hynes, G. M., Kerr, S. M., and Willison, K. R. (1997). Tissue-specific Subunit of the Mouse Cytosolic Chaperonin-Containing TCP-1 1. *FEBS Lett.* 402 (1), 53–56. doi:10.1016/s0014-5793(96)01501-3

Kubota, H., Hynes, G., and Willison, K. (1995). The Eighth Cct Gene, Cctq, Encoding the Theta Subunit of the Cytosolic Chaperonin Containing TCP-1. *Gene* 154 (2), 231–236. doi:10.1016/0378-1119(94)00880-2

Kubota, H., Yokota, S.-i., Yanagi, H., and Yura, T. (1999b). Structures and Co-regulated Expression of the Genes Encoding Mouse Cytosolic Chaperonin CCT Subunits. *Eur. J. Biochem.* 262 (2), 492–500. doi:10.1046/j.1432-1327.1999.00405.x

Kubota, H., Yokota, S.-i., Yanagi, H., and Yura, T. (2000). Transcriptional Regulation of the Mouse Cytosolic Chaperonin Subunit Gene Ccta/t-Complex Polypeptide 1 by Selenocysteine tRNA Gene Transcription Activating Factor Family Zinc Finger Proteins. *J. Biol. Chem.* 275 (37), 28641–28648. doi:10.1074/jbc.M005009200

Kubota, S., Kubota, H., and Nagata, K. (2006). Cytosolic Chaperonin Protects Folding Intermediates of Gβ from Aggregation by Recognizing Hydrophobic β-strands. *Proc. Natl. Acad. Sci. U.S.A.* 103 (22), 8360–8365. doi:10.1073/pnas.0600195103

Lee, M. W., Bassiouni, R., Sparrow, N. A., Iketani, A., Boohaker, R. J., Moskowitz, C., et al. (2014). The CT20 Peptide Causes Detachment and Death of Metastatic Breast Cancer Cells by Promoting Mitochondrial Aggregation and Cytoskeletal Disruption. *Cell Death Dis.* 5, e1249. doi:10.1038/cddis.2014.225

Leitner, A., Joachimiak, L. A., Bracher, A., Mönkemeyer, L., Walzthoeni, T., Chen, B., et al. (2012). The Molecular Architecture of the Eukaryotic Chaperonin TRiC/CCT. *Structure* 20 (5), 814–825. doi:10.1016/j.str.2012.03.007

Leslie, K., Lang, C., Devgan, G., Azare, J., Berishaj, M., Gerald, W., et al. (2006). Cyclin D1 Is Transcriptionally Regulated by and Required for Transformation by Activated Signal Transducer and Activator of Transcription 3. *Cancer Res.* 66 (5), 2544–2552. doi:10.1158/0008-5472.CAN-05-2203

Li, L.-J., Zhang, L.-S., Han, Z.-J., He, Z.-Y., Chen, H., and Li, Y.-M. (2017). Chaperonin Containing TCP-1 Subunit 3 Is Critical for Gastric Cancer Growth. *Oncotarget* 8 (67), 111470–111481. doi:10.18632/oncotarget.22838

Li, W., Xu, Y., Wang, X., Cao, G., Bu, W., Wang, X., et al. (2020). circCCT3 Modulates Vascular Endothelial Growth Factor A and Wnt Signaling to Enhance Colorectal Cancer Metastasis through Sponging miR-613. *DNA Cell Biol.* 39 (1), 118–125. doi:10.1089/dna.2019.5139

Lin, Y.-F., Tsai, W.-P., Liu, H.-G., and Liang, P.-H. (2009). Intracellular β-Tubulin/Chaperonin Containing TCP1-β Complex Serves as a Novel Chemotherapeutic Target against Drug-Resistant Tumors. *Cancer Res.* 69 (17), 6879–6888. doi:10.1158/0008-5472.CAN-08-4700

Lindquist, S., and Craig, E. A. (1988). The Heat-Shock Proteins. *Annu. Rev. Genet.* 22, 631–677. doi:10.1146/annurev.ge.22.120188.003215

Liou, A. K. F., McCormack, E. A., and Willison, K. R. (1998). The Chaperonin Containing TCP-1 (CCT). Displays a Single-Ring Mediated Disassembly and Reassembly Cycle. *Biol. Chem.* 379 (3), 311–319. doi:10.1515/bchm.1998.379.3.311

Liou, A. K. F., and Willison, K. R. (1997). Elucidation of the Subunit Orientation in CCT (Chaperonin Containing TCP1) from the Subunit Composition of CCT Micro-complexes. *Embo J.* 16 (14), 4311–4316. doi:10.1093/emboj/16.14.4311

Liu, J., Huang, L., Zhu, Y., He, Y., Zhang, W., Lei, T., et al. (2021a). Exploring the Expression and Prognostic Value of the TCP1 Ring Complex in Hepatocellular Carcinoma and Overexpressing its Subunit 5 Promotes HCC Tumorigenesis. *Front. Oncol.* 11, 739660. doi:10.3389/fonc.2021.739660

Liu, L., Wu, Q., Zhong, W., Chen, Y., Zhang, W., Ren, H., et al. (2020). Microarray Analysis of Differential Gene Expression in Alzheimer's Disease Identifies Potential Biomarkers with Diagnostic Value. *Med. Sci. Monit.* 26, e919249. doi:10.12659/MSM.919249

Liu, P., Kong, L., Jin, H., Wu, Y., Tan, X., and Song, B. (2019a). Differential Secretome of Pancreatic Cancer Cells in Serum-Containing Conditioned Medium Reveals CCT8 as a New Biomarker of Pancreatic Cancer Invasion and Metastasis. *Cancer Cell Int.* 19, 262. doi:10.1186/s12935-019-0980-1

Liu, Q., Qi, Y., Kong, X., Wang, X., Zhang, W., Zhai, J., et al. (2021b). Molecular and Clinical Characterization of CCT2 Expression and Prognosis via Large-Scale Transcriptome Profile of Breast Cancer. *Front. Oncol.* 11, 614497. doi:10.3389/fonc.2021.614497

Liu, X., Lin, C.-Y., Lei, M., Yan, S., Zhou, T., and Erikson, R. L. (2005). CCT Chaperonin Complex Is Required for the Biogenesis of Functional Plk1. *Mol. Cell Biol.* 25 (12), 4993–5010. doi:10.1128/mcb.25.12.4993-5010.2005

Liu, Y.-J., Kumar, V., Lin, Y.-F., and Liang, P.-H. (2017). Disrupting CCT-β : β-tubulin Selectively Kills CCT-β Overexpressed Cancer Cells through MAPKs Activation. *Cell Death Dis.* 8 (9), e3052. doi:10.1038/cddis.2017.425

Liu, Y., Zhang, X., Lin, J., Chen, Y., Qiao, Y., Guo, S., et al. (2019b). CCT3 Acts Upstream of YAP and TFCP2 as a Potential Target and Tumour Biomarker in Liver Cancer. *Cell Death Dis.* 10 (9), 644. doi:10.1038/s41419-019-1894-5

Llorca, O., Martin-Benito, J., Grantham, J., Ritco-Vonsovici, M., Willison, K. R., Carrascosa, J. L., et al. (2001). The 'sequential Allosteric Ring' Mechanism in the Eukaryotic Chaperonin-Assisted Folding of Actin and Tubulin. *EMBO J.* 20 (15), 4065–4075. doi:10.1093/emboj/20.15.4065

Llorca, O., Martin-Benito, J., Ritco-Vonsovici, M., Grantham, J., Hynes, G. M., Willison, K. R., et al. (2000). Eukaryotic Chaperonin CCT Stabilizes Actin and Tubulin Folding Intermediates in Open Quasi-Native Conformations. *EMBO J.* 19 (22), 5971–5979. doi:10.1093/emboj/19.22.5971

Llorca, O., McCormack, E. A., Hynes, G., Grantham, J., Cordell, J., Carrascosa, J. L., et al. (1999a). Eukaryotic Type II Chaperonin CCT Interacts with Actin through Specific Subunits. *Nature* 402 (6762), 693–696. doi:10.1038/45294

Lu, K.-Y., Quan, B., Sylvester, K., Srivastava, T., Fitzgerald, M. C., and Derbyshire, E. R. (2020). Plasmodium Chaperonin TRiC/CCT Identified as a Target of the Antihistamine Clemastine Using Parallel Chemoproteomic Strategy. *Proc. Natl. Acad. Sci. U.S.A.* 117 (11), 5810–5817. doi:10.1073/pnas.1913525117

Machida, K., Masutani, M., Kobayashi, T., Mikami, S., Nishino, Y., Miyazawa, A., et al. (2012). Reconstitution of the Human Chaperonin CCT by Co-expression of the Eight Distinct Subunits in Mammalian Cells. *Protein Expr. Purif.* 82 (1), 61–69. doi:10.1016/j.pep.2011.11.010

Marco, S., Valpuesta, J. M. a., Rivas, G. n., AndrÃ©s, G. n., San MartÃn, C., and Carrascosa, J. L. (1993). A Structural Model for the GroEL Chaperonin. *FEMS Microbiol. Lett.* 106 (3), 301–308. doi:10.1111/j.1574-6968.1993.tb05980.x

Martín-Benito, J., Bertrand, S., Hu, T., Ludtke, P. J., McLaughlin, J. N., Willardson, B. M., et al. (2004). Structure of the Complex between the Cytosolic Chaperonin CCT and Phosducin-like Protein. *Proc. Natl. Acad. Sci. U.S.A.* 101 (50), 17410–17415. doi:10.1073/pnas.0405070101

Miller, M. C., Doyle, G. V., and Terstappen, L. W. M. M. (2010). Significance of Circulating Tumor Cells Detected by the CellSearch System in Patients with Metastatic Breast Colorectal and Prostate Cancer. *J. Oncol.* 2010, 1–8. doi:10.1155/2010/617421

Min, W., Angileri, F., Luo, H., Lauria, A., Shanmugasundaram, M., Almerico, A. M., et al. (2014). A Human CCT5 Gene Mutation Causing Distal Neuropathy Impairs Hexadecamer Assembly in an Archaeal Model. *Sci. Rep.* 4, 6688. doi:10.1038/srep06688

Myslinski, E., Krol, A., and Carbon, P. (1998). ZNF76 and ZNF143 Are Two Human Homologs of the Transcriptional Activator Staf. *J. Biol. Chem.* 273 (34), 21998–22006. doi:10.1074/jbc.273.34.21998

Neef, D. W., Turski, M. L., and Thiele, D. J. (2010). Modulation of Heat Shock Transcription Factor 1 as a Therapeutic Target for Small Molecule Intervention in Neurodegenerative Disease. *PLoS Biol.* 8 (1), e1000291. doi:10.1371/journal.pbio.1000291

Neganova, I., Vilella, F., Atkinson, S. P., Lloret, M., Passos, J. F., von Zglinicki, T., et al. (2011). An Important Role for CDK2 in G1 to S Checkpoint Activation and DNA Damage Response in Human Embryonic Stem Cells. *Stem Cells* 29 (4), 651–659. doi:10.1002/stem.620

Nitika, Porter, C. M., Truman, A. W., and Truttmann, M. C. (2020). Post-translational Modifications of Hsp70 Family Proteins: Expanding the Chaperone Code. *J. Biol. Chem.* 295 (31), 10689–10708. doi:10.1074/jbc.REV120.011666

Nollen, E. A. A., Garcia, S. M., van Haaften, G., Kim, S., Chavez, A., Morimoto, R. I., et al. (2004). Genome-wide RNA Interference Screen Identifies Previously Undescribed Regulators of Polyglutamine Aggregation. *Proc. Natl. Acad. Sci. U.S.A.* 101 (17), 6403–6408. doi:10.1073/pnas.0307697101

Noormohammadi, A., Khodakarami, A., Gutierrez-Garcia, R., Lee, H. J., Koyuncu, S., König, T., et al. (2016). Somatic Increase of CCT8 Mimics Proteostasis of Human Pluripotent Stem Cells and Extends *C. elegans* Lifespan. *Nat. Commun.* 7, 13649. doi:10.1038/ncomms13649

Oftedal, B. E., Maio, S., Handel, A. E., White, M. P. J., Howie, D., Davis, S., et al. (2021). The Chaperonin CCT8 Controls Proteostasis Essential for T Cell Maturation, Selection, and Function. *Commun. Biol.* 4 (1), 681. doi:10.1038/s42003-021-02203-0

Pappenberger, G., Wilsher, J. A., Mark Roe, S., Counsell, D. J., Willison, K. R., and Pearl, L. H. (2002). Crystal Structure of the CCTγ Apical Domain: Implications for Substrate Binding to the Eukaryotic Cytosolic Chaperonin. *J. Mol. Biol.* 318 (5), 1367–1379. doi:10.1016/s0022-2836(02)00190-0

Park, S. H., Jeong, S., Kim, B. R., Jeong, Y. A., Kim, J. L., Na, Y. J., et al. (2020). Activating CCT2 Triggers Gli-1 Activation during Hypoxic Condition in Colorectal Cancer. *Oncogene* 39 (1), 136–150. doi:10.1038/s41388-019-0972-6

Pavel, M., Imarisio, S., Menzies, F. M., Jimenez-Sanchez, M., Siddiqi, F. H., Wu, X., et al. (2016). CCT Complex Restricts Neuropathogenic Protein Aggregation via Autophagy. *Nat. Commun.* 7, 13821. doi:10.1038/ncomms13821

Pereira, J. H., McAndrew, R. P., Sergeeva, O. A., Ralston, C. Y., King, J. A., and Adams, P. D. (2017). Structure of the Human TRiC/CCT Subunit 5 Associated with Hereditary Sensory Neuropathy. *Sci. Rep.* 7 (1), 3673. doi:10.1038/s41598-017-03825-3

Peters, M. J., Broer, L., Willemen, H. L. D. M., Eiriksdottir, G., Hocking, L. J., Holliday, K. L., et al. (2013). Genome-wide Association Study Meta-Analysis of Chronic Widespread Pain: Evidence for Involvement of the 5p15.2 Region. *Ann. Rheum. Dis.* 72 (3), 427–436. doi:10.1136/annrheumdis-2012-201742

Plimpton, R. L., Cuéllar, J., Lai, C. W. J., Aoba, T., Makaju, A., Franklin, S., et al. (2015). Structures of the Gβ-CCT and PhLP1-Gβ-CCT Complexes Reveal a Mechanism for G-Protein β-subunit Folding and Gβγ Dimer Assembly. *Proc. Natl. Acad. Sci. U.S.A.* 112 (8), 2413–2418. doi:10.1073/pnas.1419595112

Powers, E. T., Morimoto, R. I., Dillin, A., Kelly, J. W., and Balch, W. E. (2009). Biological and Chemical Approaches to Diseases of Proteostasis Deficiency. *Annu. Rev. Biochem.* 78 (1), 959–991. doi:10.1146/annurev.biochem.052308.114844

Priya, S., Sharma, S. K., Sood, V., Mattoo, R. U. H., Finka, A., Azem, A., et al. (2013). GroEL and CCT Are Catalytic Unfoldases Mediating Out-Of-Cage Polypeptide Refolding without ATP. *Proc. Natl. Acad. Sci. U.S.A.* 110 (18), 7199–7204. doi:10.1073/pnas.1219867110

Qian, T., Cui, L., Liu, Y., Cheng, Z., Quan, L., Zeng, T., et al. (2020). High Expression of Chaperonin-Containing TCP1 Subunit 3 May Induce Dismal Prognosis in Multiple Myeloma. *Pharmacogenomics J.* 20 (4), 563–573. doi:10.1038/s41397-019-0145-6

Qiu, X., He, X., Huang, Q., Liu, X., Sun, G., Guo, J., et al. (2015). Overexpression of CCT8 and its Significance for Tumor Cell Proliferation, Migration and Invasion in Glioma. *Pathology - Res. Pract.* 211 (10), 717–725. doi:10.1016/j.prp.2015.04.012

Qu, H., Zhu, F., Dong, H., Hu, X., and Han, M. (2020). Upregulation of CCT-3 Induces Breast Cancer Cell Proliferation through miR-223 Competition and Wnt/β-Catenin Signaling Pathway Activation. *Front. Oncol.* 10, 533176. doi:10.3389/fonc.2020.533176

Reissmann, S., Joachimiak, L. A., Chen, B., Meyer, A. S., Nguyen, A., and Frydman, J. (2012). A Gradient of ATP Affinities Generates an Asymmetric Power Stroke Driving the Chaperonin TRIC/CCT Folding Cycle. *Cell Rep.* 2 (4), 866–877. doi:10.1016/j.celrep.2012.08.036

Reissmann, S., Parnot, C., Booth, C. R., Chiu, W., and Frydman, J. (2007). Essential Function of the Built-In Lid in the Allosteric Regulation of Eukaryotic and Archaeal Chaperonins. *Nat. Struct. Mol. Biol.* 14 (5), 432–440. doi:10.1038/nsmb1236

Rivenzon-Segal, D., Wolf, S. G., Shimon, L., Willison, K. R., and Horovitz, A. (2005). Sequential ATP-Induced Allosteric Transitions of the Cytoplasmic Chaperonin Containing TCP-1 Revealed by EM Analysis. *Nat. Struct. Mol. Biol.* 12 (3), 233–237. doi:10.1038/nsmb901

Roh, S.-H., Kasembeli, M., Bakthavatsalam, D., Chiu, W., and Tweardy, D. (2015). Contribution of the Type II Chaperonin, TRiC/CCT, to Oncogenesis. *Ijms* 16 (11), 26706–26720. doi:10.3390/ijms161125975

Roh, S.-H., Kasembeli, M., Galaz-Montoya, J. G., Trnka, M., Lau, W. C.-Y., Burlingame, A., et al. (2016). Chaperonin TRiC/CCT Modulates the Folding and Activity of Leukemogenic Fusion Oncoprotein AML1-ETO. *J. Biol. Chem.* 291 (9), 4732–4741. doi:10.1074/jbc.M115.684878

Rommelaere, H., Van Troys, M., Gao, Y., Melki, R., Cowan, N. J., Vandekerckhove, J., et al. (1993). Eukaryotic Cytosolic Chaperonin Contains T-Complex Polypeptide 1 and Seven Related Subunits. *Proc. Natl. Acad. Sci. U.S.A.* 90 (24), 11975–11979. doi:10.1073/pnas.90.24.11975

Roobol, A., and Carden, M. J. (1999). Subunits of the Eukaryotic Cytosolic Chaperonin CCT Do Not Always Behave as Components of a Uniform Hetero-Oligomeric Particle. *Eur. J. Cell Biol.* 78 (1), 21–32. doi:10.1016/S0171-9335(99)80004-1

Roobol, A., Grantham, J., Whitaker, H. C., and Carden, M. J. (1999a). Disassembly of the Cytosolic Chaperonin in Mammalian Cell Extracts at Intracellular Levels of K+ and ATP. *J. Biol. Chem.* 274 (27), 19220–19227. doi:10.1074/jbc.274.27.19220

Roobol, A., Sahyoun, Z. P., and Carden, M. J. (1999b). Selected Subunits of the Cytosolic Chaperonin Associate with Microtubules Assembled *In Vitro*. *J. Biol. Chem.* 274 (4), 2408–2415. doi:10.1074/jbc.274.4.2408

Rüßmann, F., Stemp, M. J., Mönkemeyer, L., Etchells, S. A., Bracher, A., and Hartl, F. U. (2012). Folding of Large Multidomain Proteins by Partial Encapsulation in the Chaperonin TRiC/CCT. *Proc. Natl. Acad. Sci. U.S.A.* 109 (52), 21208–21215. doi:10.1073/pnas.1218836109

Sanchez-Vega, F., Mina, M., Armenia, J., Chatila, W. K., Luna, A., La, K. C., et al. (2018). Oncogenic Signaling Pathways in the Cancer Genome Atlas. *Cell* 173 (2), 321–e10. doi:10.1016/j.cell.2018.03.035

Sergeeva, O. A., Chen, B., Haase-Pettingell, C., Ludtke, S. J., Chiu, W., and King, J. A. (2013). Human CCT4 and CCT5 Chaperonin Subunits Expressed in *Escherichia coli* Form Biologically Active Homo-Oligomers. *J. Biol. Chem.* 288 (24), 17734–17744. doi:10.1074/jbc.m112.443929

Sergeeva, O. A., Haase-Pettingell, C., and King, J. A. (2019). Co-expression of CCT Subunits Hints at TRiC Assembly. *Cell Stress Chaperones* 24 (6), 1055–1065. doi:10.1007/s12192-019-01028-5

Sergeeva, O. A., Tran, M. T., Haase-Pettingell, C., and King, J. A. (2014). Biochemical Characterization of Mutants in Chaperonin Proteins CCT4 and CCT5 Associated with Hereditary Sensory Neuropathy. *J. Biol. Chem.* 289 (40), 27470–27480. doi:10.1074/jbc.M114.576033

Shahmoradian, S. H., Galaz-Montoya, J. G., Schmid, M. F., Cong, Y., Ma, B., Spiess, C., et al. (2013). TRiC's Tricks Inhibit Huntingtin Aggregation. *Elife* 2, e00710. doi:10.7554/eLife.00710

Shi, X., Cheng, S., and Wang, W. (2018). Suppression of CCT3 Inhibits Malignant Proliferation of Human Papillary Thyroid Carcinoma Cell. *Oncol. Lett.* 15 (6), 9202–9208. doi:10.3892/ol.2018.8496

Shimon, L., Hynes, G. M., McCormack, E. A., Willison, K. R., and Horovitz, A. (2008). ATP-Induced Allostery in the Eukaryotic Chaperonin CCT is Abolished by the Mutation G345D in CCT4 that Renders Yeast Temperature-Sensitive for Growth. *J. Mol. Biol.* 377 (2), 469–477. doi:10.1016/j.jmb.2008.01.011

Showalter, A. E., Martini, A. C., Nierenberg, D., Hosang, K., Fahmi, N. A., Gopalan, P., et al. (2020). Investigating Chaperonin-Containing TCP-1 Subunit 2 as an Essential Component of the Chaperonin Complex for Tumorigenesis. *Sci. Rep.* 10 (1), 798. doi:10.1038/s41598-020-57602-w

Siegers, K., Waldmann, T., Leroux, M. R., Grein, K., Shevchenko, A., Schiebel, E., et al. (1999). Compartmentation of Protein Folding Invivo: Sequestration of Non-native Polypeptide by the Chaperonin-GimC System. *EMBO J.* 18 (1), 75–84. doi:10.1093/emboj/18.1.75

Silver, L. M., Artzt, K., and Bennett, D. (1979). A Major Testicular Cell Protein Specified by a Mouse T/t Complex Gene. *Cell* 17 (2), 275–284. doi:10.1016/0092-8674(79)90153-3

Simizu, S., and Osada, H. (2000). Mutations in the Plk Gene Lead to Instability of Plk Protein in Human Tumour Cell Lines. *Nat. Cell Biol.* 2 (11), 852–854. doi:10.1038/35041102

Soares, H., Penque, D., Mouta, C., and Rodrigues-Pousada, C. (1994). A Tetrahymena Orthologue of the Mouse Chaperonin Subunit CCT Gamma and its Coexpression with Tubulin during Cilia Recovery. *J. Biol. Chem.* 269 (46), 29299–29307. doi:10.1016/s0021-9258(19)62044-2

Sontag, E. M., Joachimiak, L. A., Tan, Z., Tomlinson, A., Housman, D. E., Glabe, C. G., et al. (2013). Exogenous Delivery of Chaperonin Subunit Fragment ApiCCT1 Modulates Mutant Huntingtin Cellular Phenotypes. *Proc. Natl. Acad. Sci. U.S.A.* 110 (8), 3077–3082. doi:10.1073/pnas.1222663110

Sot, B., Rubio-Muñoz, A., Leal-Quintero, A., Martínez-Sabando, J., Marcilla, M., Roodveldt, C., et al. (2017). The Chaperonin CCT Inhibits Assembly of α-synuclein Amyloid Fibrils by a Specific, Conformation-dependent Interaction. *Sci. Rep.* 7 (1), 40859. doi:10.1038/srep40859

Spiess, C., Miller, E. J., McClellan, A. J., and Frydman, J. (2006). Identification of the TRiC/CCT Substrate Binding Sites Uncovers the Function of Subunit Diversity in Eukaryotic Chaperonins. *Mol. cell* 24 (1), 25–37. doi:10.1016/j.molcel.2006.09.003

Stein, K. C., Kriel, A., and Frydman, J. (2019). Nascent Polypeptide Domain Topology and Elongation Rate Direct the Cotranslational Hierarchy of Hsp70 and TRiC/CCT. *Mol. Cell* 75 (6), 1117–1130. doi:10.1016/j.molcel.2019.06.036

Steinemann, M., Schlosser, A., Jank, T., and Aktories, K. (2018). The Chaperonin TRiC/CCT Is Essential for the Action of Bacterial Glycosylating Protein Toxins like *Clostridium difficile* Toxins A and B. *Proc. Natl. Acad. Sci. U.S.A.* 115 (38), 9580–9585. doi:10.1073/pnas.1807658115

Sternlicht, H., Farr, G. W., Sternlicht, M. L., Driscoll, J. K., Willison, K., and Yaffe, M. B. (1993). The T-Complex Polypeptide 1 Complex Is a Chaperonin for Tubulin and Actin *In Vivo*. *Proc. Natl. Acad. Sci. U.S.A.* 90 (20), 9422–9426. doi:10.1073/pnas.90.20.9422

Stirling, P. C., Cuéllar, J., Alfaro, G. A., El Khadali, F., Beh, C. T., Valpuesta, J. M., et al. (2006). PhLP3 Modulates CCT-Mediated Actin and Tubulin Folding via Ternary Complexes with Substrates. *J. Biol. Chem.* 281 (11), 7012–7021. doi:10.1074/jbc.m513235200

Tam, S., Geller, R., Spiess, C., and Frydman, J. (2006). The Chaperonin TRiC Controls Polyglutamine Aggregation and Toxicity through Subunit-specific Interactions. *Nat. Cell Biol.* 8 (10), 1155–1162. doi:10.1038/ncb1477

Tam, S., Spiess, C., Auyeung, W., Joachimiak, L., Chen, B., Poirier, M. A., et al. (2009). The Chaperonin TRiC Blocks a Huntingtin Sequence Element that Promotes the Conformational Switch to Aggregation. *Nat. Struct. Mol. Biol.* 16 (12), 1279–1285. doi:10.1038/nsmb.1700

Tang, N., Cai, X., Peng, L., Liu, H., and Chen, Y. (2020). TCP1 Regulates Wnt7b/β-Catenin Pathway through P53 to Influence the Proliferation and Migration of Hepatocellular Carcinoma Cells. *Sig Transduct. Target Ther.* 5 (1), 169. doi:10.1038/s41392-020-00278-5

Thulasiraman, V., Yang, C. F., and Frydman, J. (1999). *In Vivo* newly Translated Polypeptides Are Sequestered in a Protected Folding Environment. *Embo J.* 18 (1), 85–95. doi:10.1093/emboj/18.1.85

Tokumoto, M., Horiguchi, R., Nagahama, Y., Ishikawa, K., and Tokumoto, T. (2000). Two Proteins, a Goldfish 20S Proteasome Subunit and the Protein Interacting with 26S Proteasome, Change in the Meiotic Cell Cycle. *Eur. J. Biochem.* 267 (1), 97–103. doi:10.1046/j.1432-1327.2000.00962.x

Tong, M., Smeekens, J. M., Xiao, H., and Wu, R. (2020). Systematic Quantification of the Dynamics of Newly Synthesized Proteins Unveiling Their Degradation Pathways in Human Cells. *Chem. Sci.* 11 (13), 3557–3568. doi:10.1039/c9sc06479f

Tracy, C. M., Gray, A. J., Cuéllar, J., Shaw, T. S., Howlett, A. C., Taylor, R. M., et al. (2014). Programmed Cell Death Protein 5 Interacts with the Cytosolic Chaperonin Containing Tailless Complex Polypeptide 1 (CCT) to Regulate β-Tubulin Folding. *J. Biol. Chem.* 289 (7), 4490–4502. doi:10.1074/jbc.M113.542159

Trent, J. D., Nimmesgern, E., Wall, J. S., Hartl, F.-U., and Horwich, A. L. (1991). A Molecular Chaperone from a Thermophilic Archaebacterium Is Related to the Eukaryotic Protein T-Complex Polypeptide-1. *Nature* 354 (6353), 490–493. doi:10.1038/354490a0

Trinidad, A. G., Muller, P. A. J., Cuellar, J., Klejnot, M., Nobis, M., Valpuesta, J. M., et al. (2013). Interaction of P53 with the CCT Complex Promotes Protein Folding and Wild-type P53 Activity. *Mol. Cell* 50 (6), 805–817. doi:10.1016/j.molcel.2013.05.002

Vallin, J., and Grantham, J. (2019). The Role of the Molecular Chaperone CCT in Protein Folding and Mediation of Cytoskeleton-Associated Processes: Implications for Cancer Cell Biology. *Cell Stress Chaperones* 24 (1), 17–27. doi:10.1007/s12192-018-0949-3

Valpuesta, J. M., Llorca, O., Smyth, M. G., Carrascosa, J. L., Willison, K. R., Radermacher, M., et al. (1999b). 3D Reconstruction of the ATP-Bound Form of CCT Reveals the Asymmetric Folding Conformation of a Type II Chaperonin. *Nat. Struct. Biol.* 6 (7), 639–642. doi:10.1038/10689

Valpuesta, J. M., Martı´n-Benito, J., Gómez-Puertas, P., Carrascosa, J. L., and Willison, K. R. (2002). Structure and Function of a Protein Folding Machine: the Eukaryotic Cytosolic Chaperonin CCT. *FEBS Lett.* 529 (1), 11–16. doi:10.1016/s0014-5793(02)03180-0

Wang, G., Zhang, M., Meng, P., Long, C., Luo, X., Yang, X., et al. (2022). Anticarin-β Shows a Promising Anti-osteosarcoma Effect by Specifically Inhibiting CCT4 to Impair Proteostasis. *Acta Pharm. Sin. B.* doi:10.1016/j.apsb.2021.12.024

Wang, X., Venable, J., LaPointe, P., Hutt, D. M., Koulov, A. V., Coppinger, J., et al. (2006). Hsp90 Cochaperone Aha1 Downregulation Rescues Misfolding of CFTR in Cystic Fibrosis. *Cell* 127 (4), 803–815. doi:10.1016/j.cell.2006.09.043

Wells, C. A., Dingus, J., and Hildebrandt, J. D. (2006). Role of the Chaperonin CCT/TRiC Complex in G Protein βγ-Dimer Assembly. *J. Biol. Chem.* 281 (29), 20221–20232. doi:10.1074/jbc.M602409200

Willison, K. R. (2018). The Substrate Specificity of Eukaryotic Cytosolic Chaperonin CCT. *Phil. Trans. R. Soc. B* 373, 20170192. doi:10.1098/rstb.2017.0192

Won, K.-A., Schumacher, R. J., Farr, G. W., Horwich, A. L., and Reed, S. I. (1998). Maturation of Human Cyclin E Requires the Function of Eukaryotic Chaperonin CCT. *Mol. Cell Biol.* 18 (12), 7584–7589. doi:10.1128/mcb.18.12.7584

Xie, H., Hu, H., Chang, M., Huang, D., Gu, X., Xiong, X., et al. (2016a). Identification of Chaperones in a MPP+-induced and ATRA/TPA-differentiated SH-Sy5y Cell PD Model. *Am. J. Transl. Res.* 8 (12), 5659–5671.

Xie, X., Yi, Z., Sinha, S., Madan, M., Bowen, B. P., Langlais, P., et al. (2016b). Proteomics Analyses of Subcutaneous Adipocytes Reveal Novel Abnormalities in Human Insulin Resistance. *Obesity* 24 (7), 1506–1514. doi:10.1002/oby.21528

Xu, G., Bu, S., Wang, X., Zhang, H., and Ge, H. (2020). Suppression of CCT3 Inhibits the Proliferation and Migration in Breast Cancer Cells. *Cancer Cell Int.* 20, 218. doi:10.1186/s12935-020-01314-8

Xu, W.-X., Song, W., Jiang, M.-P., Yang, S.-J., Zhang, J., Wang, D.-D., et al. (2021). Systematic Characterization of Expression Profiles and Prognostic Values of the Eight Subunits of the Chaperonin TRiC in Breast Cancer. *Front. Genet.* 12, 637887. doi:10.3389/fgene.2021.637887

Yam, A. Y., Xia, Y., Lin, H.-T. J., Burlingame, A., Gerstein, M., and Frydman, J. (2008). Defining the TRiC/CCT Interactome Links Chaperonin Function to Stabilization of Newly Made Proteins with Complex Topologies. *Nat. Struct. Mol. Biol.* 15 (12), 1255–1262. doi:10.1038/nsmb.1515

Yamauchi, T., Nishiyama, M., Moroishi, T., Yumimoto, K., and Nakayama, K. I. (2014). MDM2 Mediates Nonproteolytic Polyubiquitylation of the DEAD-Box RNA Helicase DDX24. *Mol. Cell Biol.* 34 (17), 3321–3340. doi:10.1128/MCB.00320-14

Yamazaki, Y., Kubota, H., Nozaki, M., and Nagata, K. (2003). Transcriptional Regulation of the Cytosolic Chaperonin θ Subunit Gene, Cctq, by Ets Domain Transcription Factors Elk-1, Sap-1a, and Net in the Absence of Serum Response Factor. *J. Biol. Chem.* 278 (33), 30642–30651. doi:10.1074/jbc.M212242200

Yang, J. W., Czech, T., Felizardo, M., Baumgartner, C., and Lubec, G. (2006). Aberrant Expression of Cytoskeleton Proteins in hippocampus from Patients with Mesial Temporal Lobe Epilepsy. *Amino Acids* 30 (4), 477–493. doi:10.1007/s00726-005-0281-y

Yang, X., Ren, H., Shao, Y., Sun, Y., Zhang, L., Li, H., et al. (2018). Chaperonin-containing T-complex P-rotein 1 S-ubunit 8 P-romotes C-ell M-igration and I-nvasion in H-uman E-sophageal S-quamous C-ell C-arcinoma by R-egulating α-actin and β-tubulin E-xpression. *Int. J. Oncol.* 52 (6), 2021–2030. doi:10.3892/ijo.2018.4335

Yao, L., Zou, X., and Liu, L. (2019). The TCP1 Ring Complex Is Associated with Malignancy and Poor Prognosis in Hepatocellular Carcinoma. *Int. J. Clin. Exp. Pathol.* 12 (9), 3329–3343.

Ying, Z., Tian, H., Li, Y., Lian, R., Li, W., Wu, S., et al. (2017). CCT6A Suppresses SMAD2 and Promotes Prometastatic TGF-β Signaling. *J. Clin. Invest* 127 (5), 1725–1740. doi:10.1172/JCI90439

Yokota, S.-i., Kayano, T., Ohta, T., Kurimoto, M., Yanagi, H., Yura, T., et al. (2000a). Proteasome-dependent Degradation of Cytosolic Chaperonin CCT. *Biochem. Biophysical Res. Commun.* 279 (2), 712–717. doi:10.1006/bbrc.2000.4011

Yokota, S.-i., Yamamoto, Y., Shimizu, K., Momoi, H., Kamikawa, T., Yamaoka, Y., et al. (2001a). Increased Expression of Cytosolic Chaperonin CCT in Human Hepatocellular and Colonic Carcinoma. *Cell Stress Chaper* 6 (4), 345–350. doi:10.1379/1466-1268(2001)006<0345:ieoccc>2.0.co;2

Yokota, S.-i., Yanagi, H., Yura, T., and Kubota, H. (1999). Cytosolic Chaperonin Is Up-Regulated during Cell Growth. *J. Biol. Chem.* 274 (52), 37070–37078. doi:10.1074/jbc.274.52.37070

Yokota, S.-i., Yanagi, H., Yura, T., and Kubota, H. (2001b). Cytosolic Chaperonin-Containing T-Complex Polypeptide 1 Changes the Content of a Particular Subunit Species Concomitant with Substrate Binding and Folding Activities during the Cell Cycle. *Eur. J. Biochem.* 268 (17), 4664–4673. doi:10.1046/j.1432-1327.2001.02393.x

Yokota, S.-i., Yanagi, H., Yura, T., and Kubota, H. (2000b). Upregulation of Cytosolic Chaperonin CCT Subunits during Recovery from Chemical Stress that Causes Accumulation of Unfolded Proteins. *Eur. J. Biochem.* 267 (6), 1658–1664. doi:10.1046/j.1432-1327.2000.01157.x

Yoo, B. C., Vlkolinsky, R., Engidawork, E., Cairns, N., Fountoulakis, M., and Lubec, G. (2001). Differential Expression of Molecular Chaperones in Brain of Patients with Down Syndrome. *Electrophoresis* 22 (6), 1233–1241. doi:10.1002/1522-2683()22:6<1233::aid-elps1233>3.0.co;2-m

Yu, H., Lee, H., Herrmann, A., Buettner, R., and Jove, R. (2014). Revisiting STAT3 Signalling in Cancer: New and Unexpected Biological Functions. *Nat. Rev. Cancer* 14 (11), 736–746. doi:10.1038/nrc3818

Zang, Y., Jin, M., Wang, H., Cui, Z., Kong, L., Liu, C., et al. (2016). Staggered ATP Binding Mechanism of Eukaryotic Chaperonin TRiC (CCT) Revealed through High-Resolution Cryo-EM. *Nat. Struct. Mol. Biol.* 23 (12), 1083–1091. doi:10.1038/nsmb.3309

Zeng, G., Wang, J., Huang, Y., Lian, Y., Chen, D., Wei, H., et al. (2019). Overexpressing CCT6A Contributes to Cancer Cell Growth by Affecting the G1-To-S Phase Transition and Predicts A Negative Prognosis in Hepatocellular Carcinoma. *Ott* 12, 10427–10439. doi:10.2147/OTT.S229231

Zhang, J., Ye, C., Ruan, X., Zan, J., Xu, Y., Liao, M., et al. (2014). The Chaperonin CCTα Is Required for Efficient Transcription and Replication of Rabies Virus. *Microbiol. Immunol.* 58 (10), 590–599. doi:10.1111/1348-0421.12186

Zhang, Q., Yu, D., Seo, S., Stone, E. M., and Sheffield, V. C. (2012). Intrinsic Protein-Protein Interaction-Mediated and Chaperonin-Assisted Sequential Assembly of Stable Bardet-Biedl Syndrome Protein Complex, the BBSome. *J. Biol. Chem.* 287 (24), 20625–20635. doi:10.1074/jbc.M112.341487

Zhang, T., Shi, W., Tian, K., and Kong, Y. (2020). Chaperonin Containing T-Complex Polypeptide 1 Subunit 6A Correlates with Lymph Node Metastasis, Abnormal Carcinoembryonic Antigen and Poor Survival Profiles in Non-small Cell Lung Carcinoma. *World J. Surg. Onc* 18 (1), 156. doi:10.1186/s12957-020-01911-x

Zhao, X., Chen, X.-Q., Han, E., Hu, Y., Paik, P., Ding, Z., et al. (2016). TRiC Subunits Enhance BDNF Axonal Transport and Rescue Striatal Atrophy in Huntington's Disease. *Proc. Natl. Acad. Sci. U.S.A.* 113 (38), E5655–E5664. doi:10.1073/pnas.1603020113

Zou, Q., Yang, Z.-l., Yuan, Y., Li, J.-h., Liang, L.-f., Zeng, G.-x., et al. (2013). Clinicopathological Features and CCT2 and PDIA2 Expression in Gallbladder Squamous/adenosquamous Carcinoma and Gallbladder Adenocarcinoma. *World J. Surg. Onc* 11 (1), 143. doi:10.1186/1477-7819-11-143

**Conflict of Interest:** The authors declare that AK is a shareholder in Seva Therapeutics, Inc.

The remaining authors declare that the research was conducted in the absence of any commercial or financial relationships that could be construed as a potential conflict of interest.

**Publisher's Note:** All claims expressed in this article are solely those of the authors and do not necessarily represent those of their affiliated organizations, or those of the publisher, the editors and the reviewers. Any product that may be evaluated in this article, or claim that may be made by its manufacturer, is not guaranteed or endorsed by the publisher.

frontiers | Frontiers in Cell and Developmental Biology

MINI REVIEW
published: 16 May 2022
doi: 10.3389/fcell.2022.921739

# *Plasmodium falciparum* Molecular Chaperones: Guardians of the Malaria Parasite Proteome and Renovators of the Host Proteome

*Gregory L. Blatch*[1,2,3]*

[1]The Vice Chancellery, The University of Notre Dame Australia, Fremantle, WA, Australia, [2]Biomedical Biotechnology Research Unit, Department of Biochemistry and Microbiology, Rhodes University, Grahamstown, South Africa, [3]Biomedical Research and Drug Discovery Research Group, Faculty of Health Sciences, Higher Colleges of Technology, Sharjah, United Arab Emirates

*Plasmodium falciparum* is a unicellular protozoan parasite and causative agent of the most severe form of malaria in humans. The malaria parasite has had to develop sophisticated mechanisms to preserve its proteome under the changing stressful conditions it confronts, particularly when it invades host erythrocytes. Heat shock proteins, especially those that function as molecular chaperones, play a key role in protein homeostasis (proteostasis) of *P. falciparum*. Soon after invading erythrocytes, the malaria parasite exports a large number of proteins including chaperones, which are responsible for remodeling the infected erythrocyte to enable its survival and pathogenesis. The infected host cell has parasite-resident and erythrocyte-resident chaperones, which appear to play a vital role in the folding and functioning of *P. falciparum* proteins and potentially host proteins. This review critiques the current understanding of how the major chaperones, particularly the Hsp70 and Hsp40 (or J domain proteins, JDPs) families, contribute to proteostasis of the malaria parasite-infected erythrocytes.

**Keywords: heat shock proteins, molecular chaperones and co-chaperones, malaria parasite, parasitophorous vacuole, proteostasis**

OPEN ACCESS

***Edited by:***
*Francesco Fazi,*
*Sapienza University of Rome, Italy*

***Reviewed by:***
*Paul R. Gilson,*
*Burnet Institute, Australia*

***Correspondence:**
*Gregory L. Blatch*
*g.blatch@ru.ac.za*

***Specialty section:***
*This article was submitted to Signaling, a section of the journal Frontiers in Cell and Developmental Biology*

***Received:*** *16 April 2022*
***Accepted:*** *28 April 2022*
***Published:*** *16 May 2022*

***Citation:***
*Blatch GL (2022) Plasmodium falciparum Molecular Chaperones: Guardians of the Malaria Parasite Proteome and Renovators of the Host Proteome. Front. Cell Dev. Biol. 10:921739. doi: 10.3389/fcell.2022.921739*

## INTRODUCTION

The deadliest human malaria parasite, *Plasmodium falciparum,* has a reduced genome, and yet appears to have dedicated a significant proportion of its genes (~2%) to molecular chaperones (Sargeant et al., 2006), the guardians of protein folding. This suggests that the structural integrity of the proteome is an important aspect of the survival of the malaria parasite. Interestingly, an unusually high proportion of *P. falciparum* proteins (24–30%) are rich in asparagine (N) and glutamine (Q), particularly poly-N repeats (Singh et al., 2004; Pallarès et al., 2018), which have been found to have a tendancy to aggregate (Halfmann et al., 2011). Furthermore, a key phase in the pathology of malaria, is the invasion of host erythrocytes by the parasite, which it completely remodels by exporting over 400 parasite proteins, including a substantial proportion (~5%) of molecular chaperones (Cortés et al., 2020). This massive renovation of the host cell potentially requires unique protein folding pathways involving both parasite and host molecular chaperones (Pesce and Blatch, 2014; Gabriela et al., 2022). This review will critique the evidence indicating that heat shock proteins serving as molecular chaperones, especially Hsp70 and Hsp40 (also called J domain proteins, JDPs) families, are

highly adapted to maintaining the structural and functional integrity of the proteomes of the parasite and potentially the host erythrocyte.

## PfHSP70s ARE THE GUARDIANS OF THE PARASITE-RESIDENT AND EXPORTED PROTEOME

*P. falciparum* has only six Hsp70s (PfHsp70s; Shonhai et al., 2007; Shonhai, 2021) and four Hsp90s (PfHsp90s; Shahinas and Pillai, 2021). However, there is a highly expanded complement of JDPs, with 49 members (PfJDPs; Botha et al., 2007; Njunge et al., 2013; Pesce and Blatch, 2014; Dutta et al., 2021a).

All six PfHsp70s appear to be finely tuned to the malaria parasite lifecycle, playing an important role in parasite survival and virulence (Przyborski et al., 2015), with most being essential (Zhang et al., 2018), and a number of them shown to be inhibited by small molecules with anti-malarial activity (Chiang et al., 2009; Cockburn et al., 2011; Cockburn et al., 2014; Zininga et al. 2017a; Zininga et al. 2017b; Zininga et al. 2017c). The canonical and highly abundant cytoplasmic and nuclear *P. falciparum* Hsp70-1 (PfHsp70-1; Kumar et al., 1991; Pesce et al., 2008) has been shown to be essential (Zhang et al., 2018). PfHsp70-1 is regulated by a number of co-chaperones, including JDPs which deliver specialized substrates (Pesce et al., 2008; Botha et al., 2011; Njunge et al., 2015), *P. falciparum* Hsp70/Hsp90 organizing protein which enables transfer of substrates to PfHsp90 (PfHop; Gitau et al., 2012; Zininga et al., 2015), and the cytosolic Hsp70-like protein, PfHsp70-z (an Hsp110), serving as a nucleotide exchange factor (Zininga et al., 2016). The cytoplasmic PfHsp70-z is also essential (Muralidharan et al., 2012; Zhang et al., 2018), which may well be due to its highly effective protein aggregation suppression activity (Zininga et al., 2016). PfHsp70-1 has also been shown to have high ATPase activity (Matambo et al., 2004; Misra and Ramachandran, 2009; Makumire et al., 2021) and strong aggregation suppression activity (Botha et al., 2011), suggesting that it is a superior chaperone compared to human Hsp70s (Anas et al., 2020). Overall, the evidence suggests that PfHsp70-1 and PfHsp70-z are major players in proteostasis of the parasite cytoplasm.

In the endoplasmic reticulum (ER), there are two Hsp70s, PfHsp70-2 (a BiP/Grp78 homologue) and PfHsp70-y (a Hsp110/Grp170 homologue). PfHsp70-2 is essential (Zhang et al., 2018), and has been proposed to be involved in protein translocation into the ER, working with a PfJDP (PfSec63) and the PfSec translocon (Tuteja, 2007; Blatch and Zimmermann, 2009; Cortés et al., 2020; Shonhai, 2021). PfHsp70-2 was found to functionally associate with another PfJDP (Pfj2) and a protein disulfide isomerase (PDI-8) in the oxidative folding of ER proteins (Cobb et al., 2017). PfHsp70-y has also been shown to be essential, and to potentially interact with, and serve as a nucleotide exchange factor for PfHsp70-2, analogous to the cytoplasmic PfHsp70-z-PfHsp70-1 interaction (Zhang et al., 2018; Kudyba et al., 2019). Overall, the data suggest that these chaperones play an important role in protein quality control and proteostasis within the ER.

Very little is known about the proposed mitochondrial PfHsp70-3, except for the observation that PfHsp70-3 interacted with at least two N-rich malarial antigens (LaCount et al., 2005). Like PfHsp70-3, other PfHsp70s (PfHsp70-1, PfHsp70-z, and PfHsp70-x) have been reported to exhibit a preference for N-rich substrates (Muralidharan et al., 2012; Mabate et al., 2018; Lebepe et al., 2020; Rajapandi, 2020). Therefore, there is growing evidence that PfHsp70s may be finely tuned for the protection of unstable N-rich *P. falciparum* proteins from misfolding and aggregation.

PfHsp70-x is the only exported member of the PfHsp70 family, and has been shown to be localized to the PV and erythrocyte cytosol where it is found free or associated with PfJDPs (PFE0055c and PFA0660w) in mobile lipid containing complexes called J-Dots (Külzer et al., 2012; Grover et al., 2013; Behl and Mishra. 2019). Interestingly, PfHsp70-x is not essential; however, knockout compromised virulence (Charnaud et al., 2017), while knockdown compromised growth under stressful conditions similar to febrile episodes (Day et al., 2019). Recently, the crystal structures of the ATPase (Day et al., 2019) and substrate binding domains (Schmidt and Vakonakis, 2020) of PfHsp70-x were elucidated. Interestingly, PfHsp70-x contains an N-terminal signal sequence for secretion through the ER, but not the *Plasmodium* export element (PEXEL; Marti et al., 2004; Hiller et al., 2004), which has been shown to be required for the export of many *P. falciparum* proteins through the *Plasmodium* translocon of exported proteins (PTEX; de Koning-Ward et al., 2009; Beck et al., 2014; Elsworth et al., 2014; Elsworth et al., 2016). PfHsp70-x, like certain other PEXEL-negative *P. falciparum* proteins (PNEPs), is also successfully exported through the PTEX translocon (Rhiel et al., 2016). We are yet to elucidate exactly how proteins synthesized off the ribosome in the parasite cytosol, are threaded through the ER, across the plasma membrane, through the PV and the PV membrane, and into the erythrocyte cytosol or *via* the Maurer's Cleft to the membrane, where they are folded and begin functioning. However, there is some evidence emerging that suggests that PfHsp70-2 and PfHsp70-x (and potentially other chaperones/co-chaperones such as PfJDPs) may collaborate with the core threading machinery of PTEX, a class I AAA + ATPase (PfHsp101; Russo et al., 2010; Matthews et al., 2019) in the chaperoning of exported *P. falciparum* proteins. For example, it has been shown that PfHsp101 is localized to the ER and the PV (Russo et al., 2010), and is able to preferentially associate with certain PEXEL-containing proteins within these compartments (Gabriela et al., 2022). PfHsp70-2 has been shown to not only interact with proteins secreted into the PV, but also with exported proteins, including the main virulence factor *P. falciparum* erythrocyte membrane protein 1 (PfEMP1; Saridaki et al., 2008; Batinovic et al., 2017; Cortés et al., 2020). In addition, it has been reported that PfHsp70-x associates with PfHsp101 (Charnaud et al., 2017;

Cobb et al., 2017; Zhang et al., 2018) and PfEMP1 (Külzer et al., 2012). Therefore, in addition to its role in protein quality control and proteostasis in the ER, PfHsp70-2 may be playing a major role in the protein trafficking of secreted proteins, and in collaboration with PfHsp70-x also involved in the trafficking of exported proteins. It is tempting to speculate that two protein trafficking and folding pathways exist for exported proteins: 1) a pathway for PEXEL-containing proteins with PfHsp101 being the main chaperone and PfHsp70-2 and PfHsp70-x being auxiliary chaperones; and 2) a pathway for PNEPs with PfHsp70-2 and PfHsp70-x being the main chaperones which hand over to PfHsp101 in the PV or as a component of PTEX.

## PfJDPs HARNESS THE CHAPERONE POWER OF PARASITE AND HOST HSP70s

PfJDPs are ubiquitous, expressed in all compartments of the parasite, in the PV and in the host cell (Dutta et al., 2021a). There is emerging evidence that they play an important role in protein trafficking, folding, assembly and protection from misfolding and aggregation under stressful conditions (Daniyan et al., 2016; Dutta et al., 2021a). The majority of the PfJDPs are essential (Maier et al., 2008; Zhang et al., 2018), and nearly half them are exported into the erythrocyte and play a crucial role in promoting parasite virulence (Dutta et al., 2021a).

A number of the parasite-resident PfJDPs, have been identified as potential co-chaperone of PfHsp70-1 (PfHsp40/PF14_0359, Botha et al., 2011, Anas et al., 2020; PFB0595w, Njunge et al., 2015; and Pfj4/PFL0565w, Pesce et al., 2008). Like PfHsp70-1, PfHsp40 is essential (Zhang et al., 2018), cytosolic, constitutively expressed, and upregulated under stressful conditions (Botha et al., 2011). While they are the homologous chaperone pair to the canonical cytosolic human Hsp70-JDP pair (HSPA1A-DNAJA1), there are subtle but critical structural, biochemical and functional differences, with the *P. falciparum* pair shown to be a more effective chaperone machine (Anas et al., 2020). Furthermore, PfHsp40 has been found to be farnesylated and palmitoylated, leading to membrane localization (Mathews et al., 2021). Notably, farnesyl-PfHsp40 may well be the essential isoform of this PfJDP, as inhibition of farnesylation significantly compromised survival of the parasite under stress conditions.

PfHsp70-PfJDP pairs have also been identified within the ER, and appear to play an important role in protein translocation (PfHsp70-2 and PfSec63/PF13_0102; Marapana et al., 2018) and protein folding and quality control within that compartment (PfHsp70-2 and Pfj2/PF11_0099; Cobb et al., 2017). At least one PfJDP has been shown to be secreted through the ER, and partially localized to the PV (PFF1415c; Khosh-Naucke et al., 2018). PFF1415c was found to be essential for growth of erythrocyte-stage parasites; however, its precise function is yet to be determined. Pfj1 (PFD0462w) is the only PfJDP reported to be localized to the apicoplast (Kumar et al., 2010), which was contrary to a previous report which proposed it was targeted to the mitochondrion (Watanabe, 1987). Pfj1 has an unusually long and unique C-terminal region, and has been proposed to be capable of binding to the apicoplast genome and play a role in DNA replication (Kumar et al., 2010). Interesting, Pfj1 has been shown to have a functional J domain (Nicoll et al., 2007), and therefore is likely to associate with a partner Hsp70; however, none of the PfHsp70s have been shown to localize to the apicoplast.

A number of recent reports suggest that the exported PfJDPs may serve as co-chaperones of not only the exported PfHsp70-x, but also the host Hsp70. As mentioned in the previous section, two of the exported PfJDPs (PFA0660w and PFE0055c) associate with PfHsp70-x in J-dots within the erythrocyte cytosol (Külzer et al., 2010; Külzer et al., 2012; Grover et al., 2013; Petersen et al., 2016), and have been shown to be co-chaperones of PfHsp70-x (Daniyan et al., 2016; Dutta et al., 2021b). It has been proposed that these J-dots play a role in the trafficking and folding of exported proteins (Külzer et al., 2012; Behl et al., 2019; Gabriela et al., 2022). Interestingly, one of the J-Dot PfJDPs, PFE0055c, was found to be essential (Zhang et al., 2018), while the other (PFA0660w) was not. However, functional disruption of PFA0660w was found to causes defects in knob formation and cytoadherence, with further genetic and biochemical studies suggesting that the role of PFA0660w in host cell modification involved host Hsp70 (Diehl et al., 2021; **Table 1**). This finding is consistent with a previous study using a yeast two-hybrid system, which reported an interaction between three exported PfJDPs (PFA0660w, PFE0055c, and PFB0090c) and human Hsp70 (Jha et al., 2017; **Table 1**). PFB0090c, also called knob-associated Hsp40 (KAHsp40; structurally similar to PFE0055c and PFA0660w), has been shown to interact with components of PTEX and knobs, and may be involved in the genesis of knob complexes (Acharya et al., 2012). It is well established that the knob protein complex does not contain PfHsp70-x, but rather, host chaperones (Hsp70, Hsp90, and Hop), and there is significant evidence that human Hsp70 is involved in the assembly of knob protein complexes (Banumathy et al., 2002; Alampalli et al., 2018). Hence, it is plausible that PFB0090c occurs in a common complex with human Hsp70, and potentially serves as its co-chaperone (**Table 1**).

The largest group of PfJDPs are those members containing a J domain with a corrupted HPD motif (so-called type IVs), most of which appear to be exported (Botha et al., 2007; Njunge et al., 2013; Daniyan and Blatch, 2017). In fact, there is evidence that a number of the exported type IV PfJDPs are essential for parasite survival (e.g., PFB0085c and PF14_0013; Zhang et al., 2018), required for growth or survival under febrile conditions [e.g., PFA0110w, the ring-infected erythrocyte surface antigen protein (RESA); Silva et al., 2005; Diez-Silva et al., 2012], or involved in pathogenesis (e.g., PF10_0381; knockout causes loss of knobs; Maier et al., 2008). Recently, an exported type IV PfJDP, called eCiJP/PF11_0034 (and a paralogue of PF10_0381), was found to localize to J-Dots, associate with the erythrocyte cytoskeleton, and to potentially interact with host Hsp70 (HSPA1A) (Sahu et al., 2022; **Table 1**).

**TABLE 1 |** Exported PfJDPs shown to functionally associate with PfHsp70-x or human Hsp70.

| PlasmoDB | Common name | Proposed function | Hsp70 partner | References |
|---|---|---|---|---|
| PFA0660w | | Localized to J-Dots; Folding of exported proteins (e.g., PfEMP1) | PfHsp70-x; hHsp70 | Külzer et al. (2010; 2012); Grover et al. (2013); Daniyan et al. (2016); Jha et al. (2017); Behl et al. (2019); Diehl et al. (2021) |
| PFE0055c | | Localized to J-Dots; Folding of exported proteins (e.g., PfEMP1) | PfHsp70-x; hHsp70 | Küzer et al. (2010; 2012); Jha et al. (2017); Dutta et al. (2021b) |
| PFB0090c | KAHsp40 | Localized to knobs; Folding and assembly of knob complexes | hHsp70 | Acharya et al. (2012); Jha et al. (2017) |
| PF110034 | eCiJP | Localized to J-Dots and the erythrocyte cytoskeleton; Folding of exported proteins; Folding and assembly of the cytoskeleton | PfHsp70-x; hHsp70 | Sahu et al. (2022) |

## CONCLUSION

The malaria parasite has adapted to its pathological co-existence with the human host, enabling it to overcome the extreme physiological and cellular challenges that it faces, particularly during the erythrocytic stages of the life cycle. *P. falciparum* appears to have finely tuned its molecular chaperone machinery to be highly efficient, particularly its PfHsp70-PfJDP pairs, which are found in most compartments of the parasite-infected erythrocyte. Most of these *P. falciparum* PfHsp70-PfJDP partnerships appears to have evolved to efficiently protect the N-repeat-rich parasite proteome from the toxic effects of aggregation and misfolding. Furthermore, and perhaps as importantly, the parasite appears to have harnessed the host Hsp70 chaperone machinery to enable it to renovate the infected erythrocyte for its survival and pathology. The molecular details of this host-parasite interface represent an important frontier of future research endeavours.

## AUTHOR CONTRIBUTIONS

GB developed the conceptual framework for this review and wrote the article.

## FUNDING

GB acknowledges the financial support of Higher Colleges of Technology, UAE (Interdisciplinary Research Grant, IRG, grant number 213471), and Rhodes University, South Africa (Rated Researcher Grant).

## REFERENCES

Acharya, P., Chaubey, S., Grover, M., and Tatu, U. (2012). An Exported Heat Shock Protein 40 Associates with Pathogenesis-Related Knobs in *Plasmodium falciparum* Infected Erythrocytes. *PloS One* 7, e44605. doi:10.1371/journal.pone.0044605

Alampalli, S. V., Grover, M., Chandran, S., Tatu, U., and Acharya, P. (2018). Proteome and Structural Organization of the Knob Complex on the Surface of the *Plasmodium* Infected Red Blood Cell. *Proteomics Clin. Appl.* 12, e1600177. doi:10.1002/prca.201600177

Anas, M., Shukla, A., Tripathi, A., Kumari, V., Prakash, C., Nag, P., et al. (2020). Structural-functional Diversity of Malaria Parasite's PfHSP70-1 and PfHSP40 Chaperone Pair Gives an Edge over Human Orthologs in Chaperone-Assisted Protein Folding. *Biochem. J.* 477, 3625–3643. doi:10.1042/bcj20200434

Banumathy, G., Singh, V., and Tatu, U. (2002). Host Chaperones Are Recruited in Membrane-Bound Complexes by *Plasmodium falciparum*. *J. Biol. Chem.* 277, 3902–3912. doi:10.1074/jbc.m110513200

Batinovic, S., McHugh, E., Chisholm, S. A., Matthews, K., Liu, B., Dumont, L., et al. (2017). An Exported Protein-Interacting Complex Involved in the Trafficking of Virulence Determinants in *Plasmodium*-Infected Erythrocytes. *Nat. Commun.* 8, 16044. doi:10.1038/ncomms16044

Beck, J. R., Muralidharan, V., Oksman, A., and Goldberg, D. E. (2014). PTEX Component HSP101 Mediates Export of Diverse Malaria Effectors into Host Erythrocytes. *Nature* 511, 592–595. doi:10.1038/nature13574

Behl, A., and Mishra, P. C. (2019). Structural Insights into the Binding Mechanism of *Plasmodium falciparum* Exported Hsp40-Hsp70 Chaperone Pair. *Comput. Biol. Chem.* 83, 107099. doi:10.1016/j.compbiolchem.2019.107099

Behl, A., Kumar, V., and Bisht, A. (2019). Cholesterol Bound *Plasmodium falciparum* Co-chaperone 'PFA0660w'complexes with Major Virulence Factor 'PfEMP1'via Chaperone 'PfHsp70-X. *Sci. Rep.* 9, 1–7. doi:10.1038/s41598-019-39217-y

Botha, M., Pesce, E.-R., and Blatch, G. L. (2007). The Hsp40 Proteins of *Plasmodium falciparum* and Other Apicomplexa: Regulating Chaperone Power in the Parasite and the Host. *Int. J. Biochem. Cell Biol.* 39, 1781–1803. doi:10.1016/j.biocel.2007.02.011

Botha, M., Chiang, A. N., Needham, P. G., Stephens, L. L., Hoppe, H. C., Külzer, S., et al. (2011). *Plasmodium falciparum* Encodes a Single Cytosolic Type I Hsp40 that Functionally Interacts with Hsp70 and Is Upregulated by Heat Shock. *Cell Stress Chaperones* 16, 389–401. doi:10.1007/s12192-010-0250-6

Charnaud, S. C., Dixon, M. W. A., Nie, C. Q., Chappell, L., Sanders, P. R., Nebl, T., et al. (2017). The Exported Chaperone Hsp70-X Supports Virulence Functions for *Plasmodium falciparum* Blood Stage Parasites. *PLoS One* 12, e0181656. doi:10.1371/journal.pone.0181656

Chiang, A. N., Valderramos, J.-C., Balachandran, R., Chovatiya, R. J., Mead, B. P., Schneider, C., et al. (2009). Select Pyrimidinones Inhibit the Propagation of the Malarial Parasite, *Plasmodium falciparum*. *Bioorg. Med. Chem.* 17, 1527–1533. doi:10.1016/j.bmc.2009.01.024

Cobb, D. W., Florentin, A., Fierro, M. A., Krakowiak, M., Moore, J. M., and Muralidharan, V. (2017). The Exported Chaperone PfHsp70x Is Dispensable for the *Plasmodium falciparum* Intraerythrocytic Life Cycle. *MSphere* 2, e00363–17. doi:10.1128/mSphere.00363-17

Cockburn, I. L., Pesce, E. R., Pryzborski, J. M., Davies-Coleman, M. T., Clark, P. G., Keyzers, R. A., et al. (2011). Screening for Small Molecule Modulators of Hsp70 Chaperone Activity Using Protein Aggregation Suppression Assays: Inhibition of the Plasmodial Chaperone PfHsp70-1. *Biol. Chem.* 392, 431–438. doi:10.1515/BC.2011.040

Cockburn, I. L., Boshoff, A., Pesce, E.-R., and Blatch, G. L. (2014). Selective Modulation of Plasmodial Hsp70s by Small Molecules with Antimalarial Activity. *Biol. Chem.* 395, 1353–1362. doi:10.1515/hsz-2014-0138

Cortés, G. T., Wiser, M. F., and Gómez-Alegría, C. J. (2020). Identification of *Plasmodium falciparum* HSP70-2 as a Resident of the *Plasmodium* Export Compartment. *Heliyon* 6, e04037.

Daniyan, M. O., and Blatch, G. L. (2017). Plasmodial Hsp40s: New Avenues for Antimalarial Drug Discovery. *Curr. Pharm. Des.* 23, 4555–4570. doi:10.2174/1381612823666170124142439

Daniyan, M. O., Boshoff, A., Prinsloo, E., Pesce, E.-R., and Blatch, G. L. (2016). The Malarial Exported PFA0660w Is an Hsp40 Co-chaperone of PfHsp70-X. *PLoS ONE* 11, e0148517. doi:10.1371/journal.pone.0148517

Day, J., Passecker, A., Beck, H.-P., and Vakonakis, I. (2019). The *Plasmodium falciparum* Hsp70-X Chaperone Assists the Heat Stress Response of the Malaria Parasite. *FASEB J.* 33, 14611–14624. doi:10.1096/fj.201901741r

de Koning-Ward, T. F., Gilson, P. R., Boddey, J. A., Rug, M., Smith, B. J., Papenfuss, A. T., et al. (2009). A Newly Discovered Protein Export Machine in Malaria Parasites. *Nature* 459, 945–949. doi:10.1038/nature08104

Diehl, M., Roling, L., Rohland, L., Weber, S., Cyrklaff, M., Sanchez, C. P., et al. (2021). Co-chaperone Involvement in Knob Biogenesis Implicates Host-Derived Chaperones in Malaria Virulence. *PLoS Pathog.* 17, e1009969. doi:10.1371/journal.ppat.1009969

Diez-Silva, M., Park, Y., Huang, S., Bow, H., Mercereau-Puijalon, O., Deplaine, G., et al. (2012). Pf155/RESA Protein Influences the Dynamic Micro-Circulatory Behavior of Ring-Stage *Plasmodium falciparum* Infected Red Blood Cells. *Sci. Rep.* 2, 614. doi:10.1038/srep00614

Dutta, T., Pesce, E.-R., Maier, A. G., and Blatch, G. L. (2021a). Role of the J Domain Protein Family in the Survival and Pathogenesis of *Plasmodium falciparum*. *Adv. Exp. Med. Biol.* 1340, 97–123. doi:10.1007/978-3-030-78397-6_4

Dutta, T., Singh, H., Gestwicki, J. E., and Blatch, G. L. (2021b). Exported Plasmodial J Domain Protein, PFE0055c, and PfHsp70-X Form a Specific Co-chaperone-chaperone Partnership. *Cell Stress Chaperones* 26, 355–366. doi:10.1007/s12192-020-01181-2

Elsworth, B., Matthews, K., Nie, C. Q., Kalanon, M., Charnaud, S. C., Sanders, P. R., et al. (2014). PTEX Is an Essential Nexus for Protein Export in Malaria Parasites. *Nature* 511, 587–591. doi:10.1038/nature13555

Elsworth, B., Sanders, P. R., Nebl, T., Batinovic, S., Kalanon, M., Nie, C. Q., et al. (2016). Proteomic Analysis Reveals Novel Proteins Associated with the *Plasmodium* Protein Exporter PTEX and a Loss of Complex Stability upon Truncation of the Core PTEX Component, PTEX150. *Cell. Microbiol.* 18, 1551–1569. doi:10.1111/cmi.12596

Gabriela, M., Matthews, K. M., Boshoven, C., Kouskousis, B., Jonsdottir, T. K., Bullen, H. E., et al. (2022). A Revised Mechanism for How *Plasmodium falciparum* Recruits and Exports Proteins into its Erythrocytic Host Cell. *PLoS Pathog.* 18, e1009977. doi:10.1371/journal.ppat.1009977

Gitau, G. W., Mandal, P., Blatch, G. L., Przyborski, J., and Shonhai, A. (2012). Characterisation of the *Plasmodium falciparum* Hsp70-Hsp90 Organising Protein (PfHop). *Cell Stress Chaperones* 17, 191–202. doi:10.1007/s12192-011-0299-x

Grover, M., Chaubey, S., Ranade, S., and Tatu, U. (2013). Identification of an Exported Heat Shock Protein 70 in *Plasmodium falciparum*. *Parasite* 20, 2. doi:10.1051/parasite/2012002

Halfmann, R., Alberti, S., Krishnan, R., Lyle, N., O'Donnell, C. W., King, O. D., et al. (2011). Opposing Effects of Glutamine and Asparagine Govern Prion Formation by Intrinsically Disordered Proteins. *Mol. Cell* 43, 72–84. doi:10.1016/j.molcel.2011.05.013

Hiller, N. L., Bhattacharjee, S., van Ooij, C., Liolios, K., Harrison, T., LopezEstraño, C., et al. (2004). A Host-Targeting Signal in Virulence Proteins Reveals a Secretome in Malarial Infection. *Science* 306, 1934–1937. doi:10.1126/science.1102737

Jha, P., Laskar, S., Dubey, S., Bhattacharyya, M. K., and Bhattacharyya, S. (2017). *Plasmodium* Hsp40 and Human Hsp70: A Potential Cochaperone-Chaperone Complex. *Mol. Biochem. Parasitol.* 214, 10–13. doi:10.1016/j.molbiopara.2017.03.003

Khosh-Naucke, M., Becker, J., Mesén-Ramírez, P., Kiani, P., Birnbaum, J., Fröhlke, U., et al. (2018). Identification of Novel Parasitophorous Vacuole Proteins in *P. falciparum* Parasites Using BioID. *Int. J. Med. Microbiol.* 308, 13–24. doi:10.1016/j.ijmm.2017.07.007

Kudyba, H. M., Cobb, D. W., Fierro, M. A., Florentin, A., Ljolje, D., Singh, B., et al. (2019). The Endoplasmic Reticulum Chaperone PfGRP170 Is Essential for Asexual Development and Is Linked to Stress Response in Malaria Parasites. *Cell Microbiol.* 21, e13042. doi:10.1111/cmi.13042

Külzer, S., Rug, M., Brinkmann, K., Cannon, P., Cowman, A., Lingelbach, K., et al. (2010). Parasite-encoded Hsp40 Proteins Define Novel Mobile Structures in the Cytosol of the *P. falciparum*-Infected Erythrocyte. *Cell Microbiol.* 12, 1398–1420. doi:10.1111/j.1462-5822.2010.01477.x

Külzer, S., Charnaud, S., Dagan, T., Riedel, J., Mandal, P., Pesce, E. R., et al. (2012). *Plasmodium falciparum*-encoded Exported Hsp70/hsp40 Chaperone/co-Chaperone Complexes within the Host Erythrocyte. *Cell Microbiol.* 14, 1784–1795. doi:10.1111/j.1462-5822.2012.01840.x

Kumar, N., Koski, G., Harada, M., Aikawa, M., and Zheng, H. (1991). Induction and Localization of *Plasmodium falciparum* Stress Proteins Related to the Heat Shock Protein 70 Family. *Mol. Biochem. Parasitol.* 48, 47–58. doi:10.1016/0166-6851(91)90163-z

Kumar, A., Tanveer, A., Biswas, S., Ram, E. V. S. R., Gupta, A., Kumar, B., et al. (2010). Nuclear-encoded DnaJ Homologue of *Plasmodium falciparum* interacts with Replicationori of the Apicoplast Genome. *Mol. Microbiol.* 75, 942–956. doi:10.1111/j.1365-2958.2009.07033.x

LaCount, D. J., Vignali, M., Chettier, R., Phansalkar, A., Bell, R., Hesselberth, J. R., et al. (2005). A Protein Interaction Network of the Malaria Parasite *Plasmodium falciparum*. *Nature* 438, 103–107. doi:10.1038/nature04104

Lebepe, C. M., Matambanadzo, P. R., Makhoba, X. H., Achilonu, I., Zininga, T., and Shonhai, A. (2020). Comparative Characterization of *Plasmodium falciparum* Hsp70-1 Relative to E. coli DnaK Reveals the Functional Specificity of the Parasite Chaperone. *Biomolecules* 10, 856. doi:10.3390/biom10060856

Mabate, B., Zininga, T., Ramatsui, L., Makumire, S., Achilonu, I., Dirr, H. W., et al. (2018). Structural and Biochemical Characterization of *Plasmodium falciparum* Hsp70-X Reveals Functional Versatility of its C-Terminal EEVN Motif. *Proteins* 86, 1189–1201. doi:10.1002/prot.25600

Maier, A. G., Rug, M., O'Neill, M. T., Brown, M., Chakravorty, S., Szestak, T., et al. (2008). Exported Proteins Required for Virulence and Rigidity of *Plasmodium falciparum*-Infected Human Erythrocytes. *Cell* 134, 48–61. doi:10.1016/j.cell.2008.04.051

Makumire, S., Dongola, T. H., Chakafana, G., Tshikonwane, L., Chauke, C. T., Maharaj, T., et al. (2021). Mutation of GGMP Repeat Segments of *Plasmodium falciparum* Hsp70-1 Compromises Chaperone Function and Hop Co-chaperone Binding. *Ijms* 22, 2226. doi:10.3390/ijms22042226

Marapana, D. S., Dagley, L. F., Sandow, J. J., Nebl, T., Triglia, T., Pasternak, M., et al. (2018). Plasmepsin V Cleaves Malaria Effector Proteins in a Distinct Endoplasmic Reticulum Translocation Interactome for Export to the Erythrocyte. *Nat. Microbiol.* 3, 1010–1022. doi:10.1038/s41564-018-0219-2

Marti, M., Good, R. T., Rug, M., Knuepfer, E., and Cowman, A. F. (2004). Targeting Malaria Virulence and Remodeling Proteins to the Host Erythrocyte. *Science* 306, 1930–1933. doi:10.1126/science.1102452

Matambo, T. S., Odunuga, O. O., Boshoff, A., and Blatch, G. L. (2004). Overproduction, Purification, and Characterization of the *Plasmodium falciparum* Heat Shock Protein 70. *Protein Expr. Purif.* 33, 214–222. doi:10.1016/j.pep.2003.09.010

Mathews, E. S., Jezewski, A. J., and Odom John, A. R. (2021). Protein Prenylation and Hsp40 in Thermotolerance of *Plasmodium falciparum* Malaria Parasites. *mBio* 12, e0076021. doi:10.1128/mBio.00760-21

Matthews, K. M., Kalanon, M., and de Koning-Ward, T. F. (2019). Uncoupling the Threading and Unfoldase Actions of *Plasmodium* HSP101 Reveals Differences in Export between Soluble and Insoluble Proteins. *mBio* 10, e01106–19. doi:10.1128/mBio.01106-19

Misra, G., and Ramachandran, R. (2009). Hsp70-1 from *Plasmodium falciparum*: Protein Stability, Domain Analysis and Chaperone Activity. *Biophys. Chem.* 142, 55–64. doi:10.1016/j.bpc.2009.03.006

Muralidharan, V., Oksman, A., Pal, P., Lindquist, S., and Goldberg, D. E. (2012). *Plasmodium falciparum* Heat Shock Protein 110 Stabilizes the Asparagine Repeat-Rich Parasite Proteome during Malarial Fevers. *Nat. Commun.* 3, 1310. doi:10.1038/ncomms2306

Nicoll, W. S., Botha, M., McNamara, C., Schlange, M., Pesce, E.-R., Boshoff, A., et al. (2007). Cytosolic and ER J-Domains of Mammalian and Parasitic Origin Can Functionally Interact with DnaK. *Int. J. Biochem. Cell Biol.* 39, 736–751. doi:10.1016/j.biocel.2006.11.006

Njunge M., J., Ludewig H., M., Boshoff, A., Pesce, E.-R., and Blatch L., G. (2013). Hsp70s and J Proteins of *Plasmodium* Parasites Infecting Rodents and Primates: Structure, Function, Clinical Relevance, and Drug Targets. *Curr. Pharm. Des.* 19, 387–403. doi:10.2174/138161213804143734

Njunge, J. M., Mandal, P., Przyborski, J. M., Boshoff, A., Pesce, E.-R., and Blatch, G. L. (2015). PFB0595w Is a *Plasmodium falciparum* J Protein that Co-localizes with PfHsp70-1 and Can Stimulate its *In Vitro* ATP Hydrolysis Activity. *Int. J. Biochem. Cell Biol.* 62, 47–53. doi:10.1016/j.biocel.2015.02.008

Pallare`s, I., de Groot, N. S., Iglesias, V., Sant'Anna, R., Biosca, A., Ferna`ndez-Busquets, X., et al. (2018). Discovering Putative Prion-like Proteins in *Plasmodium falciparum*: a Computational and Experimental Analysis. *Front. Microbiol.* 9, 1737.

Pesce, E.-R., and Blatch, G. L. (2014). Plasmodial Hsp40 and Hsp70 Chaperones: Current and Future Perspectives. *Parasitology* 141, 1167–1176. doi:10.1017/s003118201300228x

Pesce, E.-R., Acharya, P., Tatu, U., Nicoll, W. S., Shonhai, A., Hoppe, H. C., et al. (2008). The *Plasmodium falciparum* Heat Shock Protein 40, Pfj4, Associates with Heat Shock Protein 70 and Shows Similar Heat Induction and Localisation Patterns. *Int. J. Biochem. Cell Biol.* 40, 2914–2926. doi:10.1016/j.biocel.2008.06.011

Petersen, W., Külzer, S., Engels, S., Zhang, Q., Ingmundson, A., Rug, M., et al. (2016). J-dot Targeting of an Exported HSP40 in *Plasmodium falciparum*-infected Erythrocytes. *Int. J. Parasitol.* 46, 519–525. doi:10.1016/j.ijpara.2016.03.005

Przyborski, J. M., Diehl, M., and Blatch, G. L. (2015). Plasmodial Hsp70s Are Functionally Adapted to the Malaria Parasite Life Cycle. *Front. Mol. Biosci.* 2, 34. doi:10.3389/fmolb.2015.00034

Rajapandi, T. (2020). Chaperoning of Asparagine Repeat-Containing Proteins in *Plasmodium falciparum*. *J Parasit. Dis.* 44, 687–693. doi:10.1007/s12639-020-01251-3

Rhiel, M., Bittl, V., Tribensky, A., Charnaud, S. C., Strecker, M., Müller, S., et al. (2016). Trafficking of the Exported *P. falciparum* Chaperone PfHsp70x. *Sci. Rep.* 6, 36174. doi:10.1038/srep36174

Russo, I., Babbitt, S., Muralidharan, V., Butler, T., Oksman, A., and Goldberg, D. E. (2010). Plasmepsin V Licenses *Plasmodium* Proteins for Export into the Host Erythrocyte. *Nature* 463, 632–636. doi:10.1038/nature08726

Sahu, W., Bai, T., Panda, P. K., Mazumder, A., Das, A., Ojha, D. K., et al. (2022). *Plasmodium falciparum* HSP40 Protein eCiJp Traffics to the Erythrocyte Cytoskeleton and Interacts with the Human HSP70 Chaperone HSPA1. *FEBS Lett.* 596, 95–111. doi:10.1002/1873-3468.14255

Sargeant, T. J., Marti, M., Caler, E., Carlton, J. M., Simpson, K., Speed, T. P., et al. (2006). Lineage-specific Expansion of Proteins Exported to Erythrocytes in Malaria Parasites. *Genome Biol.* 7, R12. doi:10.1186/gb-2006-7-2-r12

Saridaki, T., Sanchez, C. P., Pfahler, J., and Lanzer, M. (2008). A Conditional Export System Provides New Insights Into Protein Export in *Plasmodium falciparum*-Infected Erythrocytes. *Cell Microbiol.* 1, 2483–2495. doi:10.1111/j.1462-5822.2008.01223.x

Schmidt, J., and Vakonakis, I. (2020). Structure of the Substrate-Binding Domain of *Plasmodium falciparum* Heat-Shock Protein 70-x. *Acta Cryst. Sect. F.* 76, 495–500. doi:10.1107/s2053230x2001208x

Shahinas, D., and Pillai, D. R. (2021). Role of Hsp90 in *Plasmodium falciparum* Malaria. *Adv. Exp. Med. Biol.* 1340, 125–139. doi:10.1007/978-3-030-78397-6_5

Shonhai, A., Boshoff, A., and Blatch, G. L. (2007). The Structural and Functional Diversity of Hsp70 Proteins from *Plasmodium falciparum*. *Protein Sci.* 16, 1803–1818. doi:10.1110/ps.072918107

Shonhai, A. (2021). The Role of Hsp70s in the Development and Pathogenicity of *Plasmodium falciparum*. *Adv. Exp. Med. Biol.* 340, 75–95. doi:10.1007/978-3-030-78397-6_3

Silva, M. D., Cooke, B. M., Guillotte, M., Buckingham, D. W., Sauzet, J.-P., Scanf, C. L., et al. (2005). A Role for the *Plasmodium falciparum* RESA Protein in Resistance against Heat Shock Demonstrated Using Gene Disruption. *Mol. Microbiol.* 56, 990–1003. doi:10.1111/j.1365-2958.2005.04603.x

Singh, G. P., Chandra, B. R., Bhattacharya, A., Akhouri, R. R., Singh, S. K., and Sharma, A. (2004). Hyper-expansion of Asparagines Correlates with an Abundance of Proteins with Prion-like Domains in *Plasmodium falciparum*. *Mol. Biochem. Parasitol.* 137, 307–319. doi:10.1016/j.molbiopara.2004.05.016

Tuteja, R. (2007). Unraveling the Components of Protein Translocation Pathway in Human Malaria Parasite *Plasmodium falciparum*. *Archives Biochem. Biophysics* 467, 249–260. doi:10.1016/j.abb.2007.08.031

Watanabe, J. (1987). Cloning and Characterization of Heat Shock Protein DnaJ Homologues from *Plasmodium falciparum* and Comparison with Ring Infected Erythrocyte Surface Antigen. *Mol. Biochem. Parasitol.* 88, 253–258. doi:10.1016/s0166-6851(97)00073-x

Zhang, M., Wang, C., Otto, T. D., Oberstaller, J., Liao, X., Adapa, S. R., et al. (2018). Uncovering the Essential Genes of the Human Malaria Parasite *Plasmodium falciparum* by Saturation Mutagenesis. *Science* 360, eaap7847. doi:10.1126/science.aap7847

Zimmermann, R., and Blatch, G. L. (2009). A Novel Twist to Protein Secretion in Eukaryotes. *Trends Parasitol.* 25, 147–150. doi:10.1016/j.pt.2009.01.002

Zininga, T., Makumire, S., Gitau, G. W., Njunge, J. M., Pooe, O. J., Klimek, H., et al. (2015). *Plasmodium falciparum* Hop (PfHop) Interacts with the Hsp70 Chaperone in a Nucleotide-dependent Fashion and Exhibits Ligand Selectivity. *PLoS One* 10, e0135326. doi:10.1371/journal.pone.0135326

Zininga, T., Achilonu, I., Hoppe, H., Prinsloo, E., Dirr, H. W., and Shonhai, A. (2016). *Plasmodium falciparum* Hsp70-Z, an Hsp110 Homologue, Exhibits Independent Chaperone Activity and Interacts with Hsp70-1 in a Nucleotide-dependent Fashion. *Cell Stress Chaperones* 21, 499–513. doi:10.1007/s12192-016-0678-4

Zininga, T., Pooe, O. J., Makhado, P. B., Ramatsui, L., Prinsloo, E., Achilonu, I., et al. (2017a). Polymyxin B Inhibits the Chaperone Activity of *Plasmodium falciparum* Hsp70. *Cell Stress Chaperones* 22, 707–715. doi:10.1007/s12192-017-0797-6

Zininga, T., Anokwuru, C., Sigidi, M., Tshisikhawe, M., Ramaite, I., Traoré, A., et al. (2017b). Extracts Obtained from Pterocarpus Angolensis DC and Ziziphus Mucronata Exhibit Antiplasmodial Activity and Inhibit Heat Shock Protein 70 (Hsp70) Function. *Molecules* 22, 1224. doi:10.3390/molecules22071224

Zininga, T., Ramatsui, L., Makhado, P., Makumire, S., Achilinou, I., Hoppe, H., et al. (2017c). (−)-Epigallocatechin-3-Gallate Inhibits the Chaperone Activity of *Plasmodium falciparum* Hsp70 Chaperones and Abrogates Their Association with Functional Partners. *Molecules* 22, 2139. doi:10.3390/molecules22122139

**Conflict of Interest:** The author declares that the research was conducted in the absence of any commercial or financial relationships that could be construed as a potential conflict of interest.

frontiers | Frontiers in Cell and Developmental Biology

ORIGINAL RESEARCH
published: 06 June 2022
doi: 10.3389/fcell.2022.920569

# HLH-1 Modulates Muscle Proteostasis During *Caenorhabditis elegans* Larval Development

*Khairun Nisaa and Anat Ben-Zvi**

*Department of Life Sciences, Ben-Gurion University of the Negev, Beer Sheva, Israel*

Muscle proteostasis is shaped by the myogenic transcription factor MyoD which regulates the expression of chaperones during muscle differentiation. Whether MyoD can also modulate chaperone expression in terminally differentiated muscle cells remains open. Here we utilized a temperature-sensitive (ts) conditional knockdown nonsense mutation in MyoD ortholog in *C. elegans,* HLH-1, to ask whether MyoD plays a role in maintaining muscle proteostasis post myogenesis. We showed that *hlh-1* is expressed during larval development and that *hlh-1* knockdown at the first, second, or third larval stages resulted in severe defects in motility and muscle organization. Motility defects and myofilament organization were rescued when the clearance of *hlh-1(ts)* mRNA was inhibited, and *hlh-1* mRNA levels were restored. Moreover, *hlh-1* knockdown modulated the expression of chaperones with putative HLH-1 binding sites in their promoters, supporting HLH-1 role in muscle maintenance during larval development. Finally, mild disruption of *hlh-1* expression during development resulted in earlier dysregulation of muscle maintenance and function during adulthood. We propose that the differentiation transcription factor, HLH-1, contributes to muscle maintenance and regulates cell-specific chaperone expression post differentiation. HLH-1 may thus impact muscle proteostasis and potentially the onset and manifestation of sarcopenia.

**Keywords: *Caenorhabditis elegans* (c. elegans), development, MyoD, *hlh-1*, myosin, proteostasis, chaperone**

OPEN ACCESS

***Edited by:***
*Linda M. Hendershot,*
*St. Jude Children's Research Hospital, United States*

***Reviewed by:***
*Patricija Van Oosten-Hawle, University of Leeds, United Kingdom*
*Viraj Ichhaporia, EMD Serono, United States*

***Correspondence:**
*Anat Ben-Zvi*
*anatbz@bgu.ac.il*

***Specialty section:***
*This article was submitted to Signaling, a section of the journal Frontiers in Cell and Developmental Biology*

***Received:*** *14 April 2022*
***Accepted:*** *18 May 2022*
***Published:*** *06 June 2022*

***Citation:***
*Nisaa K and Ben-Zvi A (2022) HLH-1 Modulates Muscle Proteostasis During Caenorhabditis elegans Larval Development. Front. Cell Dev. Biol. 10:920569. doi: 10.3389/fcell.2022.920569*

## 1 INTRODUCTION

The ability to maintain a functional proteome throughout life is vital for long-term organismal health (Shai et al., 2014; Sala et al., 2017; Meller and Shalgi, 2021). Cells cope with protein damage by employing highly conserved quality control systems that repair or remove the damaged proteins to maintain proteostasis (Bar-Lavan et al., 2016a; Bett, 2016; Jackson and Hewitt, 2016). The cellular chaperone machinery is involved in many cellular processes, including *de novo* folding, assembly and disassembly of protein complexes, protein translocation across membranes, proteolytic degradation, and unfolding and reactivation of stress-denatured proteins (Makhnevych and Houry, 2012; Bar-Lavan et al., 2016a; Bett, 2016; Jackson and Hewitt, 2016; Craig, 2018; Nillegoda et al., 2018). Chaperones unfold, refold and reactivate proteins to gain or recover their function (Rosenzweig et al., 2019). The regulation and specificity of chaperone-based reactions can be mediated by co-chaperones choosing the substrate, presenting it to the chaperone, and coordinating chaperone-substrate binding and release cycles (Kampinga and Craig, 2010; Bar-Lavan et al., 2016a; Rosenzweig et al., 2019). As its folding advances, a substrate can be identified by different chaperones or co-chaperones, resulting in substrate overlap, shuffling, and collaboration between various chaperone

machinery (Bar-Lavan et al., 2016a; Rosenzweig et al., 2019). These chaperone or co-chaperone interactions constitute the chaperone network (Brehme et al., 2014; Shemesh et al., 2021).

Most chaperones are ubiquitously expressed, yet chaperone and co-chaperone expression levels display tissue-specific patterns (Brehme et al., 2014; Shemesh et al., 2021). These patterns are conserved and linked to the cellular proteome's folding demands, suggesting that the proteome diversity and differential cellular folding requirements shape the chaperone network in multicellular organisms (Shemesh et al., 2021). Such tailoring of the chaperone system to the proteome needs enables cells to respond to their unique folding requirements, contributing to tissue-specific vulnerability in protein-misfolding diseases (Basha et al., 2020; Thiruvalluvan et al., 2020; Vonk et al., 2020). While it is still an open question how chaperone expression is regulated in a tissue-specific manner, a role for differentiation transcription factors that establish the cell-specific proteome in defining the chaperone network is well-established (Nisaa and Ben-Zvi, 2021). One well-characterized example is the role of the myogenic transcription factor, MyoD, and its' *Caenorhabditis elegans* ortholog, HLH-1 (Fukushige and Krause, 2005), in regulating chaperone expression during muscle differentiation (Sugiyama et al., 2000; Bar-Lavan et al., 2016b; Echeverria et al., 2016; Tiago et al., 2021).

The chaperone network is rewired during muscle differentiation, resulting in the induced expression of some chaperones and repression of others (Bar-Lavan et al., 2016b; Echeverria et al., 2016; Nisaa and Ben-Zvi, 2021). This muscle-specific expression pattern remains consistent across development and aging (Brehme et al., 2014; Shemesh et al., 2021). Chaperones that are upregulated during myogenesis also show muscle-specific differential expression in adult muscle tissues (muscle chaperones). This pattern is conserved from human to worm (Bar-Lavan et al., 2016b; Shemesh et al., 2021). MyoD/HLH-1 can regulate the expression of most muscle chaperones associated with this conserved muscle expression pattern (Bar-Lavan et al., 2016b; Echeverria et al., 2016), and it has functional binding sites at the promoters of most muscle chaperones (Sugiyama et al., 2000; Bar-Lavan et al., 2016b). Disrupting MyoD/HLH-1 function or mutating its' binding sites abolish muscle chaperones' expression during myoblasts differentiation, while its ectopic expression induces chaperone expression (Bar-Lavan et al., 2016b; Echeverria et al., 2016). While MyoD/HLH-1 modulates muscle chaperone expression during differentiation, a role for HLH-1 in maintaining muscle proteostasis later in life was not determined. Here, we asked whether HLH-1 plays a role in muscle maintenance post myogenesis by knocking down *hlh-1* expression at different points during *C. elegans* development.

# 2 MATERIALS AND METHODS

## 2.1 Nematodes and Growth Conditions

Nematodes were grown on NGM plates seeded with the *Escherichia coli* OP50-1 strain and maintained at 15°C. Age-synchronized embryos were obtained by placing for 3–5 h ~25 adults on fresh plates at 15°C, as in (Dror et al., 2020). Nematodes were either maintained at 15°C for the duration of an experiment or shifted to 25°C at specific time points during development (**Figures 1A,B**). Unless otherwise stated, animals' motility, muscle organization, or gene expression were examined on the first day of adulthood before the onset of egg-laying (young adults, YA). A list of strains used in this work is included in **Supplementary Table S1**. All strains were outcrossed to our N2 stock at least four times. Cross-strains were generated using standard *C. elegans* procedures. Animals' genotype was confirmed by single worm PCR using Phire Animal Tissue Direct PCR Kit (F-170L, Thermo Scientific) with primers that amplified the area of the mutation as in (Meshnik et al., 2022). Primer sequences used in this study are listed in **Supplementary Table S2**.

## 2.2 Temperature Shift Experiments

Wild type (WT), *hlh-1(cc561), smg-6(*ok1794), or *hlh-1(cc561); smg-6(ok1794)* embryos laid at 15°C were shifted to 25°C at the first (L1, I), second (L2, II), third (L3, III), or fourth (L4, IV) larval stage and maintained at 25°C until they reached the YA stage. As a control (Ctrl), embryos laid at 15°C were allowed to develop at 15°C until the YA stage (**Figure 1A**). YA motility, muscle organization, or mRNA levels were then examined. Cultivation times at 15°C and 25°C for each experimental condition are noted (**Figure 1B**). We treated all examined strains in parallel for each experimental condition when comparing different strains.

## 2.3 Motility Assay

To determine motility rates, we counted the number of changes in bending direction at mid-body (thrashes) per minute of age-synchronized animals (N = 3, $n$ = 30), as in (Dror et al., 2020).

## 2.4 Feeding RNA Interference

Synchronized embryos (N = 3, $n$ > 30) were placed on plates seeded with *E. coli* strain HT115 (DE3) transformed with the indicated RNA interference (RNAi) vectors, *smg-2* or *smg-7*, (obtained from the Vidal RNAi library) or empty vector (EV) control (pL4440), as previously described (Dror et al., 2020). The efficiency of the RNAi treatment was determined using qPCR to examine the mRNA levels of *smg-2* or *smg-7*. The efficiency of mRNA knockdown ranged between 50–90%.

## 2.5 Confocal Imaging

Adult animals expressing MYO-3 tagged with GFP (strains DM8005 or RW1596) were fixed with 4% paraformaldehyde, as previously described (Karady et al., 2013). Alternatively, adult animals were fixed with 4% paraformaldehyde, permeabilized with ice-cold acetone, and stained with Rhodamine-Phalloidin (1: 10; 00027, Biotium). Treated samples were imaged using a Leica DM5500 confocal microscope through a 63x 1.0 numerical aperture objective with a 488 nm or 532 lines for excitation, respectively.

## 2.6 RNA Levels

RNA was extracted from age-synchronized animals using GENEzol TriRNA Pure Kit (GZXD200, Geneaid), and was

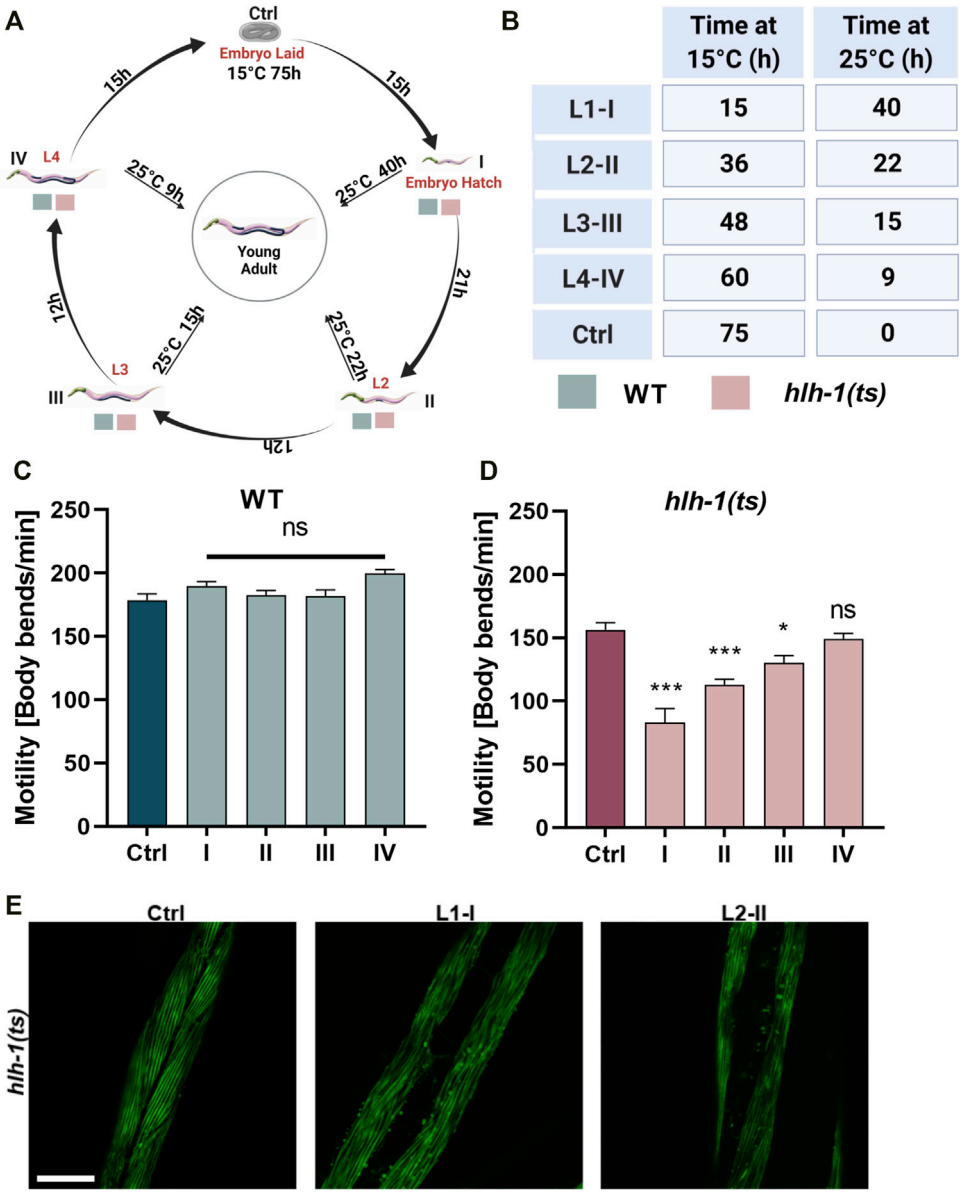


**FIGURE 1 |** Differentiation transcription factor HLH-1 is required for muscle maintenance during larval development. **(A)** Schematic representation of the experimental setup. Wild type (WT) or *hlh-1(ts)* embryos were placed on seeded plates at 15°C. Animals were maintained at 15°C (Ctrl) or shifted to 25°C at the indicated times, corresponding to specific larval stages (L1-I, L2-II, L3-III, and L4-IV). Young adults (YA, before the onset of egg-laying) were then analyzed for motility, myofilament organization, and chaperone expression. **(B)** A list of treatments duration (in hours) at 15°C and 25°C for each group (Ctrl and I-IV). **(C–D)** Motility rates of temperature-shifted YA. Thrashing rates were scored on day one of adulthood for WT **(C)** or *hlh-1(ts)* **(D)** animals grown at 15°C for the duration of the experiment (Ctrl-75 h) or shifted to 25°C at the indicated times (I-15h, II-36h, III-46 h or IV-60 h). Data are means ± 1 standard error of the mean (1SE). Data were analyzed using one-way ANOVA followed by a Dunnett's post-hoc test (N = 3, $n = 30$). (*) denotes $p < 0.05$, (**) denotes $p < 0.01$, (***) denotes $p < 0.001$, and (ns) denotes $p > 0.05$, compared with Ctrl animals maintain at 15°C. **(E)** Representative images of age-synchronized *hlh-1(ts)* animals that express MYO-3::GFP. Animals were grown at 15°C for the duration of the experiment (Ctrl) or shifted to 25°C at L1-I or L2-II. Animals were collected and fixed at the YA stage, and myofilaments were imaged. The scale bar is 25 μm. Panels A–B were created using BioRender.com.

then treated with DNA Free™ DNA removal kit (AM 1906, Invitrogen). For cDNA synthesis, RNA was reverse-transcribed using the iScript™ cDNA Synthesis Kit (1708891, Bio-Rad). mRNA levels were measured using quantitative PCR, performed on a C1000 Thermal Cycler (Bio-Rad) with KAPA SYBRFAST qPCR Master Mix (KK4602, KAPA Biosystems), as in (Meshnik et al., 2022). Relative transcript levels were determined by averaging the $C_T$ of triplicate values for the genes examined and normalizing those to $C_T$ values obtained for 18S rRNA of the same sample using the $2_T^{-\Delta\Delta CT}$ method (Livak and Schmittgen, 2001). List of primes used in this work are provided in **Supplementary Table S2**.

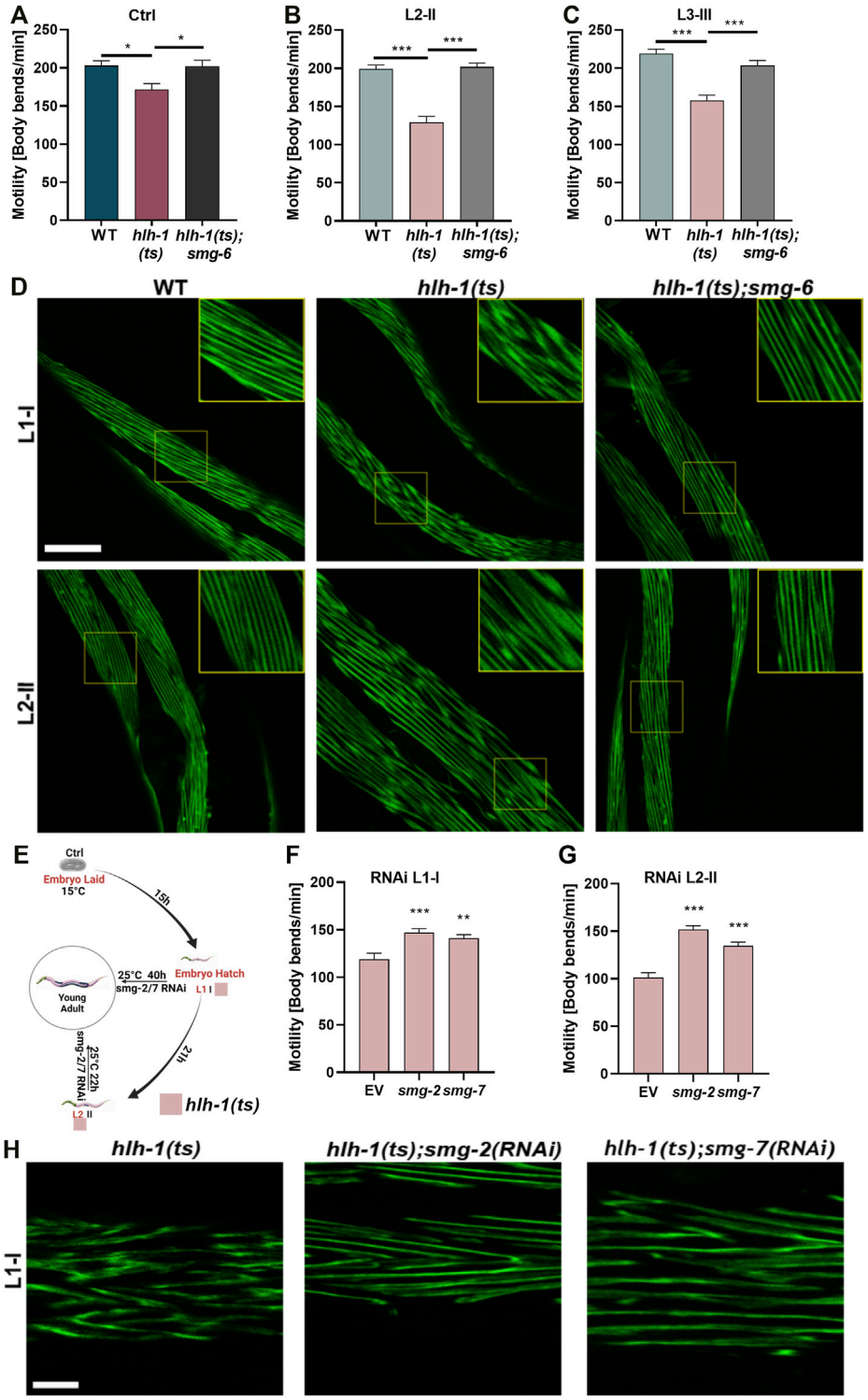


**FIGURE 2 |** Blocking the RNA-mediated decay pathway rescues animals' motility. **(A–C)** Motility rates of wild type (WT), *hlh-1(ts),* or *hlh-1(ts);smg-6*. Thrashing rates of age-synchronized WT, *hlh-1(ts),* or *hlh-1(ts);smg-6* grown at 15°C for the experiment duration **(A)** or shifted to 25°C at L2 [II, **(B)**] or L3 [III, **(C)**] larval stages. Data are means ± 1 standard error of the mean (1SE). Data were analyzed using one-way ANOVA followed by a Tukey's post hoc test (N = 3, $n = 20$). (*) denotes $p < 0.05$, and (***) denotes $p < 0.001$ compared with WT. **(D)** Representative images of temperature-shifted animals expressing MYO-3:GFP. WT, *hlh-1(ts)*, or *hlh-1(ts);smg-6* animals were shifted to 25°C at L1-I or L2-II. YA were collected and fixed, and myofilaments were imaged. The scale bar is 25 μm. Inserts are a 2-fold magnification of the boxed area. **(E)** Schematic representation of the experimental setup. *hlh-1(ts)* embryos were laid on seeded plates at 15°C. Age-synchronized *hlh-1(ts)* animals were

(*Continued*)

**FIGURE 2 |** moved to RNAi plates seeded with *smg-2*, *smg-7*, or empty vector (EV) control, and plates were shifted to 25°C at L1 (I) or L2 (II) larval stages. YAs were then analyzed for motility and myofilament organization. **(F–G)** Motility rates of *hlh-1(ts) smg(RNAi)* treated animals. Thrashing rates of age-synchronized *hlh-1(ts)* animals that were moved to RNAi plates seeded with *smg-2*, *smg-7*, or EV control and shifted to 25°C at L1 **(F)** or L2 **(G)** larval stages. Data are means ± 1 standard error of the mean (1SE). Data were analyzed using one-way ANOVA followed by a Dunnett's post hoc test (N = 3, *n* = 60). (**) denotes $p < 0.01$ and (***) denotes $p < 0.001$ compared with EV control. **(H)** Representative images of *hlh-1(ts) smg(RNAi)* treated myofilament. Age-synchronized *hlh-1(ts)* animals expressing MYO-3:GFP were treated with *smg-2*, *smg-7*, or EV control RNAi at 25°C as in G, and myofilaments were imaged. The scale bar is 7.5 μm. Panel E was created using BioRender.com.

## 2.7 Statistical Analysis

To test the null hypothesis that *hlh-1* or chaperone mRNA levels are reduced in *hlh-1(ts)* animals compared to WT (**Supplementary Figures S1A, S4C**), we used a one-way analysis of variance (ANOVA) followed by Bonferroni's post hoc test. We used one-way ANOVA followed by Dunnett's post hoc test to compare motility rates or mRNA levels between Ctrl and temperature shifted animals (**Figures 1C,D** and **Supplementary Figure S3U–W**, respectively). We used the same test to compare motility rates between *smg-2*, or *smg-7* RNAi treated animals and EV control at different knockdown stages (**Figures 2F,G**). We used one-way ANOVA followed by Tukey's post hoc test to compare motility rates between WT, *hlh-1(cc561),* or *hlh-1(cc561); smg-6(ok1794)* mutant animals treated as Ctrl, L2-II or L3-III (**Figures 2A–C**). We used the Wilcoxon Mann-Whitney rank sum test to ask whether muscle chaperone expression levels are reduced in *hlh-1*(ts) compared to WT animals (**Figure 3** and **Supplementary Figure S3A–T**) or to ask whether *hlh-1* levels are elevated in *hlh-1(ts);smg-6* mutant animals treated as Ctrl, L2-II or L3-III compared to *hlh-1(ts)* or WT (**Supplementary Figure S2**). The same test was used to ask whether the motility of *hlh-1(ts)* animals was reduced compared to WT animals maintained at 15°C at different larval and adult stages (**Figures 4A–C** and **Supplementary Figure S4A–B**). Bonferroni correction was applied to adjust *p* values when gene expression was compared under two conditions. Data are presented as bar graphs showing means ± 1 standard error of the mean (1SE). The numbers of biological repeats (N) and individuals (n) in each condition tested are noted in the figure legends.

# 3 RESULTS

## 3.1 HLH-1 is Required for Muscle Maintenance During Larval Development

*hlh-1* is expressed during larval development, with mRNA and protein expression detected in all larval stages (L1-L4) (Harfe et al., 1998; Toudji-Zouaz et al., 2021). During early larval development (L1-L2), HLH-1 plays a role in postembryonic muscle differentiation of the 14 body-wall muscle cells derived from the M-lineage (Harfe et al., 1998; Krause and Liu, 2012). In agreement, we detected *hlh-1* mRNA expression in larvae. This expression declined with age (**Supplementary Figure S1**) (Gerstein et al., 2014).

To ask whether HLH-1 affects muscle postembryonic maintenance, we utilized a nonsense mutant allele, *hlh-1(cc561ts)* (hereafter designated as *hlh-1(ts)*), that gives rise to a truncated protein. The phenotype is attributed to insufficient HLH-1 levels, as overexpression of the truncated mRNA or disruption of the nonsense-mediated decay (NMD) pathway rescues *hlh-1(ts)* phenotypes. The *hlh-1(ts)* mutation behaves like a conditional knockdown, likely because the nonsense-mediated decay pathway activity is modulated by temperature (Harfe et al., 1998; Cali et al., 1999). Whereas the animals appear wild-type at low cultivation temperatures, and there is minimal impact on *hlh-1* levels (**Supplementary Figure S1**), motility, and body wall muscles organization (Gieseler et al., 2000; Gieseler et al., 2002). The mutation is fully evident at high cultivation temperatures, showing defective embryonic and postembryonic muscle differentiation and L1-arrest phenotype (Harfe et al., 1998). We thus used *hlh-1(ts)* temperature-sensitive behavior to knock down *hlh-1* levels at different stages during larval development and examine its impact on muscle maintenance.

Age synchronized wild-type (WT) or *hlh-1(ts)* embryos were allowed to hatch and develop under permissive conditions (15°C). Animals were shifted to the restrictive conditions (25°C) at first (L1, I), second (L2, II), third (L3, III), or fourth (L4, IV) larval stages (**Figure 1A**) and then maintained under restrictive conditions for the duration of the experiment (**Figure 1B**). The motility of temperature-shifted young adult animals (YA), measured as thrashing rates, was compared to that of YA animals maintained at the permissive conditions for the duration of the experiment (Ctrl, **Figures 1A,B**). Whereas the motility of WT larvae shifted to the restrictive conditions was unaffected, motility of *hlh-1(ts)* animals shifted at L1, L2, or L3, but not L4, was significantly reduced (1.8-, 1.4-, and 1.2-fold, respectively, ANOVA followed by a Dunnett's post hoc test, **Figures 1C,D**). Thus, disrupting *hlh-1* expression during larval development affects muscle function, supporting a postembryonic role for HLH-1 in muscle maintenance.

The postembryonic differentiation of M-lineage derived body-wall muscles can occur in the absence of HLH-1, and it is completed before the L3 stage (Harfe et al., 1998; Krause and Liu, 2012). To determine if the impact of *hlh-1* knockdown on motility was specific to the M-derived body-wall muscle cells or general, we examined whether and which body-wall muscle cells display disrupted myofilament organization. For that, we monitored myosin heavy chain A (MYO-3) organization using an MYO-3::GFP tagged protein. L1-or L2-shifted *hlh-1(ts)* animals (L1-I and L2-II, respectively) exhibited disrupted myofilament structure and MYO-3::GFP mislocalization in most muscle cells, while animals maintained at permissive conditions were unaffected (**Figure 1E**). Thus, *hlh-1* is required to maintain embryonic and postembryonic differentiated body-wall muscles.

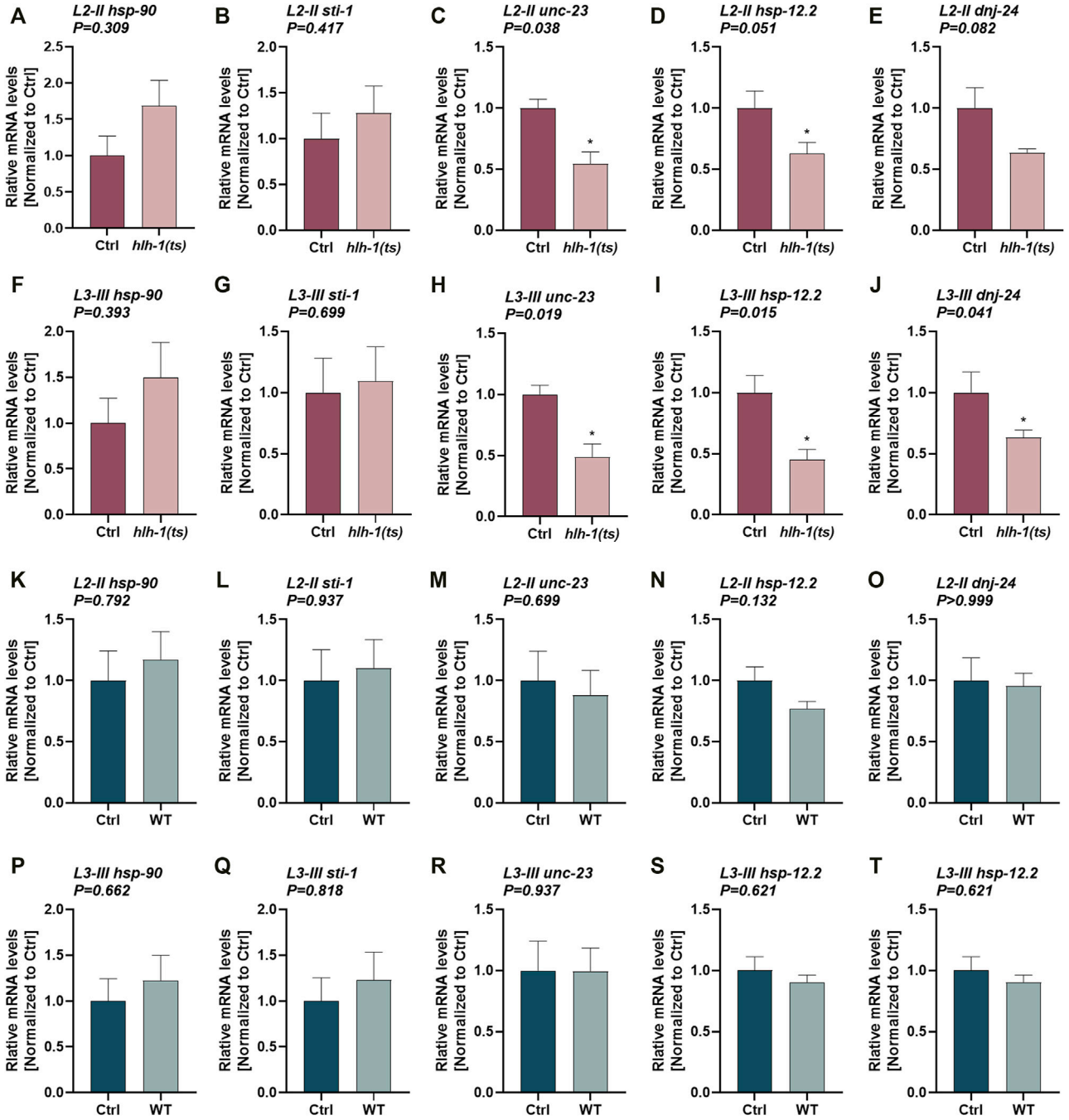


**FIGURE 3 |** The expression of HLH-1-dependent chaperones during larval development. **(A–T)** Expression levels of chaperones in *hlh-1(ts)* animals. Relative mRNA levels of HLH-1-dependent chaperones, *hsp-90*, *sti-1*, *unc-23*, *hsp-12.2*, or *dnj-24*, in age synchronized *hlh-1(ts)* **(A–J)** or WT **(K–T)** animals, shifted to 25°C at L2-II [**(A-E)** and **(K-O)**] or L3-III [**(F-J)** and **(P-T)**] larval stages. Expression levels were compared with the same strain animals maintained at 15°C (Ctrl). Data are means ± 1 standard error of the mean (1SE). Data were analyzed using the Wilcoxon Mann-Whitney rank sum test compared with the same strain Ctrl treated animals (N ≥ 4).

## 3.2 Restoring *hlh-1* mRNA During Development Rescues Muscle Proteostasis

We next asked whether inhibiting the NMD pathway can restore muscle maintenance by disrupting the expression of the *smg* mRNA surveillance genes, using animals harboring a mutation in *smg-6(ok1794)* (hereafter designated as *smg-6*). Double mutant *hlh-1(ts); smg-6* animals that were maintained under permissive conditions (Ctrl) showed no or a mild increase in *hlh-1* mRNA levels compared to *hlh-1(ts)* or WT animals (Wilcoxon Mann-Whitney rank sum test, $p = 0.2$, and $p = 0.028$, respectively; **Supplementary Figure S2A–B**). In agreement, the mild motility reduction (1.15-fold) of Ctrl treated *hlh-1(ts)* animals compared

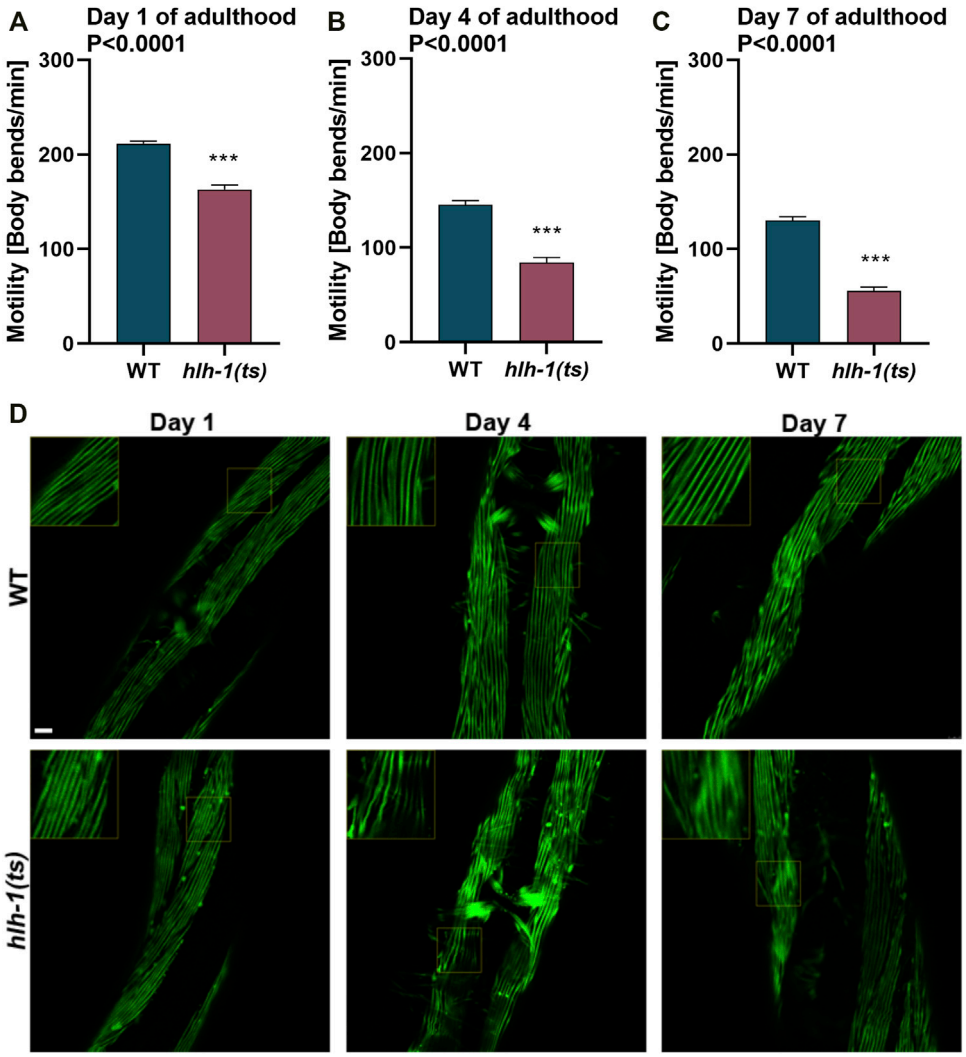


**FIGURE 4 |** Mild disruption of *hlh-1* expression during development severely impact muscle maintenance later in adulthood. **(A–C)** Motility rates of WT or *hlh-1(ts)* adults. Thrashing rates of age-synchronized WT or *hlh-1(ts)* animals maintained at 15°C were examined on days 1 **(A)**, 4 **(B)**, or 7 **(C)** of adulthood. Data are means ± 1 standard error of the mean (1SE). Data were analyzed using the Wilcoxon Mann-Whitney rank sum test compared with WT (N = 3, $n \geq 30$). **(D)** Representative images of WT or *hlh-1(ts)* animals that express MYO-3::GFP. Age-synchronized WT or *hlh-1(ts)* animals maintained at 15°C were collected and fixed on days 1, 4, or 7 of adulthood, and myofilaments were imaged. Inserts are a 2-fold magnification of the boxed area. The scale bar is 10 μm.

to WT animals was abolished in the double mutant *hlh-1(ts); smg-6* animals (ANOVA followed by a Tukey's post hoc test, $p \leq 0.05$; **Figure 2A**). This behavior was more apparent in temperature-shifted animals than in Ctrl-treated animals. *hlh-1* mRNA levels in animals shifted at L2-II or L3-III were significantly higher for *hlh-1(ts);smg-6* than for *hlh-1(ts)* mutant or WT animals, restoring and even raising *hlh-1* mRNA levels (Wilcoxon Mann-Whitney rank sum test, $p = 0.028$; **Supplementary Figure S2C–F**). Likewise, the reduced motility of L2-or L3-shifted *hlh-1(ts)* animals compared to WT (129 ± 8 vs. 199 ± 5 bends per minute and 158 ± 7 vs. 219 ± 5 bends per minute, respectively) was rescued in *hlh-1(ts);smg-6* shifted animals (202 ± 5 and 204 ± 6 bends per minute, respectively, ANOVA followed by a Tukey's post hoc test, $p \leq 0.001$; **Figures 2B,C**). Furthermore, the severe MYO-3::GFP mislocalization observed in *hlh-1(ts)* animals shifted at L1-I or L2-II was abrogated in *hlh-1(ts);smg-6* animals (**Figure 2D**). Thus, the observed developmental muscle maintenance phenotypes are dependent on HLH-1.

One possible interpretation of our results is that the mild reduction in *hlh-1* mRNA levels during embryogenesis alone gives rise to the muscle defects observed during development under permissive conditions. We thus asked whether inhibiting the NMD pathway past embryogenesis can still rescue muscle defects in temperature-shifted larvae to address this possibility. We knocked down the expression of *smg* genes during larval development by introducing RNAi against *smg-2* or *smg-7* only once we shifted the animals to the restrictive conditions (**Figure 2E**). The motility of *hlh-1(ts)* temperature-shifted L1-I or L2-II animals treated with *smg-*

*2(RNAi)* or *smg-7(RNAi)* was significantly improved compared to animals treated with empty vector (EV) control (~1.4- and ~1.2-fold, respectively, ANOVA followed by a Dunnett's post hoc test, $p \leq 0.01$; **Figures 2F,G**). Likewise, MYO-3:GFP mislocalization observed in EV control-treated *hlh-1(ts)* L1-I shifted animals was strongly reduced in *smg-2(RNAi)* or *smg-7(RNAi)* treated L1-I shifted animals (**Figure 2H**). Taken together, HLH-1 is required for muscle maintenance during larval development.

## 3.3 HLH-1 Knockdown During Larval Development Modulates Muscle Chaperone Expression

MyoD/HLH-1 can regulate chaperone expression during muscle differentiation (Sugiyama et al., 2000; Bar-Lavan et al., 2016b; Echeverria et al., 2016; Tiago et al., 2021). To ask whether HLH-1 also regulates chaperones' expression during larval development, we examined the expression of chaperones that are *hlh-1*-dependent or *hlh-1*-independent. While *hlh-1*-dependent chaperones were shown to have putative HLH-1 occupancy sites at their promoter and respond to modulation of *hlh-1* expression levels in embryos, *hlh-1*-independent chaperones lack such features. We first compared mRNA levels of chaperones in Ctrl and L2-II and L3-III temperature-shifted *hlh-1(ts)* (**Figures 3A–J**) or WT (**Figure 3K**-T) animals using qPCR. *unc-23*, *hsp-12.2*, and *dnj-24* showed reduced expression in L2-II (**Figures 3C–E**) and L3-III (**Figures 3H–J**) temperature-shifted *hlh-1(ts)* animals compared to animals maintained under permissive conditions, but not in WT animals (Wilcoxon Mann-Whitney rank sum test; **Supplementary Figure S3M–O, R–T**). *unc-23*, *hsp-12.2*, and *dnj-24* reduced expression was rescued in temperature-shifted *hlh-1(ts); smg-6* animals (ANOVA followed by a Dunnett's post hoc test; **Supplementary Figure S3U–W**), when *hlh-1* levels are elevated (**Supplementary Figure S2C–F**). The expression levels of the other two *hlh-1*-dependent chaperones, *hsp-90* and *sti-1*, were not significantly different (Wilcoxon Mann-Whitney rank sum test). *hsp-90* and *sti-1* are highly and ubiquitously expressed chaperones, and changes in their expression in one tissue might not be apparent. While *unc-23*, *hsp-12.2*, and *dnj-24* are also expressed in other tissues, their expression is enriched in muscle cells (Roy et al., 2002; Fox et al., 2007; Kuntz et al., 2012). Indeed, their expression pattern clusters with muscle-specific genes during embryogenesis, showing a myogenesis-induced expression pattern (while *hsp-90* and *sti-1* do not) (Bar-Lavan et al., 2016b). In contrast, when we examined the expression levels of five *hlh-1*-independent chaperones (**Supplementary Figure S3**), only *hsp-17* showed reduced expression in temperature-shifted *hlh-1(ts)* animals (**Supplementary Figure S3A, F**). However, it was similarly affected in temperature-shifted WT animals (Wilcoxon Mann-Whitney rank sum test; **Supplementary Figure S3K, P**). Thus, *hlh-1*-dependent chaperone expression can be modulated by *hlh-1* knockdown during larval development, suggesting that HLH-1 could contribute to muscle proteostasis.

## 3.4 Disruption in *hlh-1* Expression During Embryonic or Larval Development Results in Early Onset of Muscle Deterioration

RNAi knockdown of *hlh-1* in adulthood shows no impact on muscle function in adulthood (Mergoud Dit Lamarche et al., 2018). In agreement, the motility of L4 temperature-shifted *hlh-1(ts)* animals was similar to animals grown under permissive conditions (**Figure 1D**). These data suggest that HLH-1 has no role in muscle maintenance during adulthood. However, *hlh-1* function during embryonic and larval development could impact muscle proteome and proteostasis and thus modulate muscle maintenance later in life. To address this possibility, we ask whether the mild reduction in *hlh-1* mRNA levels (**Supplementary Figure S1**) and its' associated phenotypes (**Figure 1E**, **2A**, and **Supplementary Figure S4A–C**) observed in *hlh-1(ts)* animals maintained at permissive conditions has implications on muscle maintenance in adulthood. The motility of *hlh-1(ts)* animals was mildly reduced compared to WT during larval development (~1.15-fold, Wilcoxon Mann-Whitney rank sum test; **Supplementary Figure S4A–B**). However, with age, motility decline became more pronounced (**Figures 4A–C**). By day four of adulthood, *hlh-1(ts)* animals' thrashing rate was reduced by 1.7-fold compared to WT (Wilcoxon Mann-Whitney rank sum test, $p < 0.001$; **Figure 4B**). Motility declined further by day 7 of adulthood (2.3-fold compared to WT, Wilcoxon Mann-Whitney rank sum test, $p < 0.0001$; **Figure 4C**). Of note, while WT motility declined by 1.6-fold with age, *hlh-1(ts)* motility declined by 3-fold. Likewise, myofilament organization was disrupted with age. MYO-3 and actin filaments disruption was apparent already at day 4 of adulthood. By day 7 of adulthood, MYO-3 and actin organization were disrupted in most body wall muscle cells (**Figure 4D** and **Supplementary Figure S4D**). In contrast, MYO-3 organization in WT animals remained intact, as previously observed (Ben-Zvi et al., 2009). Thus, the mild decline in *hlh-1* expression levels associated with mild or no changes in muscle maintenance during larval development (**Figures 1E**,F, **2A**, and **Supplementary Figure S4A–C**) is sufficient to disrupt the muscle folding environment and thus muscle maintenance in adulthood.

# 4 DISCUSSION

Chaperone expression is differentially regulated across cell types during cellular differentiation to establish tissue-specific chaperone networks (Nisaa and Ben-Zvi, 2021; Shemesh et al., 2021). Differentiation transcription factors play a role in the rewiring of the chaperone network in parallel to setting the cellular proteome (Luo et al., 1991; Bar-Lavan et al., 2016b; Piri et al., 2016; Zha et al., 2019; Nisaa and Ben-Zvi, 2021). Specifically for muscle cells, MyoD/HLH-1 was shown to directly regulate chaperone expression (Sugiyama et al., 2000; Bar-Lavan et al., 2016b; Echeverria et al., 2016; Tiago et al., 2021). Tissue-specific chaperone networks are also maintained in adult tissues and deteriorate with age (Brehme et al., 2014; Sala et al., 2017;

Shemesh et al., 2021). Here, we asked whether a differentiation transcription factor can be involved in muscle maintenance later in life. To address this question, we set out to examine the effects of conditional knockdown of *C. elegans* MyoD, HLH-1, at different stages of larval development.

We first established that *hlh-1* is expressed during larval development and is required for motility and muscle organization, although the effect was most pronounced in early larval stages (**Figures 1**, **2**). Furthermore, we showed that disrupting *hlh-1* expression during L2-L3 larval stages resulted in reduced expression of some HLH-1-dependent chaperones but not HLH-1-independent chaperones (**Figure 3**). Finally, we showed that even a mild reduction in *hlh-1* expression during embryogenesis and larval development with no or mild impact on motility and muscle organization in YA showed faster deterioration of muscles during aging (**Figure 4**). Taken together, we propose a role for MyoD/HLH-1 in the maintenance of muscle proteostasis.

## 4.1 HLH-1-dependent Chaperones Shape the Muscle Chaperone Folding Capacity

Muscle chaperones, most of which are *hlh-1*-dependent, are required for muscle proteostasis (Bar-Lavan et al., 2016b; Nisaa and Ben-Zvi, 2021; Shemesh et al., 2021). Disrupting the expression of a single muscle chaperone by knockdown or overexpression often affects muscle proteome folding and function and, for some chaperones, can even disrupt muscle differentiation (Landsverk et al., 2007; Frumkin et al., 2014; Papsdorf et al., 2014; Bar-Lavan et al., 2016b; Echeverria et al., 2016; Nisaa and Ben-Zvi, 2021; Tiago et al., 2021). For example, DNJ-24, UNC-23, HSP-90, and STI-1 are localized to the sarcomere, and when any are disrupted, myosin is disorganized (Meissner et al., 2011; Frumkin et al., 2014; Papsdorf et al., 2014; Rahmani et al., 2015; Bar-Lavan et al., 2016b). Indeed, when the functional association of chaperones that are upregulated in human skeletal muscle (and their *C. elegans* homologs) was examined, most were required for muscle function, and more than half were causal or associated with muscle diseases (Shemesh et al., 2021). For example, mutations in DNAJB6 (homolog of *dnj-24*) lead to Limb-girdle muscular dystrophy 1E, and mutations in HSPB8 (homolog of *hsp-12.2*) or BAG2 (homolog of *unc-23*) were associated with myopathies (Sarparanta et al., 2012; Al-Tahan et al., 2019; Diofano et al., 2020). Moreover, the knockdown of muscle chaperone expression activated a muscle-specific stress response (Guisbert et al., 2013). The tight regulation of muscle chaperones is most apparent when overexpression of chaperones, including HSP-90, HSP-1, and UNC-45, disrupt, rather than improve, muscle proteostasis (Landsverk et al., 2007; Papsdorf et al., 2014; Bar-Lavan et al., 2016b; Echeverria et al., 2016; Nisaa and Ben-Zvi, 2021). Thus, MyoD/HLH-1 modulates the regulation of muscle chaperones. In turn, muscle chaperones directly contribute to muscle health, supporting a role for MyoD/HLH-1 in muscle-specific regulation of chaperone expression to address the specific folding needs of the muscle proteome.

## 4.2 The Function of HLH-1 During Embryonic and Larval Development Shapes Muscle Proteostasis in Adulthood

*hlh-1* knockdown in adulthood has no impact on muscle maintenance later in life, suggesting that HLH-1 mainly functions in embryos and developing larvae (Mergoud Dit Lamarche et al., 2018). This developmental role is supported by the observed decline in *hlh-1* requirement during larval development (**Figure 1D**) and the low *hlh-1* levels detected in young adults (**Supplementary Figure S1**). While it is likely that HLH-1 has no active role in muscle maintenance during adulthood, even mild disruption in *hlh-1* expression during larval development strongly impacted muscle maintenance in adulthood (**Figure 4** and **Supplementary Figure S4**). The impact of *hlh-1* disruption suggests that the basal state of muscle proteostasis early in adulthood can substantially affect muscle maintenance in aging. In agreement, aggregation prone poly-glutamine extended repeat model (Q35) in *hlh-1(ts)* background show increase aggregation rate mainly in adulthood (Bar-Lavan et al., 2016b). A model for Duchenne muscular dystrophy (DMD), consisting of animals carrying a null mutation in dystrophin in *hlh-1(ts)* background, showed similar behavior. Animals displayed a progressive loss of motility and muscle degeneration. Disruption-associated damage that started in development became functionally apparent during *C. elegans* adulthood (Gieseler et al., 2000; Gieseler et al., 2002; Brouilly et al., 2015) as well as in mice (Megeney et al., 1999). Several studies demonstrated a role for proteostasis maintenance in this *C. elegans* DMD model (Nyamsuren et al., 2007; Brouilly et al., 2015). Specifically, deletion of the co-chaperone, STUB1 (*chn-1* in *C. elegans*), or inhibition of the proteasome partially rescued muscle function and structure in adulthood, delaying muscle wasting (Nyamsuren et al., 2007). Muscle-specific gene expression analyses comparing WT and dystrophin mutants after phenotypes were observed (L3-adult) identified significant changes in the expression of genes involved in myogenesis, supporting a role for HLH-1 in muscle maintenance (Hrach et al., 2020). We, therefore, propose that the basal proteostasis network in *hlh-1(ts)* mutant animals is limiting, which contributes to age-dependent muscle deterioration, accelerating the rate of muscle wasting.

## 4.3 Various Transcription Factors can Shape the Cell-specific Proteostasis Networks

Three myogenic transcription factors are involved in muscle differentiation during embryogenesis, HLH-1, UNC-120, and HND-1 (Fukushige and Krause, 2005; Fukushige et al., 2006; Lei et al., 2010; Kuntz et al., 2012). Like HLH-1, UNC-120 is expressed past embryogenesis and protects muscle cells later in life (Mergoud Dit Lamarche et al., 2018). Specifically, UNC-120 knockdown results in reduced expression of muscle genes, disrupted mitochondria morphology and connectivity, and accumulation of autophagic vesicles, suggesting that UNC-120 impacts muscle health. In agreement, UNC-120 overexpression

in body wall muscle cells improves muscle aging. Moreover, UNC-120 can affect the expression of some chaperones (Kuntz et al., 2012), suggesting that, like HLH-1, it can shape muscle chaperone network in adulthood.

Other transcription factors, such as the heat shock transcription factors (HSFs), regulate chaperones' expression during development (Li et al., 2016; Li et al., 2017) or modulate the muscle heat shock response (Guisbert et al., 2013). Furthermore, trans-cellular signaling modulates chaperone expression in muscle in response to changes in chaperone expression in neurons or intestine cells (O'Brien et al., 2018; Miles et al., 2022). Therefore, the chaperone system can be shaped and reshaped during development. Different transcription factors can contribute to the composition, expression levels, and thus folding capacity of muscle cells in development and aging. How these signals regulate and coordinate an intricate chaperone network that responds to tissue and organismal folding demands remains to be determined.

## DATA AVAILABILITY STATEMENT

The original contributions presented in the study are included in the article/**Supplementary Material**, further inquiries can be directed to the corresponding author.

## AUTHOR CONTRIBUTIONS

Conceptualization, AB; experimental design, KN and AB; data acquisition, KN; data analysis, KN and AB; writing and revising the text, KN and AB. All authors read and approved the final manuscript.

## FUNDING

This study was funded by the Israel Science Foundation (ISF) grant 278/18 to AB.

## ACKNOWLEDGMENTS

Some strains were provided by the Caenorhabditis Genetics Center, which is funded by the NIH National Center for Research Resources (NCRR).

## SUPPLEMENTARY MATERIAL

The Supplementary Material for this article can be found online at: https://www.frontiersin.org/articles/10.3389/fcell.2022.920569/full#supplementary-material

## REFERENCES

Al-Tahan, S., Weiss, L., Yu, H., Tang, S., Saporta, M., Vihola, A., et al. (2019). New Family with HSPB8-Associated Autosomal Dominant Rimmed Vacuolar Myopathy. *Neurol. Genet.* 5 (4), e349. doi:10.1212/NXG.0000000000000349

Bar-Lavan, Y., Shemesh, N., and Ben-Zvi, A. (2016a). Chaperone Families and Interactions in Metazoa. *Essays Biochem.* 60 (2), 237–253. doi:10.1042/EBC20160004

Bar-Lavan, Y., Shemesh, N., Dror, S., Ofir, R., Yeger-Lotem, E., and Ben-Zvi, A. (2016b). A Differentiation Transcription Factor Establishes Muscle-specific Proteostasis in *Caenorhabditis elegans*. *PLoS Genet.* 12 (12), e1006531. doi:10.1371/journal.pgen.1006531

Basha, O., Argov, C. M., Artzy, R., Zoabi, Y., Hekselman, I., Alfandari, L., et al. (2020). Differential Network Analysis of Multiple Human Tissue Interactomes Highlights Tissue-Selective Processes and Genetic Disorder Genes. *Bioinformatics* 36 (9), 2821–2828. doi:10.1093/bioinformatics/btaa034

Ben-Zvi, A., Miller, E. A., and Morimoto, R. I. (2009). Collapse of Proteostasis Represents an Early Molecular Event in *Caenorhabditis elegans* Aging. *Proc. Natl. Acad. Sci. U.S.A.* 106 (35), 14914–14919. doi:10.1073/pnas.0902882106

Bett, J. S. (2016). Proteostasis Regulation by the Ubiquitin System. *Essays Biochem.* 60 (2), 143–151. doi:10.1042/EBC20160001

Brehme, M., Voisine, C., Rolland, T., Wachi, S., Soper, J. H., Zhu, Y., et al. (2014). A Chaperome Subnetwork Safeguards Proteostasis in Aging and Neurodegenerative Disease. *Cell Rep.* 9 (3), 1135–1150. doi:10.1016/j.celrep.2014.09.042

Brouilly, N., Lecroisey, C., Martin, E., Pierson, L., Mariol, M.-C., Qadota, H., et al. (2015). Ultra-structural Time-Course Study in theC. Elegansmodel for Duchenne Muscular Dystrophy Highlights a Crucial Role for Sarcomere-Anchoring Structures and Sarcolemma Integrity in the Earliest Steps of the Muscle Degeneration Process. *Hum. Mol. Genet.* 24 (22), 6428–6445. doi:10.1093/hmg/ddv353

Cali, B. M., Kuchma, S. L., Latham, J., and Anderson, P. (1999). smg-7 Is Required for mRNA Surveillance in *Caenorhabditis elegans*. *Genetics* 151 (2), 605–616. doi:10.1093/genetics/151.2.605

Craig, E. A. (2018). Hsp70 at the Membrane: Driving Protein Translocation. *BMC Biol.* 16 (1), 11. doi:10.1186/s12915-017-0474-3

Diofano, F., Weinmann, K., Schneider, I., Thiessen, K. D., Rottbauer, W., and Just, S. (2020). Genetic Compensation Prevents Myopathy and Heart Failure in an *In Vivo* Model of Bag3 Deficiency. *PLoS Genet.* 16 (11), e1009088. doi:10.1371/journal.pgen.1009088

Dror, S., Meidan, T. D., Karady, I., and Ben-Zvi, A. (2020). Using *Caenorhabditis elegans* to Screen for Tissue-specific Chaperone Interactions. *J. Vis. Exp.* 160, e61140. doi:10.3791/61140

Echeverría, P. C., Briand, P.-A., and Picard, D. (2016). A Remodeled Hsp90 Molecular Chaperone Ensemble with the Novel Cochaperone Aarsd1 Is Required for Muscle Differentiation. *Mol. Cell Biol.* 36 (8), 1310–1321. doi:10.1128/MCB.01099-15

Fox, R. M., Watson, J. D., Von Stetina, S. E., McDermott, J., Brodigan, T. M., Fukushige, T., et al. (2007). The Embryonic Muscle Transcriptome of *Caenorhabditis elegans*. *Genome Biol.* 8 (9), R188. doi:10.1186/gb-2007-8-9-r188

Frumkin, A., Dror, S., Pokrzywa, W., Bar-Lavan, Y., Karady, I., Hoppe, T., et al. (2014). Challenging Muscle Homeostasis Uncovers Novel Chaperone Interactions in *Caenorhabditis elegans*. *Front. Mol. Biosci.* 1, 21. doi:10.3389/fmolb.2014.00021

Fukushige, T., Brodigan, T. M., Schriefer, L. A., Waterston, R. H., and Krause, M. (2006). Defining the Transcriptional Redundancy of Early Bodywall Muscle Development in *C. elegans*: Evidence for a Unified Theory of Animal Muscle Development. *Genes Dev.* 20 (24), 3395–3406. doi:10.1101/gad.1481706

Fukushige, T., and Krause, M. (2005). The Myogenic Potency of HLH-1 Reveals Wide-Spread Developmental Plasticity in earlyC. Elegansembryos. *Development* 132 (8), 1795–1805. doi:10.1242/dev.01774

Gerstein, M. B., Rozowsky, J., Yan, K. K., Wang, D., Cheng, C., Brown, J. B., et al. (2014). Comparative Analysis of the Transcriptome across Distant Species. *Nature* 512 (7515), 445–448. doi:10.1038/nature13424

Gieseler, K., Grisoni, K., Mariol, M.-C., and Ségalat, L. (2002). Overexpression of Dystrobrevin Delays Locomotion Defects and Muscle Degeneration in a Dystrophin-Deficient *Caenorhabditis elegans*. *Neuromuscul. Disord.* 12 (4), 371–377. doi:10.1016/s0960-8966(01)00330-3

Gieseler, K., Grisoni, K., and Ségalat, L. (2000). Genetic Suppression of Phenotypes Arising from Mutations in Dystrophin-Related Genes in *Caenorhabditis elegans*. *Curr. Biol.* 10 (18), 1092–1097. doi:10.1016/s0960-9822(00)00691-6

Guisbert, E., Czyz, D. M., Richter, K., McMullen, P. D., and Morimoto, R. I. (2013). Identification of a Tissue-Selective Heat Shock Response Regulatory Network. *PLoS Genet.* 9 (4), e1003466. doi:10.1371/journal.pgen.1003466

Harfe, B. D., Branda, C. S., Krause, M., Stern, M. J., and Fire, A. (1998). MyoD and the Specification of Muscle and Non-muscle Fates during Postembryonic Development of the *C. elegans* Mesoderm. *Development* 125 (13), 2479–2488. doi:10.1242/dev.125.13.2479

Hrach, H. C., O'Brien, S., Steber, H. S., Newbern, J., Rawls, A., and Mangone, M. (2020). Transcriptome Changes during the Initiation and Progression of Duchenne Muscular Dystrophy in *Caenorhabditis elegans*. *Hum. Mol. Genet.* 29 (10), 1607–1623. doi:10.1093/hmg/ddaa055

Jackson, M. P., and Hewitt, E. W. (2016). Cellular Proteostasis: Degradation of Misfolded Proteins by Lysosomes. *Essays Biochem.* 60 (2), 173–180. doi:10.1042/EBC20160005

Kampinga, H. H., and Craig, E. A. (2010). The HSP70 Chaperone Machinery: J Proteins as Drivers of Functional Specificity. *Nat. Rev. Mol. Cell Biol.* 11 (8), 579–592. doi:10.1038/nrm2941

Karady, I., Frumkin, A., Dror, S., Shemesh, N., Shai, N., and Ben-Zvi, A. (2013). Using *Caenorhabditis elegans* as a Model System to Study Protein Homeostasis in a Multicellular Organism. *J. Vis. Exp.* 82, e50840. doi:10.3791/50840

Krause, M., and Liu, J. (2012). Somatic Muscle Specification during Embryonic and Post-embryonic Development in the nematodeC. Elegans. *Wiley Interdiscip Rev. Dev. Biol.* 1 (2), 203–214. doi:10.1002/wdev.15

Kuntz, S. G., Williams, B. A., Sternberg, P. W., and Wold, B. J. (2012). Transcription Factor Redundancy and Tissue-specific Regulation: Evidence from Functional and Physical Network Connectivity. *Genome Res.* 22 (10), 1907–1919. doi:10.1101/gr.133306.111

Landsverk, M. L., Li, S., Hutagalung, A. H., Najafov, A., Hoppe, T., Barral, J. M., et al. (2007). The UNC-45 Chaperone Mediates Sarcomere Assembly through Myosin Degradation in *Caenorhabditis elegans*. *J. Cell Biol.* 177 (2), 205–210. doi:10.1083/jcb.200607084

Lei, H., Fukushige, T., Niu, W., Sarov, M., Reinke, V., and Krause, M. (2010). A Widespread Distribution of Genomic CeMyoD Binding Sites Revealed and Cross Validated by ChIP-Chip and ChIP-Seq Techniques. *PLoS One* 5 (12), e15898. doi:10.1371/journal.pone.0015898

Li, J., Chauve, L., Phelps, G., Brielmann, R. M., and Morimoto, R. I. (2016). E2F Coregulates an Essential HSF Developmental Program that Is Distinct from the Heat-Shock Response. *Genes Dev.* 30 (18), 2062–2075. doi:10.1101/gad.283317.116

Li, J., Labbadia, J., and Morimoto, R. I. (2017). Rethinking HSF1 in Stress, Development, and Organismal Health. *Trends Cell Biol.* 27 (12), 895–905. doi:10.1016/j.tcb.2017.08.002

Livak, K. J., and Schmittgen, T. D. (2001). Analysis of Relative Gene Expression Data Using Real-Time Quantitative PCR and the 2−ΔΔCT Method. *Methods* 25 (4), 402–408. doi:10.1006/meth.2001.1262

Luo, Y., Amin, J., and Voellmy, R. (1991). Ecdysterone Receptor Is a Sequence-specific Transcription Factor Involved in the Developmental Regulation of Heat Shock Genes. *Mol. Cell Biol.* 11 (7), 3660–3675. doi:10.1128/mcb.11.7.3660-3675.1991

Makhnevych, T., and Houry, W. A. (2012). The Role of Hsp90 in Protein Complex Assembly. *Biochim Biophys Acta.* 1823 (3), 674–682. doi:10.1016/j.bbamcr.2011.09.001

Megeney, L. A., Kablar, B., Perry, R. L. S., Ying, C., May, L., and Rudnicki, M. A. (1999). Severe Cardiomyopathy in Mice Lacking Dystrophin and MyoD. *Proc. Natl. Acad. Sci. U.S.A.* 96 (1), 220–225. doi:10.1073/pnas.96.1.220

Meissner, B., Rogalski, T., Viveiros, R., Warner, A., Plastino, L., Lorch, A., et al. (2011). Determining the Sub-cellular Localization of Proteins within *Caenorhabditis elegans* Body Wall Muscle. *PLoS One* 6 (5), e19937. doi:10.1371/journal.pone.0019937

Meller, A., and Shalgi, R. (2021). The Aging Proteostasis Decline: From Nematode to Human. *Exp. Cell Res.* 399 (2), 112474. doi:10.1016/j.yexcr.2021.112474

Mergoud Dit Lamarche, A., Molin, L., Pierson, L., Mariol, M.-C., Bessereau, J.-L., Gieseler, K., et al. (2018). UNC-120/SRF Independently Controls Muscle Aging and Lifespan in *Caenorhabditis elegans*. *Aging Cell* 17 (2), e12713. doi:10.1111/acel.12713

Meshnik, L., Bar-Yaacov, D., Kasztan, D., Neiger, T., Cohen, T., Kishner, M., et al. (2022). Mutant *C. elegans* Mitofusin Leads to Selective Removal of mtDNA Heteroplasmic Deletions across Generations to Maintain Fitness. *BMC Biol.* 20 (1), 40. doi:10.1186/s12915-022-01241-2

Miles, J., Townend, S., Smith, W., Westhead, D. R., and van Oosten-Hawle, P. (2022). Transcellular Chaperone Signaling Is an Intercellular Stress-Response Distinct from the HSF-1 Mediated HSR. *biorxiv*. doi:10.1101/2022.03.17.484707

Nillegoda, N. B., Wentink, A. S., and Bukau, B. (2018). Protein Disaggregation in Multicellular Organisms. *Trends Biochem. Sci.* 43 (4), 285–300. doi:10.1016/j.tibs.2018.02.003

Nisaa, K., and Ben-Zvi, A. (2022). Chaperone Networks Are Shaped by Cellular Differentiation and Identity. *Trends Cell Biol.* 32 (6), 470–474. doi:10.1016/j.tcb.2021.11.001

Nyamsuren, O., Faggionato, D., Loch, W., Schulze, E., and Baumeister, R. (2007). A Mutation in CHN-1/CHIP Suppresses Muscle Degeneration in *Caenorhabditis elegans*. *Dev. Biol.* 312 (1), 193–202. doi:10.1016/j.ydbio.2007.09.033

O'Brien, D., Jones, L. M., Good, S., Miles, J., Vijayabaskar, M. S., Aston, R., et al. (2018). A PQM-1-Mediated Response Triggers Transcellular Chaperone Signaling and Regulates Organismal Proteostasis. *Cell Rep.* 23 (13), 3905–3919. doi:10.1016/j.celrep.2018.05.093

Papsdorf, K., Sacherl, J., and Richter, K. (2014). The Balanced Regulation of Hsc70 by DNJ-13 and UNC-23 Is Required for Muscle Functionality. *J. Biol. Chem.* 289 (36), 25250–25261. doi:10.1074/jbc.M114.565234

Piri, N., Kwong, J. M. K., Gu, L., and Caprioli, J. (2016). Heat Shock Proteins in the Retina: Focus on HSP70 and Alpha Crystallins in Ganglion Cell Survival. *Prog. Retin. Eye Res.* 52, 22–46. doi:10.1016/j.preteyeres.2016.03.001

Rahmani, P., Rogalski, T., and Moerman, D. G. (2015). TheC. elegansUNC-23 Protein, a Member of the BCL-2-Associated Athanogene (BAG) Family of Chaperone Regulators, Interacts with HSP-1 to Regulate Cell Attachment and Maintain Hypodermal Integrity. *Worm* 4 (2), e1023496. doi:10.1080/21624054.2015.1023496

Rosenzweig, R., Nillegoda, N. B., Mayer, M. P., and Bukau, B. (2019). The Hsp70 Chaperone Network. *Nat. Rev. Mol. Cell Biol.* 20, 665–680. doi:10.1038/s41580-019-0133-3

Roy, P. J., Stuart, J. M., Lund, J., and Kim, S. K. (2002). Chromosomal Clustering of Muscle-Expressed Genes in *Caenorhabditis elegans*. *Nature* 418 (6901), 975–979. doi:10.1038/nature01012

Sala, A. J., Bott, L. C., and Morimoto, R. I. (2017). Shaping Proteostasis at the Cellular, Tissue, and Organismal Level. *J. Cell Biol.* 216 (5), 1231–1241. doi:10.1083/jcb.201612111

Sarparanta, J., Jonson, P. H., Golzio, C., Sandell, S., Luque, H., Screen, M., et al. (2012). Mutations Affecting the Cytoplasmic Functions of the Co-chaperone DNAJB6 Cause Limb-Girdle Muscular Dystrophy. *Nat. Genet.* 44 (4), 450S451–455452. doi:10.1038/ng.1103

Shai, N., Shemesh, N., and Ben-Zvi, A. (2014). Remodeling of Proteostasis upon Transition to Adulthood Is Linked to Reproduction Onset. *Curr. Genomics* 15 (2), 122–129. doi:10.2174/1389202915666140221005023

Shemesh, N., Jubran, J., Dror, S., Simonovsky, E., Basha, O., Argov, C., et al. (2021). The Landscape of Molecular Chaperones across Human Tissues Reveals a Layered Architecture of Core and Variable Chaperones. *Nat. Commun.* 12 (1), 2180. doi:10.1038/s41467-021-22369-9

Sugiyama, Y., Suzuki, A., Kishikawa, M., Akutsu, R., Hirose, T., Waye, M. M. Y., et al. (2000). Muscle Develops a Specific Form of Small Heat Shock Protein Complex Composed of MKBP/HSPB2 and HSPB3 during Myogenic Differentiation. *J. Biol. Chem.* 275 (2), 1095–1104. doi:10.1074/jbc.275.2.1095

Thiruvalluvan, A., de Mattos, E. P., Brunsting, J. F., Bakels, R., Serlidaki, D., Barazzuol, L., et al. (2020). DNAJB6, a Key Factor in Neuronal Sensitivity to Amyloidogenesis. *Mol. Cell* 78 (2), 346–358. doi:10.1016/j.molcel.2020.02.022

Tiago, T., Hummel, B., Morelli, F. F., Basile, V., Vinet, J., Galli, V., et al. (2021). Small Heat-Shock Protein HSPB3 Promotes Myogenesis by Regulating the Lamin B Receptor. *Cell Death Dis.* 12 (5), 452. doi:10.1038/s41419-021-03737-1

Toudji-Zouaz, A., Bertrand, V., and Barrière, A. (2021). Imaging of Native Transcription and Transcriptional Dynamics *In Vivo* Using a Tagged Argonaute Protein. *Nucleic Acids Res.* 49 (15), e86. doi:10.1093/nar/gkab469

Vonk, W. I. M., Rainbolt, T. K., Dolan, P. T., Webb, A. E., Brunet, A., and Frydman, J. (2020). Differentiation Drives Widespread Rewiring of the Neural Stem Cell Chaperone Network. *Mol. Cell* 78 (2), 329–345. doi:10.1016/j.molcel.2020.03.009

Zha, J., Ying, M., Alexander-Floyd, J., and Gidalevitz, T. (2019). HSP-4/BiP Expression in Secretory Cells Is Regulated by a Developmental Program and Not by the Unfolded Protein Response. *PLoS Biol.* 17 (3), e3000196. doi:10.1371/journal.pbio.3000196

**Conflict of Interest:** The authors declare that the research was conducted in the absence of any commercial or financial relationships that could be construed as a potential conflict of interest.

**Publisher's Note:** All claims expressed in this article are solely those of the authors and do not necessarily represent those of their affiliated organizations, or those of the publisher, the editors and the reviewers. Any product that may be evaluated in this article, or claim that may be made by its manufacturer, is not guaranteed or endorsed by the publisher.

frontiers | Frontiers in Cell and Developmental Biology

MINI REVIEW
published: 13 July 2022
doi: 10.3389/fcell.2022.967875

# Selective Secretion of KDEL-Bearing Proteins: Mechanisms and Functions

*F. C. Palazzo, R. Sitia* and T. Tempio*

*Division of Genetics and Cell Biology Vita-Salute San Raffaele University and IRCCS San Raffaele Scientific Institute, Milan, Italy*

In multicellular organisms, cells must continuously exchange messages with the right meaning, intensity, and duration. Most of these messages are delivered through cognate interactions between membrane and secretory proteins. Their conformational maturation is assisted by a vast array of chaperones and enzymes, ensuring the fidelity of intercellular communication. These folding assistants reside in the early secretory compartment (ESC), a functional unit that encompasses endoplasmic reticulum (ER), intermediate compartment and cis-Golgi. Most soluble ESC residents have C-terminal KDEL-like motifs that prevent their transport beyond the Golgi. However, some accumulate in the ER, while others in downstream stations, implying different recycling rates. Moreover, it is now clear that cells can actively secrete certain ESC residents but not others. This essay discusses the physiology of their differential intracellular distribution, and the mechanisms that may ensure selectivity of release.

**Keywords: KDEL receptors, protein quality control, protein secretion, ERp44, PDI, protein folding, endoplasmic recticulum, Golgi**

OPEN ACCESS

***Edited by:***
*Silvia Masciarelli,*
*Sapienza University of Rome, Italy*

***Reviewed by:***
*Boaz Tirosh,*
*Hebrew University of Jerusalem, Israel*

****Correspondence:***
*R. Sitia*
*sitia.roberto@hsr.it*

***Specialty section:***
*This article was submitted to Signaling, a section of the journal Frontiers in Cell and Developmental Biology*

***Received:*** *13 June 2022*
***Accepted:*** *24 June 2022*
***Published:*** *13 July 2022*

***Citation:***
*Palazzo FC, Sitia R and Tempio T (2022) Selective Secretion of KDEL-Bearing Proteins: Mechanisms and Functions. Front. Cell Dev. Biol. 10:967875. doi: 10.3389/fcell.2022.967875*

## THE ASSEMBLY LINE FOR SECRETORY PROTEINS

Secreted proteins are key messengers in cell-to-cell communication. The composition of the secretome depends on selective cargo export and retention/retrieval mechanisms. Key players in the latter are KDEL receptors (KRs), present in three isoforms in mammals. Through the recognition of C-terminal sequence KDEL, or variants thereof (e.g., KTEL, RDEL, HDEL), they prevent the secretion of the many and very abundant soluble chaperones and enzymes (Munro and Pelham, 1987), that assist the folding of a diverse secretome. These folding assistants operate in the early secretory compartment (ESC), a term we use herein to define the ER, intermediate compartment and cis-Golgi. Its stepwise organization is perfectly suited to time the many posttranslational modifications that cargoes need to attain their native structure.

Cargo proteins proceed along the ESC like cars in assembly lines: yet, workers must stay in place to execute their tasks in a precise order. How can few KRs retain the numerous resident proteins? And how are the latter distributed in ESC to operate in the optimal sequence along the folding-assembly line? Compelling evidence shows that KDEL-bearing proteins distribute differently along ESC, depending on the balance between retention and forward movement, in a self-assembling multiple phase separation system (Gilchrist et al., 2006; Anelli et al., 2007; Tempio et al., 2021). This structure allows sequential checkpoints in the biogenesis and quality control (QC) of complex cargo proteins. **Figure 1** summarizes our hypothetical model of ESC as a chromatography column (Anelli et al., 2015) packed with supramolecular complexes of chaperones and enzymes (Booth & Koch, 1989; Meunier et al., 2002). The propensity of resident proteins to interact with each other, as well as redox oscillations, pH differences and increasing/decreasing concentration of salts and metals might determine the size of the beads, which would distribute accordingly, like the stones that remain in a

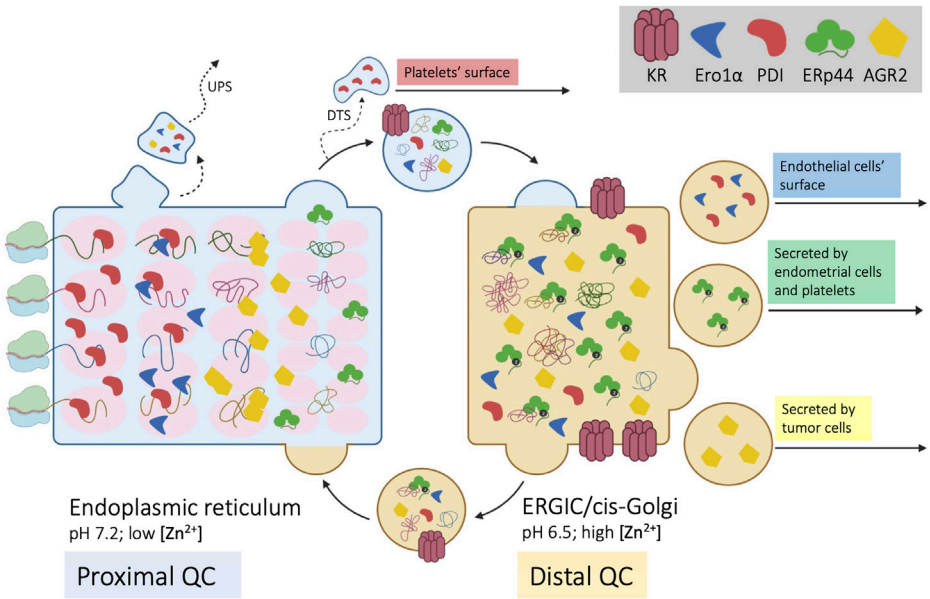


**FIGURE 1 |** Self-sorting of chaperones and cargoes along the early secretory compartment (ESC). Four nascent cargo proteins are depicted on the left side of the cartoon as they cotranslationally translocate into the ER. Here, they encounter a series of chaperones and enzymes, that help their folding and prevent aggregation (proximal QC). The pink ovals represent supramolecular complexes with different diffusibility, with which cargo proteins sequentially interact. Once they reach a native, compact conformation, cargoes no longer interact with the matrix and can proceed towards downstream stations of the secretory pathway. ESC residents that reach the Golgi are instead retrieved by KRs. Unlike PDI, ERp44 reaches faster the distal compartment (ERGIC/cis-Golgi) to patrol the assembly of complex, multimeric proteins (distal QC). ERp44 retrieves also Ero1α and other enzymes that lack KDEL motifs (Prx4, ERAP1, FGE/SuMF1). Some proteins might be retro-translocated from the ER to the cytosol and exported via unconventional pathways of secretion (UPS). As shown in the right part of the cartoon, some ESC residents elude KRs' retention/retrieval and are found also extracellularly. During megakaryocyte maturation, PDI is routed towards smooth ER fragments called "dense tubular system" (DTS). PDI and Ero1α are also found on the surface of endothelial cells, whilst ERp44 is secreted during decidualization of primary endometrial cells. AGR2 is instead abundantly secreted by tumor cells or upon inflammation.

sieve. In their route to secretion, newly synthesized, unfolded cargo proteins interact with the column matrices. On the one hand, these interactions favor folding and prevent aggregation of cargo proteins. On the other, they can further increase the matrix size, making the retention system hardly saturable (Reddy et al., 1996; Meunier et al., 2002).

Only compact cargoes that no longer interact with the column matrices can proceed further. For many complex cargoes, however, the folding schedule is not complete within the proximal QC checkpoints. Thus, some chaperones and enzymes evade the ER and patrol the arrival of complex molecules in the ERGIC and cis-Golgi compartments, operating a distal QC. For example, IgM and adiponectin are transported further downstream to oligomerize under the assistance of ERp44 (Hampe et al., 2015; Anelli and Sitia 2018; Giannone et al., 2022). Indeed, despite having a RDEL motif, ERp44 accumulates distally with respect to other ESC residents, like PDI. The faster rate at which it exits from the ER depends in part on interactions with the cargo receptor ERGIC53 (Tempio et al., 2021). Moreover, unlike PDI, ERp44 is not part of the BiP containing primary matrix (Meunier et al., 2002).

To further complicate the issue, some proteins acting primarily in the ER do not contain known localization signals. An outstanding example is Ero1α, a glycosylated flavoenzyme playing a crucial role in oxidative protein folding (Cabibbo et al., 2000; Mezghrani et al., 2001). Interestingly, while the yeast Ero1p contains an essential C-terminal tail mediating its association with the ER membrane (Pagani et al., 2001), this tail is absent from human Ero1α and Ero1β. As a matter of fact, to be retained/retrieved the two flavoproteins hijack the KDEL and RDEL motifs of PDI and ERp44 with whom they associate. The loss of an intrinsic localization motif from Ero1α and Ero1β likely reflects the need to perform new functions in metazoan with respect to unicellular yeast. In stressed mammalian cells, for instance, Ero1α can reach the Golgi, increase its oxidase activity upon phosphorylation by Fam20C, and return to the ER with ERp44 (Anelli et al., 2003; Zhang et al., 2018) or be secreted by certain cell types (Swiatkowska et al., 2010).

This scenario depicts a continuous flow of proteins in ESC that self-sort in functional order. Some, more "static", are part of slowly diffusing supramolecular complexes with a low propensity to exit the ER (**Figure 1**). Others, more "dynamic", cycle rapidly between ER and Golgi. Prototypes of the two are PDI and ERp44. Intriguingly, both retain Ero1α and are released by certain cell types, playing important functions extracellularly. Hereafter, we'll use the term secretion to indicate active and specific transport, whilst release will encompass also non-specific mechanisms that involve loss of membrane integrity.

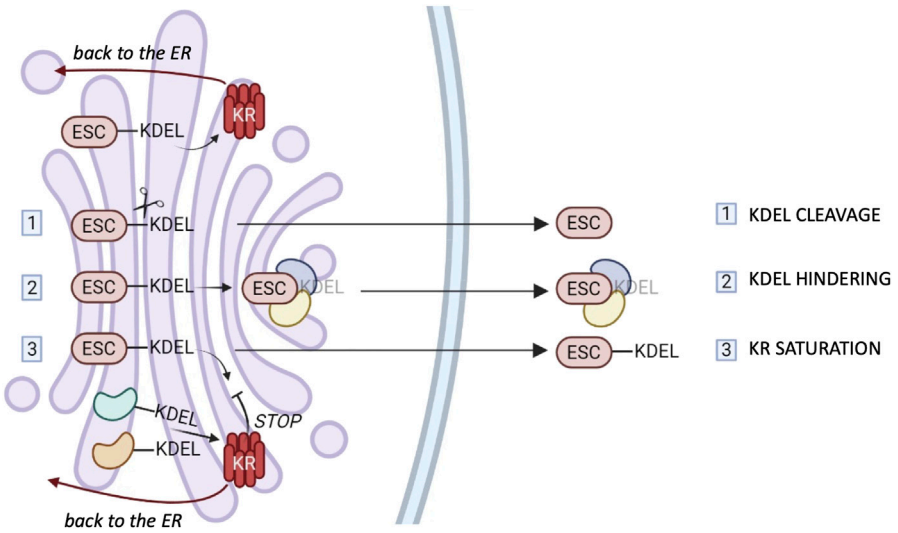


**FIGURE 2 |** ESCape mechanisms. Most ER chaperones and enzymes are characterized by the presence of a C-terminal motif KDEL or variants thereof which mediates their retrieval to the ER via binding to one of the three KDEL receptors (KR). The cartoon summarizes possible mechanisms that these proteins might exploit to elude KRs' surveillance. 1) Selective secretion by cleavage of the KDEL retention motifs. 2) Selective secretion upon binding of bulky clients that hinder KDEL-motifs. 3) Release upon weak KR retrieval activity due to client overload and/or Golgi basification. The different tissue distribution or preferential saturation/inhibition of individual KRs might sustain the selective secretion of chaperones or groups of them (see text for references).

## WHAT DETERMINES THE EXIT OF ESC PROTEINS?

### Loss of Membrane Integrity

Passive release upon severe stress, necrosis or pyroptosis could make ESC resident proteins a subset of damage-associated molecular pattern (DAMPs) molecules. These non-specific mechanisms can hardly allow the selective externalization of single or groups of molecules, even though being part of large multimolecular complexes might retard diffusion. This could yield a temporal hierarchy of release from damaged cells, in this way informing the organism of the nature of the incumbent danger.

### Specific Release of ESC Residents

How can ESC residents bearing KDEL motifs escape KR surveillance? Several mechanisms can be hypothesized, and they are summarized in **Figure 2**.

First of all, a selective proteolysis might remove the KDEL-like motif (step I in **Figure 2**). However, convincing evidence for this mechanism is missing.

Secondly, there could be the hindering of retrieval motifs by bulky clients (step II), proof of which has been obtained in the case of calreticulin (Johnson et al., 2001).

Moreover, considering that KRs are pH-sensitive (Bräuer et al., 2019), basification of the Golgi stacks might weaken their overall activity. Client overload, also, could transiently saturate KR-dependent retrieval systems (step III), but neither of these mechanisms would be sufficient to explain selective secretion of chaperones. In our hands, even when very abundantly overexpressed, ERp44 was not secreted, nor did it induce the secretion of other residents (Anelli et al., 2003; Vavassori et al., 2013). The structural similarities of the three KR argue against gross differences in their binding affinities for clients. Yet, the three human KRs are likely to serve different functions. Accordingly, their relative abundance changes in different tissues or cells (www.proteinatlas.org). However, it is still unclear whether they bind preferentially certain clients in the lumen, or different signaling molecules in the cytosol (Cancino et al., 2013; Luini et al., 2014). More detailed comparisons might reveal mechanisms that allow ER resident secretion by selective inhibition (or saturation) of a single KR. Intriguingly, in some cell types, KR1 can reach the plasma membrane, supposedly through clathrin-dependent transport carriers (Jia et al., 2021), in association with PDI, ERp57 and ERp5 (Bartels et al., 2019). It remains to be seen what allows KR1 to travel further and how its client oxidoreductases elude the other KRs. Specific secretion could be achieved if selected KDEL-bearing proteins arrive with forward-moving cargo transporters, as described for ERp44 (Tempio et al., 2021).

### Unconventional Secretory Pathway

Some proteins that lack a leader sequence (e.g., IL-1β, FGF2 or thioredoxin) are actively secreted by living cells via diverse pathways (Sitia & Rubartelli, 2020). In many cases, their precursors can translocate into lysosomes, or reach them by autophagic pathways (Duran et al., 2010; Dupont et al., 2011). Particularly in hematopoietic cells, lysosomes can fuse with the plasma membrane, releasing their contents in the extracellular space. It is possible that also ESC residents follow this route. Concentration of soluble proteins in ESC subregions might recruit autophagosomes leading to selective secretion.

Moreover, in conditions of ER stress, prion protein and calreticulin are shunted to the cytosol in the process of pre-emptive quality control (Orsi et al., 2006; Snapp et al., 2006). It has also been proposed that, upon harsh ER stress, some ER chaperones can be translocated to the cytosol in a process defined "ER reflux" (Igbaria et al., 2019; Sicari et al., 2021). Then, from the cytosol, these proteins might also follow chaperone-mediated unconventional secretory pathways to reach the extracellular space.

## EXTRACELLULAR FUNCTIONS OF ESC RESIDENTS

The "selective secretion" of proteins that are normally retained inside may represent a novel code that cells use to interact with each other. When secreted, ESC residents can interfere directly or indirectly with ligands, receptors and the signals generated by their interactions. In any case, to reflect specific pathophysiologic conditions their release should be regulated in time and space.

Although several lines of evidence suggest new roles for "mis-localized" ESC residents, the transport mechanisms and functions are still controversial. Even in systems in which selective secretion is documented, only a minor fraction of the ESC resident in question is found extracellularly (Soares Moretti and Martins Laurindo, 2017). This does not diminish the potential pathophysiological implications, though. Considering the almost virtual space in immunological and neural synapses and between cells in contact, even few molecules may reach concentrations sufficient to exert relevant biological phenomena. Rarely does evolution leave important pathways to chance: hence, the release of ESC components by living and unstressed cells would be most likely linked to tightly regulated paths.

### Blood Clotting

There is ample evidence that the presence of PDI in the extracellular space impacts blood clotting, virus entry and other pathophysiological events (Gallina et al., 2002; Markovic et al., 2004; Furie & Flaumenhaft, 2014; Fraternale et al., 2021; Xu et al., 2021). In the ER, PDI is present in high concentration, up to 0.2–0.5 mM (Lyles & Gilbert, 1991; Laurindo et al., 2012), making it a well-known marker of this compartment.

Its presence in the medium and on the surface of some cell types has been widely reported (Araujo et al., 2017; Wu & Essex, 2020). During vascular injury, for example, activated platelets and endothelial cells release PDI in the extracellular space (Cho et al., 2012; Bowley et al., 2017; Sharda & Furie, 2018). Moreover, they present also PDI molecules on their surface, which interact with $\beta_3$ integrins (Cho et al., 2012; Ponamarczuk et al., 2018). Given its role in blood clotting, one would expect PDI secretion being mostly short range, essentially of paracrine nature.

Upon platelet activation, also other thiol isomerases, such as ERp5, ERp57, ERp72, ERp44 and ERp29 are exported into the medium or bound to the outer leaflet of the plasma membrane (Holbrook et al., 2010; Tanaka et al., 2020; Wu & Essex, 2020). Whether their export depends on aspecific release or active secretion is still debated. For instance, during megakaryocyte maturation, PDI and ERp57 molecules that will be found in platelets do not follow the normal Golgi-secretory vesicles route. Rather, they accumulate in a subcellular compartment called "dense tubular system", which derives from the smooth ER of megakaryocytes (Crescente et al., 2016). Additionally, it has been proposed that stimulated endothelial cells secrete PDI in Gro-α-containing granules (Jasuja et al., 2010). Within these granules, PDI might hide its KDEL and elude retrieval, as described for calreticulin (Johnson et al., 2001).

Anyway, whatever is the transport mechanism, paramount are the pathophysiologic consequences of thiol isomerases appearance outside the cell.

### Potential Synergies in the Redox Control of Extracellular Thiol Isomerases

Not only their abundance but also the redox state of PDI and other oxidoreductases are bound to determine their extracellular function. PDI molecules found on activated platelets are mainly in their reduced state (Essex & Wu, 2018), while the reverse is true in vascular smooth muscle cells (Tanaka et al., 2016, 2019). In the ER, PDI oxidation depends largely on the selective binding of Ero1α to it's a domain. Yet, part of PDI must remain reduced to mediate disulfide isomerization. In the extracellular space, its redox state depends on the presence of non-protein couples (e.g., GSH-GSSG) or redox enzymes such as thioredoxin, QSOX or Ero1α. Thus, other cell types can modulate the ultimate function of PDI and other oxidoreductases. The reversible modifications of the catalytic cysteines of these enzymes are powerful molecular switches. Thus, the presence of oxidants in constrained extracellular spaces is particularly relevant. For this reason, the detection of also Ero1α on the surface of activated platelets is not trivial (Swiatkowska et al., 2010). In the ER, and also in test tubes, Ero1α re-oxidizes PDI at the expense of $O_2$ molecules (Appenzeller-Herzog et al., 2010). Therefore, their vicinity on the platelets surface would fuel oxidative equivalents that sustain clotting through disulfide bond formation or isomerization in extracellular substrates (Swiatkowska et al., 2010). As the ER localization of Ero1α depends also on ERp44, its release would involve at least two control levels. In cells actively secreting PDI, also the surveillance of ERp44 must be eluded by Ero1α. What if Ero1α is released by other cells in which ERp44 is inactive or itself secreted?

The localization and cycling of ERp44 are controlled by zinc- and pH-dependent conformational changes that expose its client binding site and RDEL motif (Vavassori et al., 2013; Watanabe et al., 2019; Tempio & Anelli, 2020). O-glycosylated ERp44 is secreted by primary and immortalized endometrial cells (Sannino et al., 2014) suggesting transport through the canonical secretory pathway. If not in all, in most cell types, lowering zinc concentration induces rather selectively the secretion of ERp44 and its clients. Upon pH manipulation, instead, ERp44 is retained while its cargos Ero1α, Prx4 and ERAP1 are secreted.

## Cancer and Inflammation

Like ERp44, the small thioredoxin family member AGR2 lacks the resolving cysteine in its active motif and is hence better suited for an isomerase/holdase than an oxidoreductase function (Moidu et al., 2020). Despite its KTEL motif warrants ESC residency, it has a reduced binding affinity for the KRs (Raykhel et al., 2007; Alanen et al., 2011). This could explain its well documented secretion in response to physiological and/or pathological conditions. Indeed, besides its established intracellular roles in the folding, trafficking, and assembly of mucins, EGF receptors and other cysteine-rich proteins (Delom et al., 2020; Moidu et al., 2020), AGR2 has been found secreted or bound to the plasma membrane (Chevet et al., 2013; Dumartin et al., 2017). In cancer, these extracellular localizations of AGR2 have been proposed to modulate matrix remodeling, metastasis progression and support angiogenesis (Delom et al., 2018). Enhanced AGR2 secretion by ER stressed cells is thought also to modulate pro-inflammatory signals, particularly in inflammatory bowel disease (Maurel et al., 2019). The presence of O-glycans in extracellular AGR2 suggests that it follows the canonical secretory route (Clarke et al., 2015; Tian et al., 2018; Moidu et al., 2020).

## Conclusions and Open Questions

After the finding that cells exchange bits of cytosol and membranes with each other, another pillar of cell biology fell apart with the detection on the plasma membrane or in the extracellular fluids of proteins traditionally used as markers of the ESC. Is this "extracellular folding compartment" a new way that cells use to communicate with each other? Are moonlighting and multitasking obligatory features of proteins in multicellular organisms? In this respect, we can imagine an intercellular compartment in which individual folding components are provided by different cells.

The presence of small redox compounds and enzymes in the extracellular space becomes crucial. For instance, stressed cells release cysteine, thioredoxin and other stress associated molecular pattern (SAMPs) molecules, often through unconventional secretory pathways, that dictate the intensity and duration of inflammatory responses (Sitia & Rubartelli, 2020; Yang et al., 2021). It is tempting to speculate that fundamental decisions, like thrombus initiation, depend on the simultaneous release of synergizing compounds by different cells.

A key issue is the mechanism(s) of secretion. Posttranslational modifications, glycan processing in particular, can provide powerful cues to decipher the route ESC residents follow to reach the extracellular space. Indeed, the release of O-glycosylated ERp44 and AGR2 argues in favor of passage through the Golgi. Since sugar bound asparagines are converted to aspartates by cytosolic glycanases, an accurate characterization of suitably engineered reporters might shed some light on this important issue. It is possible that multiple pathways exist that regulate the export of luminal ESC residents as biological signals, like in the case of the diverse unconventional pathways used by leaderless proteins (Sitia & Rubartelli, 2020).

An increased knowledge on these secretory pathways and their regulation may allow manipulating key pathophysiological circuits, including inflammation, angiogenesis, and blood clotting, in this way reestablishing homeostasis.

Overall, this could be also important to find new therapeutic targets for diseases still having great unmet medical needs.

## AUTHOR CONTRIBUTIONS

All authors listed have made a substantial, direct, and intellectual contribution to the work and approved it for publication.

## FUNDING

This work was supported by grants from Cariplo, AIRC IG 2019—ID. 23285 and Ministero dell'Università e Ricerca (PRIN 2017XA5J5N).

## ACKNOWLEDGMENTS

We thank Percillia Oliveira and Andrea Orsi for suggestions and critical reading of the manuscript. The help of Tiziana Anelli, by all means Mrs ERp44, which has been invaluable.

## REFERENCES

Alanen, H. I., Raykhel, I. B., Luukas, M. J., Salo, K. E. H., and Ruddock, L. W. (2011). Beyond KDEL: The Role of Positions 5 and 6 in Determining ER Localization. *J. Mol. Biol.* 409 (3), 291–297. doi:10.1016/j.jmb.2011.03.070

Anelli, T., Alessio, M., Bachi, A., Bergamelli, L., Bertoli, G., Camerini, S., et al. (2003). Thiol-mediated Protein Retention in the Endoplasmic Reticulum: The Role of ERp44. *EMBO J.* 22 (19), 5015–5022. doi:10.1093/emboj/cdg491

Anelli, T., Ceppi, S., Bergamelli, L., Cortini, M., Masciarelli, S., Valetti, C., et al. (2007). Sequential Steps and Checkpoints in the Early Exocytic Compartment during Secretory IgM Biogenesis. *Embo J.* 26 (19), 4177–4188. doi:10.1038/sj.emboj.7601844

Anelli, T., Sannino, S., and Sitia, R. (2015). Proteostasis and "Redoxtasis" in the Secretory Pathway: Tales of Tails from ERp44 and Immunoglobulins. *Free Radic. Biol. Med.* 83, 323–330. doi:10.1016/j.freeradbiomed.2015.02.020

Anelli, T., and Sitia, R. (2018). "CHAPTER 3.4. Mechanisms of Oxidative Protein Folding and Thiol-dependent Quality Control: Tales of Cysteines and Cystines," in *Oxidative Folding of Proteins: Basic Principles, Cellular Regulation and Engineering*. Editor M. Feige (London, United Kingdom: The Royal Society of Chemistry), 249–266. doi:10.1039/9781788013253-00249

Appenzeller-Herzog, C., Riemer, J., Zito, E., Chin, K.-T., Ron, D., Spiess, M., et al. (2010). Disulphide Production by Ero1α-PDI Relay Is Rapid and Effectively Regulated. *Embo J.* 29 (19), 3318–3329. doi:10.1038/emboj.2010.203

Araujo, T. L. S., Zeidler, J. D., Oliveira, P. V. S., Dias, M. H., Armelin, H. A., and Laurindo, F. R. M. (2017). Protein Disulfide Isomerase Externalization in Endothelial Cells Follows Classical and Unconventional Routes. *Free Radic. Biol. Med.* 103, 199–208. doi:10.1016/j.freeradbiomed.2016.12.021

Bartels, A. K., Göttert, S., Desel, C., Schäfer, M., Krossa, S., Scheidig, A. J., et al. (2019). KDEL Receptor 1 Contributes to Cell Surface Association of Protein Disulfide Isomerases. *Cell Physiol. Biochem.* 52 (4), 580–868. doi:10.33594/000000059

Booth, C., and Koch, G. L. E. (1989). Perturbation of Cellular Calcium Induces Secretion of Luminal ER Proteins. *Cell* 59 (4), 729–737. doi:10.1016/0092-8674(89)90019-6

Bowley, S. R., Fang, C., Merrill-Skoloff, G., Furie, B. C., and Furie, B. (2017). Protein Disulfide Isomerase Secretion Following Vascular Injury Initiates a Regulatory Pathway for Thrombus Formation. *Nat. Commun.* 8, 14151. doi:10.1038/ncomms14151

Bräuer, P., Parker, J. L., Gerondopoulos, A., Zimmermann, I., Seeger, M. A., Barr, F. A., et al. (2019). Structural Basis for pH-dependent Retrieval of ER Proteins from the Golgi by the KDEL Receptor. *Science* 363 (6431), 1103–1107. doi:10.1126/science.aaw2859

Cabibbo, A., Pagani, M., Fabbri, M., Rocchi, M., Farmery, M. R., Bulleid, N. J., et al. (2000). ERO1-L, a Human Protein that Favors Disulfide Bond Formation in the Endoplasmic Reticulum. *J. Biol. Chem.* 275 (7), 4827–4833. doi:10.1074/jbc.275.7.4827

Cancino, J., Jung, J. E., and Luini, A. (2013). Regulation of Golgi Signaling and Trafficking by the KDEL Receptor. *Histochem Cell Biol.* 140 (4), 395–405. doi:10.1007/s00418-013-1130-9

Chevet, E., Fessart, D., Delom, F., Mulot, A., Vojtesek, B., Hrstka, R., et al. (2013). Emerging Roles for the Pro-oncogenic Anterior Gradient-2 in Cancer Development. *Oncogene* 32 (20), 2499–2509. doi:10.1038/onc.2012.346

Cho, J., Kennedy, D. R., Lin, L., Huang, M., Merrill-Skoloff, G., Furie, B. C., et al. (2012). Protein Disulfide Isomerase Capture during Thrombus Formation *In Vivo* Depends on the Presence of β3 Integrins. *Blood* 120 (3), 647–655. doi:10.1182/blood-2011-08-372532

Clarke, C., Rudland, P., and Barraclough, R. (2015). The Metastasis-Inducing Protein AGR2 Is O-Glycosylated upon Secretion from Mammary Epithelial Cells. *Mol. Cell Biochem.* 408 (1–2), 245–252. doi:10.1007/s11010-015-2502-3

Crescente, M., Pluthero, F. G., Li, L., Lo, R. W., Walsh, T. G., Schenk, M. P., et al. (2016). Intracellular Trafficking, Localization, and Mobilization of Platelet-Borne Thiol Isomerases. *Atvb* 36 (6), 1164–1173. doi:10.1161/ATVBAHA.116.307461

Delom, F., Mohtar, M. A., Hupp, T., and Fessart, D. (2020). The Anterior Gradient-2 Interactome. *Am. J. Physiology-Cell Physiology* 318 (1), C40–C47. doi:10.1152/ajpcell.00532.2018

Delom, F., Nazaraliyev, A., and Fessart, D. (2018). The Role of Protein Disulphide Isomerase AGR2 in the Tumour Niche. *Biol. Cell* 110 (12), 271–282. doi:10.1111/boc.201800024

Dumartin, L., Alrawashdeh, W., Trabulo, S. M., Radon, T. P., Steiger, K., Feakins, R. M., et al. (2017). ER Stress Protein AGR2 Precedes and Is Involved in the Regulation of Pancreatic Cancer Initiation. *Oncogene* 36 (22), 3094–3103. doi:10.1038/onc.2016.459

Dupont, N., Jiang, S., Pilli, M., Ornatowski, W., Bhattacharya, D., and Deretic, V. (2011). Autophagy-based Unconventional Secretory Pathway for Extracellular Delivery of IL-1β. *EMBO J.* 30 (23), 4701–4711. doi:10.1038/emboj.2011.398

Duran, J. M., Anjard, C., Stefan, C., Loomis, W. F., and Malhotra, V. (2010). Unconventional Secretion of Acb1 Is Mediated by Autophagosomes. *J. Cell Biol.* 188 (4), 527–536. doi:10.1083/jcb.200911154

Essex, D. W., and Wu, Y. (2018). Multiple Protein Disulfide Isomerases Support Thrombosis. *Curr. Opin. Hematol.* 25 (5), 395–402. doi:10.1097/MOH.0000000000000449

Fraternale, A., Zara, C., De Angelis, M., Nencioni, L., Palamara, A. T., Retini, M., et al. (2021). Intracellular Redox-Modulated Pathways as Targets for Effective Approaches in the Treatment of Viral Infection. *Ijms* 22 (7), 3603. doi:10.3390/ijms22073603

Furie, B., and Flaumenhaft, R. (2014). Thiol Isomerases in Thrombus Formation. *Circ. Res.* 114 (7), 1162–1173. doi:10.1161/CIRCRESAHA.114.301808

Gallina, A., Hanley, T. M., Mandel, R., Trahey, M., Broder, C. C., Viglianti, G. A., et al. (2002). Inhibitors of Protein-Disulfide Isomerase Prevent Cleavage of Disulfide Bonds in Receptor-Bound Glycoprotein 120 and Prevent HIV-1 Entry. *J. Biol. Chem.* 277 (52), 50579–50588. doi:10.1074/jbc.M204547200

Giannone, C., Chelazzi, M. R., Orsi, A., Anelli, T., Nguyen, T., Buchner, J., et al. (2022). Biogenesis of Secretory Immunoglobulin M Requires Intermediate Non-native Disulfide Bonds and Engagement of the Protein Disulfide Isomerase ERp44. *EMBO J.* 41 (3), e108518. doi:10.15252/embj.2021108518

Gilchrist, A., Au, C. E., Hiding, J., Bell, A. W., Fernandez-Rodriguez, J., Lesimple, S., et al. (2006). Quantitative Proteomics Analysis of the Secretory Pathway. *Cell* 127 (6), 1265–1281. doi:10.1016/j.cell.2006.10.036

Hampe, L., Radjainia, M., Xu, C., Harris, P. W. R., Bashiri, G., Goldstone, D. C., et al. (2015). Regulation and Quality Control of Adiponectin Assembly by Endoplasmic Reticulum Chaperone ERp44. *J. Biol. Chem.* 290 (29), 18111–18123. doi:10.1074/jbc.M115.663088

Holbrook, L.-M., Watkins, N. A., Simmonds, A. D., Jones, C. I., Ouwehand, W. H., and Gibbins, J. M. (2010). Platelets Release Novel Thiol Isomerase Enzymes Which Are Recruited to the Cell Surface Following Activation. *Br. J. Haematol.* 148 (4), 627–637. doi:10.1111/j.1365-2141.2009.07994.x

Igbaria, A., Merksamer, P. I., Trusina, A., Tilahun, F., Johnson, J. R., Brandman, O., et al. (2019). Chaperone-mediated Reflux of Secretory Proteins to the Cytosol during Endoplasmic Reticulum Stress. *Proc. Natl. Acad. Sci. U.S.A.* 116 (23), 11291–11298. doi:10.1073/pnas.1904516116

Jasuja, R., Furie, B., and Furie, B. C. (2010). Endothelium-derived but Not Platelet-Derived Protein Disulfide Isomerase Is Required for Thrombus Formation *In Vivo*. *Blood* 116 (22), 4665–4674. doi:10.1182/blood-2010-04-278184

Jia, J., Yue, X., Zhu, L., Jing, S., Wang, Y., Gim, B., et al. (2021). KDEL Receptor Is a Cell Surface Receptor that Cycles between the Plasma Membrane and the Golgi via Clathrin-Mediated Transport Carriers. *Cell. Mol. Life Sci.* 78 (3), 1085–1100. doi:10.1007/s00018-020-03570-3

Johnson, S., Michalak, M., Opas, M., and Eggleton, P. (2001). The Ins and Outs of Calreticulin: from the ER Lumen to the Extracellular Space. *Trends Cell Biol.* 11 (3), 122–129. doi:10.1016/s0962-8924(01)01926-2

Laurindo, F. R. M., Pescatore, L. A., and de Castro Fernandes, D. (2012). Protein Disulfide Isomerase in Redox Cell Signaling and Homeostasis. *Free Radic. Biol. Med.* 52 (9), 1954–1969. doi:10.1016/j.freeradbiomed.2012.02.037

Luini, A., Mavelli, G., Jung, J., and Cancino, J. (2014). Control Systems and Coordination Protocols of the Secretory Pathway. *F1000Prime Rep.* 6 (October), 1–7. doi:10.12703/P6-88

Lyles, M. M., and Gilbert, H. F. (1991). Catalysis of the Oxidative Folding of Ribonuclease A by Protein Disulfide Isomerase: Dependence of the Rate on the Composition of the Redox Buffer. *Biochemistry* 30 (3), 613–619. doi:10.1021/bi00217a004

Markovic, I., Stantchev, T. S., Fields, K. H., Tiffany, L. J., Tomiç, M., Weiss, C. D., et al. (2004). Thiol/disulfide Exchange Is a Prerequisite for CXCR4-Tropic HIV-1 Envelope-Mediated T-Cell Fusion during Viral Entry. *Blood* 103 (5), 1586–1594. doi:10.1182/blood-2003-05-1390

Maurel, M., Obacz, J., Avril, T., Ding, Y. P., Papadodima, O., Treton, X., et al. (2019). Control of Anterior GR Adient 2 ( AGR 2) Dimerization Links Endoplasmic Reticulum Proteostasis to Inflammation. *EMBO Mol. Med.* 11 (6), 1–19. doi:10.15252/emmm.201810120

Meunier, L., Usherwood, Y.-K., Chung, K. T., and Hendershot, L. M. (2002). A Subset of Chaperones and Folding Enzymes Form Multiprotein Complexes in Endoplasmic Reticulum to Bind Nascent Proteins. *MBoC* 13 (12), 4456–4469. doi:10.1091/mbc.e02-05-0311

Mezghrani, A., Fassio, A., Benham, A., Simmen, T., Braakman, I., and Sitia, R. (2001). Manipulation of Oxidative Protein Folding and PDI Redox State in Mammalian Cells. *EMBO J.* 20 (22), 6288–6296. doi:10.1093/emboj/20.22.6288

Moidu, N. A., A Rahman, N. S., Syafruddin, S. E., Low, T. Y., and Mohtar, M. A. (2020). Secretion of Pro-oncogenic AGR2 Protein in Cancer. *Heliyon* 6 (9), e05000. doi:10.1016/j.heliyon.2020.e05000

Munro, S., and Pelham, H. R. B. (1987). A C-Terminal Signal Prevents Secretion of Luminal ER Proteins. *Cell* 48 (5), 899–907. doi:10.1016/0092-8674(87)90086-9

Orsi, A., Fioriti, L., Chiesa, R., and Sitia, R. (2006). Conditions of Endoplasmic Reticulum Stress Favor the Accumulation of Cytosolic Prion Protein. *J. Biol. Chem.* 281 (41), 30431–30438. doi:10.1074/jbc.M605320200

Pagani, M., Pilati, S., Bertoli, G., Valsasina, B., and Sitia, R. (2001). The C-Terminal Domain of Yeast Ero1p Mediates Membrane Localization and Is Essential for Function. *FEBS Lett.* 508 (1), 117–120. doi:10.1016/s0014-5793(01)03034-4

Raykhel, I., Alanen, H., Salo, K., Jurvansuu, J., Nguyen, V. D., Latva-Ranta, M., et al. (2007). A Molecular Specificity Code for the Three Mammalian KDEL Receptors. *J. Cell Biol.* 179 (6), 1193–1204. doi:10.1083/jcb.200705180

Reddy, P., Sparvoli, A., Fagioli, C., Fassina, G., and Sitia, R. (1996). Formation of Reversible Disulfide Bonds with the Protein Matrix of the Endoplasmic Reticulum Correlates with the Retention of Unassembled Ig Light Chains. *EMBO J.* 15 (9), 2077–2085. doi:10.1002/j.1460-2075.1996.tb00561.x

Sannino, S., Anelli, T., Cortini, M., Masui, S., Degano, M., Fagioli, C., et al. (2014). Progressive Quality Control of Secretory Proteins in the Early Secretory

Compartment by ERp44. *J. Cell Sci.* 127 (19), 4260–4269. doi:10.1242/jcs.153239

Sharda, A., and Furie, B. (2018). Regulatory Role of Thiol Isomerases in Thrombus Formation. *Expert Rev. Hematol.* 11 (5), 437–448. doi:10.1080/17474086.2018.1452612

Sicari, D., Centonze, F. G., Pineau, R., Le Reste, P. J., Negroni, L., Chat, S., et al. (2021). Reflux of Endoplasmic Reticulum Proteins to the Cytosol Inactivates Tumor Suppressors. *EMBO Rep.* 22 (5), 1–13. doi:10.15252/embr.202051412

Sitia, R., and Rubartelli, A. (2020). Evolution, Role in Inflammation, and Redox Control of Leaderless Secretory Proteins. *J. Biol. Chem.* 295 (22), 7799–7811. doi:10.1074/jbc.REV119.008907

Snapp, E. L., Sharma, A., Lippincott-Schwartz, J., and Hegde, R. S. (2006). Monitoring Chaperone Engagement of Substrates in the Endoplasmic Reticulum of Live Cells. *Proc. Natl. Acad. Sci. U.S.A.* 103 (17), 6536–6541. doi:10.1073/pnas.0510657103

Soares Moretti, A. I., and Martins Laurindo, F. R. (2017). Protein Disulfide Isomerases: Redox Connections in and Out of the Endoplasmic Reticulum. *Archives Biochem. Biophysics* 617, 106–119. doi:10.1016/j.abb.2016.11.007

Swiatkowska, M., Padula, G., Michalec, L., Stasiak, M., Skurzynski, S., and Cierniewski, C. S. (2010). Ero1α Is Expressed on Blood Platelets in Association with Protein-Disulfide Isomerase and Contributes to Redox-Controlled Remodeling of αIIbβ3. *J. Biol. Chem.* 285 (39), 29874–29883. doi:10.1074/jbc.M109.092486

Swiatkowska, M., Popielarski, M., Stasiak, M., Bednarek, R., Studzian, M., Pulaski, L., et al. (2018). Contribution of Activated Beta3 Integrin in the PDI Release from Endothelial Cells. *Front. Biosci.* 23 (9), 1612–1627. doi:10.2741/4663

Tanaka, L. Y., Araújo, H. A., Hironaka, G. K., Araujo, T. L. S., Takimura, C. K., Rodriguez, A. I., et al. (20161979). Peri/Epicellular Protein Disulfide Isomerase Sustains Vascular Lumen Caliber through an Anticonstrictive Remodeling Effect. *Hypertension* 67 (3), 613–622. doi:10.1161/HYPERTENSIONAHA.115.06177

Tanaka, L. Y., Araujo, T. L. S., Rodriguez, A. I., Ferraz, M. S., Pelegati, V. B., Morais, M. C. C., et al. (2019). Peri/epicellular Protein Disulfide Isomerase-A1 Acts as an Upstream Organizer of Cytoskeletal Mechanoadaptation in Vascular Smooth Muscle Cells. *Am. J. Physiology-Heart Circulatory PhysiologyHeart Circulatory Physiology* 316 (3), H566–H579. doi:10.1152/ajpheart.00379.2018

Tanaka, L. Y., Oliveira, P. V. S., and Laurindo, F. R. M. (2020). Peri/Epicellular Thiol Oxidoreductases as Mediators of Extracellular Redox Signaling. *Antioxidants Redox Signal.* 33 (4), 280–307. doi:10.1089/ars.2019.8012

Tempio, T., and Anelli, T. (2020). The Pivotal Role of ERp44 in Patrolling Protein Secretion. *J. Cell Sci.* 133 (21), jcs240366. doi:10.1242/jcs.240366

Tempio, T., Orsi, A., Sicari, D., Valetti, C., Yoboue, E. D., Anelli, T., et al. (2021). A Virtuous Cycle Operated by ERp44 and ERGIC-53 Guarantees Proteostasis in the Early Secretory Compartment. *IScience* 24 (3), 102244. doi:10.1016/j.isci.2021.102244

Tian, S., Hu, J., Tao, K., Wang, J., Chu, Y., Li, J., et al. (2018). Secreted AGR2 Promotes Invasion of Colorectal Cancer Cells via Wnt11-Mediated Non-canonical Wnt Signaling. *Exp. Cell Res.* 364 (2), 198–207. doi:10.1016/j.yexcr.2018.02.004

Vavassori, S., Cortini, M., Masui, S., Sannino, S., Anelli, T., Caserta, I. R., et al. (2013). A pH-Regulated Quality Control Cycle for Surveillance of Secretory Protein Assembly. *Mol. Cell* 50 (6), 783–792. doi:10.1016/j.molcel.2013.04.016

Watanabe, S., Amagai, Y., Sannino, S., Tempio, T., Anelli, T., Harayama, M., et al. (2019). Zinc Regulates ERp44-dependent Protein Quality Control in the Early Secretory Pathway. *Nat. Commun.* 10 (1), 1–16. doi:10.1038/s41467-019-08429-1

Wu, Y., and Essex, D. W. (2020). Vascular Thiol Isomerases in Thrombosis: The Yin and Yang. *J. Thromb. Haemost.* 18 (11), 2790–2800. doi:10.1111/jth.15019

Xu, X., Chiu, J., Chen, S., and Fang, C. (2021). Pathophysiological Roles of Cell Surface and Extracellular Protein Disulfide Isomerase and Their Molecular Mechanisms. *Br. J. Pharmacol.* 178 (15), 2911–2930. doi:10.1111/bph.15493

Yang, H., Lundbäck, P., Ottosson, L., Erlandsson-Harris, H., Venereau, E., Bianchi, M. E., et al. (2021). Redox Modifications of Cysteine Residues Regulate the Cytokine Activity of HMGB1. *Mol. Med.* 27 (1), 58. doi:10.1186/s10020-021-00307-1

Zhang, J., Zhu, Q., Wang, X. e., Yu, J., Chen, X., Wang, J., et al. (2018). Secretory Kinase Fam20C Tunes Endoplasmic Reticulum Redox State via Phosphorylation of Ero1α. *Embo J.* 37 (14), 1–16. doi:10.15252/embj.201798699

**Conflict of Interest:** The authors declare that the research was conducted in the absence of any commercial or financial relationships that could be construed as a potential conflict of interest.

**Publisher's Note:** All claims expressed in this article are solely those of the authors and do not necessarily represent those of their affiliated organizations, or those of the publisher, the editors and the reviewers. Any product that may be evaluated in this article, or claim that may be made by its manufacturer, is not guaranteed or endorsed by the publisher.

frontiers | Frontiers in Cell and Developmental Biology

REVIEW
published: 22 July 2022
doi: 10.3389/fcell.2022.930205

# The Anti-Leukemia Effect of Ascorbic Acid: From the Pro-Oxidant Potential to the Epigenetic Role in Acute Myeloid Leukemia

*S. Travaglini*[1], *C. Gurnari*[1,2], *S. Antonelli*[1], *G. Silvestrini*[1], *N. I. Noguera*[1,3], *T. Ottone*[1,3] *and M. T. Voso*[1,3]*

[1]Department of Biomedicine and Prevention, University of Rome Tor Vergata, Rome, Italy, [2]Department of Translational Hematology and Oncology Research, Taussig Cancer Institute, Cleveland Clinic, Cleveland, OH, United States, [3]Neuro-Oncohematology Unit, IRCCS Fondazione Santa Lucia, Rome, Italy

OPEN ACCESS

**Edited by:**
*Silvia Masciarelli,*
*Sapienza University of Rome, Italy*

**Reviewed by:**
*Margreet C. M. Vissers,*
*University of Otago, New Zealand*
*King Pan N. G.,*
*KK Women's and Children's Hospital, Singapore*

***Correspondence:**
*M. T. Voso*
*voso@med.uniroma2.it*

**Specialty section:**
*This article was submitted to Signaling, a section of the journal Frontiers in Cell and Developmental Biology*

**Received:** *27 April 2022*
**Accepted:** *24 June 2022*
**Published:** *22 July 2022*

**Citation:**
*Travaglini S, Gurnari C, Antonelli S, Silvestrini G, Noguera NI, Ottone T and Voso MT (2022) The Anti-Leukemia Effect of Ascorbic Acid: From the Pro-Oxidant Potential to the Epigenetic Role in Acute Myeloid Leukemia. Front. Cell Dev. Biol. 10:930205. doi: 10.3389/fcell.2022.930205*

Data derived from high-throughput sequencing technologies have allowed a deeper understanding of the molecular landscape of Acute Myeloid Leukemia (AML), paving the way for the development of novel therapeutic options, with a higher efficacy and a lower toxicity than conventional chemotherapy. In the antileukemia drug development scenario, ascorbic acid, a natural compound also known as Vitamin C, has emerged for its potential anti-proliferative and pro-apoptotic activities on leukemic cells. However, the role of ascorbic acid (vitamin C) in the treatment of AML has been debated for decades. Mechanistic insight into its role in many biological processes and, especially, in epigenetic regulation has provided the rationale for the use of this agent as a novel anti-leukemia therapy in AML. Acting as a co-factor for 2-oxoglutarate-dependent dioxygenases (2-OGDDs), ascorbic acid is involved in the epigenetic regulations through the control of TET (ten-eleven translocation) enzymes, epigenetic master regulators with a critical role in aberrant hematopoiesis and leukemogenesis. In line with this discovery, great interest has been emerging for the clinical testing of this drug targeting leukemia epigenome. Besides its role in epigenetics, ascorbic acid is also a pivotal regulator of many physiological processes in human, particularly in the antioxidant cellular response, being able to scavenge reactive oxygen species (ROS) to prevent DNA damage and other effects involved in cancer transformation. Thus, for this wide spectrum of biological activities, ascorbic acid possesses some pharmacologic properties attractive for anti-leukemia therapy. The present review outlines the evidence and mechanism of ascorbic acid in leukemogenesis and its therapeutic potential in AML. With the growing evidence derived from the literature on situations in which the use of ascorbate may be beneficial *in vitro* and *in vivo*, we will finally discuss how these insights could be included into the rational design of future clinical trials.

**Keywords: acute myeloid leukemia, ascorbic acid, epigenetic regulation, oxidative stress, vitamin C**

## INTRODUCTION

Acute myeloid leukemia (AML) is a heterogeneous clonal disorder characterized by the uncontrolled proliferation of undifferentiated myeloid progenitor cells in the bone marrow and peripheral blood. Advances in DNA sequencing technologies have provided a detailed knowledge of the molecular landscape of AML, with a better understanding of the disease pathogenesis and prognosis (The Cancer Genome Atlas Research Network, 2013; Papaemmanuil et al., 2016; Awada et al., 2021). Despite high heterogeneity, the spectrum of genetic alterations have highlighted the presence of recurrent mutations in genes encoding epigenetic regulators (Gallipoli et al., 2015), including DNA methyltransferase 3A (DNMT3A), Ten-eleven-translocation 2 (TET2), Wilms' tumor 1 (WT1), and isocitrate dehydrogenase 1 and 2 (IDH1/2) (Kunimoto and Nakajima, 2017). The study of the molecular architecture of such cases unveiled that alterations of these genes often represent founding events in the clonal hierarchy, suggesting their essential role in early phase of leukemia ontogenesis (Papaemmanuil et al., 2013; Hirsch et al., 2018; Yoshimi et al., 2019).

Epigenetic mechanisms play a major role in normal and, particularly, in malignant hematopoiesis, where the presence of recurrent alterations in transcription factors and chromatin regulators are able to drive hematopoietic malignancies (Hu and Shilatifard, 2016; Fennell et al., 2019). Epigenetic modifiers are a large and varied group of proteins involved in the modification of DNA at cytosine residues and post-translational acetylation and methylation of histones, whose aberrations lead to dysregulation of critical genes that control cell growth, differentiation and apoptosis, all important mechanisms in the pathogenesis of AML (Hou and Tien, 2016; Pastore and Levine, 2016). In contrast to genetic changes, epigenetic modifications refer to changes in gene expression, and are frequently reversible, providing the opportunities for targeted treatment (Wouters and Delwel, 2016).

A wide range of therapeutic strategies that target epigenetic alterations in AML have been successfully tested in preclinical studies and several drugs have already gained approval for clinical use, with the final goal to reverse epigenetic dysfunctions (Bewersdorf et al., 2019). Since these discoveries, a number of selective inhibitors of mutant FLT3, IDH1 and IDH2 have been developed and are now approved by the Food and Drug Administration, and drugs that target the potential epigenetic writers (DOT1L, PRMT5), readers (BRD2/3/4) and erasers (HDAC, LSD1) are currently under investigation (Das et al., 2021). However, the therapeutic efficacy of epigenetic drugs as single agents seems to be limited (Bewersdorf et al., 2019).

Ascorbic acid, also known as vitamin C or ascorbate, at physiological levels potentiates the effects of hypomethylating agents (HMA) by both causing DNA demethylation through active and passive mechanisms and selectively killing tumor cells (Ruiz et al., 2015; Liu et al., 2016; Gillberg et al., 2018). Indeed, ascorbic acid is an essential factor for epigenetic regulation and many studies reported that it also displays a pro-oxidant activity when used at high concentrations, in particular on various type of cancer cells, suggesting it as an emerging epigenetic therapy (Chen et al., 2005; Chen et al., 2008).

Besides its role in epigenetics, ascorbic acid is a pivotal regulator of many physiological processes in humans (Giansanti et al., 2021), including cellular immune responses (Ströhle et al., 2011), and represents an antioxidant molecule involved in the reactive oxygen species (ROS) scavenging that prevent oxidative DNA damage and other effects, which may lead to cancer transformation.

In this review, we provide an overview of the role of ascorbate as an essential factor for epigenetic regulation, highlighting its anti-leukemic mechanisms of action, currently under investigation in the treatment of AML.

## ASCORBIC ACID: STRUCTURE, BIOSYNTHESIS AND UPTAKE

Ascorbic acid represents a wide spectrum antioxidant and an essential nutrient for humans. This vitamin exists in two redox states, ascorbate, the reduced active form, and dehydroascorbic acid (DHA), its oxidized form. At physiological conditions, ascorbic acid loses a proton to form the ascorbate anion (AscH−), the predominant ionic form of vitamin C, that can be oxidized by losing two protons, giving rise first to ascorbate radical ($Asc^{-}$) and then to a fully oxidized DHA (Ferrada et al., 2021).

Unlike most mammals, humans are unable to synthesize ascorbic acid from oxidated glucose, missing the gulonolactone (L-) oxidase (GULO), a key enzyme involved in the catalysis of the last enzymatic step in ascorbate synthesis, and are thereby dependent on vitamin C intake from the diet (Du et al., 2012). The dietary daily requirement of vitamin C is 75–90 mg/day, which is usually taken under the form of both ascorbate and DHA (Valdés, 2006; Testa et al., 2021). Indeed, even if DHA levels are extremely low under physiological conditions (Du et al., 2012), it is rapidly recycled back to ascorbate by DHA reductase, using glutathione (GSH) as a reducing agent (Mandl et al., 2009). This recycling process occurs intracellularly, where vitamin C is involved in several biological processes. Thus, its exogenous uptake is attained through the presence of specific membrane transporters, which determine the distribution of this molecule between extra- and intra- cellular compartments. Both ascorbic acid and DHA can be transported across the plasma membrane, although by distinct carriers (Savini et al., 2008). Under physiologic conditions, vitamin C is mainly present in plasma as ascorbate and is actively absorbed in the gastrointestinal tract, particularly at the level of the enterocytes of the small intestine (May, 2011; Du et al., 2012).

Ascorbate is transported into mammalians cells in an energy-dependent fashion, requiring two types of sodium-dependent transporters, SVCT1 and SVCT2, encoded by *SLC23A1* and *SLC23A2* genes, respectively, which show distinct tissue distributions (Tsukaguchi et al., 1999; Sotiriou et al., 2002; May, 2011). Conversely, DHA can be internalized by facilitative hexose transporters, particularly via GLUT1 and GLUT3 (Rumsey et al., 1997; Rumsey et al., 1999), encoded by

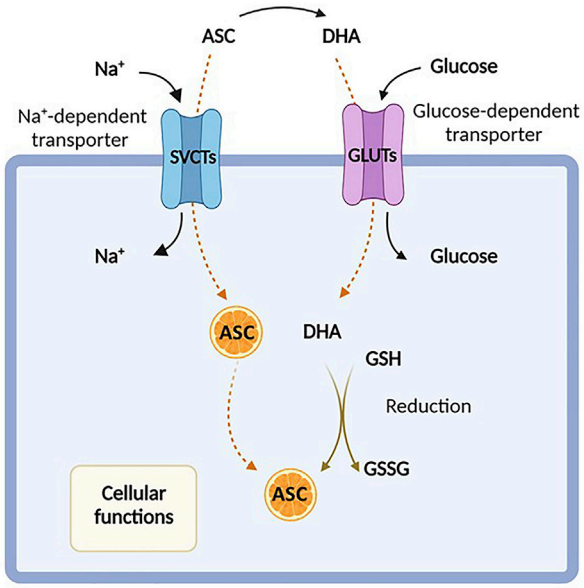


**FIGURE 1 |** Ascorbic acid uptake. Ascorbic acid, also known as Vitamin C, enters the cell either in its reduced form (ascorbate, ASC) by sodium-dependent vitamin C transporters (SVCTs) or in its oxidized form (dehydroascorbate, DHA) *via* facilitative glucose transporters (GLUTs). In the cytosol, DHA is rapidly reduced back to ASC in the presence of glutathione (GSH). Created with Biorender.com.

the *SLC2A1* and *SLC2A3* genes, and then converted back to ascorbic acid (Savini et al., 2008) (**Figure 1**). As mentioned above, DHA is present at extremely low concentration in the blood of healthy subjects and at much higher levels in the intestine, and its uptake is inhibited by excess glucose (Vera et al., 1993; Malo and Wilson, 2000; Corpe et al., 2013; Lykkesfeldt and Tveden-Nyborg, 2019). However, the intracellular transport of DHA by GLUT transporters is not usually considered the principal route of uptake, even if the impact of ascorbate and/or DHA to cellular transport *in vivo* is not fully elucidated (Rumsey and Levine, 1998).

Vitamin C uptake and its whole body distribution is essential for many biochemical processes, some of them also influencing tumor growth and spread (Wohlrab et al., 2017). Indeed, the ascorbate concentration in plasma and tissues represent one of the main risk factor for cancer incidence (Linowiecka et al., 2020). Several studies reported also that cancer patients are more likely to experience vitamin C deficiency due to a variety of factors such as decreased oral intake, inflammation, infection, and disease phases, particularly following chemotherapy and hematopoietic stem cells (HSCs) transplantation, resulting in shorter survival (Caraballoso et al., 2003; Mayland et al., 2005; Nannya et al., 2014; Wilson et al., 2014; Rasheed et al., 2019; White et al., 2020). Furthermore, it has also been indicated a potential role of vitamin C transporters in human cancer (Caprile et al., 2009; Hong et al., 2013; Aguilera et al., 2016). Particularly, genetic polymorphisms in the *SVTC2* gene have been associated to several types of tumor, including lymphoma, breast, head and neck, and gastric cancers (Ngo et al., 2019). Liu et al. (2020) showed that *GLUT3* gene expression was significantly reduced in leukemic blasts compared with normal hematopoietic cells, suggesting a defective ability in the absorption mechanisms. Furthermore, while limited data on vitamin C status are available in hematological malignancies (Aldoss et al., 2014; Nannya et al., 2014; Huijskens et al., 2016), it has been recently showed that in AML patients, plasma ascorbate levels were decreased at disease onset as opposed to healthy controls and the achievement of complete remission associated with increased values, albeit at lower-than-normal levels (Aldoss et al., 2014; Nannya et al., 2014; Huijskens et al., 2016).

## THE MULTIFACTORIAL ROLE OF ASCORBIC ACID UNDER PHYSIOLOGICAL CONDITION

Ascorbic acid takes part in many biochemical processes in humans, acting as an essential enzymatic cofactor, a reducing and antioxidant agent and a scavenger of ROS in biological systems. The wide spectrum of its biological functions relies on its role as a specific cofactor for the catalytic activity of the 2-oxoglutarate-dependent dioxygenases (2-OGDDs), which catalyze the addition of hydroxyl group to various substrates (Kuiper and Vissers, 2014). For instance, under physiological conditions, ascorbate is essential in the biosynthesis of collagen, the most abundant extracellular protein, promoting the proper folding of the stable collagen triple-helix conformation (Phillips et al., 1994). By increasing the extracellular matrix components, these mechanisms are supposed to prevent cancer spread, thus walling in tumors (Cameron and Rotman, 1972; Cameron et al., 1979). In addition, ascorbate may also act as a cofactor in the hydroxylation of the hypoxia inducible factor-1 α (HIF-1α), a transcription factor that regulates the expression of specific genes involved in the cellular response to hypoxia (Ivan et al., 2001; Jaakkola et al., 2001; Schofield and Ratcliffe, 2004; Ratcliffe, 2013; Simon, 2016). Under normoxic conditions, the hydroxylation of these proline residues induces proteasomal degradation of HIF-1α. In case of hypoxia, a scenarios which is very common in cancer, or in absence of ascorbate, hydroxylation is inhibited and HIF-1α is stabilized thereby initiating its downstream effects (Flashman et al., 2010). Furthermore, ascorbic acid, as a cofactor, is also involved in other important hydroxylation reactions, essential for catecholamines, L-carnitine, cholesterol and amino acids synthesis (Chatterjee et al., 1975).

Consistent with its role as a cofactor, ascorbic acid regulates DNA and histone methylation thanks to its ability to modulate 2-OGDD enzymes, which encompass demethylases involved in epigenetic regulation and in the maintenance of genomic stability (Cimmino et al., 2018). Particularly, the TET proteins are responsible for the active DNA demethylation and regulate gene transcription by converting 5-methylcytosine (5mC) to 5-hydroxymethylcytosine (5hmC), further to 5-formylcytosine (5fC) and 5-carboxylcytosine (5caC), to produce an unmethylated cytosine, thus completing the process of DNA active demethylation (Tahiliani et al., 2009; Ito et al., 2011). Ascorbic acid sustains and promotes the catalytic activity of

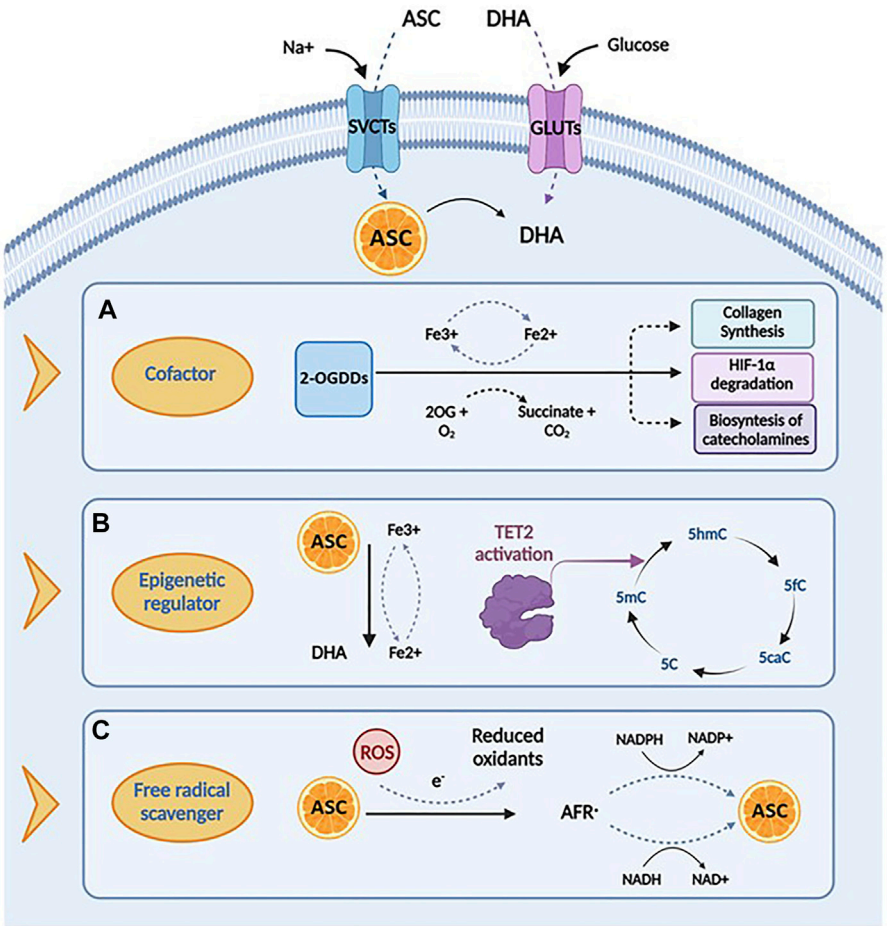


**FIGURE 2 |** Biological functions and mechanisms of action of ascorbic acid. **(A)** Ascorbic acid plays an important role in several biological processes by acting as a cofactor for 2-oxoglutarate dependent dioxygenases (2-OGDDs) that have a wide range of biological functions, including collagen synthesis, HIF-1α degradation and biosyntesis of catecholamines. **(B)** Ascorbic acid can act as an epigenetic regulator by enanching the activity of TET2 enzyme, that catalyzes the conversion of 5-methylcytosine (5-mC), into 5-hydroxymethylcytosine (5-hmC), inducing DNA demethylation. **(C)** Ascorbic acid has important roles in scavenging free radicals, having the ability to donate an electron to reactive oxygen species (ROS) to form a relatively stable ascorbyl-free radical (AFR). Created with Biorender.com.

TET enzymes, most likely reducing $Fe^{3+}$ to $Fe^{2+}$ (Kuiper and Vissers, 2014). Recent studies have demonstrated that ascorbic acid, as a direct regulator of TET activity, may enhance 5hmC generation, in a time- and dose-dependent fashion (Yin et al., 2013; Young et al., 2015). Two mechanisms have been proposed to explain the stimulatory effect of ascorbate on TET enzymatic activity. The first is related to its role as a cofactor, capable to directly bound the catalytic domain of TET proteins by enhancing their enzymatic activity (Hore et al., 2016); this finding is also supported by the evidence that other antioxidant compounds do not show effects on TET activity in *in vitro* models (Tahiliani et al., 2009; Ito et al., 2011; Chen et al., 2013; Dickson et al., 2013; Minor et al., 2013; Yin et al., 2013). The second hypothesis posits a different mechanism, suggesting that the stimulatory role of ascorbate on TET activity is associated to its ability to promote the reduction of $Fe^{3+}$ to $Fe^{2+}$ (Hore et al., 2016).

In addition to its function as a cofactor of several enzymes, ascorbic acid is involved in many biological processes acting as an electron donor. At physiological concentrations, ascorbate is a potent free radical scavenger, with a protective effect against oxidative damage caused by ROS, commonly produced during normal cellular metabolism (Gaziano et al., 2012). The antioxidant mechanisms of ascorbic acid are based on its capacity to reduce potentially damaging ROS and produce chemically inert resonance-stabilized ascorbate radicals (AFR). The AFR is reduced back to ascorbate intracellularly by the activity of $NADH^{-}$ and NADPH dependent reductases, which display high affinity for the generated radicals (Duarte and Lunec, 2005; Santos-Sánchez et al., 2019). In case of accumulation of AFR in areas not accessible to these enzymes, two AFR molecules may either react with each other or dismutate to form one molecule each of ascorbate and DHA (Bielski et al., 1981). These may be then converted back into ascorbic acid for reuse or may be metabolized with further release of additional electrons (May et al., 2001; Wilson, 2002; Duarte and Lunec, 2005). This mechanism underlines the cytoprotective functions of Vitamin C, involved in the first line of antioxidant defense, including

prevention of DNA mutation induced by oxidation (Noroozi et al., 1998; Pflaum et al., 1998; Lutsenko et al., 2002), protection of lipids against peroxidative damage (Barja et al., 1994; Sweetman et al., 1997), and repair of oxidized amino acid residues to maintain protein integrity (Kimura et al., 1992; Sweetman et al., 1997; Cadenas et al., 1998). The multifactorial roles of ascorbate discussed above are summarized in **Figure 2**.

## ASCORBATE AS A KEY EPIGENETIC REGULATOR INVOLVED IN HEMATOPOIETIC STEM CELL FUNCTION AND LEUKEMOGENESIS

As previously mentioned, among the various biological effects induced by ascorbic acid, emerging evidences suggest its key role in the epigenetic reprogramming, an effect related to the ability of ascorbic acid to act as an electron donor and, particularly, a cofactor for 2-OGDDs. These enzymes require 2-oxoglutarate (2-OG) and molecular oxygen, as substrates, and non-heme iron (Fe2+) and ascorbic acid, as cofactors; therefore, the reduction of both substrates or cofactors result in a decreased activity of these enzymes (McDonough et al., 2010; Vissers et al., 2014; Martínez-Reyes and Chandel, 2020; Crake et al., 2021). This superfamily of enzymes include key epigenetic regulators of histone demethylation and DNA hydroxymethylation, which have been shown to have crucial roles in the epigenetic regulation of stem cells and cancer (Cimmino et al., 2018). These evidences are of particular interest for AML because many of these demethylase enzymes, which require ascorbate as a cofactor, are deregulated in the process of leukemogenesis (Das et al., 2021), including lysin-specific demethylases (Castelli et al., 2018), the Jumonji C (JmjC) domain containing histone demethylases (JHDMs) (Wang et al., 2011a; Staehle et al., 2021), the ALKB homolog (ALKBH) family of nucleic acid demethylases (Gerken et al., 2007; Yi et al., 2010) and TET enzymes (Castelli et al., 2018; Das et al., 2021). Of the context discussed above, it has been recently demonstrated that ascorbic acid, acting as an epigenetic modulator could promote DNA demethylation in embryonic stem cells (ESCs), stimulate the reprogramming of fibroblast to induced pluripotent stem cells (iPSCs) and humper the aberrant self-renewal of HSCs, through the stimulation of JHDM activity (Chung et al., 2010; Esteban et al., 2010; Cimmino et al., 2018). Recent studies on JHDMs have also clearly demonstrated the involvement of these enzymes in disease initiation and progression, suggesting new attractive targets for myeloid malignancies.

Particularly, several studies have investigated the specific relationship between the activity of TET enzymes, ascorbate and the development of hematologic malignancies. It has been recently reported that ascorbic acid can protect HSCs from epigenetic alterations driving leukemia progression, stimulating the catalytic activity of TET enzymes, which are known as *bona fide* tumour suppressors of the hematopoietic lineage. Among *TET* genes, alterations in *TET2* are frequently reported in myeloid disorders, occurring in 10% of *de novo* AML, 30% of myelodysplastic syndrome (MDS) and almost 50% of chronic myelomonocytic leukemia (CMML) cases (Delhommeau et al., 2009; Papaemmanuil et al., 2016). TET2 is one of the principal epigenetic regulator of normal and malignant hematopoiesis, being able to regulate the differentiation and self-renewal of HSCs (Nakajima and Kunimoto, 2014), and is one of the most commonly mutated genes reported at high allele frequency in $CD34^+$ hematopoietic stem and progenitor cells (HSPCs). These evidences suggested that *TET2* mutations are early clonal events of the leukemic transformation in cells with multi-lineage potential.

Acting as a co- factor for the 2-OGDDs, ascorbate sustains and promotes the activity of TET enzymes, as already demonstrated by *in vitro* and *in vivo* evidences (Agathocleous et al., 2017; Cimmino et al., 2017; Vissers and Das, 2018). Two recent studies provide novel insights on how ascorbic acid regulates HSC functions and leukemogenesis by the enhancement and restoration of TET2 function, respectively.

In the first, Agathocleous et al. reported that vitamin C deficiency might play a role in leukemia progression. Interestingly, the authors showed that the more immature population of stem and progenitor cells display higher levels of ascorbate than more differentiated cells. Accordingly, they found also an overexpression of the *Slc23a2* gene, which provides instructions for making a protein involved in vitamin C uptake in HSCs/MPPs (multipotent progenitors), determining an accumulation of ascorbate levels, which decreased with differentiation (Agathocleous et al., 2017). Using *Gulo*-depleted mice, which are unable to synthesize ascorbate from glucose, they showed that ascorbate depletion increased HSC pool, in part as a consequence of Tet2 reduced activity, a scenario which was reversed by dietary vitamin C supplementation. These findings suggest the beneficial role of ascorbate treatment in the setting of *TET2* mutated leukemia. Furthermore, the presence of additional internal tandem duplications (ITDs) in the juxtamembrane domain of *FLT3* cooperated with ascorbate deprivation in acceleration of leukemia development (Agathocleous et al., 2017), phenocopying *TET2* loss.

In a second, independent study Cimmino et al. established a reversible mouse model with *Tet2* knockout. *Tet2*-deficient mice showed defective self-renewal and differentiation capacity of HSC/HPC (hematopoietic progenitor cell), and defective genomic hydroxymethylation and DNA hypermethylation. Treatment with ascorbic acid pharmacologically mimicked TET2 restoration, inducing a reversal of defective DNA methylation and cell differentiation. As *TET2* mutations are almost exclusively heterozygous, ascorbic acid was found capable to stimulate the activity of the non-mutated *TET2* allele, leading to genome-wide DNA demethylation, differentiation and cell death. These evidences also suggest that the persistence of TET2 deficiency is needed to maintain leukemic self-renewal (Cimmino et al., 2017). Furthermore, the authors showed the ability of ascorbate to enhance the activity of poly(ADP ribose) polymerase (PARP) inhibitor to induce cell

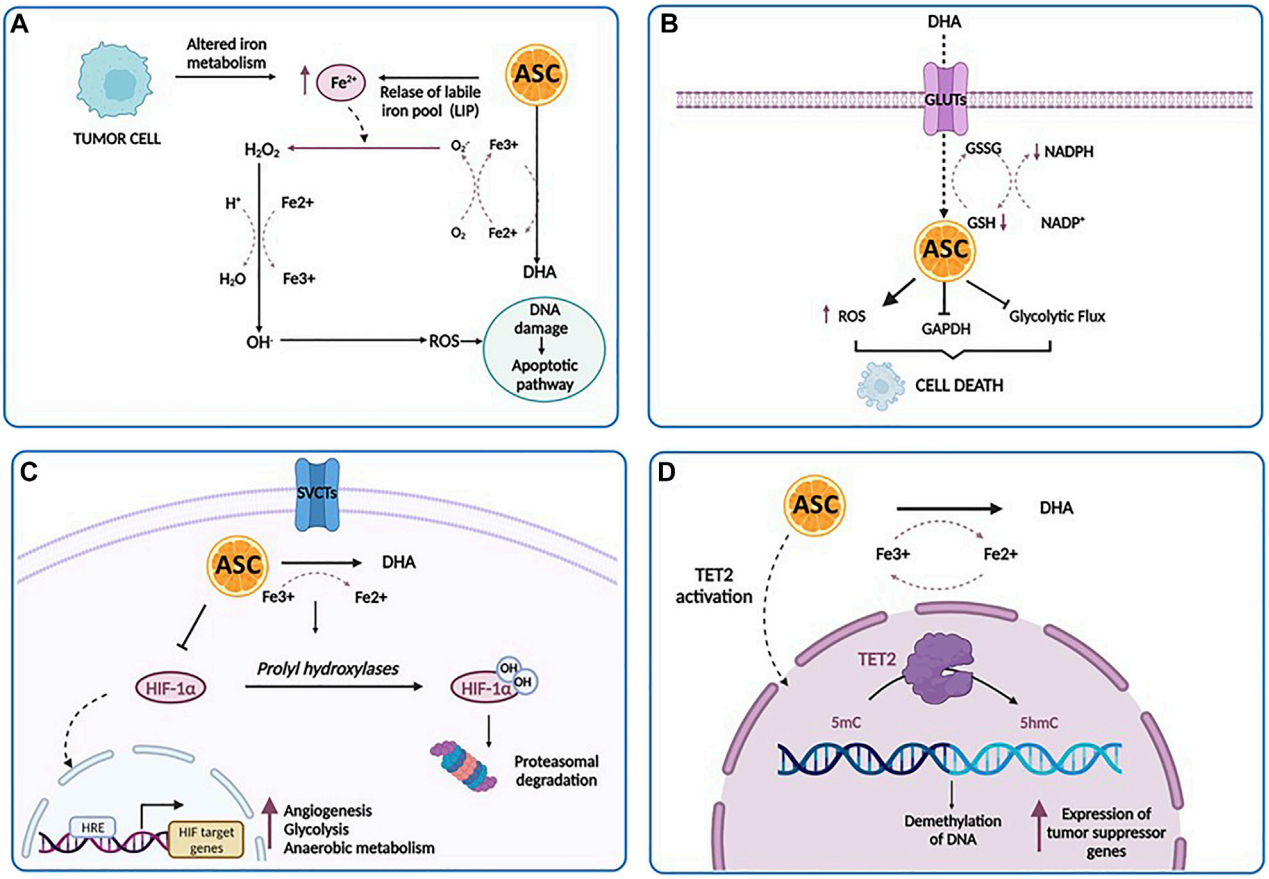


**FIGURE 3 |** The anti-cancer effects of ascorbic acid. **(A)** A high concentration of ascorbic acid (ASC) increases the labile iron pool (LIP) of tumor cells, induces the production of increased level of ROS directly damaging mitochondria and DNA, and ultimately stimulates apoptotic pathways. **(B)** Tumor cells can uptake DHA at higher rates and then internally reduce it to ASC. This reduction triggers scavenging of glutathione (GSH), inducing oxidative stress, the inactivation of glyceraldehyde 3-phosphate dehydrogenase (GAPDH), the inhibition of glycolytic flux, an energy crisis and cell death. **(C)** In the hypoxic conditions of tumor microenvironment, there is a repression of HIF-1α hydroxilation. As a result, HIF-1α accumulates in the cytoplasm and translocates into the nucleus, promoting the transcription of its targets involved in prcesses such as angiogenesis, glycolysis and anaerobic metabolism, metastasis and resistance to therapy. Under ascorbic acid treatment, HIF-1α is hydroxylated by the prolyl hydroxylases, ultimately leading to polyubiquitination and proteasomal degratadion of HIF-1α. **(D)** Ascorbic acid binds to the catalytic domain of TET and facilitates DNA demethylation and re-expression of important tumor suppressor genes. Created with Biorender.com.

death, providing a safe and effective combination strategy to selectively target TET deficiency in cancer (Cimmino et al., 2017).

Altogether, these data suggest that the restoration of TET2 activity *via* ascorbate supplementation could provide an opportunity to reverse disease progression in AML cases linked to heterozygous loss-of-function mutations in *TET2*, pointing out to its role as a potentially non-toxic therapy for TET-associated malignancies (Agathocleous et al., 2017; Cimmino et al., 2017).

## THE ANTI-CANCER EFFECTS OF ASCORBIC ACID AT PHARMACOLOGIC DOSES

Among its many effects on cellular functions and metabolism, ascorbic acid has also shown a powerful anti-cancer effect against a number of human cell lines. Indeed, while generally regarded as an antioxidant, ascorbic acid may also have prooxidant activities at high pharmacological concentrations (Noguera et al., 2017), obtained by intravenous administration, and in the presence of free transition metal ions, especially iron. Particularly, ascorbate catalyzes the reduction of $Fe^{3+}$ to $Fe^{2+}$, leading to the formation of $H_2O_2$, through the so-called Fenton reaction, and exerting a cytostatic and cytotoxic effect against tumor cells, without harming normal cells. This pro-oxidant potential has been investigated in many studies in the prevention and treatment of cancers and is proposed to be dose-dependent (Putchala et al., 2013). Among the possible mechanisms, four main biological pathways have been proposed to explain how high-dose ascorbate targets several vulnerabilities of tumor cells: intracellular iron metabolism, DHA uptake *via* GLUT1, hypoxia pathways and epigenetic regulators (**Figure 3**).

One of the major determinants of ascorbate-mediated tumor cytotoxicity is represented by the amount and the availability of intracellular iron. The labile iron pool (LIP) represents a source of intracellular iron available for exchange between various cellular

compartments (Kakhlon and Cabantchik, 2002). The intracellular iron concentration has a key role in the ascorbate-mediated cytotoxicity, related to the formation of $H_2O_2$ and .OH, which directly damages mitochondria and DNA, stimulating apoptotic pathways. Particularly, tumor cells displayed low levels of antioxidant enzymes and an impaired redox balance in respect of their normal counterpart, rendering these cells more vulnerable to oxidative stress and identifying pro-oxidant stimulations as a strategy to induce their death (Moloney and Cotter, 2018). According to these findings, Schoenfeld et al. have explored in detail the sensitivity of glioblastoma and non-small cell lung cancer (NSCLS) cell lines to ascorbate and have demonstrated that an altered iron metabolism, associated with disturbances in oxidative stress, induces an increased level of mitochondrial ROS, ultimately leading to an increase in the level of LIP and sensitivity of cancer cells to ascorbic acid (Schoenfeld et al., 2017). Interestingly, a dual relationship exists between LIP and ascorbate: pharmacological doses of ascorbate increase LIP in tumor cells, whereas an increased LIP in tumor cells enhances the toxicity of pharmacological doses of ascorbate (Du et al., 2015). Moreover, elevated LIP levels have been found in several tumor cell types as opposed to their normal counterpart, such as breast cancer cells, T-cell lymphoma and RAS-transformed cells (Yang and Stockwell, 2008; Kiessling et al., 2009; Pinnix et al., 2010). Accordingly, one could speculate that the intravenous iron injection may represent a powerful strategy to sensitize tumor cells to ascorbic acid via increased LIP levels (McCarty and Contreras, 2014).

The second mechanism involves DHA, the reversible oxidized form of ascorbic acid, based on the findings that tumor cells have the peculiar ability to uptake DHA at much higher rates and then internally reduce it to ascorbic acid (Nauman et al., 2018). As reported by Yun et al. (2015), in *KRAS* and *BRAF*-mutated colorectal cancer, this reduction triggers scavenging of glutathione (GSH), induces oxidative stress, inactivates glyceraldehyde 3-phosphate dehydrogenase (GAPDH), inhibits glycolytic flux and leads to an energy crisis with subsequent cell death (van der Reest and Gottlieb, 2016). Acting as a glycolytic inhibitor, high-dose ascorbate could represent an effective strategy against tumor cells, frequently characterized by high glycolytic activity. The third anti-tumor mechanism is based on the activity of ascorbate as a cofactor for 2-OGDDs, including HIF-hydroxylases (Ozer and Bruick, 2007). As reported above, in the hypoxic condition of tumor microenvironment, there is a repression of HIF-1α hydroxylation, associated with HIF activity. HIF-1α promotes the transition of tumor cells from aerobic to anaerobic metabolism, increasing glycolysis to maintain energy production (Masoud and Li, 2015). Thus, it is conceivable that the previously discussed DHA mechanism works in conjunction with the oxygen pathways alterations, leading to a global disruption of metabolic functioning in the tumor cell, that trigger cell death (Nauman et al., 2018). Furthermore, several studies have reported elevated levels of HIF-1α in AML, where it mediates the capacity of leukemic cells to migrate and invade extramedullary sites, suggesting that hypoxia and HIF-mediated signaling may play a crucial role in leukemia. Thus, targeting HIF with ascorbic acid could represent a potentially useful approach in AML treatment (Wang et al., 2011b; Kawada et al., 2013; Forristal et al., 2015; Gao et al., 2015).

Lastly, ascorbate modulates DNA demethylation and epigenetically reprograms cancer cells through the interaction with TET enzymes family (Blaschke et al., 2013; Ito et al., 2013). Binding to the catalytic domain, it facilitates TET-mediated DNA demethylation and re-expression of important tumor suppressor genes, with subsequent increase in chemosensitivity (Blaschke et al., 2013; Shenoy et al., 2017).

## TARGETING AML DRIVER MUTATIONS USING ASCORBIC ACID: FROM *IN VITRO* EXPERIENCES TO CLINICAL TRIALS

Despite a growing body of evidence suggesting the anti-cancer properties of ascorbic acid, few data are available on its role for the treatment of AML.

In an *in vitro* study, Parker and coworkers demonstrated that ascorbate, at concentrations of 0.25–1 mM, was able to induce a dose- and time-dependent inhibition of proliferation in various AML cell lines (HL-60, acute promyelocytic leukemia cell line NB4, retinoic acid-resistant APL cell line NB4-R1, K562 chronic myelogenous leukemia cell line, and KG1), and primary blasts (Park et al., 2004). The induction of apoptosis in these cells was due, at least in part, to the excessive increase of $H_2O_2$ levels (Park, 2013).

Another study performed by Kawada et al. (2013) attempted to determine whether high ascorbate may exert significant cytotoxic effects against human leukemic cells, K562, HL60, Jurkat (T-lymphoblastic leukemia) and Raji (B-lymphoblastic leukemia), and normal hematopoietic cells, confirming that the specific cytotoxic effects on leukemic cells were caused by the production of $H_2O_2$ with an effect directly proportional to the dose employed. These data were confirmed *in vivo*, whereby the intravenous administration of high ascorbate repressed the proliferation of leukemic cells injected in NSG (NOD scid gamma) mice. Moreover, the authors also showed that high dose ascorbate markedly inhibited the expression of HIF-1α in leukemic cells by blocking the transcriptional activation of NF-kB, constitutively upregulated in many types of leukemia and associated with leukemic progression (Braun et al., 2006; Packham, 2008; Reikvam et al., 2009).

Accordingly, Mastrangelo et al. (2015) tested the effects of high concentrations (0.5–7 mM) of ASC on a variety of human myeloid cell lines, HL60, K562, U937, NB4, NB4-R4 and arsenic trioxide ($As_2O_3$, ATO)-resistant NB4 (NB4/As), showing the high sensitivity of myeloid leukemia cell lines to the pro-oxidant effects of high doses ascorbate, with an average cytotoxic concentration of 3 mM. Surprisingly, ASC was found significantly more effective than ATO as a single agent in inducing apoptotic cell death in HL60 human cell lines *in vitro*. Since ATO also functions as a pro-oxidant factor, in a second study, Noguera et al. (2017) tested the effects of ascorbate in combination with ATO on AML and APL primary blasts and cell lines, including NB4, NB4-R4, NB4-ATO-R, and MV4-11

[AML-M5 derived cell line with t(4;11) and *FLT3*-ITD mutations], showing a synergistic effect. Particularly, the combination treatment was highly effective in APL samples, displaying a cytotoxic mechanism linked to ROS overproduction within leukemic cells and consequent induction of apoptosis. Moreover, high concentrations of ascorbate were able to downregulate the phosphorylation of FLT3 and its downstream target proteins STAT5a/b, suggesting the potential activity of the drug also in the subset of *FLT3*-ITD positive AML. In an attempt to further characterize the mechanistic underpinnings underlying the efficacy of ascorbic acid in the APL setting, the same authors found that the fusion protein PML/RARα inhibits NRF2 (NF-E2 p45-related factor 2) functions. This is a transcription factor that orchestrates cellular adaptive responses to stress, and whose nuclear transfer is prevented by ascorbate treatment, thereby enhancing its degradation into the cytoplasm. As a result, the inhibition of the NRF2 oxidative stress pathway clarifies the peculiar sensitivity of APL cells to the pro-oxidant activity of high-dose ascorbate and suggest its potential use in APL patients, especially in those resistant to ATO/retinoic acid treatment (Banella et al., 2019). Moreover, ascorbate also shows the ability to induce cell death by targeting glycolytic metabolism in primary AML blasts, through the inhibition of hexokinase 1/2 (HK1/2) and GLUT1 in hematopoietic cells, and, in combination with the metabolic inhibitor buformin, also decreases mitochondrial respiration and ATP production, sparing healthy $CD34^+$ cells. Overall, these data clearly depict an effect of ascorbate on glycolysis and contribute to elucidate the targets and mechanisms through which this therapeutic agent exerts its anti-cancer effects (Banella et al., 2022).

Another study investigated instead the combinatorial effect in AML cells of low-dose of ascorbate with decitabine, an HMA widely used in the treatment of AML in elderly patients, not suitable for conventional intensive chemotherapy. Potentially, one of the mechanisms for the efficacy of decitabine treatment is the upregulation of TET2 proteins, among others. Acting as a direct regulator of TET activity, ascorbate increases 5hmc levels and potentially sensitizes patients to decitabine. Indeed, *in vitro* studies showed that this combination in NB4 and HL60 cells resulted in the most significant upregulation of the activity of TET2 enzyme. Furthermore, *in vivo* results displayed a synergistic effect of this two agents, which are able to improve the complete remission (CR) rate in elderly AML patients (Zhao et al., 2018). Overall, these observations are of potential interest particularly for MDS and AML patients, who could have an additional benefit from adding ascorbic acid to HMA therapy.

Interestingly, ascorbate specifically interacts with the C-terminus catalytic domain of TET2, inducing effects not shown with other strong reducing chemicals (Yin et al., 2013). As already mentioned, ascorbate can act as an epigenetic therapeutic in the presence of heterozygous *TET2* mutations by restoring TET2 activity and providing an opportunity for reversing disease progression in AML cases linked to heterozygous loss-of-function mutations in *TET2*. Thus, the proposed mechanism of action requires the presence of residual functional enzyme (Das et al., 2021). However, TET2 mutations frequently occur in combination with other lesions, but little is known about how the genomic makeup may impact the up-regulation of TET2 activity induced by ascorbic acid as well as its subsequent effects on cell differentiation and survival (Papaemmanuil et al., 2016; Das et al., 2021). To further muddy the waters of the intertwining relation between TET enzymes and ascorbate in myeloid disorders, a reduced TET2 activity may also result from mutations in *IDH1*, *IDH2* and *WT1*, frequently reported in AML (**Figure 4**). In the presence of such mutations, IDH enzymes produce 2-hydroxyglutarate (2-HG), an oncometabolite able to acts as a competitor for TET2, instead of its physiological substrate, 2-oxoglutarate (2-OG) (Figueroa et al., 2010), causing functional inactivation of TET2 enzyme. Moreover, the presence of mutated WT1, prevent the recruitment of TET2 to DNA and the activation of the WT1-target genes expression. These findings provide the evidence of decreased TET2 activity in both context of *IDH* and *WT1* mutations, and are in line with a recent study reporting TET2 deficiency in up to 74% of patients with myeloid disorders, a result that goes beyond the mere presence of *TET2* mutations. Indeed, loss of TET2 functions by mutations or down-modulation due to various mechanisms have been identified as a common lynchpin of myeloid malignancies, as also indicated by the meta-analysis performed in the above-mentioned study (Gurnari et al., 2022). The implications of this are obvious, and suggest the potential application of ascorbate in settings beyond the disruption of TET2-IDH-WT1 pathway, which is the scenario where we would expect its maximal therapeutic efficacy, as also demonstrated by anecdotal case reports (Das et al., 2019). Furthermore, TET3 upregulation has also been invoked as a potential mechanism compensating the general TET2opathy of myeloid disorders, and has been linked to better survival outcomes in MDS with TET2 deficiency. Perhaps, ascorbate treatment may rescue the fraction of patients not able to contra-balance TET2 loss, thereby improving their dismal clinical outcomes (Gurnari et al., 2021, 2022).

As said, IDH1/2 mutations alter the epigenome of AML cells. Mingay and coworkers explored the effect of ascorbic acid in the setting of a murine leukemic model expressing $IDH1^{R132H}$ mutation. Ascorbate treatment induced a reduction in cell proliferation and an increased expression of genes involved in leukocyte differentiation in $IDH1^{R132H}$ mice, not observed in $IDH1^{wt}$ counterparts. These marked effects on cell differentiation were related to the induction of demethylation at the level of DNA binding sites of the hematopoietic transcription factors CEBPβ, HIF-1α, RUNX1 and PU.1 (Mingay et al., 2018). The previously mentioned study by Cimmino et al. (2017) provided the evidence that ascorbic acid treatment is able to induce the restoration of TET2 function in various leukemia models, by blocking aberrant self-renewal and leukemia progression. Indeed, mimicking TET2 restoration ascorbate treatment suppresses leukemic colony formation and leukemic progression of primary human leukemia patient-derived xenografts (PDX). Finally, a recent study investigated the effects of ascorbate on cell growth and differentiation of SKM-1 AML cell line, harbouring both *TET2* and *TP53* mutations, showing a

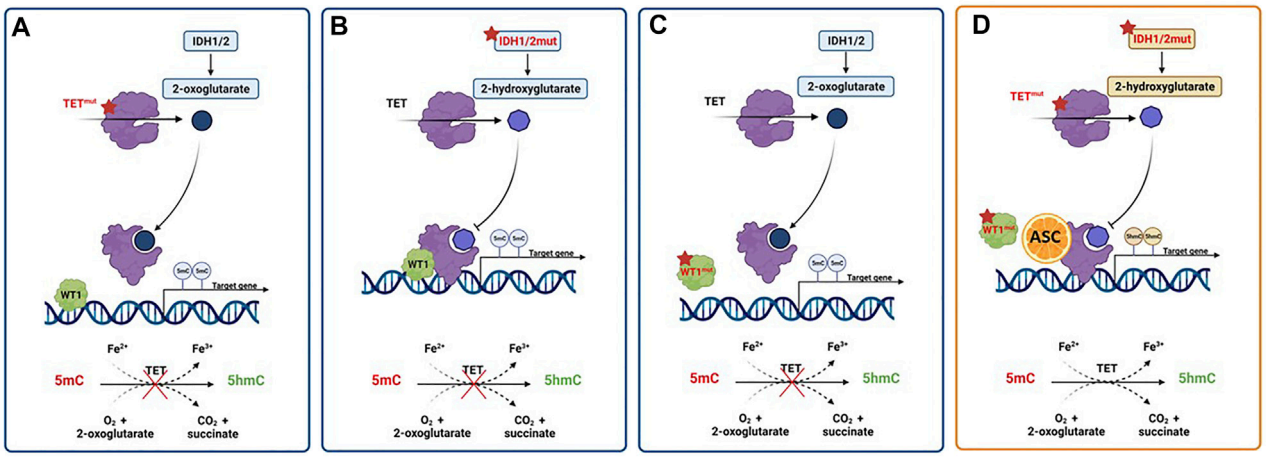


**FIGURE 4 |** Activity of pharmacologic doses of ascorbic acid in AML with TET2, IDH1/2 or WT1 altered pathways. **(A)** TET2 mutations result in a nonfunctional enzyme with hypermethylation of gene promoters, and prevention of oxidation of 5-methylcytosine (5mC) to 5-hydroxymethylcytosine (5hmc). **(B)** The presence of gain-of-function mutations in IDH1/2 genes results in the overproduction of the oncometabolite 2-hydroxyglutarate (2-HG) with the inhibition of TET2 activity. **(C)** WT1 mutations hamper the ability of TET2 to bind and activate WT1, inhibiting the expression of WT1-target genes. **(D)** Ascorbic acid treatment mimics TET2 restoration, inducing a reversal of defective DNA methylation and cell differentiation, ultimately inhibiting tumor progression. Created with Biorender.com.

beneficial anti-proliferative effect also in this subgroup of adverse-risk AML (Smith-Díaz et al., 2021).

Taken together these results identify ascorbic acid as a novel metabolic tumor suppressor involved in epigenetic remodeling and highlighted that supra-physiological doses could prevent myeloid disease progression, pointing out to its role as a potentially non-toxic therapy, especially for TET-deficient malignancies (Agathocleous et al., 2017; Cimmino et al., 2017; Guan et al., 2020). These observations suggest the incorporation of high-dose ascorbate as an adjuvant to standard chemotherapy or HMA therapy in clinical trials. Indeed, many clinical trials (NCT03682029, NCT03999723) are currently investigating the effects of ascorbate alone or as an add-on to classic therapeutic schemes of AML and myeloid disorders. Beyond HMA, specific lines of research are exploring the possibility of combining ascorbate with class I/II histone deacetylases (HDAC) (Zhang et al., 2017) or sirtuin activators (Sun et al., 2018), with the rationale of regulating TET dioxygenase-dependent effects of vitamin C (Guan et al., 2021). A peculiar application currently under investigation is the scenario of clonal hematopoiesis of indeterminate potential (CHIP) or its age-related counterpart ARCH (age-related clonal hematopoiesis), especially sustained by *TET2* mutations, where the consideration of a simple, over-the-counter supplementation of high-dose of vitamin C may represent an appealing option in decelerating progression to overt, fully-blown myeloid neoplasms (MDS/AML) (Miller and Steensma, 2020). To this end, a recent study showed that elderly individuals with inadequate vitamin C dietary intakes and plasma concentrations had higher odds of ARCH, typically TET2-related (Chen et al., 2021).

By this virtue, ascorbate could provide therapeutic opportunities able to overcome the TET2 impairment typical of myeloid neoplasms by re-establishing the net, residual TET-dioxygenase activity. Indeed, it is known that when TET2 expression is downregulated, two other dioxygenases (TET1, and especially TET3) maintain a minimal enzymatic activity critical for cell survival (Gurnari et al., 2022). Given the current evidence, newer approaches of personalized medicine should take into account not only cytogenetic and mutational characteristics but also both transcriptomic changes (e.g., RNA-seq) and assessment of vitamin C levels in patients at AML onset. This information would enable the identification of therapeutic vulnerabilities in individual patients (e.g., ascorbate in TET2-IDH-WT1 impairment and/or vitamin C-deficient patients). Ideally, with the use of sophisticated methods of artificial intelligence, one could speculate that the *in silico* creation of "digital twins" would allow testing of multiple, combinatorial therapeutic strategies (including ascorbate, conventional cytotoxic, HMA or new targeted agents), ultimately providing the best drugs to combine with this agent in a "synthetic lethally" fashion (Björnsson et al., 2019).

That said, the exact position of ascorbate in the therapeutic arsenal of AML is yet to be clearly defined. Future data derived from ongoing clinical trials will shed light on its role within the treatment algorithm of AML, a disease where still only less than 30% of patients become long-term survivors and for which new treatment options are urgently needed.

## CONCLUSION

The therapeutic potential of ascorbic acid in leukemia have been known for several decades. In particular, the observation that leukemic patients display low vitamin C plasma levels, due to the increased uptake by the actively proliferating leukocytes (Stephens and Hawley, 1936; Kyhos et al., 1945; Barkhan and Howard, 1958) suggested the rationale for the use of high-doses of ascorbic acid, not only as a prophylactic measure, but also to treat

a number of pathologic conditions, including cancer (Pauling, 1980). Its role as an anti-cancer agent has long been debated and the identification of potential mechanisms through which ascorbate exerts its biologic and pharmacologic activities, lead to hypothesize a new window of therapeutic opportunities.

Recent investigations highlighted the role of ascorbic acid as a critical regulator of cellular epigenetic processes, and a potential drug in the therapeutic armamentarium of acute myeloid leukemia through its stimulatory effect on TET2 function. Being epigenetic dysregulation a hallmark of AML and playing such a central role in the initiation and maintenance of the disease, the possibility to overcome the dysregulated gene-expression programs through an ascorbate based-epigenetic therapy represents a promising and cost-effective anti-leukemia approach.

Overall, these findings suggest the clinical benefit that could derive from the use of ascorbic acid both as a dietary supplement or as a therapeutic agent. Despite the wide number of *in vitro* experiments demonstrates the anti-leukemia activity of ascorbic acid, the lack of robust evidences about the precise mechanism of action, the tolerability and timing of pharmacological doses of ascorbic acid *in vivo* did not allow to design appropriate clinical trials. Future clinical trials are warranted to identify patients and specific AML subgroups who may benefit the most from this therapeutic strategy.

## AUTHOR CONTRIBUTIONS

ST, CG, and MV composed, edited and finalized the review. SA, GS, and TO designed the figure and reviewed the text. All authors contributed to the article and approved the submitted version.

## FUNDING

This work was supported by AIRC 5x1000 call "Metastatic disease: the key unmet need in oncology" to MYNERVA project, #21267 (Myeloid Neoplasms Research Venture AIRC. A detailed description of the MYNERVA project is available at http://www.progettoagimm.it), PRIN grant No. 2017WXR7ZT to MV, and Ministero della Salute, Rome, Italy (Finalizzata 2018, NET-2018-12365935, Personalized medicine program on myeloid neoplasms: characterization of the patient's genome for clinical decision making and systematic collection of real world data to improve quality of health care).

## REFERENCES

Agathocleous, M., Meacham, C. E., Burgess, R. J., Piskounova, E., Zhao, Z., Crane, G. M., et al. (2017). Ascorbate Regulates Haematopoietic Stem Cell Function and Leukaemogenesis. *Nature* 549, 476–481. doi:10.1038/nature23876

Aguilera, O., Muñoz-Sagastibelza, M., Torrejón, B., Borrero-Palacios, A., Del Puerto-Nevado, L., Martínez-Useros, J., et al. (2016). Vitamin C Uncouples the Warburg Metabolic Switch in KRAS Mutant Colon Cancer. *Oncotarget* 7, 47954–47965. doi:10.18632/oncotarget.10087

Aldoss, I., Mark, L., Vrona, J., Ramezani, L., Weitz, I., Mohrbacher, A. M., et al. (2014). Adding Ascorbic Acid to Arsenic Trioxide Produces Limited Benefit in Patients with Acute Myeloid Leukemia Excluding Acute Promyelocytic Leukemia. *Ann. Hematol.* 93, 1839–1843. doi:10.1007/s00277-014-2124-y

Awada, H., Durmaz, A., Gurnari, C., Kishtagari, A., Meggendorfer, M., Kerr, C. M., et al. (2021). Machine Learning Integrates Genomic Signatures for Subclassification beyond Primary and Secondary Acute Myeloid Leukemia. *Blood* 138, 1885–1895. doi:10.1182/blood.2020010603

Banella, C., Catalano, G., Travaglini, S., Divona, M., Masciarelli, S., Guerrera, G., et al. (2019). PML/RARa Interferes with NRF2 Transcriptional Activity Increasing the Sensitivity to Ascorbate of Acute Promyelocytic Leukemia Cells. *Cancers* 12, 95. doi:10.3390/cancers12010095

Banella, C., Catalano, G., Travaglini, S., Pelosi, E., Ottone, T., Zaza, A., et al. (2022). Ascorbate Plus Buformin in AML: A Metabolic Targeted Treatment. *Cancers* 14, 2565. doi:10.3390/cancers14102565

Barja, G., López-Torres, M., Pérez-Campo, R., Rojas, C., Cadenas, S., Prat, J., et al. (1994). Dietary Vitamin C Decreases Endogenous Protein Oxidative Damage, Malondialdehyde, and Lipid Peroxidation and Maintains Fatty Acid Unsaturation in the guinea Pig Liver. *Free Radic. Biol. Med.* 17, 105–115. doi:10.1016/0891-5849(94)90108-2

Barkhan, P., and Howard, A. N. (1958). Distribution of Ascorbic Acid in Normal and Leukaemic Human Blood. *Biochem. J.* 70, 163–168. doi:10.1042/bj0700163

Bewersdorf, J. P., Shallis, R., Stahl, M., and Zeidan, A. M. (2019). Epigenetic Therapy Combinations in Acute Myeloid Leukemia: what Are the Options? *Ther. Adv. Hematol.* 10, 204062071881669. doi:10.1177/2040620718816698

Bielski, B. H. J., Allen, A. O., and Schwarz, H. A. (1981). Mechanism of the Disproportionation of Ascorbate Radicals. *J. Am. Chem. Soc.* 103, 3516–3518. doi:10.1021/ja00402a042

Björnsson, B., Borrebaeck, C., Borrebaeck, C., Elander, N., Gasslander, T., Gawel, D. R., et al. (2019). Digital Twins to Personalize Medicine. *Genome Med.* 12, 4. doi:10.1186/s13073-019-0701-3

Blaschke, K., Ebata, K. T., Karimi, M. M., Zepeda-Martínez, J. A., Goyal, P., Mahapatra, S., et al. (2013). Vitamin C Induces Tet-dependent DNA Demethylation and a Blastocyst-like State in ES Cells. *Nature* 500, 222–226. doi:10.1038/nature12362

Braun, T., Carvalho, G., Fabre, C., Grosjean, J., Fenaux, P., and Kroemer, G. (2006). Targeting NF-Kb in Hematologic Malignancies. *Cell. Death Differ.* 13, 748–758. doi:10.1038/sj.cdd.4401874

Cadenas, S., Rojas, C., and Barja, G. (1998). Endotoxin Increases Oxidative Injury to Proteins in guinea Pig Liver: Protection by Dietary Vitamin C. *Pharmacol. Toxicol.* 82, 11–18. doi:10.1111/j.1600-0773.1998.tb01391.x

Cameron, E., Pauling, L., and Leibovitz, B. (1979). Ascorbic Acid and Cancer: a Review. *Cancer Res.* 39, 663–681.

Cameron, E., and Rotman, D. (1972). Ascorbic Acid, Cell Proliferation, and Cancer. *Lancet* 299, 542. doi:10.1016/s0140-6736(72)90215-2

Caprile, T., Salazar, K., Astuya, A., Cisternas, P., Silva-Alvarez, C., Montecinos, H., et al. (2009). The Na+-dependent L-Ascorbic Acid Transporter SVCT2 Expressed in Brainstem Cells, Neurons, and Neuroblastoma Cells Is Inhibited by Flavonoids. *J. Neurochem.* 108, 563–577. doi:10.1111/j.1471-4159.2008.05788.x

Caraballoso, M., Sacristan, M., Serra, C., and Bonfill Cosp, X. (2003). Drugs for Preventing Lung Cancer in Healthy People. *Cochrane database Syst. Rev.*, CD002141. doi:10.1002/14651858.CD002141

Castelli, G., Pelosi, E., and Testa, U. (2018). Targeting Histone Methyltransferase and Demethylase in Acute Myeloid Leukemia Therapy. *Ott* Vol. 11, 131–155. doi:10.2147/OTT.S145971

Chatterjee, I. B., Majumder, A. K., Nandi, B. K., and Subramanian, N. (1975). Synthesis and Some Major Functions of Vitamin C in Animals. *Ann. N. Y. Acad. Sci.* 258, 24–47. doi:10.1111/j.1749-6632.1975.tb29266.x

Chen, J., Guo, L., Zhang, L., Wu, H., Yang, J., Liu, H., et al. (2013). Vitamin C Modulates TET1 Function during Somatic Cell Reprogramming. *Nat. Genet.* 45, 1504–1509. doi:10.1038/ng.2807

Chen, J., Nie, D., Wang, X., Wang, L., Wang, F., Zhang, Y., et al. (2021). Enriched Clonal Hematopoiesis in Seniors with Dietary Vitamin C Inadequacy. *Clin. Nutr. ESPEN* 46, 179–184. doi:10.1016/j.clnesp.2021.10.014

Chen, Q., Espey, M. G., Krishna, M. C., Mitchell, J. B., Corpe, C. P., Buettner, G. R., et al. (2005). Pharmacologic Ascorbic Acid Concentrations Selectively Kill Cancer Cells: Action as a Pro-drug to Deliver Hydrogen Peroxide to Tissues. *Proc. Natl. Acad. Sci. U.S.A.* 102, 13604–13609. doi:10.1073/pnas.0506390102

Chen, Q., Espey, M. G., Sun, A. Y., Pooput, C., Kirk, K. L., Krishna, M. C., et al. (2008). Pharmacologic Doses of Ascorbate Act as a Prooxidant and Decrease Growth of Aggressive Tumor Xenografts in Mice. *Proc. Natl. Acad. Sci. U.S.A.* 105, 11105–11109. doi:10.1073/pnas.0804226105

Chung, T.-L., Brena, R. M., Kolle, G., Grimmond, S. M., Berman, B. P., Laird, P. W., et al. (2010). Vitamin C Promotes Widespread yet Specific DNA Demethylation of the Epigenome in Human Embryonic Stem Cells. *Stem Cells* 28, 1848–1855. doi:10.1002/stem.493

Cimmino, L., Dolgalev, I., Wang, Y., Yoshimi, A., Martin, G. H., Wang, J., et al. (2017). Restoration of TET2 Function Blocks Aberrant Self-Renewal and Leukemia Progression. *Cell.* 170, 1079–1095. e20. doi:10.1016/j.cell.2017.07.032

Cimmino, L., Neel, B. G., and Aifantis, I. (2018). Vitamin C in Stem Cell Reprogramming and Cancer. *Trends Cell. Biol.* 28, 698–708. doi:10.1016/j.tcb.2018.04.001

Corpe, C. P., Eck, P., Wang, J., Al-Hasani, H., and Levine, M. (2013). Intestinal Dehydroascorbic Acid (DHA) Transport Mediated by the Facilitative Sugar Transporters, GLUT2 and GLUT8. *J. Biol. Chem.* 288, 9092–9101. doi:10.1074/jbc.M112.436790

Crake, R. L. I., Burgess, E. R., Royds, J. A., Phillips, E., Vissers, M. C. M., and Dachs, G. U. (2021). The Role of 2-Oxoglutarate Dependent Dioxygenases in Gliomas and Glioblastomas: A Review of Epigenetic Reprogramming and Hypoxic Response. *Front. Oncol.* 11, 619300. doi:10.3389/fonc.2021.619300

Das, A. B., Kakadia, P. M., Wojcik, D., Pemberton, L., Browett, P. J., Bohlander, S. K., et al. (2019). Clinical Remission Following Ascorbate Treatment in a Case of Acute Myeloid Leukemia with Mutations in TET2 and WT1. *Blood Cancer J.* 9, 82. doi:10.1038/s41408-019-0242-4

Das, A. B., Smith-Díaz, C. C., and Vissers, M. C. M. (2021). Emerging Epigenetic Therapeutics for Myeloid Leukemia: Modulating Demethylase Activity with Ascorbate. *haematol* 106, 14–25. doi:10.3324/haematol.2020.259283

Delhommeau, F., Dupont, S., Valle, V. D., James, C., Trannoy, S., Massé, A., et al. (2009). Mutation inTET2in Myeloid Cancers. *N. Engl. J. Med.* 360, 2289–2301. doi:10.1056/NEJMoa0810069

Dickson, K. M., Gustafson, C. B., Young, J. I., Züchner, S., and Wang, G. (2013). Ascorbate-induced Generation of 5-hydroxymethylcytosine Is Unaffected by Varying Levels of Iron and 2-oxoglutarate. *Biochem. Biophysical Res. Commun.* 439, 522–527. doi:10.1016/j.bbrc.2013.09.010

Du, J., Cullen, J. J., and Buettner, G. R. (2012). Ascorbic Acid: Chemistry, Biology and the Treatment of Cancer. *Biochimica Biophysica Acta (BBA) - Rev. Cancer* 1826, 443–457. doi:10.1016/j.bbcan.2012.06.003

Du, J., Wagner, B. A., Buettner, G. R., and Cullen, J. J. (2015). Role of Labile Iron in the Toxicity of Pharmacological Ascorbate. *Free Radic. Biol. Med.* 84, 289–295. doi:10.1016/j.freeradbiomed.2015.03.033

Duarte, T. L., and Lunec, J. (2005). ReviewPart of the Series: From Dietary Antioxidants to Regulators in Cellular Signalling and Gene ExpressionReview: When Is an Antioxidant Not an Antioxidant? A Review of Novel Actions and Reactions of Vitamin C. *Free Radic. Res.* 39, 671–686. doi:10.1080/10715760500104025

Esteban, M. A., Wang, T., Qin, B., Yang, J., Qin, D., Cai, J., et al. (2010). Vitamin C Enhances the Generation of Mouse and Human Induced Pluripotent Stem Cells. *Cell. Stem Cell.* 6, 71–79. doi:10.1016/j.stem.2009.12.001

Fennell, K. A., Bell, C. C., and Dawson, M. A. (2019). Epigenetic Therapies in Acute Myeloid Leukemia: where to from Here? *Blood* 134, 1891–1901. doi:10.1182/blood.2019003262

Ferrada, L., Magdalena, R., Barahona, M. J., Ramírez, E., Sanzana, C., Gutiérrez, J., et al. (2021). Two Distinct Faces of Vitamin C: AA vs. DHA. *Antioxidants* 10, 215. doi:10.3390/antiox10020215

Figueroa, M. E., Abdel-Wahab, O., Lu, C., Ward, P. S., Patel, J., Shih, A., et al. (2010). Leukemic IDH1 and IDH2 Mutations Result in a Hypermethylation Phenotype, Disrupt TET2 Function, and Impair Hematopoietic Differentiation. *Cancer Cell.* 18, 553–567. doi:10.1016/j.ccr.2010.11.015

Flashman, E., Davies, S. L., Yeoh, K. K., and Schofield, C. J. (2010). Investigating the Dependence of the Hypoxia-Inducible Factor Hydroxylases (Factor Inhibiting HIF and Prolyl Hydroxylase Domain 2) on Ascorbate and Other Reducing Agents. *Biochem. J.* 427, 135–142. doi:10.1042/BJ20091609

Forristal, C. E., Brown, A. L., Helwani, F. M., Winkler, I. G., Nowlan, B., Barbier, V., et al. (2015). Hypoxia Inducible Factor (HIF)-2α Accelerates Disease Progression in Mouse Models of Leukemia and Lymphoma but Is Not a Poor Prognosis Factor in Human AML. *Leukemia* 29, 2075–2085. doi:10.1038/leu.2015.102

Gallipoli, P., Giotopoulos, G., and Huntly, B. J. P. (2015). Epigenetic Regulators as Promising Therapeutic Targets in Acute Myeloid Leukemia. *Ther. Adv. Hematol.* 6, 103–119. doi:10.1177/2040620715577614

Gao, X. N., Yan, F., Lin, J., Gao, L., Lu, X. L., Wei, S. C., et al. (2015). AML1/ETO Cooperates with HIF1α to Promote Leukemogenesis through DNMT3a Transactivation. *Leukemia* 29, 1730–1740. doi:10.1038/leu.2015.56

Gaziano, J. M., Sesso, H. D., Christen, W. G., Bubes, V., Smith, J. P., MacFadyen, J., et al. (2012). Multivitamins in the Prevention of Cancer in Men. *JAMA* 308, 1871–1880. doi:10.1001/jama.2012.14641

Gerken, T., Girard, C. A., Tung, Y.-C. L., Webby, C. J., Saudek, V., Hewitson, K. S., et al. (2007). The Obesity-Associated *FTO* Gene Encodes a 2-oxoglutarate-dependent Nucleic Acid Demethylase. *Science* 318, 1469–1472. doi:10.1126/science.1151710

Giansanti, M., Karimi, T., Faraoni, I., and Graziani, G. (2021). High-Dose Vitamin C: Preclinical Evidence for Tailoring Treatment in Cancer Patients. *Cancers* 13, 1428. doi:10.3390/cancers13061428

Gillberg, L., Ørskov, A. D., Liu, M., Harsløf, L. B. S., Jones, P. A., and Grønbæk, K. (2018). Vitamin C - A New Player in Regulation of the Cancer Epigenome. *Seminars Cancer Biol.* 51, 59–67. doi:10.1016/j.semcancer.2017.11.001

Guan, Y., Greenberg, E. F., Hasipek, M., Chen, S., Liu, X., Kerr, C. M., et al. (2020). Context Dependent Effects of Ascorbic Acid Treatment in TET2 Mutant Myeloid Neoplasia. *Commun. Biol.* 3, 493. doi:10.1038/s42003-020-01220-9

Guan, Y., Hasipek, M., Tiwari, A. D., Maciejewski, J. P., and Jha, B. K. (2021). TET-Dioxygenase Deficiency in Oncogenesis and its Targeting for Tumor-Selective Therapeutics. *Seminars Hematol.* 58, 27–34. doi:10.1053/j.seminhematol.2020.12.002

Gurnari, C., Pagliuca, S., Guan, Y., Adema, V., Hershberger, C. E., Ni, Y., et al. (2022). TET2 Mutations as a Part of DNA Dioxygenase Deficiency in Myelodysplastic Syndromes. *Blood Adv.* 6, 100–107. doi:10.1182/bloodadvances.2021005418

Gurnari, C., Pagliuca, S., and Visconte, V. (2021). The Interactome between Metabolism and Gene Mutations in Myeloid Malignancies. *Ijms* 22, 3135. doi:10.3390/ijms22063135

Hirsch, C. M., Nazha, A., Kneen, K., Abazeed, M. E., Meggendorfer, M., Przychodzen, B. P., et al. (2018). Consequences of Mutant TET2 on Clonality and Subclonal Hierarchy. *Leukemia* 32, 1751–1761. doi:10.1038/s41375-018-0150-9

Hong, S.-W., Lee, S.-H., Moon, J.-H., Hwang, J. J., Kim, D. E., Ko, E., et al. (2013). SVCT-2 in Breast Cancer Acts as an Indicator for L-Ascorbate Treatment. *Oncogene* 32, 1508–1517. doi:10.1038/onc.2012.176

Hore, T. A., von Meyenn, F., Ravichandran, M., Bachman, M., Ficz, G., Oxley, D., et al. (2016). Retinol and Ascorbate Drive Erasure of Epigenetic Memory and Enhance Reprogramming to Naïve Pluripotency by Complementary Mechanisms. *Proc. Natl. Acad. Sci. U.S.A.* 113, 12202–12207. doi:10.1073/pnas.1608679113

Hou, H.-A., and Tien, H.-F. (2016). Mutations in Epigenetic Modifiers in Acute Myeloid Leukemia and Their Clinical Utility. *Expert Rev. Hematol.* 9, 447–469. doi:10.1586/17474086.2016.1144469

Hu, D., and Shilatifard, A. (2016). Epigenetics of Hematopoiesis and Hematological Malignancies. *Genes. Dev.* 30, 2021–2041. doi:10.1101/gad.284109.116

Huijskens, M. J. A. J., Wodzig, W. K. W. H., Walczak, M., Germeraad, W. T. V., and Bos, G. M. J. (2016). Ascorbic Acid Serum Levels Are Reduced in Patients with Hematological Malignancies. *Results Immunol.* 6, 8–10. doi:10.1016/j.rinim.2016.01.001

Ito, S., Shen, L., Dai, Q., Wu, S. C., Collins, L. B., Swenberg, J. A., et al. (2011). Tet Proteins Can Convert 5-methylcytosine to 5-formylcytosine and 5-carboxylcytosine. *Science* 333, 1300–1303. doi:10.1126/science.1210597

Ito, S., Shen, L., Dai, Q., Wu, S. C., Collins, L. B., Swenberg, J. A., et al. (2013). Tet Proteins Can Convert 5-Methylcytosine to 5-Formylcytosine and 5-Carboxylcytosine. *Science* 333, 1300–1303. doi:10.1126/science.1210597

Ivan, M., Kondo, K., Yang, H., Kim, W., Valiando, J., Ohh, M., et al. (2001). HIFα Targeted for VHL-Mediated Destruction by Proline Hydroxylation:

Implications for O 2 Sensing. *Science* 292, 464–468. doi:10.1126/science.1059817

Jaakkola, P., Mole, D. R., Tian, Y.-M., Wilson, M. I., Gielbert, J., Gaskell, S. J., et al. (2001). Targeting of HIF-α to the von Hippel-Lindau Ubiquitylation Complex by O 2 -Regulated Prolyl Hydroxylation. *Science* 292, 468–472. doi:10.1126/science.1059796

Kakhlon, O., and Cabantchik, Z. I. (2002). The Labile Iron Pool: Characterization, Measurement, and Participation in Cellular Processes1 1This Article Is Part of a Series of Reviews on "Iron and Cellular Redox Status." the Full List of Papers May Be Found on the Homepage of the Journal. *Free Radic. Biol. Med.* 33, 1037–1046. doi:10.1016/S0891-5849(02)01006-7

Kawada, H., Kaneko, M., Sawanobori, M., Uno, T., Matsuzawa, H., Nakamura, Y., et al. (2013). High Concentrations of L-Ascorbic Acid Specifically Inhibit the Growth of Human Leukemic Cells via Downregulation of HIF-1α Transcription. *PLoS One* 8, e62717. doi:10.1371/journal.pone.0062717

Kiessling, M. K., Klemke, C. D., Kaminski, M. M., Galani, I. E., Krammer, P. H., and Gülow, K. (2009). Inhibition of Constitutively Activated Nuclear Factor-Kb Induces Reactive Oxygen Species- and Iron-dependent Cell Death in Cutaneous T-Cell Lymphoma. *Cancer Res.* 69, 2365–2374. doi:10.1158/0008-5472.CAN-08-3221

Kimura, H., Yamada, Y., Morita, Y., Ikeda, H., and Matsuo, T. (1992). Dietary Ascorbic Acid Depresses Plasma and Low Density Lipoprotein Lipid Peroxidation in Genetically Scorbutic Rats. *J. Nutr.* 122, 1904–1909. doi:10.1093/jn/122.9.1904

Kuiper, C., and Vissers, M. C. M. (2014). Ascorbate as a Co-factor for Fe- and 2-oxoglutarate Dependent Dioxygenases: Physiological Activity in Tumor Growth and Progression. *Front. Oncol.* 4, 359. doi:10.3389/fonc.2014.00359

Kunimoto, H., and Nakajima, H. (2017). Epigenetic Dysregulation of Hematopoietic Stem Cells and Preleukemic State. *Int. J. Hematol.* 106, 34–44. doi:10.1007/s12185-017-2257-6

Kyhos, E. D., Sevringhaus, E. L., and Hagedorn, D. (1945). Large Doses of Ascorbic Acid in Treatment of Vitamin C Deficiencies. *Arch. Intern. Med.* 75, 407–412. doi:10.1001/archinte.1945.00210300053006

Linowiecka, K., Foksinski, M., and Brożyna, A. A. (2020). Vitamin C Transporters and Their Implications in Carcinogenesis. *Nutrients* 12, 3869. doi:10.3390/nu12123869

Liu, J., Hong, J., Han, H., Park, J., Kim, D., Park, H., et al. (2020). Decreased Vitamin C Uptake Mediated by SLC2A3 Promotes Leukaemia Progression and Impedes TET2 Restoration. *Br. J. Cancer* 122, 1445–1452. doi:10.1038/s41416-020-0788-8

Liu, M., Ohtani, H., Zhou, W., Ørskov, A. D., Charlet, J., Zhang, Y. W., et al. (2016). Vitamin C Increases Viral Mimicry Induced by 5-Aza-2′-Deoxycytidine. *Proc. Natl. Acad. Sci. U.S.A.* 113, 10238–10244. LP – 10244. doi:10.1073/pnas.1612262113

Lutsenko, E. A., Cárcamo, J. M., and Golde, D. W. (2002). Vitamin C Prevents DNA Mutation Induced by Oxidative Stress. *J. Biol. Chem.* 277, 16895–16899. doi:10.1074/jbc.M201151200

Lykkesfeldt, J., and Tveden-Nyborg, P. (2019). The Pharmacokinetics of Vitamin C. *Nutrients* 11, 2412. doi:10.3390/nu11102412

Malo, C., and Wilson, J. X. (2000). Glucose Modulates Vitamin C Transport in Adult Human Small Intestinal Brush Border Membrane Vesicles. *J. Nutr.* 130, 63–69. doi:10.1093/jn/130.1.63

Mandl, J., Szarka, A., and Bánhegyi, G. (2009). Vitamin C: Update on Physiology and Pharmacology. *Br. J. Pharmacol.* 157, 1097–1110. doi:10.1111/j.1476-5381.2009.00282.x

Martínez-Reyes, I., and Chandel, N. S. (2020). Mitochondrial TCA Cycle Metabolites Control Physiology and Disease. *Nat. Commun.* 11, 102. doi:10.1038/s41467-019-13668-3

Masoud, G. N., and Li, W. (2015). HIF-1α Pathway: Role, Regulation and Intervention for Cancer Therapy. *Acta Pharm. Sin. B* 5, 378–389. doi:10.1016/j.apsb.2015.05.007

Mastrangelo, D., Massai, L., Lo Coco, F., Noguera, N. I., Borgia, L., Fioritoni, G., et al. (2015). Cytotoxic Effects of High Concentrations of Sodium Ascorbate on Human Myeloid Cell Lines. *Ann. Hematol.* 94, 1807–1816. doi:10.1007/s00277-015-2464-2

May, J. M., Qu, Z., and Li, X. (2001). Requirement for GSH in Recycling of Ascorbic Acid in Endothelial Cells. *Biochem. Pharmacol.* 62, 873–881. doi:10.1016/s0006-2952(01)00736-5

May, J. M. (2011). The SLC23 Family of Ascorbate Transporters: Ensuring that You Get and Keep Your Daily Dose of Vitamin C. *Br. J. Pharmacol.* 164, 1793–1801. doi:10.1111/j.1476-5381.2011.01350.x

Mayland, C. R., Bennett, M. I., and Allan, K. (2005). Vitamin C Deficiency in Cancer Patients. *Palliat. Med.* 19, 17–20. doi:10.1191/0269216305pm970oa

McCarty, M. F., and Contreras, F. (2014). Increasing Superoxide Production and the Labile Iron Pool in Tumor Cells May Sensitize Them to Extracellular Ascorbate. *Front. Oncol.* 4, 249. doi:10.3389/fonc.2014.00249

McDonough, M. A., Loenarz, C., Chowdhury, R., Clifton, I. J., and Schofield, C. J. (2010). Structural Studies on Human 2-oxoglutarate Dependent Oxygenases. *Curr. Opin. Struct. Biol.* 20, 659–672. doi:10.1016/j.sbi.2010.08.006

Miller, P. G., and Steensma, D. P. (2020). Implications of Clonal Hematopoiesis for Precision Oncology. *JCO Precis. Oncol.* 4, 639–646. doi:10.1200/PO.20.00144

Mingay, M., Chaturvedi, A., Bilenky, M., Cao, Q., Jackson, L., Hui, T., et al. (2018). Vitamin C-Induced Epigenomic Remodelling in IDH1 Mutant Acute Myeloid Leukaemia. *Leukemia* 32, 11–20. doi:10.1038/leu.2017.171

Minor, E. A., Court, B. L., Young, J. I., and Wang, G. (2013). Ascorbate Induces Ten-Eleven Translocation (Tet) Methylcytosine Dioxygenase-Mediated Generation of 5-hydroxymethylcytosine. *J. Biol. Chem.* 288, 13669–13674. doi:10.1074/jbc.C113.464800

Moloney, J. N., and Cotter, T. G. (2018). ROS Signalling in the Biology of Cancer. *Seminars Cell. & Dev. Biol.* 80, 50–64. doi:10.1016/j.semcdb.2017.05.023

Nakajima, H., and Kunimoto, H. (2014). TET2 as an Epigenetic Master Regulator for Normal and Malignant Hematopoiesis. *Cancer Sci.* 105, 1093–1099. doi:10.1111/cas.12484

Nannya, Y., Shinohara, A., Ichikawa, M., and Kurokawa, M. (2014). Serial Profile of Vitamins and Trace Elements during the Acute Phase of Allogeneic Stem Cell Transplantation. *Biol. Blood Marrow Transplant.* 20, 430–434. doi:10.1016/j.bbmt.2013.12.554

Nauman, G., Gray, J., Parkinson, R., Levine, M., and Paller, C. (2018). Systematic Review of Intravenous Ascorbate in Cancer Clinical Trials. *Antioxidants* 7, 89. doi:10.3390/antiox7070089

Ngo, B., Van Riper, J. M., Cantley, L. C., and Yun, J. (2019). Targeting Cancer Vulnerabilities with High-Dose Vitamin C. *Nat. Rev. Cancer* 19, 271–282. doi:10.1038/s41568-019-0135-7

Noguera, N. I., Pelosi, E., Angelini, D. F., Piredda, M. L., Guerrera, G., Piras, E., et al. (2017). High-dose Ascorbate and Arsenic Trioxide Selectively Kill Acute Myeloid Leukemia and Acute Promyelocytic Leukemia Blasts *In Vitro*. *Oncotarget* 8, 32550–32565. doi:10.18632/oncotarget.15925

Noroozi, M., Angerson, W. J., and Lean, M. E. (1998). Effects of Flavonoids and Vitamin C on Oxidative DNA Damage to Human Lymphocytes. *Am. J. Clin. Nutr.* 67, 1210–1218. doi:10.1093/ajcn/67.6.1210

Ozer, A., and Bruick, R. K. (2007). Non-heme Dioxygenases: Cellular Sensors and Regulators Jelly Rolled into One? *Nat. Chem. Biol.* 3, 144–153. doi:10.1038/nchembio863

Packham, G. (2008). The Role of NF-Kb in Lymphoid Malignancies. *Br. J. Haematol.* 143, 3–15. doi:10.1111/j.1365-2141.2008.07284.x

Papaemmanuil, E., Gerstung, M., Bullinger, L., Gaidzik, V. I., Paschka, P., Roberts, N. D., et al. (2016). Genomic Classification and Prognosis in Acute Myeloid Leukemia. *N. Engl. J. Med.* 374, 2209–2221. doi:10.1056/NEJMoa1516192

Papaemmanuil, E., Gerstung, M., Malcovati, L., Tauro, S., Gundem, G., Van Loo, P., et al. (2013). Clinical and Biological Implications of Driver Mutations in Myelodysplastic Syndromes. *Blood* 122, 3616–3627. quiz 3699. doi:10.1182/blood-2013-08-518886

Park, S., Han, S.-S., Park, C. H., Hahm, E.-R., Lee, S. J., Park, H. K., et al. (2004). L-ascorbic Acid Induces Apoptosis in Acute Myeloid Leukemia Cells via Hydrogen Peroxide-Mediated Mechanisms. *Int. J. Biochem. Cell. Biol.* 36, 2180–2195. doi:10.1016/j.biocel.2004.04.005

Park, S. (2013). The Effects of High Concentrations of Vitamin C on Cancer Cells. *Nutrients* 5, 3496–3505. doi:10.3390/nu5093496

Pastore, F., and Levine, R. L. (2016). Epigenetic Regulators and Their Impact on Therapy in Acute Myeloid Leukemia. *Haematologica* 101, 269–278. doi:10.3324/haematol.2015.140822

Pauling, L. (1980). Vitamin C Therapy of Advanced Cancer. *N. Engl. J. Med.* 302, 694–695. doi:10.1056/NEJM198003203021219

Pflaum, M., Kielbassa, C., Garmyn, M., and Epe, B. (1998). Oxidative DNA Damage Induced by Visible Light in Mammalian Cells: Extent, Inhibition

by Antioxidants and Genotoxic Effects. *Mutat. Research/DNA Repair* 408, 137–146. doi:10.1016/s0921-8777(98)00029-9

Phillips, C. L., Combs, S. B., and Pinnell, S. R. (1994). Effects of Ascorbic Acid on Proliferation and Collagen Synthesis in Relation to the Donor Age of Human Dermal Fibroblasts. *J. Investigative Dermatology* 103, 228–232. doi:10.1111/1523-1747.ep12393187

Pinnix, Z. K., Miller, L. D., Wang, W., D'Agostino, R., Kute, T., Willingham, M. C., et al. (2010). Ferroportin and Iron Regulation in Breast Cancer Progression and Prognosis. *Sci. Transl. Med.* 2, 43ra56. doi:10.1126/scitranslmed.3001127

Putchala, M. C., Ramani, P., Sherlin, H. J., Premkumar, P., and Natesan, A. (2013). Ascorbic Acid and its Pro-oxidant Activity as a Therapy for Tumours of Oral Cavity - A Systematic Review. *Archives Oral Biol.* 58, 563–574. doi:10.1016/j.archoralbio.2013.01.016

Rasheed, M., Simmons, G., Fisher, B., Leslie, K., Reed, J., Roberts, C., et al. (2019). Reduced Plasma Ascorbic Acid Levels in Recipients of Myeloablative Conditioning and Hematopoietic Cell Transplantation. *Eur. J. Haematol.* 103, 329–334. doi:10.1111/ejh.13287

Ratcliffe, P. J. (2013). Oxygen Sensing and Hypoxia Signalling Pathways in Animals: the Implications of Physiology for Cancer. *J. Physiol.* 591, 2027–2042. doi:10.1113/jphysiol.2013.251470

Reikvam, H., Olsnes, A. M., Gjertsen, B. T., Ersvar, E., and Bruserud, O. (2009). Nuclear Factor-Kb Signaling: A Contributor in Leukemogenesis and a Target for Pharmacological Intervention in Human Acute Myelogenous Leukemia. *Crit. Rev. Oncog.* 15, 1–41. doi:10.1615/critrevoncog.v15.i1-2.10

Ruiz, M. A., Rivers, A., Ibanez, V., Vaitkus, K., Mahmud, N., DeSimone, J., et al. (2015). Hydroxymethylcytosine and Demethylation of Theγ-Globingene Promoter during Erythroid Differentiation. *Epigenetics* 10, 397–407. doi:10.1080/15592294.2015.1039220

Rumsey, S. C., Kwon, O., Xu, G. W., Burant, C. F., Simpson, I., and Levine, M. (1997). Glucose Transporter Isoforms GLUT1 and GLUT3 Transport Dehydroascorbic Acid. *J. Biol. Chem.* 272, 18982–18989. doi:10.1074/jbc.272.30.18982

Rumsey, S. C., and Levine, M. (1998). Absorption, Transport, and Disposition of Ascorbic Acid in Humans. *J. Nutr. Biochem.* 9, 116–130. doi:10.1016/S0955-2863(98)00002-3

Rumsey, S. C., Welch, R. W., Garraffo, H. M., Ge, P., Lu, S.-F., Crossman, A. T., et al. (1999). Specificity of Ascorbate Analogs for Ascorbate Transport. *J. Biol. Chem.* 274, 23215–23222. doi:10.1074/jbc.274.33.23215

Santos-Sánchez, N. F., Salas-Coronado, R., Villanueva-Cañongo, C., and Hernández-Carlos, B. (2019). "Antioxidant Compounds and Their Antioxidant Mechanism," in *Antioxidants*. Editor E. Shalaby (Rijeka: IntechOpen). doi:10.5772/intechopen.85270

Savini, I., Rossi, A., Pierro, C., Avigliano, L., and Catani, M. V. (2008). SVCT1 and SVCT2: Key Proteins for Vitamin C Uptake. *Amino Acids* 34, 347–355. doi:10.1007/s00726-007-0555-7

Schoenfeld, J. D., Sibenaller, Z. A., Mapuskar, K. A., Wagner, B. A., Cramer-Morales, K. L., Furqan, M., et al. (2017). O2·− and H2O2-Mediated Disruption of Fe Metabolism Causes the Differential Susceptibility of NSCLC and GBM Cancer Cells to Pharmacological Ascorbate. *Cancer Cell.* 32, 268. doi:10.1016/j.ccell.2017.07.008

Schofield, C. J., and Ratcliffe, P. J. (2004). Oxygen Sensing by HIF Hydroxylases. *Nat. Rev. Mol. Cell. Biol.* 5, 343–354. doi:10.1038/nrm1366

Shenoy, N., Bhagat, T., Nieves, E., Stenson, M., Lawson, J., Choudhary, G. S., et al. (2017). Upregulation of TET Activity with Ascorbic Acid Induces Epigenetic Modulation of Lymphoma Cells. *Blood Cancer J.* 7, e587. doi:10.1038/bcj.2017.65

Simon, M. C. (2016). The Hypoxia Response Pathways - Hats off. *N. Engl. J. Med.* 375, 1687–1689. doi:10.1056/NEJMcibr1610065

Smith-Díaz, C. C., Magon, N. J., McKenzie, J. L., Hampton, M. B., Vissers, M. C. M., and Das, A. B. (2021). Ascorbate Inhibits Proliferation and Promotes Myeloid Differentiation in TP53-Mutant Leukemia. *Front. Oncol.* 11, 709543. doi:10.3389/fonc.2021.709543

Sotiriou, S., Gispert, S., Cheng, J., Wang, Y., Chen, A., Hoogstraten-Miller, S., et al. (2002). Ascorbic-acid Transporter Slc23a1 Is Essential for Vitamin C Transport into the Brain and for Perinatal Survival. *Nat. Med.* 8, 514–517. doi:10.1038/0502-514

Staehle, H. F., Pahl, H. L., and Jutzi, J. S. (2021). The Cross Marks the Spot: The Emerging Role of JmjC Domain-Containing Proteins in Myeloid Malignancies. *Biomolecules* 11, 1911. doi:10.3390/biom11121911

Stephens, D. J., and Hawley, E. E. (1936). The Partition of Reduced Ascorbic Acid in Blood. *J. Biol. Chem.* 115, 653–658. doi:10.1016/S0021-9258(18)74704-2

Strohle, A., Wolters, M., and Hahn, A. (2011). Micronutrients at the Interface between Inflammation and Infection Ascorbic Acid and Calciferol. Part 2: Calciferol and the Significance of Nutrient Supplements. *Iadt* 10, 64–74. doi:10.2174/187152811794352097

Sun, J., He, X., Zhu, Y., Ding, Z., Dong, H., Feng, Y., et al. (2018). SIRT1 Activation Disrupts Maintenance of Myelodysplastic Syndrome Stem and Progenitor Cells by Restoring TET2 Function. *Cell. Stem Cell.* 23, 355–369. e9. doi:10.1016/j.stem.2018.07.018

Sweetman, S. F., Strain, J. J., and McKelvey-Martin, V. J. (1997). Effect of Antioxidant Vitamin Supplementation on DNA Damage and Repair in Human Lymphoblastoid Cells. *Nutr. Cancer* 27, 122–130. doi:10.1080/01635589709514513

Tahiliani, M., Koh, K. P., Shen, Y., Pastor, W. A., Bandukwala, H., Brudno, Y., et al. (2009). Conversion of 5-methylcytosine to 5-hydroxymethylcytosine in Mammalian DNA by MLL Partner TET1. *Science* 324, 930–935. doi:10.1126/science.1170116

Testa, U., Pelosi, E., and Castelli, G. (2021). New Promising Developments for Potential Therapeutic Applications of High-Dose Ascorbate as an Anticancer Drug. *Hematology/Oncology Stem Cell. Ther.* 14, 179–191. doi:10.1016/j.hemonc.2020.11.002

The Cancer Genome Atlas Research Network (2013). Genomic and Epigenomic Landscapes of Adult De Novo Acute Myeloid Leukemia. *N. Engl. J. Med.* 368, 2059–2074. doi:10.1056/NEJMoa1301689

Tsukaguchi, H., Tokui, T., Mackenzie, B., Berger, U. V., Chen, X.-Z., Wang, Y., et al. (1999). A Family of Mammalian Na+-dependent L-Ascorbic Acid Transporters. *Nature* 399, 70–75. doi:10.1038/19986

Valdés, F. (2006). Vitamin C. *Actas Dermosifiliogr.* 97, 557–568. doi:10.1016/s0001-7310(06)73466-4

van der Reest, J., and Gottlieb, E. (2016). Anti-cancer Effects of Vitamin C Revisited. *Cell. Res.* 26, 269–270. doi:10.1038/cr.2016.7

Vera, J. C., Rivas, C. I., Fischbarg, J., and Golde, D. W. (1993). Mammalian Facilitative Hexose Transporters Mediate the Transport of Dehydroascorbic Acid. *Nature* 364, 79–82. doi:10.1038/364079a0

Vissers, M. C. M., and Das, A. B. (2018). Potential Mechanisms of Action for Vitamin C in Cancer: Reviewing the Evidence. *Front. Physiol.* 9, 809. doi:10.3389/fphys.2018.00809

Vissers, M. C. M., Kuiper, C., and Dachs, G. U. (2014). Regulation of the 2-oxoglutarate-dependent Dioxygenases and Implications for Cancer. *Biochem. Soc. Trans.* 42, 945–951. doi:10.1042/BST20140118

Wang, T., Chen, K., Zeng, X., Yang, J., Wu, Y., Shi, X., et al. (2011a). The Histone Demethylases Jhdm1a/1b Enhance Somatic Cell Reprogramming in a Vitamin-C-dependent Manner. *Cell. Stem Cell.* 9, 575–587. doi:10.1016/j.stem.2011.10.005

Wang, Y., Liu, Y., Malek, S. N., Zheng, P., and Liu, Y. (2011b). Targeting HIF1α Eliminates Cancer Stem Cells in Hematological Malignancies. *Cell. Stem Cell.* 8, 399–411. doi:10.1016/j.stem.2011.02.006

White, R., Nonis, M., Pearson, J. F., Burgess, E., Morrin, H. R., Pullar, J. M., et al. (2020). Low Vitamin C Status in Patients with Cancer Is Associated with Patient and Tumor Characteristics. *Nutrients* 12, 2338. doi:10.3390/nu12082338

Wilson, J. X. (2002). The Physiological Role of Dehydroascorbic Acid. *FEBS Lett.* 527, 5–9. doi:10.1016/s0014-5793(02)03167-8

Wilson, M. K., Baguley, B. C., Wall, C., Jameson, M. B., and Findlay, M. P. (2014). Review of High-Dose Intravenous Vitamin C as an Anticancer Agent. *Asia-Pac J. Clin. Oncol.* 10, 22–37. doi:10.1111/ajco.12173

Wohlrab, C., Phillips, E., and Dachs, G. U. (2017). Vitamin C Transporters in Cancer: Current Understanding and Gaps in Knowledge. *Front. Oncol.* 7. doi:10.3389/fonc.2017.00074

Wouters, B. J., and Delwel, R. (2016). Epigenetics and Approaches to Targeted Epigenetic Therapy in Acute Myeloid Leukemia. *Blood* 127, 42–52. doi:10.1182/blood-2015-07-604512

Yang, W. S., and Stockwell, B. R. (2008). Synthetic Lethal Screening Identifies Compounds Activating Iron-dependent, Nonapoptotic Cell Death in

Oncogenic-RAS-Harboring Cancer Cells. *Chem. Biol.* 15, 234–245. doi:10.1016/j.chembiol.2008.02.010

Yi, C., Jia, G., Hou, G., Dai, Q., Zhang, W., Zheng, G., et al. (2010). Iron-catalysed Oxidation Intermediates Captured in a DNA Repair Dioxygenase. *Nature* 468, 330–333. doi:10.1038/nature09497

Yin, R., Mao, S.-Q., Zhao, B., Chong, Z., Yang, Y., Zhao, C., et al. (2013). Ascorbic Acid Enhances Tet-Mediated 5-methylcytosine Oxidation and Promotes DNA Demethylation in Mammals. *J. Am. Chem. Soc.* 135, 10396–10403. doi:10.1021/ja4028346

Yoshimi, A., Lin, K.-T., Wiseman, D. H., Rahman, M. A., Pastore, A., Wang, B., et al. (2019). Coordinated Alterations in RNA Splicing and Epigenetic Regulation Drive Leukaemogenesis. *Nature* 574, 273–277. doi:10.1038/s41586-019-1618-0

Young, J. I., Züchner, S., and Wang, G. (2015). Regulation of the Epigenome by Vitamin C. *Annu. Rev. Nutr.* 35, 545–564. doi:10.1146/annurev-nutr-071714-034228

Yun, J., Mullarky, E., Lu, C., Bosch, K. N., Kavalier, A., Rivera, K., et al. (2015). Vitamin C Selectively Kills KRAS and BRAF Mutant Colorectal Cancer Cells by Targeting GAPDH. *Science* 350, 1391–1396. doi:10.1126/science.aaa5004

Zhang, Y. W., Wang, Z., Xie, W., Cai, Y., Xia, L., Easwaran, H., et al. (2017). Acetylation Enhances TET2 Function in Protecting against Abnormal DNA Methylation during Oxidative Stress. *Mol. Cell.* 65, 323–335. doi:10.1016/j.molcel.2016.12.013

Zhao, H., Zhu, H., Huang, J., Zhu, Y., Hong, M., Zhu, H., et al. (2018). The Synergy of Vitamin C with Decitabine Activates TET2 in Leukemic Cells and Significantly Improves Overall Survival in Elderly Patients with Acute Myeloid Leukemia. *Leukemia Res.* 66, 1–7. doi:10.1016/j.leukres.2017.12.009

**Conflict of Interest:** The authors declare that the research was conducted in the absence of any commercial or financial relationships that could be construed as a potential conflict of interest.

frontiers | Frontiers in Cell and Developmental Biology

TYPE Original Research
PUBLISHED 22 August 2022
DOI 10.3389/fcell.2022.924848



OPEN ACCESS

EDITED BY
Daniel G. S. Capelluto,
Virginia Tech, United States

REVIEWED BY
Yanfen Liu,
ShanghaiTech University, China
Chiara Giannone,
Vita-Salute San Raffaele University, Italy

*CORRESPONDENCE
Linda M. Hendershot,
Linda.hendershot@stjude.org

†PRESENT ADDRESS
Christina Oikonomou,
Genmab, Utrecht, Netherlands
Candace A. Hayes,
MS3 Lewis Katz School of Medicine,
Temple University, Philadelphia, PA,
United States

SPECIALTY SECTION
This article was submitted to Signaling, a section of the journal Frontiers in Cell and Developmental Biology

RECEIVED 20 April 2022
ACCEPTED 04 July 2022
PUBLISHED 22 August 2022

CITATION
Mann MJ, Flory AR, Oikonomou C, Hayes CA, Melendez-Suchi C and Hendershot LM (2022), Identification of two rate-limiting steps in the degradation of partially folded immunoglobulin light chains. *Front. Cell Dev. Biol.* 10:924848. doi: 10.3389/fcell.2022.924848



# Identification of two rate-limiting steps in the degradation of partially folded immunoglobulin light chains

Melissa J. Mann[1], Ashley R. Flory[1], Christina Oikonomou[1,2†], Candace A. Hayes[3†], Chris Melendez-Suchi[1] and Linda M. Hendershot[1,2*]

[1]St Jude Children's Research Hospital, Memphis, TN, United States, [2]University of Tennessee Health Science Center, Memphis, TN, United States, [3]Rhodes College, Memphis, TN, United States

Antibody monomers are produced from two immunoglobulin heavy chains and two light chains that are folded and assembled in the endoplasmic reticulum This process is assisted and monitored by components of the endoplasmic reticulum quality control machinery; an outcome made more fraught by the unusual genetic machinations employed to produce a seemingly unlimited antibody repertoire. Proper functioning of the adaptive immune system is as dependent on the success of this operation, as it is on the ability to identify and degrade those molecules that fail to reach their native state. In this study, two rate-limiting steps were identified in the degradation of a non-secreted κ light chain. Both focus on the constant domain ($C_L$), which has evolved to fold rapidly and very stably to serve as a catalyst for the folding of the heavy chain $C_H1$ domain. The first hurdle is the reduction of the disulfide bond in the $C_L$ domain, which is required for retrotranslocation to the cytosol. In spite of being reduced, the $C_L$ domain retains structure, giving rise to the second rate-limiting step, the unfolding of this domain at the proteasome, which results in a stalled degradation intermediate.

KEYWORDS

**ER quality control, ERAD, Ig light chain, proteasome, degradation**

## Introduction

Our immune systems are able to produce antibodies to a seemingly limitless number of antigens. In fact, a recent study estimated that the potential human antibody repertoire may approach a quintrillion unique molecules (Briney et al., 2019). If each antibody was encoded by a separate DNA segment, an absurd number of genome equivalents would be required to produce them. Instead, this incredible feat is made possible through a complex series of molecular manipulations of antibody genes. The variable regions of the heavy and light chain, which provide the antigen recognition capability of antibody, are assembled from three distinct sets of immunoglobulin (Ig) gene families for the heavy chain: Variable ($V_H$), Diversity ($D_H$), and Joining ($J_H$), and two each for the κ and λ light chains ($V_κ$, $J_κ$ and

$V_\lambda$, $J_\lambda$). One DNA segment from each of these heavy and light chain gene families must be successfully recombined, and non-templated nucleotides are added to the ends of the DNA segments prior to their relegation to produce a heavy chain and light chain variable region. In addition, the assembled variable region is subjected to hypermutation to increase antigen affinity (Kenter and Feeney, 2019; Vajda et al., 2021). While this clearly adds to the diversity of the repertoire, from a standpoint of protein folding it represents a veritable nightmare. And yet, absolute fidelity in antibody maturation is required for proper functioning of the immune system.

Like nearly all secreted or cell surface proteins, immunoglobulins are produced in the endoplasmic reticulum, where a dedicated ER quality control (ERQC) system assists and monitors the maturation of nascent proteins. Monomeric IgG antibodies are covalently assembled from two identical γ heavy chains and two identical either κ or λ light chains, which possess four and two Ig domains, respectively, whereas pentameric IgM antibodies are covalently assembled from ten μ heavy chains consisting of five Ig domains, ten light chains, and a J or joining chain. Each Ig domain is approximately 100 amino acids in length and folds into an anti-parallel β barrel structure that is secured with a disulfide bond between highly conserved cysteines in strands 2 and 6 (Oreste et al., 2021). Antibodies have been subjected to numerous *in vitro* and *in vivo* folding studies that have provided significant understanding of the molecular and cellular checkpoints that ensure fidelity of their maturation (Feige et al., 2010). These studies reveal that although most Ig domains can fold and form their intra-domain disulfide bond independently or after homodimerization (Lilie et al., 1994), the first constant domain of the heavy chain ($C_H1$) domain is unique in that it remains reduced (Lee et al., 1999) and unstructured (Feige et al., 2009) prior to assembly with a light chain. The unfolded $C_H1$ domain reacts with BiP, which serves to retain the incompletely assembled heavy chain in the ER, and deletion of the $C_H1$ domain results in the secretion of partially assembled antibody intermediates (Hendershot et al., 1987). Contact with the well-folded constant domain $C_L$ of a light chain nucleates oxidative folding of the $C_H1$ domain, allowing the completely folded and assembled antibody to be released from BiP and secreted (Feige et al., 2009). In the case of pre-B cells, the surrogate light chain is responsible for associating with the $C_H1$ domain of the μ chains, and deletion of the $C_H1$ domain of the μ heavy chain locus adversely affects B cell development (Shaffer and Schlissel, 1997). Thus, checkpoints for Ig gene rearrangements are also assessed through the protein quality control system and focus on the ability of a well-folded $C_L$ domain to induce folding of the $C_H1$ domain.

Given the unusual mechanisms needed to produce the vast antibody repertoire, as well as the extremely high biosynthetic rate achieved in plasma cells, it is to be expected that some genetic manipulations, and even random mistakes during normal synthesis, will produce antibody subunits that fail to fold or assemble properly. The presence of a single unfolded domain requires that the heavy or light chain be targeted for degradation, which occurs through the actions of the ER associated degradation (ERAD) system (Wu and Rapoport, 2018; Needham et al., 2019). Once the decision has been made to degrade an unfolded/misfolded client, it must be targeted and inserted into a protein channel, referred to as the retrotranslocon or dislocon, for extraction to the cytosol where it will be degraded by the proteasome. A number of components of the retrotranslocon have been identified, although it appears there is some heterogeneity in the composition of individual retrotranslocons (Lilley and Ploegh, 2005; Carvalho et al., 2006; Vembar and Brodsky, 2008; Olzmann et al., 2013). One of the translocon components, Hrd1, is a multi-pass integral membrane protein that forms part of the channel itself (Carvalho et al., 2010; Stein et al., 2014). Hrd1 possesses E3 ubiquitin ligase activity with the RING domain oriented to the cytosol (Gardner et al., 2000; Deak and Wolf, 2001). Upon emerging into the cytosol, the ERAD client becomes poly-ubiquitinated, which can occur on a number of amino acids, including serine, threonine, and cysteine, in addition to the prototypical lysine residue (Cadwell and Coscoy, 2005; Wang et al., 2007; Ishikura et al., 2010; Shimizu et al., 2010). In addition to Hrd1, a limited number of other ER-associated E3 ligases have been identified (Kostova et al., 2007). The attached ubiquitin chain provides a recognition motif for the p97/VCP complex (Meyer et al., 2002) that is associated with the ER membrane (Ye et al., 2004; Ye et al., 2005). The AAA-ATPase, p97, provides the energy to extract ERAD clients from the ER membranes. With the possible exception of the cholera toxin A1 subunit (Kothe et al., 2005; Moore et al., 2013), all integral membrane, as well as soluble, luminal ERAD clients examined thus far require the activity of p97 for their disposal.

To understand the cellular checkpoints and requirements for the degradation of an Ig subunit that fails to mature properly and how a well-folded domain affects these, we chose the NS1 Ig light chain. It is comprised of a variable region ($V_L$) that forms its disulfide bond but folds unstably and a well-folded, oxidized constant domain ($C_L$). We found that although the $V_L$ domain must be reduced (Knittler et al., 1995; Okuda-Shimizu and Hendershot, 2007) and is the target of ubiquitination in the cytosol (Shimizu et al., 2010), reduction of the $C_L$ domain represents a more significant rate-limiting step in its retrotranslocation. The $C_L$ domain either maintains or re-achieves structure once in the cytosol explaining the lack of ubiquitination of this domain. Unfolding of the $C_L$ at proteasome represents a second rate-limiting step in its degradation.

TABLE 1 Primers used to make NS1 mutants.

| Site/AA substitution | Forward primer | Reverse primer |
|---|---|---|
| NS1-N28/V30T | GCCAGTGAGAATGTGaccACTTATGTTTCCTGG | CCAGGAAACATAAGTggtCACATTCTCACTGGC |
| NS1-N53/Y55T | GCATCCAACCGGaccACTGGGGTCCCC | GGGGACCCCAGTggtCCGGTTGGATGC |
| NS1-N100/G100N | CACGTTCGGAaacGGGACCAAGC | TACGGATAGCTGTAACCC |
| NS1-N129/G129N | AACATCTGGAaatGCCTCAGTCGTGTG | AACTGCTCACTGGATGGT |
| NS1-N157/V159T | ACAAAATGGCaccCTGAACAGTTG | CGTTCACTGCCATCAATC |
| NS1-Vmut and Cmut-N157/V159T | ACAAAATGGCactCTGAACAGTTGGAC | CGTTCACTGCCATCAATC |
| NS1-N170/D170N | GGACAGCAAAaatAGCACCTACA | TGATCAGTCCAACTGTTCAG |
| NS1-VLSTK- N28/V30T | TGAGAATGTGaccGCTTATGTTGCCTGGTATCAACAGAGACCAGAG | GCGGCCCTGCAGGCCAAG |
| NS1-VLSTK- N100/G100N & A102T | gaccAGGCTGGAAATAAGACGGG | ccattTCCGAACGCGTACGGATA |
| ΔssNS1(removing ER target SS) | ACCGGATCGATCCCTCGACCTGCAGATGGGGAACATTGTAATGACCCAATCTCCCA | TGGGAGATTGGGTCATTACAATGTTCCCCATCTGCAGGTCGAGGGATCGATCCGGT |
| ΔssNS1 (M4A,M11A,M13A) | aaatccgcttccgctTCAGTAGGAGAGAGGGTC | gggagattgggtagcTACAATGTTCCCCATCTG |

# Materials and methods

## DNA constructs and generation of mutants

The non-secreted murine NS1 κ LC (Skowronek et al., 1998) and the ubiquitination-deficient NS1-$V_L$STK- (Shimizu et al., 2010) were cloned in pSVL vector. Single N-linked glycosylation consensus sites (N-X-S/T) were engineered throughout NS1 in order to monitor deglycosylation, which occurs after substrate retrotranslocation to the cytosol. Generation of these mutants was performed using the PWO enzyme (11644955001, Roche) or the Q5 mutagenesis kit (E0554S, NEB, Ipswich, MA). When glycosylation sites were added to the folded $C_L$ domain, the mutations were introduced on β turns or loops, which were mapped using the available crystal structure for the mouse $C_κ$ domain (UniProtKB - P01837) to minimize adverse effects on the natural folding of this domain. A cytosolically expressed NS1 (ΔssNS1) was engineered by removing the ER targeting signal sequence, and replacing methionines present at positions 4, 11, 13 with alanines to prevent possible alternative translation initiation sites. Primers used to create the amino acid changes in these constructs are found in Table 1. The NS1-Vmut and NS1-Cmut constructs were created in the pSVL vector using PCR-mediated, site-directed mutagenesis to replace the two cysteine codons in either the $V_L$ or $C_L$ domains with serine codons. The PDIA6 construct in the pCDNA3 vector was generously provided by Dr. Neil Bulleid (University of Glasgow, Scotland, United Kingdom), and ERdj5, also in pCDNA3, was a kind gift from Dr. Kazuhiro Nagata (Kyoto Sangyo University, Japan). Wild type p97 and the ATP hydrolysis-defective mutant p97QQ, each in the pcDNA3 vector, were considerate gifts from Dr. Yihong Ye (NIDDK, United States). The Hrd1 mutant deficient in ubiquitin ligase activity (Hrd1 C291S in pcDNA3) was kindly supplied by Dr. Yuval Reiss (Proteologics, Israel).

## Cell culture and transfections

293T human embryonic kidney cells were grown in Dulbecco's modified Eagle's medium (DMEM; 15–013-CV, Corning–cellgro, Manassas, VA) supplemented with 10% (v/v) heat-inactivated fetal bovine serum (FBS; S11150, Atlanta biologicals, Flowery Branch, GA), 2 mM L-glutamine (25–005-CI, Corning), and a 1% (v/v) antibiotic-antimycotic solution (25 μg/ml amphotenicin B, 10,000 μg/ml streptomycin, and 10,000 units of penicillin; Cellgro/Mediatech, Manassas, VA) at 37°C and 5% $CO_2$. 293T cells were plated 24 h prior to transfection, which was performed using GeneCellin (GC5000, BioCellChallenge, Toulon, France) according to the manufacturer's protocol. For all analysis, 1 μg of each indicated ERAD substrate was used per p60 dish. When p97WT, p97QQ or Hrd1C291S was co-expressed, 1.5 μg of each plasmid was used and an equal amount of empty pcDNA3.1 vector was used in the control samples. When PDIA6 or ERdj5 was co-expressed, 2 μg of the plasmid was used. The P3U.1 murine plasmacytoma cells, which naturally synthesize the NS1 κ LC, were grown in complete DMEM supplemented with 55 μM 2-mercaptoethanol (21985023, Gibco, Grand Island, NY) at 37°C and 5% $CO_2$. The Ag8.653 chain-loss variant cell line was grown in the same conditions and was used as a negative control for experiments with P3U.1 cells.

## Metabolic labeling and immunoprecipitation experiments

Twenty-four hours after transfection, cells were pre-incubated at 37°C for 30 min in 2 ml media consisting of 1x DMEM without Cys and Met ($Cys^-/Met^-$) (17-204CI, Corning), which was supplemented with 1% L-glutamine and 10% FBS dialyzed against PBS to deplete amino acids. Cells were labeled with Express [$^{35}S$] Labeling Mix (NEG072-007, PerkinElmer) for 15 min. After labeling, culture dishes were placed on ice, washed once with 2 ml cold DPBS (21–031-CV, Corning), and cells were re-incubated in 2 ml of chase media (complete DMEM supplemented with 2 mM each of unlabeled methionine (M5308, Sigma) and cysteine (C7352, Sigma). For the NS1-N157 deglycosylation experiments, cells were pre-incubated in 10 μm MG132 for 2 h and 15 min before starving. The starving, labeling and chase media all contained 10 μm MG132. Zero time points were lysed immediately in Nonidet P-40 lysis buffer (NP-40: 50 mM Tris/HCl pH 7.5, 150 mM NaCl, 0.5% Nonidet P40, 0.5% sodium deoxycholate, 0.1 mM PMSF, 1X complete protease inhibitor tablets without EDTA), and all other plates were returned to 37°C for the indicated time points. Lysates were clarified by centrifugation at 18,000 g and incubated with goat anti-mouse κ (SouthernBiotechonology) overnight at 4°C on a rotator. Protein A agarose beads (CA-PRI-0100, Repligen) were added for an hour the following morning. After washing the beads 3 times with Nonidet P-40 wash buffer (NP-40 lysis buffer with 400 mM NaCl), proteins were eluted with 2x sample buffer at 95°C. 30% of immunoprecipitated proteins were electrophoresed on polyacrylamide gels and transferred to PVDF membranes. Dry membranes were exposed to BAS storage phosphor screens (Cytiva, 28956475) and scanned using a phosphor imager (Typhoon FLA 9500 GE Healthcare) to detect signals. Signals were quantified with the ImageQuant TL software (Cytiva). Non-transfected cells were used to subtract any background signal from the samples.

## Western blot analysis

Clarified NP40-solubilized lysates were mixed with reducing sample buffer (1:1), and samples were separated on 13% SDS-polyacrylamide gels for nearly all analyses. Exceptions include studies to determine the oxidation status of our substrates in which 15% gels were used, and the Proteinase K digestion and pulse-chase experiments where 12% gels were used. Post-electrophoresis, proteins were transferred to PVDF membranes (IPFL00010, Millipore). Membranes were fixed with methanol, blocked with gelatin wash buffer, and incubated overnight with the indicated primary immune reagents in blocking buffer followed by species-specific secondary reagents, also in blocking buffer. Western blots with HRP-conjugated secondary antibodies were developed using the Pierce™ ECL (32106, Thermo Fisher Scientific, Waltham, MA), and for quantitative analysis they were scanned with the LI-COR Fc Odyssey scanner (LI-COR, Lincoln, NE). When secondary antibodies conjugated to IRDye680 or IRDye800 (Li-COR) were employed, protein bands were detected using the LI-COR Odyssey CLx Imager (LI-COR Biosciences). Analysis and quantification were performed with the Image Studio Lite software. For experiments where the oxidation status of clients was studied, cells were lysed in complete NP-40 buffer additionally supplemented with 20 mM NEthylmaleimide (NEM; E3876-5G, Sigma-Aldrich, St. Louis, MO).

For co-immunoprecipitation-coupled western blot experiments, $3 \times 10^6$ P3U.1 (κ LC expressing) or Ag8.653 ($Ig^-$) cells were used. To detect association of proteins, cells were incubated with a membrane-permeable cross-linking agent prior to lysing as described previously (Meunier et al., 2002). Briefly, cells were washed and resuspended in cold Hepes buffer (25 mM Hepes-KOH, pH 8.3 and 125 mM KCl). A 5 mg/ml solution of 3,3′-Dithiodipropionic acid di (N-hydroxysuccinimide ester) (DSP) (Sigma-Aldrich), was freshly prepared in DMSO and added to the cells to achieve a final concentration of 150 μg/ml. Cells were incubated on ice for 1h with occasional shaking. After quenching with 100 mM glycine final concentration, cells were lysed in RIPA buffer (10 mM Tris/HCl pH 7.5, 150 mM NaCl, 1% Nonidet P40, 0.2% sodium deoxycholate, 0.1% SDS, 0.1 mM PMSF, 1X complete protease inhibitor tablets without EDTA). LCs were immunoprecipitated overnight by incubating with anti-κλ-conjugated agarose beads (custom made by SouthernBiotech using their antibodies 1050–01 and 1060–01). LCs and associated proteins were eluted from the beads with 2x sample buffer, electrophoresed, and interacting proteins were analyzed by western blotting.

## Antibodies

The following antibodies were used for blotting: polyclonal goat anti-mouse κ LC (1050–01, SouthernBiotech); mouse anti-GAPDH (MAB374, Millipore); mouse anti-Hsc70 (B-6) (sc-7298, Santa Cruz Biotechnology), mouse anti-VCP/p97 (ab11433, abcam, Cambridge, MA), mouse anti-20S proteasome subunit alpha (C8) (PW8110, Biomol, Hamburg, Germany), rabbit anti-PSMC2 (HPA019238, Sigma-Aldrich), mouse anti-actin (A5441, Sigma-Aldrich), rabbit anti-PDIA6 (NBP157999, Novus Biologicals). HRP-conjugated antibodies were used at 1:10,000 dilution and include goat anti-rabbit (sc-2054), donkey anti-goat (sc-2020), and goat anti-mouse (sc-2031) all purchased from Santa Cruz Biotechnology. The rabbit anti-ERdj3 antibody was produced in our lab (Shen and Hendershot, 2005). IRdye® secondary antibodies (LI-COR Biosciences, all 1:20,000): goat anti-mouse IgG (925–32210), goat anti-rabbit IgG (925–68071), and donkey anti-goat IgG (926–68074).

## Cycloheximide chase and deglycosylation experiments

For cycloheximide (CHX) and/or MG132 chase experiments, cells were treated with 10 μM MG132 or 100 μg/ml CHX for the indicated times. The cells were lysed in 0.5 ml of NP40 lysis buffer, clarified by centrifugation at 18,000 × g for 15 min, and 1.5% of the resulting lysate was analyzed by western blotting. To remove N-linked glycans from the NS1 glyco-mutant constructs, we treated samples with Endo H (P0702L, NEB) according to the manufacturer's protocol. Samples were mixed with 2x Laemmli sample buffer and analyzed by western blotting.

## Assessment of disulfide bond content

To monitor the oxidation status of the various proteins, cells expressing the constructs of interest were washed twice with PBS containing 20 mM NEM (E3876-5G, Sigma-Aldrich) and lysed in 0.5 ml NP-40 supplemented with 0.1 mM PMSF, 1X complete protease inhibitor tablets without EDTA and 20 mM NEM.

## Concanavalin A binding experiments

Concanavalin A (Con A) beads (AL-1003, VECTOR LABORATORIES, Burlingame, CA) were used to separate glycosylated and non-glycosylated species. 293T cells were grown in p60 dishes and transfected with the mono-glycosylated NS1 client (NS1-N100). After 24 h, the cells were incubated with 10 μM MG132 in DMSO or in an equal volume of DMSO alone as a control for 3.5 h and were then lysed in 0.5 ml of NP-40 lysis buffer supplemented with 1 mM $CaCl_2$, 1 mM $MgCl_2$, 1 mM $MnCl_2$, 0.1 mM PMSF and 20 mM NEM. Clarified lysates were incubated overnight at 4°C with 2:1 v/v Con A bead slurry. Beads were centrifuged (500 × g for 5 min) and the supernatant (unbound) was collected and mixed with an equal volume of 2x non-reducing Laemmli buffer for analysis of the non-glycosylated proteins. The glycosylated proteins (bound) were eluted from the beads with a volume of 1x non-reducing Laemmli buffer equal to the total volume of the non-bound sample. The resulting pools were analyzed by western blotting.

## Partial proteolysis

Stability of indicated proteins was assessed by partial proteolysis experiments. Cells expressing the indicated constructs were lysed in 0.5 ml NP-40 devoid of protease inhibitors and PMSF. Proteinase K (V302B, PROMEGA, Madison, WI) was added to a final concentration of 20 μg/ml. Digestion was performed on ice for 25 min and was followed by a 5 min incubation with PMSF (5 mM final concentration) (Sigma) to inactivate the Proteinase K. An equal volume of 2x Laemmli sample buffer was added to samples, which were heated to 95°C for 5 min and immediately loaded onto SDS-PAGE gels for western blotting. To determine the glycosylation status of the Proteinase K resistant fragments, the samples were treated with Endo H. At the end of this reaction 2x Laemmli buffer was added, and samples were immediately analyzed by western blotting.

## Mass spectrophotometer analysis

P3U.1 and Ag8.653 cells ($1.5 \times 10^6$ of each) were incubated with 10 μM MG132 or DMSO for 3.5 h and lysed in NP40 lysis buffer. LCs were isolated by immunoprecipitated overnight with anti-mouse-κλ-conjugated agarose beads (custom made by SouthernBiotech using their antibodies 1050–01, and 1060–01) and washed 3 times in NP40 lysis buffer made to 400 mM NaCl. Beads were resuspended in 20 μL of 2x Lammeli buffer with 2-β mercaptoethanol and heated to 95°C for 5 min. Solubilized proteins were loaded on a precast 4–15% gradient gel (BioRad) and run 1 cm into the gel. The gel was then incubated for 1 h in GelCode-Blue (Thermo Scientific), destained overnight in ultrapure $H_2O$ at room temperature, and transferred to our Center for Proteomics and Metabolomics core for proteome profiling by spectral counting.

The stained portion of the gel was cut into small pieces and reduced with dithiothreitol to ensure complete breakage of disulfide bonds. Cysteine residues were alkylated by iodoacetamide to allow the recovery of Cys-containing peptides. The gel segment was washed, dried in a speed vacuum, and rehydrated with a buffer containing trypsin and incubated overnight. The next day the digested samples were acidified, and the peptides were extracted multiple times. The extracts were pooled, dried, and reconstituted in a small volume. The peptide samples were loaded on a nanoscale capillary reverse phase C18 column by a HPLC system (Thermo EasynLC 1000) and eluted by a gradient (~60 min). The eluted peptides were ionized by electrospray ionization and detected by an inline mass spectrometer (Thermo Elite). The MS spectra were collected first, and the 20 most abundant ions are sequentially isolated for MS/MS analysis. This process is cycled over the entire liquid chromatography gradient. Database searches were performed using the Sequest search engine in our in-house SPIDERS software package. All matched MS/MS spectra were filtered by mass accuracy and matching scores to reduce protein false discovery rate to ~1%. Finally, all proteins identified in one gel lane were combined.

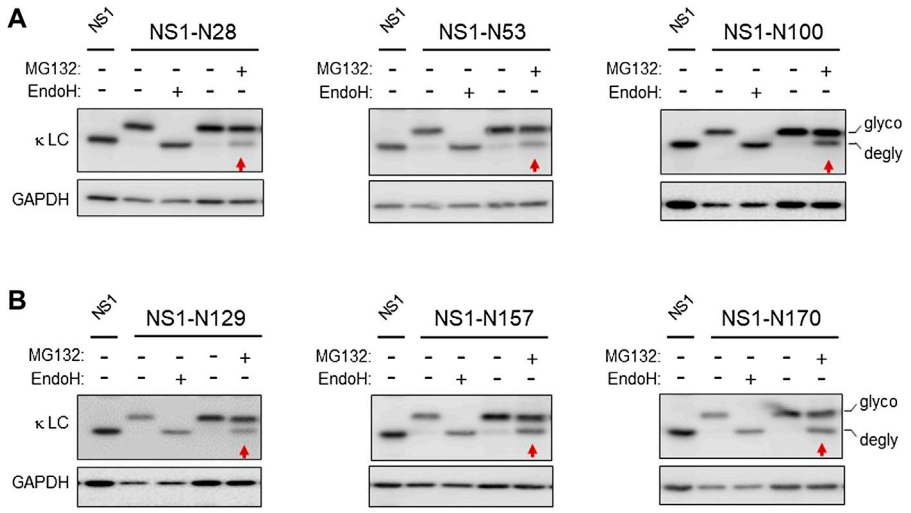


FIGURE 1
The well-folded domain in NS1 does not impede retrotranslocation. **(A)** Cells were transfected with the indicated NS1 constructs bearing a single N-linked glycan on the $V_L$ domain, and 24 h later cell lysates were prepared. Lysates were treated with (+) or without (-) Endo H to identify mobility of the deglycosylated and non-glycosylated forms of these constructs. In each case, the parental, non-glycosylated NS1 was used as a control for the mobility of the non-glycosylated form of NS1. One dish each of cells expressing the indicated glycosylated constructs were incubated with 10 μM MG132 (+) or DMSO control (-) for 3.5 h prior to lysis. Lysates were prepared, and one sample was digested with Endo H (+) as a control for mobility of the unglycosylated protein, and then samples were analyzed by SDS-PAGE-coupled western blotting with a goat anti-mouse κ antisera. Red arrows point at the deglycosylated (DG) species in each panel. **(B)** Cells were transfected with the indicated NS1 glycosylated constructs bearing a single glycan on the $C_L$ domain alone and processed as in **(A)**. Non-glycosylated NS1 was used as a control for the mobility of the non-glycosylated form of NS1. In all cases, GAPDH was used as a loading control.

# Results

## The well-folded kappa $C_L$ domain is completely retrotranslocated across the ER membrane after proteasome inhibition

The non-glycosylated NS1 κ light chain has been the focus of multiple ERAD studies (Knittler et al., 1995; Skowronek et al., 1998; Shimizu et al., 2010). Unlike most Ig light chains, it is not secreted in the absence of its partner heavy chain, due to a $V_L$ domain that does not fold stably. However, its $C_L$ domain folds well, forms its intrachain disulfide bond, and can stimulate the folding of the $C_H1$ domain of a γ heavy chain leading to the secretion of a properly antibody (Lee et al., 1999; Vanhove et al., 2001). To determine if the $C_L$ domain impeded transport across the ER membrane for degradation, we made use of the fact that N-glycanase 1 is present on the cytosolic side of the retrotranslocon and serves to deglycosylate ERAD clients as they emerge from the retrotranslocon (Suzuki et al., 2016). We engineered a single glycan acceptor sequence at three distinct sites within the unfolded $V_L$ domain (Supplementary Figure S1A). This domain becomes ubiquitinated at multiple sites when the proteasome is inhibited, (Okuda-Shimizu and Hendershot, 2007; Shimizu et al., 2010), making it likely that the VL domain enters the retrotranslocon first. Each of the N-linked glycan consensus sites engineered in the $V_L$ domain was readily glycosylated, as shown by comparing the migration of each mutant with the parental NS1 and by Endo H treatment, which cleaved the glycans and restored mobility to that of the non-glycosylated NS1. Inhibition of proteasomal activity with MG132 treatment resulted in a pool that was deglycosylated, even in the case of the NS1-N100 construct, which had the glycan positioned at the $V_L$:$C_L$ boundary (Figure 1A), revealing that the entire $V_L$ domain must reach the cytosol. We next engineered sites in the $C_L$ domain and were careful to choose positions within loops of the well-characterized Ig fold, as glycans at these positions should be less likely to interfere with domain folding (Supplementary Figure S1B). All sites were glycosylated and treatment with MG132 also resulted in deglycosylation of a similar amount of each of these modified NS1 constructs (Figure 1B). This indicated that even the well-folded $C_L$ domain, which is not ubiquitinated when the proteasome is inhibited, was fully retrotranslocated to the cytosol.

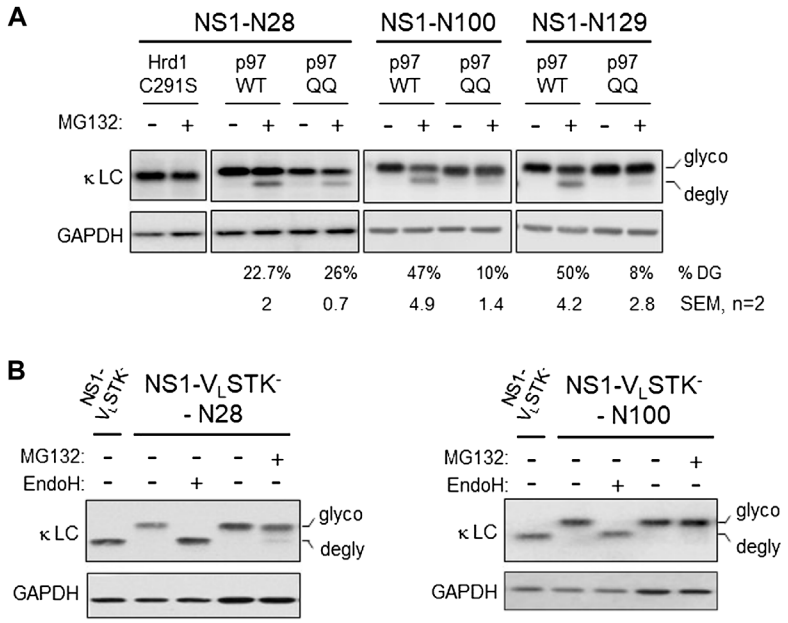


FIGURE 2
Retrotranslocation of NS1 does not require proteasomal activity but is dependent on ubiquitination and p97. **(A)** Cells were co-transfected with NS1-N28, NS1-N100, or NS1-N129 encoding constructs together with either p97 WT or ATPase inactive p97QQ mutant. The next day, a plate of each was incubated with either 10 μM MG132 (+) or DMSO (- control) for 3.5 h prior to lysis. Lysates were prepared and analyzed by SDS-PAGE coupled western blotting with goat anti-mouse κ antisera or GAPDH as a control. The percent deglycosylation was determined as the fraction of the total amount of LC and is indicated below each lane along with the calculated SEM, $n = 2$. **(B)** Cells were transfected with the NS1-$V_L$STK$^-$ construct or NS1-$V_L$STK$^-$ engineered with a single N-linked glycan on the $V_L$ domain at N28 or N100. Prior to lysis, one dish of each glycosylated construct was incubated with MG132 (+). Lysates were prepared and one sample of each glycosylated construct was treated with Endo H (+) as indicated. Samples were analyzed as in Figure 1.

## Deglycosylation is dependent on ERAD substrate ubiquitination and retrotranslocation

Each of the engineered constructs led to nearly complete glycosylation, leading us to conclude the unglycosylated pool present with proteasome inhibition was due to deglycosylation of the pool that was retrotranslocated. Nonetheless, we explored the possibility that the more rapidly migrating band observed was in fact due to MG132 stabilizing a population that never entered the ER but was normally rapidly degraded. Cycloheximide chase experiments were conducted on cells expressing the NS1-N129 construct (Supplementary Figure S2). There was no evidence the more rapidly migrating form appeared with cycloheximide treatment alone. In contrast, when cells were treated with both cycloheximide and MG132 the glycosylated form began to disappear over time, while the deglycosylated form appeared, demonstrating a precursor-product relationship. We next queried whether retrotranslocation, as measured by deglycosylation, was dependent on both ubiquitination and p97 activity. We chose three constructs including one with the engineered glycosylation site present in the $V_L$ domain (N28), one at the boundary between the two domains (N100), and one in the $C_L$ domain (N129). Co-expression of a domain negative Hrd1 mutant (C291S) inhibited deglycosylaton of the NS1-N28 protein (Figure 2A). These constructs were co-expressed with either wild-type p97 or a dominant negative mutant (QQ) and the effects on deglycosylation of monoglycosylated NS1 proteins was examined when the proteasome was inhibited. Although the mutant p97 inhibited deglycosylation, and thus retrotranslocation, of the N100 and N129 constructs, it had very little effect on the N28 construct. This implies that the $V_L$ domain of the NS1 protein can be transported at least this far into the cytosol before the activity of p97 is required to extract this ERAD client.

The lack of client deglycosylation observed with co-expression of the dominant negative Hrd1C291S mutant strongly suggested that ubiquitination was required for retrotranslocation. However, there is evidence that auto-ubiquitination of Hrd1 is critical to its activity in client dislocation *in vitro* (Baldridge and Rapoport, 2016). Hence, we examined a variant of the NS1 LC that cannot be ubiquitinated due to mutation of all lysines, serines, and threonines in the $V_L$ domain (NS1-$V_L$-STK$^-$); the well-folded $C_L$ domain is left intact and is not ubiquitinated (Shimizu et al., 2010). A single glycosylation site was engineered near the

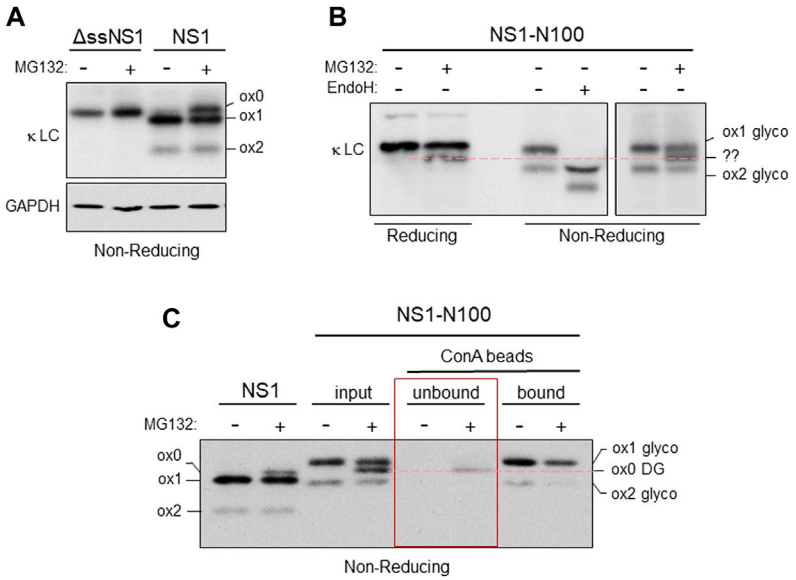


FIGURE 3
Both domains are reduced in the retrotranslocated NS1 protein. **(A)** Cells were transfected with either the cytosolically expressed ΔssNS1 or NS1. After 24 h, cells were treated with (+) or without (-) MG132, and cell lysates were prepared in NP-40 buffer containing NEM. Samples were analyzed by non-reducing SDS-PAGE-coupled western blotting with goat anti-mouse κ antisera. Migration of the various oxidation species (ox0, ox1, ox2) is indicated. **(B)** Cells expressing NS1-N100 were treated with (+) or without (-) MG132 for 3.5 h prior to lysis. Lysates were prepared and analyzed under reducing or non-reducing conditions as indicated. A portion of the lysate from cells not treated with MG132 was digested with Endo H (+) to determine the migration of the deglycosylated ox1 and ox2 species. An unidentified species (??) generated by proteasomal inhibition observed on non-reducing gels that co-migrated with reduced, deglycosylated NS1-N100 is indicated with a red dotted line. **(C)** 293T cells expressing NS1-N100 were incubated with MG132 (+) or DMSO (-). Cells were lysed in NP-40 lysing buffer supplemented with NEM, and a portion of each was kept as an input. The remaining lysate was absorbed with Con A-conjugated beads. Equivalent fractions of the Con A-unbound and the sample was eluted from the Con A beads (bound) were analyzed by SDS-PAGE conducted under non-reducing conditions and blotted with anti-κ antisera. Bands corresponding to the various redox states are indicated as is their glycosylation status. A red dotted line indicates the species generated by proteasomal inhibition observed panel B is in fact fully reduced and non-glycosylated.

N-terminus of the unfolded $V_L$ domain (N28), and a separate one was introduced near the C-terminus of this domain (N100). In this case, inhibition of the proteasome did not lead to the appearance of a significant amount of the deglycosylated form of either NS1-$V_L$-STK$^-$ construct (Figure 2B). Thus, client ubiquitination was indeed required for it to be recognized by cytosolic factors, like p97, and pulled far enough into the cytosol for the glycan at N28, or any subsequent glycans, to become accessible to N-glycanase 1.

## Retrotranslocated $C_L$ domain is reduced

Under steady state conditions, the NS1 protein populates a form in which both domains are oxidized (ox2), and a partially oxidized (ox1) form, in which only the $C_L$ domain possesses a disulfide bond (Knittler et al., 1995; Skowronek et al., 1998). The presence of the intramolecular disulfide bond can be detected by increased mobility on non-reducing SDS polyacrylamide gels (Braakman et al., 1992). To determine the redox state of NS1 after proteasome inhibition, we engineered a NS1 κ LC that was devoid of the ER targeting signal sequence (ΔssNS1), which would be synthesized in the cytosol, to serve as a control for the mobility of a completely reduced NS1 protein. When both the ΔssNS1 and the parental NS1 were electrophoresed on the same SDS polyacrylamide gel under non-reducing conditions, we found that in the absence of MG132 NS1 populated two redox forms (ox1 with an oxidized $C_L$ domain and ox2 possessing disulfide bonds in both the $V_L$ and $C_L$ domains), which is consistent with previously reported data (Skowronek et al., 1998). However, when the proteasome was inhibited, we observed an additional slower migrating band that co-migrated with the completely reduced ox0 form observed with the cytosolically expressed ΔssNS1 construct (Figure 3A). This revealed that inhibition of proteasomal degradation generated a pool of NS1 in which both the $V_L$ and $C_L$ domains were fully reduced. As the fraction of NS1 that was deglycosylated upon proteasomal degradation was similar to the amount that became fully reduced, it was likely that they represented the same pool. To test this directly, we chose the NS1-N100 construct with the single engineered N-glycan in the $V_L$ domain. Proteasome inhibition resulted in the appearance of the deglycosylated

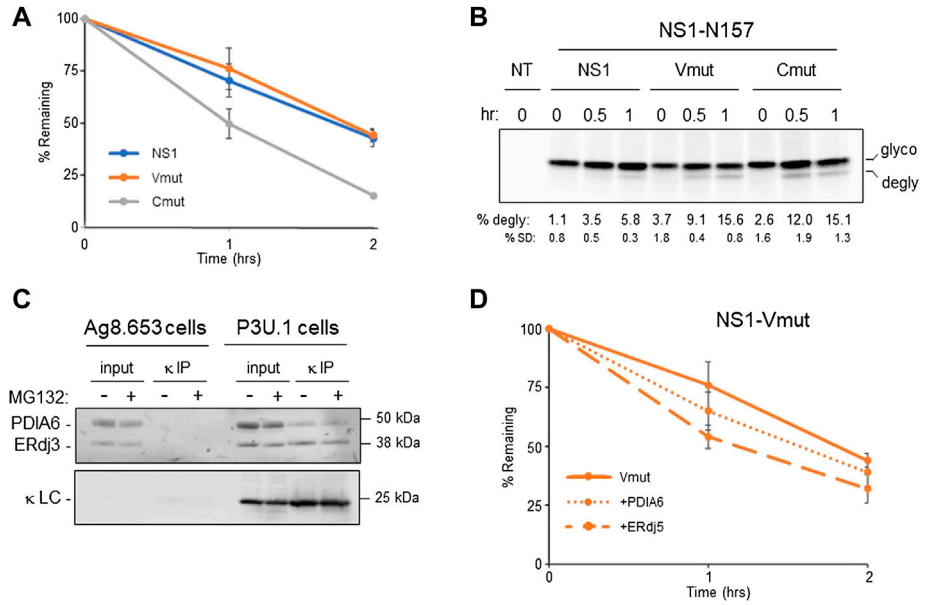


FIGURE 4
Reduction of the $C_L$ domain is a rate-limiting step in retrotranslcoation and degradation. **(A)** Cells expressing parental NS1 or a mutant in which $V_L$ (Vmut) or $C_L$ (Cmut) cysteines were substituted with serines were pulse-labeled for 15 min and chased as indicated. LC was isolated by immunoprecipitation, electrophoresed, and quantified by Phosphorimaging $n = 4$ for NS1, and $n = 3$ for the $V_L$ and $C_L$ mutants. Error bars show standard deviation. **(B)** Cells expressing parental NS1-N157 or constructs in which the $V_L$ or $C_L$ cysteines were substituted were pulse-labeled for 15 min and chased for the indicated times. As MG132 was included in the chase media, cells were incubated with MG132 for between 3 and 4 h prior to lysis depending on the time point harvested. Non-transfected (NT) cells were used to subtract background signals. Percent deglycosylation and standard deviation (SD) are shown below, $n = 4$. **(C)** Ag8.654 ($Ig^-$) and P3U.1 ($\kappa^+$) cells were incubated with MG132 (+) or DMSO (-). Prior to lysis, cells were crosslinked with DSP to retain protein:protein interactions. Lysates were prepared, a portion was removed for input, and the remainder was immunoprecipitated with polyclonal anti-κ. Samples were analyzed by reducing SDS-PAGE-coupled western blotting with rabbit anti-PDIA6, rabbit anti-ERdj3, and goat anti-κ. **(D)** The NS1-Vmut was expressed alone or co-expressed with PDIA6 or ERdj5. Cells were pulse-labeled for 15 min and chased as shown. Lysates were prepared, immunoprecipitated with anti-κ and analyzed as in **(A)**, $n = 3$ for $V_L$ mutant alone and $n = 4$ for Vmut + PDIA6 and Vmut + ERdj5.

form when the protein was analyzed under reducing conditions, and the non-MG132 treated sample separates into the ox1 and ox2 forms on non-reducing gels. Endo H treatment increased the mobility of both species, demonstrating that both were glycosylated. When NS1-N100 isolated from non-treated and MG132-treated cells was separated under non-reducing conditions, we observed a third species that migrated between the ox1 and ox2 isoforms found it the proteasome inhibited cells, but slightly slower than the deglycosylated ox1 form generated by Endo H treatment (Figure 3B). To determine if this new species represented reduced and deglycosylated NS1-N100 protein, the glycosylated pool was separated from the deglycosylated one by incubation with Concanavalin A (Con A)-conjugated beads. The Con A lectin binds N-linked glycans, allowing the glycosylated form of the protein to be readily isolated by centrifugation, leaving the deglycosylated form in the supernatant. All samples were electrophoresed under non-reducing conditions and the parental non-glycosylated NS1 was used as a control. The new species observed in proteasome-inhibited cells expressing NS1-N100 co-migrated with the ox0 form of non-glycosylated NS1 and did not bind to Con A (Figure 3C), demonstrating that the new band appearing upon MG132 treatment was deglycosylated and fully reduced.

## Reduction of the $C_L$ domain represents a significant rate-limiting step in degradation and retrotranslocation of a κ LC

The accumulation of a completely reduced species of NS1 upon inhibition of the proteasome led us to determine how much the reduction of each domain represented an impediment to the retrotranslocation and degradation of this ERAD client. We genetically ablated the disulfide bonds in the $V_L$ domain and in the $C_L$ domain separately by mutating the two cysteines in each domain to serines (Supplementary Figure S4A) and quantified the effect on the turnover of both constructs using pulse-chase experiments. Although disruption of the disulfide bond in the V domain had very little effect on the half-life of this mutant, disruption of the bond in the C domain significantly increased its turnover (Figure 4A). This revealed that breaking

TABLE 2 Identification of proteins associated with NS1.

| References | SC neg cntrl | SC -MG132 | SC + MG132 |
|---|---|---|---|
| ER chaperones | | | |
| GRP78 | 2 | 151 | 109 |
| GRP94 | 0 | 5 | 2 |
| NS1 LC | 0 | 51 | 41 |
| CALX | 0 | 5 | 0 |
| PDIA6 | 0 | 2 | 0 |
| cyto chaperones | | | |
| HSP7C | 3 | 26 | 44 |
| BAG6 | 0 | 0 | 21 |
| UBA52 | 0 | 0 | 53 |
| UPS | | | |
| PSA6 (α-core) | 0 | 0 | 2 |
| PSA7 (α-core) | 0 | 0 | 2 |
| PRS7 (base) | 0 | 0 | 2 |
| PRS4 (base) | 0 | 0 | 2 |
| Cullin-9 | 0 | 0 | 2 |

the disulfide bond in the C domain represented a rate-limiting step in the degradation of NS1. In an attempt to determine if this rate-limiting step occurred at the point of retrotranslocation, we employed constructs with a glycan engineered at N157 for the parental NS1 and each of the two domain disulfide mutants. Pulse-chase experiments revealed the glycosylated forms of all three constructs turned over somewhat faster than their non-glycosylated counterparts, perhaps due to their interaction with the lectin chaperones instead of the BiP chaperone complex. Additionally, the glycosylated Vmut possessed a shorter half-life than the glycosylated protein with both disulfide bonds intact, but disruption of the disulfide bond in the constant domain continued to have a greater effect on the turnover of NS1 (Supplementary Figure S4B). MG132-treated cells expressing these monoglycosylated clients were pulse-labeled and shorter chase periods were monitored to catch early time points in retrotranslocation. In keeping with the half-lives of these glycosylated proteins, genetic disruption of the disulfide bond in either domain led to faster retrotranslocation, as judged by deglycosylation, than the NS1 construct possessing both disulfide bonds, whereas differences between the two disulfide mutants was marginal (Figure 4B).

In an attempt to identify the PDI family member(s) responsible for reducing the disulfide bonds in NS1, we used the P3U.1 mouse plasmacytoma cells, which is the source of the NS1 construct used in our studies thus far (Yelton et al., 1978) and the Ag8.653 cells (Kearney et al., 1979), a LC loss variant of P3U.1, as a negative control. P3U.1 cells have been used in multiple studies to examine ERAD requirements for this LC (Knittler et al., 1995; Okuda-Shimizu and Hendershot, 2007). The κ LC were isolated by immunoprecipitation and subjected to mass spectrometric spectral count analysis (Supplementary File S1). Several ER chaperones were identified with the LC, including BiP and GRP94 in keeping with previous reports (Melnick et al., 1992), but since chemical cross-linking was not used to stabilize labile interactions, co-chaperones like ERdj3 or other components of the BiP chaperone complex (Meunier et al., 2002) were not identified. PDIA6 was the only PDI family member found to be associated with NS1 (Table 2 and Supplementary File S1) and has been reported to have reductase activity (Gorasia et al., 2016). To confirm this finding, lysates from P3U.1 and Ag8.653 cells were treated with the cleavable, cross-linking agent DSP, and proteins association with the NS1 κ LC were analyzed by immunoprecipitation-coupled western blotting. Membranes were blotted with antibodies specific for PDIA6, ERdj3 as a positive control, and mouse κ LC (Figure 4C). PDIA6 was detected with the LC in P3U.1 cells, but it was not isolated from κ LC-negative Ag8.653 cells. To determine if PDIA6 was responsible for reducing the $C_L$ domain, we expressed the Vmut (possessing only an oxidized C domain) alone or co-expressed it with either PDIA6 or ERdj5, another PDI family member with reductase activity, and performed pulse-chase experiments (Figure 4D). PDIA6 had a modest effect on enhancing the turnover of the NS1 Vmut, but ERdj5 had a greater effect, even though it was not detected in the spectral counts data (Supplementary File S1) or by western blotting (not shown). We also tested the effects of PDIA6 and ERdj5 co-expression on the half-life of the Cmut. PDIA6 had no effect on the turnover rate of Cmut, in keeping with the fact that genetic ablation of the disulfide bond in the $V_L$ domain did not change the half-life of the non-glycosylated NS1 LC (Supplementary Figure S4C). Somewhat unexpectedly, co-expression of ERdj5 actually decreased the turnover of the Cmut.

## The retrotranslocated, deglycosylated, and fully reduced NS1 $C_L$ domain retains structure in the cytosol

A previous *in vitro* study found that reduction of a recombinant $C_L$ domain did not significantly alter its structure (Feige et al., 2007). To determine if the fully reduced species of NS1 expressed in cells still possessed structure, lysates from non-treated or MG132-treated cells expressing the parental NS1 construct were incubated with limiting concentrations of Proteinase K to distinguish between unstructured and structured domains. Samples were electrophoresed on 12% acrylamide gels to resolve fragments of 10–12 kDa. Proteinase K digestion of NS1 from non-MG132-treated lysates (control) yielded a single, readily detectable band migrating with an apparent molecular weight of ~12 kDa. Importantly, the anti-κ antisera is specific for the constant region, which is consistent with this small fragment representing a complete, well-folded $C_L$ domain in which the

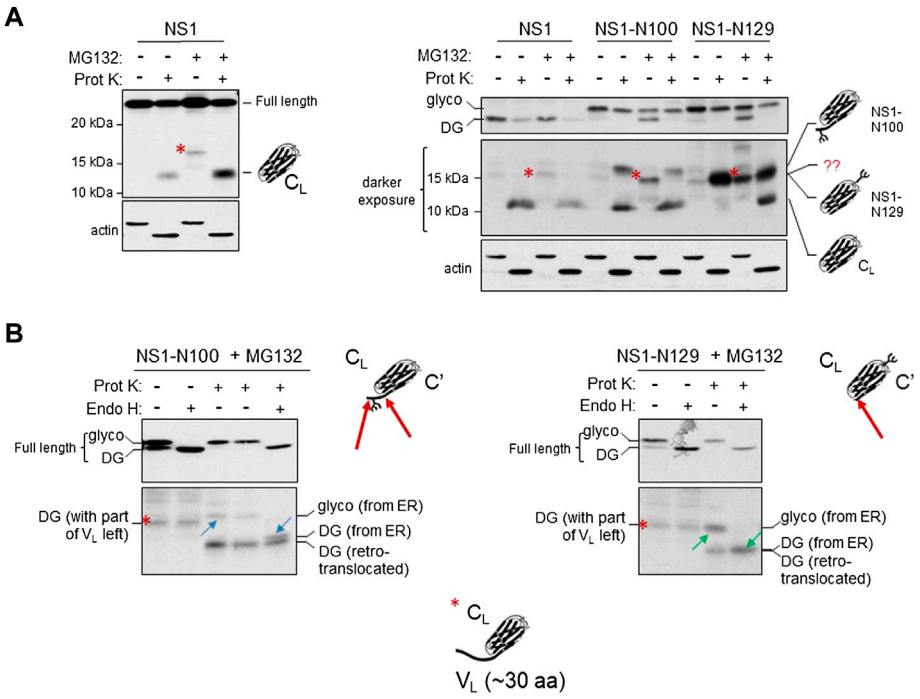


FIGURE 5
The retrotranslocated and deglycosylated $C_L$ domain maintains structure as indicated by resistance to Proteinase K digestion. **(A)** Cells were transfected with parental NS1, NS1-N100 or NS1-N129 and incubated with (+) or without (-) MG132 for 3.5 h prior to lysis. Lysates were treated with (+) or without (-) Proteinase K as described in Materials and Methods and analyzed by western blotting with anti-κ antisera. On the left, analysis of parental NS1 is shown alone, and on the right together with the two glycosylated constructs. Migration of full-length NS1 is shown in the top on right, whereas a longer exposure of the fragments generated is below. A MG132-generated fragment present with all three constructs is indicated with a red asterisk. The deduced identity of the various fragments based on data in **(B)** are portrayed with cartoon schematics. **(B)** Cells expressing the indicated glycosylated constructs were incubated with MG132 prior to lysis. Lysates were treated either with (+) or without (-) Proteinase K, and then split to allow subsequent digestion with Endo H (+) for one half and left undigested (-) for the other half as a control. The altered mobility of fragment pairs that were glycosylated and cleaved by Endo H are indicated with blue arrows for NS1-N100 or green arrows for NS1-N129. Schematic representations of Proteinase K cleavage of both proteins are shown with a red arrow on the schematic. Fragment identities and their source are indicated.

unstable $V_L$ domain had been digested (Figure 5A). When the MG132-treated sample was examined without Proteinase K treatment, we detected a band that migrated somewhat slower than an isolated $C_L$ domain (red asterisk). Proteinase K treatment of the lysate from MG132-treated cells resulted in the disappearance of this band and the appearance of an ~12 kDa band that co-migrated with the band generated in the Proteinase K treated cells in which the proteasome had not been inhibited.

Using this construct, it was not possible to establish if the protected $C_L$ band arose only from the ox1 form, which would have been in the ER lumen possessing the intramolecular disulfide bond in the $C_L$ domain, or if it also included the retrotranslocated and fully reduced ox0 isoform. To distinguish between these possibilities, we similarly examined lysates from two of the NS1 constructs possessing a single N-linked glycan; the NS1-N100 with an engineered glycan very near the C-terminus of the $V_L$ domain and the NS1-N129 with the glycan position in a loop in the $C_L$ domain. For the NS1-N100 construct, treatment of the control (no MG132) sample with Proteinase K produced two anti-κ-reactive fragments; both of which must originate from ER localized, glycosylated protein, as this is the only form present without proteasome inhibition (Figure 5A). One of these co-migrated with the Proteinase K protected fragment in the parental non-glycosylated NS1 protein. This likely represented an unglycosylated $C_L$ domain generated by proteolytic cleavage at the $V_L$:$C_L$ boundary just C-terminal of the glycan, however, the source of the slower migrating fragment was not immediately clear (Figure 5A). The same two species were present after Proteinase K digestion of MG132-treated cells, and the non-Proteinase K digested lysate from proteasome-inhibited cells again produced a fragment similar to that found with the parental NS1 protein (red asterisk). For the NS1-N129 construct, a single fragment was produced with protease digestion of lysates from untreated cells (Figure 5A). It migrated faster than the slow migrating band observed in the NS1-N100 protein and co-migrated with the red asterisk band. MG132 treatment alone generated a similar ~15 kDa fragment as

observed with the NS1 and NS1-N100 proteins, and Proteinase K digestion of the MG132-treated samples produced two fragments, including one that co-migrated with the ~15 kDa band from the non-MG132 treated cells, and the other with the ~12 kDa band observed with NS1 and NS1-N100.

To determine the source of the various fragments generated in Figure 5A when MG132 treatment was combined with or without Proteinase K digestion, lysates were further digested with endoglycosidase H (Endo H) to remove the glycan if present. In the case of the NS1-N100 construct, Endo H treatment of the MG132 lysate that was not digested with Proteinase K demonstrated the fragment (red asterisk) was not glycosylated and therefore arose from a cytosolic pool of this protein (Figure 5B). Lysates from the proteasome-inhibited cells that had been treated with Proteinase K were further digested with Endo H. This revealed the slower migrating band (blue upward arrow) was glycosylated (derived from ER) but collapsed to a band slightly larger than the isolated $C_L$ domain (blue downward arrow), whereas the fastest migrating fragment in this sample was unglycosylated and thus represented the retrotranslocated protein that had been deglycosylated by N-glycanase and was digested by Proteinase K to an isolated $C_L$ domain. Thus, it appeared that the glycan engineered just 9 amino acids from the $V_L$:$C_L$ boundary partially interfered with complete proteolysis of the $V_L$ domain (indicated with two red arrows on the cartoon) giving rise to the doublet in the Proteinase K and Endo H treated sample.

When the NS1-N129 construct was similarly examined (Figure 5B), we again found that Endo H digestion of the sample from MG132 treated cells that was not treated with Proteinase K revealed that the MG132-generated fragment (red asterisk) was not glycosylated and therefore arose from a cytosolic pool of this protein. The Proteinase K-treated sample from this glycosylated construct had produced two fragments, and Endo H digestion revealed that the slowest migrating band (green upward arrow) was glycosylated and collapsed to the non-glycosylated faster migrating $C_L$ domain (green downward arrow) after the glycan was removed. In this case the position of the engineered glycan did not interfere with complete proteolysis of the $V_L$ domain. Furthermore, the glycosylated, isolated $C_L$ domain (green upward arrow) was shown to co-migrate with the MG132-generated fragment (red asterisk). Cartoon depictions of the composition of the various bands generated as deduced from the combinations of treatments are included in the figure and Supplementary Figure S5. Together, the data presented in this figure strongly indicated that the $C_L$ domain of the deglycosylated ox0 isoform generated after MG132 treatment still possessed significant structure in the cytosol, even though the disulfide bond had been reduced. Based on the molecular weight of the MG132-generated, non-glycosylated fragment recognized by anti-κ LC antisera we deduced that it must include ~30 amino acids of the $V_L$ domain in addition to the 105 amino acid $C_L$ domain and represents an intermediate in proteasomal degradation.

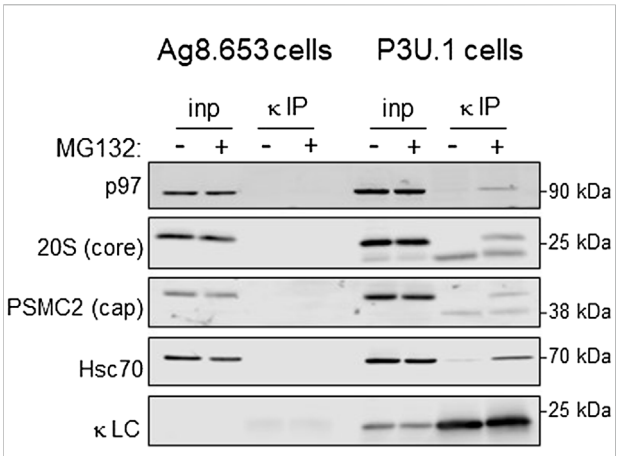


FIGURE 6
Proteasomal inhibition results in the association of retrotranslocated κ LCs with AAA-ATPase base and 20S core subunits. **(A)** P3U.1 ($κ^+$) and Ag8.653 ($Ig^-$) cells were incubated with MG132 (+) or DMSO (-) for 3.5 h. Prior to lysis, cells were crosslinked with DSP to retain protein:protein interactions. Lysates were prepared using RIPA buffer; a portion was removed for input, and the remainder was immunoprecipitated with anti-LC-conjugated agarose beads. Immunoprecipitated material (IP) and total lysate samples (input) were separated on reducing SDS-gels and analyzed by western blotting with an anti-p97, anti-20S proteasome core α subunit, anti-PSMC ATPase regulatory particle subunit, anti-Hsc70, or anti-κ LC.

## Retrotranslocated NS1 LC were associated with regulatory particle ATPases and core subunits of the proteasome when degradation was inhibited

To identify proteins that the retrotranslocated NS1 protein interacted with, we examined the spectral count data that was obtained with κ LC immunoprecipitated from the P3U.1 cells obtained with and without inhibition of the proteasome (Table 2 and Supplementary File S1). We identified several proteasome subunits associated with the LC only after MG132 treatment, including two core components of the 20S proteosome and two ATPase subunits of the proteasome regulatory particle. To validate this finding, anti-κ immunoprecipitated proteins were isolated from Ag8.653 and P3U.1 cells that were pre-treated with or without MG132 and processed for western blotting. We found that κ LCs associated with p97, regulatory subunit 7 (PSMC2) of the ATPase ring component of the proteasome cap, and the α7 subunit of the proteasome core when MG132 was used, but not in its absence, nor were they detected in anti-κ isolated material from the control Ag8.653 cells (Figure 6). In combination, these data indicate that a portion of the retrotranslocated NS1 LCs possessing a constant domain that retains structure are stably bound to the proteasome when its proteolytic activity was inhibited. Given the known dimensions of the proteasome (Rape and Jentsch, 2002), the distance from

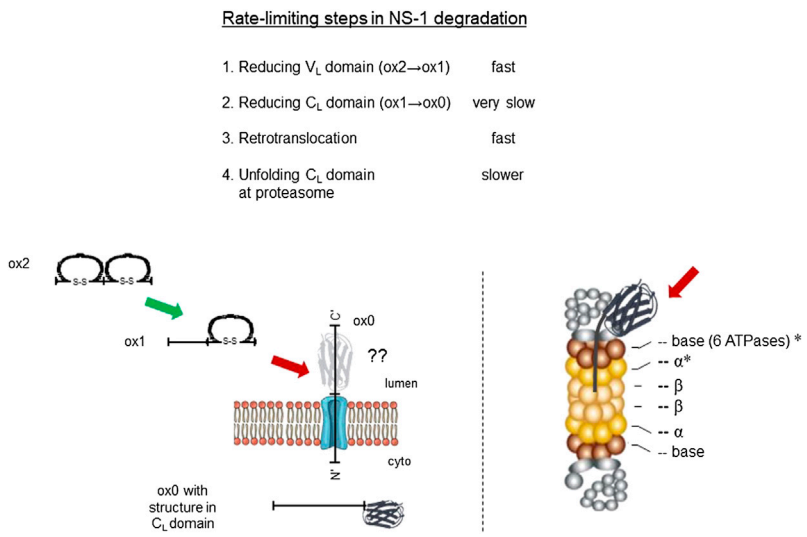


FIGURE 7
Identification of rate-limiting steps in NS1 degradation. Delineation of degradation steps revealed in this study and their relative rate of execution are shown at top. Schematic of steps in the reduction and retrotranslocation of NS1 on left, and the location of proteasomal subunits engaging the MG132-generated fragment are shown with asterisks on the right. Fast steps are indicated with a green arrow and slower ones with red arrows. The unknown conformation of the reduced $C_L$ domain as it passes through the retrotranslocon is portrayed in grey with a question mark.

the active proteolytic sites to the outside of the 20S core would require ~20 amino acids of an extended polypeptide chain and another 10–15 to cross the ATPase ring. The ~15 kDa anti-κ-reactive fragment that we observed in proteasome inhibited cells was calculated to possess ~30–35 additional amino acids of the $V_L$ domain, which would be sufficient to reach the proteolytic active site, indicating that unfolding of the structured $C_L$ domain by the ATPase ring of the proteasome represented a second rate-limiting step in the degradation of NS1 κ LCs (Figure 7).

## Discussion

Ig HC are expressed first in pre-B cells during B cell development, and the association of BiP with the unstructured $C_H1$ domain ensures the free HC are not secreted. Subsequently, LC rearrangement is initiated to produce a single LC that must induce folding of the $C_H1$ domain and release BiP, so the assembled Ig protein can be transported to the cell surface or secreted. This represents a critical checkpoint in both B cell development and in Ig assembly, and as such, LC genes have evolved to produce $C_L$ domains that fold very stably. The failure of a LC to rescue the free HC can initiate another round of LC gene rearrangements, necessitating the disposal of the LC produced first. Even once a compatible LC partner has been selected, the extremely high rate of antibody synthesis observed in plasma cells is likely to result in some failures in proper Ig maturation resulting in the need to target improperly folded subunits for degradation. The NS1 LC is an example of such a protein and provides an excellent model to ask what the requirements and checkpoints for degrading a protein when one domain fails to fold, and the other domain folds very stably and secured with a disulfide bond. Our studies revealed two checkpoints or rate-limiting steps in the degradation of this non-secreted LC (Figure 7). The first is the reduction of the $C_L$ domain. Although the $V_L$ domain of NS1 obtains a disulfide bond initially, it is readily reduced, due to its unstable fold giving rise to the ER resident ox1 form of NS1. Although we observed PDIA6 associated with NS1, over-expression of this reductase only modestly increased the turnover of the Vmut construct in which the only disulfide bond present was in the $C_L$ domain. PDIA6 over-expression had even less of an effect on the half-life of the Cmut that possessed only the $V_L$ domain disulfide bond. The interpretation of this result is complicated by the fact that genetically ablating the disulfide bond in the $V_L$ domain is not rate-limiting for NS1 turnover. Thus, it remains formally possible that PDIA6 plays a role in reducing the disulfide bond in the $V_L$ domain. Although we were unable to detect endogenous ERdj5 association with NS1, perhaps because its association is too transient to detect in these types of experiments, over-expression of ERdj5 readily increased the turnover of the Vmut construct arguing that it is responsible for reducing the disulfide in the $C_L$ domain and thus executing this rate-limiting step. Upon reduction of the $C_L$ domain, this LC is retrotranslocated and degraded so rapidly that a completely reduced, ox0 form is never observed unless proteasomal

activity is inhibited. These data argue that accessibility of this PDI family member to the disulfide bond in the $C_L$ domain is restricted by the very stable fold of this domain.

The extraction of the NS1 LC from the ER lumen required the activity of the AAA-ATPase p97 but was not dependent on proteasomal function. A group of papers from the Sitia lab has examined requirements for degradation of Ig μ heavy chain multimers (Mancini et al., 2000) and μ heavy chain-TCRα chimeras (Fagioli et al., 2001), both of which possess multiple folded domains and are covalently assembled with subunits making them very complicated ERAD clients. In both cases, interchain disulfides were shown to be reduced prior to retrotranslocation. It is noteworthy that proteasome inhibition resulted in reduction of the inter- and intra-molecular disulfide bonds of the J chain that is covalently bound to the μ chain multimers and deglycosylation of this subunit, indicating that it was dislocated to the cytosol. However, the freed μ heavy chain multimers showed no evidence of deglycosylation, arguing that this dimeric ERAD client with oxidized domains at both its N- and C-termini was not retrotranslocated in the absence of proteasomal function (Mancini et al., 2000).

Our data on the requirements for ERAD components in the extraction of NS1 from the ER are contrary to a study using proximity biotinylation, which found that this client was modified by cytosolically expressed BirA even in the presence of the p97QQ mutant, as was the NS1 $V_L$-STK$^-$ mutant that cannot be ubiquitinated (Sasset et al., 2015). Although this group found that the co-expression of a BiP trap mutant, which is not released from the client, and therefore upstream of retrotranslocation, did prevent biotinylation. Based on our data using these same mutants and constructs, it is possible that the proximity labeling experiments might be revealing continuous sampling of the cytosol by the termini of ERAD clients, which would require that BiP be released. In support of this possibility, an earlier study revealed that BiP release coincided with client retrotranslocation (Chillaron and Haas, 2000).

Somewhat less expected was our finding that, in spite of being reduced for retrotranslocation, the $C_L$ domain either retains or re-obtains structure in the cytosol. Indeed, previous studies from our lab revealed that light chain constant domains fold so rapidly in the ER that BiP trap mutants are unable to bind and prevent their folding and are more resistant to heat/chemical denaturation *in vitro* than the molecular chaperone BiP (Hellman et al., 1999). However, the observation raises the question as to the folded state of this LC as it passes through the retrotranslocon. Although the dimensions of actively translocating retrotranslocons in cells have not been determined, there have been several studies that provide insights into this point. The addition of EGFP to an ERAD client revealed that fluorescence was retained throughout retrotranslocation, arguing that either it was not unfolded during extraction or that it refolded very rapidly (Fiebiger et al., 2002). In another study, DHFR was tethered to the N-terminus of the MHC Class I protein, which is an ERAD client in the absence of assembly with $\beta_2$ microglobulin. They found that addition of methotrexate to stabilize the DHFR moiety in a fully folded state did not impede retrotranslocation (Tirosh et al., 2003). The narrowest cross-section of DHFR is 40 Å, and the dimensions of an Ig domain are 40Å × 25Å × 25Å, suggesting this domain might be able to pass through the channel with some structure intact. A cryo-EM structure obtained for yeast Hrd1 dimers complexed with Hrd3, revealed a very narrow channel (Schoebel et al., 2017), which would be incompatible with proteins retaining structure as they passed through the retrotranslocon. However, additional proteins like Der1, Usa1, and Yos9 are known to be components of retrotranslocons in yeast and mammal, which could alter the dimensions of the channel. Ig domains are comprised of 7-9 antiparallel β strands, in which strands 1-4 form one face of the structure and are disulfide bonded to the second part of the structure comprised of strands 5-7 with a Greek key topology (Bork et al., 1994). It is conceivable that reduction of the bond between strands 2 and 6 inside the ER could allow sufficient unfolding to separate the two portions of the domain, allowing it to pass through a narrower channel while retaining enough structure to refold in the cytosol. A better understanding of retrotranslocon dimensions during the extraction process is needed to determine the limitations on client structure.

The continued presence of a structured domain while this ERAD client was in the cytosol provided the second rate-limiting step in its turnover. Intriguingly, our studies detected a very sharp, anti-κ reactive intermediate migrating at ~15–16 kDa when MG132 was used without the addition of a protease. This fragment is a minor population and small enough that it runs near the dye front and is readily lost if the samples are electrophoresed to long. Based on the apparent molecular weight of this species together with the actual sequence of the NS1 protein, we calculated that this fragment was comprised of the ~12 kDa $C_L$ domain together with an additional ~30 amino acids of the $V_L$ domain. It has been estimated that the distance from the outside of the 20S proteasome to the proteolytic active site is ~70Å (Hoppe et al., 2000), which is equivalent to ~20 amino acids of an extended polypeptide chain and is consistent with the $C_L$ domain stalling ~10 amino acids from the 20S proteasome particle. This argues that the $C_L$ domain represented an impediment to entry into the proteasome core, consistent with this domain retaining structure, until it was unfolded by the AAA-ATPases found in the base of the proteasome lid (de la Pena et al., 2018). This interpretation is in keeping with our finding that two of the ring ATPases and two of the α subunits of the core 20S proteasome co-immunoprecipitated with NS1.

In summary, our studies revealed two checkpoints in the degradation of an Ig LC. First, the disulfide bond in the well-folded $C_L$ domain must be broken for the LC to be transported to the cytosol. In spite of becoming reduced, this domain retains or re-obtains structure in the cytosol. This structured

domain represents the second rate-limiting step, and it must be unfolded by the AAA-ATPases that are a component of the proteasome regulatory particle. Since all κ LC share the $C_L$ domain, these checkpoints are valid for any LC that fails to achieve its native state. Although our studies focused on a non-secreted κ LC, the Ig fold is the second most common structural motif found in metazoan proteins and is particularly abundant in cell surface receptors and secreted proteins (Muller et al., 2002). This due to a combination of the stability of Ig fold, which is secured by an intradomain disulfide bond, and the ready ability to modify the 8 loops connecting the β strands that comprise the domain. Thus, insights gained on the checkpoints for disposal of this LC are likely to be relevant for the degradation of other proteins possessing an Ig fold(s) that fail to reach their native state.

## Data availability statement

The raw data supporting the conclusions of this article will be made available by the authors, without undue reservation.

## Author contributions

LH and CO designed research, CO, MM, AF, CH, and CM-S performed the research, LH, CO, MM, and AF analyzed the data, LH, MM, CO, and AF wrote the paper.

## Funding

NIH grant GM54068 provided support for some personnel, equipment, and materials. The American Lebanese Syrian Associated Charities of St. Jude Children's Research Hospital provided further salary support and supplies.

## Acknowledgments

We thank members of the Hendershot lab and Drs. Roberto Sitia and Eelco van Anken for helpful discussions, Rachael Wood for providing the ΔssNS1 construct, and the Rhodes College Summer Plus Program that sponsored Hayes. This work was supported by National Institutes of Health Grant R01 GM54068 awarded to L.M.H. and by the American Lebanese Syrian Associated Charities of St. Jude Children's Research Hospital. The content is solely the responsibility of the authors and does not necessarily represent the official views of the National Institutes of Health.

## Conflict of interest

The authors declare that the research was conducted in the absence of any commercial or financial relationships that could be construed as a potential conflict of interest.

## Publisher's note

All claims expressed in this article are solely those of the authors and do not necessarily represent those of their affiliated organizations, or those of the publisher, the editors and the reviewers. Any product that may be evaluated in this article, or claim that may be made by its manufacturer, is not guaranteed or endorsed by the publisher.

## Supplementary material

The Supplementary Material for this article can be found online at: https://www.frontiersin.org/articles/10.3389/fcell.2022.924848/full#supplementary-material

## References

Baldridge, R. D., and Rapoport, T. A. (2016). Autoubiquitination of the Hrd1 ligase triggers protein retrotranslocation in ERAD. *Cell* 166, 394–407. doi:10.1016/j.cell.2016.05.048

Bork, P., Holm, L., and Sander, C. (1994). The immunoglobulin fold. structural classification, sequence patterns and common core. *J. Mol. Biol.* 242, 309–320. doi:10.1006/jmbi.1994.1582

Braakman, I., Helenius, J., and Helenius, A. (1992). Role of ATP and disulphide bonds during protein folding in the endoplasmic reticulum. *Nature* 356, 260–262. doi:10.1038/356260a0

Briney, B., Inderbitzin, A., Joyce, C., and Burton, D. R. (2019). Commonality despite exceptional diversity in the baseline human antibody repertoire. *Nature* 566, 393–397. doi:10.1038/s41586-019-0879-y

Cadwell, K., and Coscoy, L. (2005). Ubiquitination on nonlysine residues by a viral E3 ubiquitin ligase. *Science* 309, 127–130. doi:10.1126/science.1110340

Carvalho, P., Goder, V., and Rapoport, T. A. (2006). Distinct ubiquitin-ligase complexes define convergent pathways for the degradation of ER proteins. *Cell* 126, 361–373. doi:10.1016/j.cell.2006.05.043

Carvalho, P., Stanley, A. M., and Rapoport, T. A. (2010). Retrotranslocation of a misfolded luminal ER protein by the ubiquitin-ligase Hrd1p. *Cell* 143, 579–591. doi:10.1016/j.cell.2010.10.028

Chillaron, J., and Haas, I. G. (2000). Dissociation from BiP and retrotranslocation of unassembled immunoglobulin light chains are tightly coupled to proteasome activity. *Mol. Biol. Cell* 11, 217–226. doi:10.1091/mbc.11.1.217

de la Pena, A. H., Goodall, E. A., Gates, S. N., Lander, G. C., and Martin, A. (2018). Substrate-engaged 26S proteasome structures reveal mechanisms for ATP-hydrolysis-driven translocation. *Science* 362, eaav0725. doi:10.1126/science.aav0725

Deak, P. M., and Wolf, D. H. (2001). Membrane topology and function of Der3/Hrd1p as a ubiquitin-protein ligase (E3) involved in endoplasmic reticulum degradation. *J. Biol. Chem.* 276, 10663–10669. doi:10.1074/jbc.M008608200

Fagioli, C., Mezghrani, A., and Sitia, R. (2001). Reduction of interchain disulfide bonds precedes the dislocation of Ig-mu chains from the endoplasmic reticulum to the cytosol for proteasomal degradation. *J. Biol. Chem.* 276, 40962–40967. doi:10.1074/jbc.M107456200

Feige, M. J., Hagn, F., Esser, J., Kessler, H., and Buchner, J. (2007). Influence of the internal disulfide bridge on the folding pathway of the CL antibody domain. *J. Mol. Biol.* 365, 1232–1244. doi:10.1016/j.jmb.2006.10.049

Feige, M. J., Groscurth, S., Marcinowski, M., Shimizu, Y., Kessler, H., Hendershot, L. M., et al. (2009). An unfolded CH1 domain controls the assembly and secretion of IgG antibodies. *Mol. Cell* 34, 569–579. doi:10.1016/j.molcel.2009.04.028

Feige, M. J., Hendershot, L. M., and Buchner, J. (2010). How antibodies fold. *Trends biochem. Sci.* 35, 189–198. doi:10.1016/j.tibs.2009.11.005

Fiebiger, E., Story, C., Ploegh, H. L., and Tortorella, D. (2002). Visualization of the ER-to-cytosol dislocation reaction of a type I membrane protein. *EMBO J.* 21, 1041–1053. doi:10.1093/emboj/21.5.1041

Gardner, R. G., Swarbrick, G. M., Bays, N. W., Cronin, S. R., Wilhovsky, S., Seelig, L., et al. (2000). Endoplasmic reticulum degradation requires lumen to cytosol signaling. Transmembrane control of hrd1p by hrd3p. *J. Cell Biol.* 151, 69–82. doi:10.1083/jcb.151.1.69

Gorasia, D. G., Dudek, N. L., Safavi-Hemami, H., Perez, R. A., Schittenhelm, R. B., Saunders, P. M., et al. (2016). A prominent role of PDIA6 in processing of misfolded proinsulin. *Biochim. Biophys. Acta* 1864, 715–723. doi:10.1016/j.bbapap.2016.03.002

Hellman, R., Vanhove, M., Lejeune, A., Stevens, F. J., and Hendershot, L. M. (1999). The *in vivo* association of BiP with newly synthesized proteins is dependent on the rate and stability of folding and not simply on the presence of sequences that can bind to BiP. *J. Cell Biol.* 144, 21–30. doi:10.1083/jcb.144.1.21

Hendershot, L., Bole, D., Kohler, G., and Kearney, J. F. (1987). Assembly and secretion of heavy chains that do not associate posttranslationally with immunoglobulin heavy chain-binding protein. *J. Cell Biol.* 104, 761–767. doi:10.1083/jcb.104.3.761

Hoppe, T., Matuschewski, K., Rape, M., Schlenker, S., Ulrich, H. D., Jentsch, S., et al. (2000). Activation of a membrane-bound transcription factor by regulated ubiquitin/proteasome-dependent processing. *Cell* 102, 577–586. doi:10.1016/s0092-8674(00)00080-5

Ishikura, S., Weissman, A. M., and Bonifacino, J. S. (2010). Serine residues in the cytosolic tail of the T-cell antigen receptor alpha-chain mediate ubiquitination and endoplasmic reticulum-associated degradation of the unassembled protein. *J. Biol. Chem.* 285, 23916–23924. doi:10.1074/jbc.M110.127936

Kearney, J. F., Radbruch, A., Liesegang, B., and Rajewsky, K. (1979). A new mouse myeloma cell line that has lost immunoglobulin expression but permits the construction of antibody-secreting hybrid cell lines. *J. Immunol.* 123, 1548–1550.

Kenter, A. L., and Feeney, A. J. (2019). New insights emerge as antibody repertoire diversification meets chromosome conformation. *F1000Res* 8. doi:10.12688/f1000research.17358.1

Knittler, M. R., Dirks, S., and Haas, I. G. (1995). Molecular chaperones involved in protein degradation in the endoplasmic reticulum: Quantitative interaction of the heat shock cognate protein BiP with partially folded immunoglobulin light chains that are degraded in the endoplasmic reticulum. *Proc. Natl. Acad. Sci. U. S. A.* 92, 1764–1768. doi:10.1073/pnas.92.5.1764

Kostova, Z., Tsai, Y. C., and Weissman, A. M. (2007). Ubiquitin ligases, critical mediators of endoplasmic reticulum-associated degradation. *Semin. Cell Dev. Biol.* 18, 770–779. doi:10.1016/j.semcdb.2007.09.002

Kothe, M., Ye, Y., Wagner, J. S., De Luca, H. E., Kern, E., Rapoport, T. A., et al. (2005). Role of p97 AAA-ATPase in the retrotranslocation of the cholera toxin A1 chain, a non-ubiquitinated substrate. *J. Biol. Chem.* 280, 28127–28132. doi:10.1074/jbc.M503138200

Lee, Y.-K., Brewer, J. W., Hellman, R., and Hendershot, L. M. (1999). BiP and immunoglobulin light chain cooperate to control the folding of heavy chain and ensure the fidelity of immunoglobulin assembly. *Mol. Biol. Cell* 10, 2209–2219. doi:10.1091/mbc.10.7.2209

Lilie, H., McLaughlin, S., Freedman, R., and Buchner, J. (1994). Influence of protein disulfide isomerase (PDI) on antibody folding *in vitro*. *J. Biol. Chem.* 269, 14290–14296. doi:10.1016/s0021-9258(17)36787-x

Lilley, B. N., and Ploegh, H. L. (2005). Multiprotein complexes that link dislocation, ubiquitination, and extraction of misfolded proteins from the endoplasmic reticulum membrane. *Proc. Natl. Acad. Sci. U. S. A.* 102, 14296–14301. doi:10.1073/pnas.0505014102

Mancini, R., Fagioli, C., Fra, A. M., Maggioni, C., and Sitia, R. (2000). Degradation of unassembled soluble Ig subunits by cytosolic proteasomes: evidence that retrotranslocation and degradation are coupled events. *FASEB J.* 14, 769–778. doi:10.1096/fasebj.14.5.769

Melnick, J., Aviel, S., and Argon, Y. (1992). The endoplasmic reticulum stress protein GRP94, in addition to BiP, associates with unassembled immunoglobulin chains. *J. Biol. Chem.* 267, 21303–21306. doi:10.1016/s0021-9258(19)36608-6

Meunier, L., Usherwood, Y. K., Chung, K. T., and Hendershot, L. M. (2002). A subset of chaperones and folding enzymes form multiprotein complexes in endoplasmic reticulum to bind nascent proteins. *Mol. Biol. Cell* 13, 4456–4469. doi:10.1091/mbc.e02-05-0311

Meyer, H. H., Wang, Y., and Warren, G. (2002). Direct binding of ubiquitin conjugates by the mammalian p97 adaptor complexes, p47 and Ufd1-Npl4. *EMBO J.* 21, 5645–5652. doi:10.1093/emboj/cdf579

Moore, P., He, K., and Tsai, B. (2013). Establishment of an *in vitro* transport assay that reveals mechanistic differences in cytosolic events controlling cholera toxin and T-cell receptor alpha retro-translocation. *PLoS ONE* 8, e75801. doi:10.1371/journal.pone.0075801

Muller, A., MacCallum, R. M., and Sternberg, M. J. (2002). Structural characterization of the human proteome. *Genome Res.* 12, 1625–1641. doi:10.1101/gr.221202

Needham, P. G., Guerriero, C. J., and Brodsky, J. L. (2019). Chaperoning endoplasmic reticulum-associated degradation (ERAD) and protein conformational diseases. *Cold Spring Harb. Perspect. Biol.* 11, a033928. doi:10.1101/cshperspect.a033928

Okuda-Shimizu, Y., and Hendershot, L. M. (2007). Characterization of an ERAD pathway for nonglycosylated BiP substrates, which require Herp. *Mol. Cell* 28, 544–554. doi:10.1016/j.molcel.2007.09.012

Olzmann, J. A., Kopito, R. R., and Christianson, J. C. (2013). The mammalian endoplasmic reticulum-associated degradation system. *Cold Spring Harb. Perspect. Biol.* 5, a013185. doi:10.1101/cshperspect.a013185

Oreste, U., Ametrano, A., and Coscia, M. R. (2021). On origin and evolution of the antibody molecule. *Biol. (Basel)* 10, 140. doi:10.3390/biology10020140

Rape, M., and Jentsch, S. (2002). Taking a bite: Proteasomal protein processing. *Nat. Cell Biol.* 4, E113–E116. doi:10.1038/ncb0502-e113

Sasset, L., Petris, G., Cesaratto, F., and Burrone, O. R. (2015). The VCP/p97 and YOD1 proteins have different substrate-dependent activities in endoplasmic reticulum-associated degradation (ERAD). *J. Biol. Chem.* 290, 28175–28188. doi:10.1074/jbc.M115.656660

Schoebel, S., Mi, W., Stein, A., Ovchinnikov, S., Pavlovicz, R., DiMaio, F., et al. (2017). Cryo-EM structure of the protein-conducting ERAD channel Hrd1 in complex with Hrd3. *Nature* 548, 352–355. doi:10.1038/nature23314

Shaffer, A. L., and Schlissel, M. S. (1997). A truncated heavy chain protein relieves the requirement for surrogate light chains in early B cell development. *J. Immunol.* 159, 1265–1275.

Shen, Y., and Hendershot, L. M. (2005). ERdj3, a stress-inducible endoplasmic reticulum DnaJ homologue, serves as a cofactor for BiP's interactions with unfolded substrates. *Mol. Biol. Cell* 16, 40–50. doi:10.1091/mbc.e04-05-0434

Shimizu, Y., Okuda-Shimizu, Y., and Hendershot, L. M. (2010). Ubiquitylation of an ERAD substrate occurs on multiple types of amino acids. *Mol. Cell* 40, 917–926. doi:10.1016/j.molcel.2010.11.033

Skowronek, M. H., Hendershot, L. M., and Haas, I. G. (1998). The variable domain of nonassembled Ig light chains determines both their half-life and binding to the chaperone BiP. *Proc. Natl. Acad. Sci. U. S. A.* 95, 1574–1578. doi:10.1073/pnas.95.4.1574

Stein, A., Ruggiano, A., Carvalho, P., and Rapoport, T. A. (2014). Key steps in ERAD of luminal ER proteins reconstituted with purified components. *Cell* 158, 1375–1388. doi:10.1016/j.cell.2014.07.050

Suzuki, T., Huang, C., and Fujihira, H. (2016). The cytoplasmic peptide:N-glycanase (NGLY1) - structure, expression and cellular functions. *Gene* 577, 1–7. doi:10.1016/j.gene.2015.11.021

Tirosh, B., Furman, M. H., Tortorella, D., and Ploegh, H. L. (2003). Protein

unfolding is not a prerequisite for endoplasmic reticulum-to-cytosol dislocation. *J. Biol. Chem.* 278, 6664–6672. doi:10.1074/jbc.M210158200

Vajda, S., Porter, K. A., and Kozakov, D. (2021). Progress toward improved understanding of antibody maturation. *Curr. Opin. Struct. Biol.* 67, 226–231. doi:10.1016/j.sbi.2020.11.008

Vanhove, M., Usherwood, Y.-K., and Hendershot, L. M. (2001). Unassembled Ig heavy chains do not cycle from BiP *in vivo*, but require light chains to trigger their release. *Immunity* 15, 105–114. doi:10.1016/s1074-7613(01)00163-7

Vembar, S. S., and Brodsky, J. L. (2008). One step at a time: endoplasmic reticulum-associated degradation. *Nat. Rev. Mol. Cell Biol.* 9, 944–957. doi:10.1038/nrm2546

Wang, X., Herr, R. A., Chua, W. J., Lybarger, L., Wiertz, E. J., Hansen, T. H., et al. (2007). Ubiquitination of serine, threonine, or lysine residues on the cytoplasmic tail can induce ERAD of MHC-I by viral E3 ligase mK3. *J. Cell Biol.* 177, 613–624. doi:10.1083/jcb.200611063

Wu, X., and Rapoport, T. A. (2018). Mechanistic insights into ER-associated protein degradation. *Curr. Opin. Cell Biol.* 53, 22–28. doi:10.1016/j.ceb.2018.04.004

Ye, Y., Shibata, Y., Yun, C., Ron, D., and Rapoport, T. A. (2004). A membrane protein complex mediates retro-translocation from the ER lumen into the cytosol. *Nature* 429, 841–847. doi:10.1038/nature02656

Ye, Y., Shibata, Y., Kikkert, M., van, V. S., Wiertz, E., Rapoport, T. A., et al. (2005). Recruitment of the p97 ATPase and ubiquitin ligases to the site of retrotranslocation at the endoplasmic reticulum membrane. *Proc. Natl. Acad. Sci. U. S. A.* 102, 14132–14138. doi:10.1073/pnas.0505006102

Yelton, D. E., Diamond, B. A., Kwan, S. P., and Scharff, M. D. (1978). Fusion of mouse myeloma and spleen cells. *Curr. Top. Microbiol. Immunol.* 81, 1–7. doi:10.1007/978-3-642-67448-8_1

frontiers | Frontiers in Cell and Developmental Biology

TYPE Original Research
PUBLISHED 29 August 2022
DOI 10.3389/fcell.2022.951199



OPEN ACCESS

EDITED BY
Francesco Fazi,
Sapienza University of Rome, Italy

REVIEWED BY
Johnathan Paul Labbadia,
University College London,
United Kingdom
Derek Sieburth,
University of Southern California,
United States

*CORRESPONDENCE
Anat Ben-Zvi,
anatbz@bgu.ac.il

SPECIALTY SECTION
This article was submitted to Signaling, a section of the journal Frontiers in Cell and Developmental Biology

RECEIVED 23 May 2022
ACCEPTED 03 August 2022
PUBLISHED 29 August 2022

CITATION
Kishner M, Habaz L, Meshnik L, Meidan TD, Polonsky A and Ben-Zvi A (2022), Gonadotropin-releasing hormone-like receptor 2 inversely regulates somatic proteostasis and reproduction in Caenorhabditis elegans. *Front. Cell Dev. Biol.* 10:951199. doi: 10.3389/fcell.2022.951199



# Gonadotropin-releasing hormone-like receptor 2 inversely regulates somatic proteostasis and reproduction in *Caenorhabditis elegans*

Mor Kishner, Libat Habaz, Lana Meshnik, Tomer Dvir Meidan, Alexandra Polonsky and Anat Ben-Zvi*

Department of Life Sciences, Ben-Gurion University of the Negev, Beer Sheva, Israel

The quality control machinery regulates the cellular proteome to ensure proper protein homeostasis (proteostasis). In *Caenorhabditis elegans*, quality control networks are downregulated cell-nonautonomously by the gonadal longevity pathway or metabolic signaling at the onset of reproduction. However, how signals are mediated between the gonad and the somatic tissues is not known. Gonadotropin-releasing hormone (GnRH)-like signaling functions in the interplay between development and reproduction and have conserved roles in regulating reproduction, metabolism, and stress. We, therefore, asked whether GnRH-like signaling is involved in proteostasis collapse at the onset of reproduction. Here, we examine whether *C. elegans* orthologues of GnRH receptors modulate heat shock survival. We find that *gnrr-2* is required for proteostasis remodeling in different somatic tissues during the transition to adulthood. We show that *gnrr*-2 likely functions in neurons downstream of the gonad in the gonadal-longevity pathway and modulate the somatic regulation of transcription factors HSF-1, DAF-16, and PQM-1. In parallel, *gnrr-2* modulates egg-laying rates, vitellogenin production, and thus reproductive capacity. Taken together, our data suggest that *gnrr-2* plays a GnRH-associated role, mediating the cross-talk between the reproduction system and the soma in the decision to commit to reproduction.

KEYWORDS

**aging, gonadal longevity signaling, gonadotropin-releasing hormone (GnRH/GnRH receptor), proteostasis, stress response, reproduction, *C. elegans***

## Introduction

The age-dependent dysregulation of quality control machinery and, specifically, protein homeostasis (proteostasis), is associated with limited ability to mount stress responses, reduced folding capacity, accumulation of protein damage, and increased prevalence of protein misfolding diseases (Brehme et al., 2014; Vilchez et al., 2014; Huang et al., 2019; Morimoto, 2020; Taylor and Hetz, 2020; Aman et al., 2021; Meller and Shalgi,

2021; Shemesh et al., 2021). Transcriptional stress response programs, such as the heat shock response (HSR) and the unfolded protein responses in the ER and mitochondria ($UPR^{ER}$ and $UPR^{mt}$, respectively), are remodeled at the onset of *Caenorhabditis elegans* reproduction and in human senescent cells (Shai et al., 2014; Li et al., 2017; Taylor and Hetz, 2020; Meller and Shalgi, 2021; Sala and Morimoto, 2022). While many cytoprotective genes are upregulated under stress conditions in young adults or primary human fibroblasts, their activation is impaired in reproductive adults and senescent cells, leading to a sharp decline in stress survival (Ben-Zvi et al., 2009; Lapierre et al., 2011; Vilchez et al., 2012; Shemesh et al., 2013; Taylor and Dillin, 2013; Labbadia and Morimoto, 2015; Steinbaugh et al., 2015; Sabath et al., 2020). In *C. elegans,* HSR dysregulation is associated with a repressive chromatin state and reduced transcription of heat shock (HS) genes (Shemesh et al., 2013; Labbadia and Morimoto, 2015). Similar modifications at the chromatin state, including induction of repressive marks and reduction of activating marks, were noted in other aging organisms and senescent human cells (Meller and Shalgi, 2021; Sala and Morimoto, 2022). These findings support a broad role for stress response pathways remodeling in the age-dependent regulation of proteostasis.

Work in *C. elegans* demonstrates that reproductive competence and environmental conditions could modulate the timing of the proteostasis decline (Ben-Zvi et al., 2009; Lapierre et al., 2011; Vilchez et al., 2012; Shemesh et al., 2013; Taylor and Dillin, 2013; Labbadia and Morimoto, 2015; Shemesh et al., 2017a; Shemesh et al., 2017b; Labbadia et al., 2017; Matai et al., 2019; Shpigel et al., 2019; Sala et al., 2020). For example, disrupting germline proliferation results in the remodeling of many stress transcriptional programs, leading to maintenance of robust proteostasis while inversely modulating reproduction (Berman and Kenyon, 2006; Gerisch et al., 2007; Goudeau et al., 2011; Lapierre et al., 2011; Vilchez et al., 2012; Shemesh et al., 2013; Taylor and Dillin, 2013; Tepper et al., 2013; Labbadia and Morimoto, 2015; Steinbaugh et al., 2015; Nakamura et al., 2016; Cohen-Berkman et al., 2020). In contrast, food limitation and dietary restriction (DR) could reverse the collapse and restore the activation of the HSR even late in adulthood (Thondamal et al., 2014; Matai et al., 2019; Shpigel et al., 2019). Proteostasis collapse is therefore regulated non-autonomously in response to life history events and environmental changes. But how are these signals transmitted and integrated between tissues to mediate proteostasis collapse in the soma?

The gonadotropin-releasing hormone (GnRH) superfamily acts at the interplay between development and reproduction. This superfamily integrates internal and environmental stimuli to regulate sexual maturation and reproductive functions in vertebrates and invertebrates (Zandawala et al., 2018; Sakai et al., 2020). This G protein-coupled receptor (GPCR) superfamily is subdivided into two main subfamilies based on neuropeptides sequence conservation. GnRH receptors subfamily, including GnRH, Adipokinetic hormone (AKH), and AKH-CRZ–related peptide (ACP) binding receptors, and Corazonin (CRZ) receptors subfamily (Zandawala et al., 2018). The genome of *C. elegans* encodes eight members of the GnRH-like GPCRs superfamily (*gnrr-1* to *gnrr-8*; GNRRs) (Van der Auwera et al., 2020), the ligands of four were identified. Of the four, only *gnrr-1*, an AKH-like receptor, and its neuropeptide, *nlp-47*, regulate fecundity (Lindemans et al., 2009). Here, we asked whether *C. elegans* GnRH-like receptors could remodel proteostasis at the onset of reproduction. We identify two family members, *gnrr-2* and *gnrr-6*, as putative regulators of proteostasis collapse. We focus on *gnrr-2* and demonstrate that disrupting *gnrr-2* function or expression leads to the maintenance of robust proteostasis in adulthood. We show that *gnrr-2* acts in the gonadal longevity pathway downstream of the gonad and inversely modulates reproduction, suggesting that *gnrr-2* functions as a GnRH-like receptor.

# Materials and methods

## Nematode strains and growth conditions

A list of strains used in this work is provided in Supplementary Table S1. Mutant strains were outcrossed into our N2 strain ($n \geq 3$). Standard genetic crossing techniques were used to construct mutant strains and mutation were verify using single worm PCR (Phire Animal Tissue Direct PCR Kit, Thermo Scientific) as previously described (Meshnik et al., 2022). Nematodes were cultured using standard techniques. Animals were grown on NGM plates seeded with the *Escherichia coli* OP50-1 strain at 15°C. For RNA interference (RNAi), eggs were placed on *E. coli* strain HT115 (DE3) transformed with specified RNAi or empty vector (pL4440) control (obtained from the Ahringer or Vidal RNAi libraries). RNAi efficiency was determined using qPCR to determine the mRNA levels, as in (Dror et al., 2020). For diet supplementation of fatty acids, plates were supplemented with the detergent Tergitol (NP40; Sigma) used as control, or with AA (50 μM TCI Chemical dissolved in NP40), as in (Shemesh et al., 2017a). Unless otherwise stated, eggs, laid at 15°C, were transferred to fresh plates and grown at 25°C for the duration of an experiment. The first day of adulthood was set at 50 h after temperature shift, before the onset of egg-laying. To avoid progeny contamination, animals were moved to fresh plates during the reproductive period.

## Statistical analyses

To examine whether any *gnrr* family member improved HS survival rates compared with wild type (WT) animals, we used a one-way analysis of variance (ANOVA) followed by a Dunnett's

*post-hoc* test. To test the null hypothesis that *gnrr-2* modulated proteostasis capacity after the onset of reproduction, we used one-way ANOVA followed by a Tukey's *post-hoc* test. We used the same test to examine the impact of *gnrr-2* on reproduction. To compare proteostasis or reproduction capacity between two strains or two RNAi treatments, we used two-tailed Wilcoxon Mann-Whitney rank-sum test. To compare the expression levels of genes and assess their statistical significance, we used the Wilcoxon Mann-Whitney rank-sum test; Bonferroni correction was applied to adjust $p$ values when gene expression was also compared with *glp-1* as a positive control. Mean life spans were calculated using Kaplan-Meier survival curves and were compared using Mantel-Cox log-rank test. Data are means ±1 standard error of the mean (1 SE). Unless otherwise indicated, (*) denotes $p \leq 0.05$, and (**) denotes $p \leq 0.01$. ($N$) denotes the numbers of biological repeats, and ($n$) denotes the number individuals per experimental condition.

## *gnrr-2* deletion mutants

Genomic DNA from WT or *gnrr-2*(*ok3618*) animals was amplified with a single worm PCR Phire Animal Tissue Direct PCR Kit (Thermo Scientific) and sequenced (IDT) using primers flanking the *ok3618* deletion (Supplementary Table S2). A 417 bp deletion was identified (positions 2515-2931 of the C15H11.2a transcript), spanning *gnrr-2* exon 6, intron 6, exon 7, and its' 3′ UTR (Supplementary Figure S1). The deletion also partially disrupts the 3′ UTR of the nuclear export factor, *nxf-1* (*C15H11.3*), encoded on the opposite strand (Supplementary Figure S1). The *gnrr-2*(*tm4867*) deletion was previously characterized (Consortium, 2012). It is a 477 bp deletion spanning exons 4–6 not affecting *nxf-1* (Supplementary Figure S1). Because *nxf-1* is an essential gene involved in mRNA export from the nucleus, and mutations in *nxf-1* result in embryonic arrest and lethality (Zheleva et al., 2019), we estimate little to no effect of the *ok3618* deletion on its' function. This conclusion is further supported by the consistent results observed for the two deletion strains, and *gnrr-2* RNAi, strongly reducing the possibility that *nxf-1* contributes to the phenotypes reported.

## Heat shock assays

HS survival rates were determined as previously described (Karady et al., 2013). Briefly, age-synchronized animals were subjected to 37°C for 6 h, unless otherwise indicated, and survival was scored by monitoring SYTOX orange dye uptake ($N \geq 3$, $n > 100$). Fluorescent animals were scored as dead. For HS activation assays, plates with age-synchronized animals ($N \geq 5$) were placed in a 37°C bath for 90 min. Animals were frozen immediately following the HS. $GFP_{HS}$-expressing animals ($N \geq 3$, $n \geq 60$) were fixed 18–24 h following the HS and imaged using a Leica DM5500 confocal microscope through a 40x 1.0 numerical aperture objective with 488 nm laser line for excitation as previously described (Shpigel et al., 2019). Animals expressing GFP in the gut were scored as HS-induced. Alternately, images were analyzed using the ImageJ software (NIH), and GFP levels were determined. For HS recovery assays, age-synchronized animals were subjected to 37°C for 4 h, and recovery was scored by monitoring motility 4 h after the HS ($N \geq 5$, $n > 125$). This assay was used to score TU3401 animals that express mCherry and thus cannot be scored with SYTOX orange.

## Determination of RNA levels

RNA extraction, cDNA synthesis, and quantitative real-time PCR were performed as previously described (Shemesh et al., 2017a). Samples ($N \geq 5$) were normalized to *act-1* using the 2-ΔΔCT method. Samples were also normalized to 18S to verify that *act-1* is not modulated under these experimental conditions, and the results were consistent. A list of primers is provided in Supplementary Table S2.

## Foci quantification

Age-synchronized animals ($N \geq 3$, $n > 30$) expressing *punc-54*::Q35::YFP, were imaged using a Leica M165 FC fluorescent stereoscope with a YFP filter. The number of bright foci, discrete structures that are brighter than the surrounding fluorescence, was counted.

## Motility assays

For thrashing rates, age-synchronized animals ($N \geq 3$, $n \geq 40$) were monitored, and thrashes (changes in bending direction at mid-body) were counted, as in (Dror et al., 2020). Values are presented as bends per minute. For Stiff-body paralysis, age-synchronized *unc-52*(*ts*) mutant animals ($N \geq 12$, $n > 100$) grown at 25°C until day one of adulthood were shifted to 15°C. Motility was scored by monitoring animal movement 10 min after transfer to a new plate on day 4 of adulthood, as in (Shemesh et al., 2013). Animals that did not move were scored as paralyzed.

## DAF-16 and PQM-1 nuclear localization assay

Age-synchronized DAF-16::GFP or PQM-1::GFP animals ($N \geq 3$ and $n = 10$) were grown at 25°C until day two of adulthood. Animals were fixed, mounted, and imaged using a Leica DM5500 confocal microscope through a 40x 1.0 numerical aperture objective with 488 nm laser line for excitation as previously described (Shemesh et al., 2017a). Animals showing

nuclear-localized GFP in the majority of their intestinal cells were scored as positive. Animals were scored blind.

## *gnrr-2* localization assay

The promoter region of *gnrr-2* (1,040 bp upstream of the protein-coding region) was amplified from the genomic DNA of WT animals, cloned into pNU435 plasmid using the Gibson Assembly method (Macrogen) and verified by sequencing. All primers are listed in Supplementary Table S2. This plasmid was co-injected with a marker plasmid expressing *pmyo-3*::*mCherry* into WT animals and maintained as an extra-chromosomal array. Age-synchronized animals expressing *gnrr-2p*::*GFP* and myo-3p::mCherry were grown at 25°C. Animals were fixed at the indicated stages using paraformaldehyde (4%) and mounted on microscope slides. *gnrr-2p*::*GFP* and *myo-3p*::*mCherry* were imaged using a Leica DM5500 confocal microscope through a 40x 1.0 numerical aperture objective with 488 nm and 532 laser lines, respectively, for excitation.

## Progeny quantification

Age-synchronized animals ($N \geq 3$, $n \geq 18$) were allowed to lay eggs on seeded plates (one animal per plate). Animals were moved to freshly seeded plates every day until the end of the reproductive period, and the progeny number of each animal was scored 24–48 h later, as previously described (Shemesh et al., 2017b).

## Eggs laying rate

Age-synchronized day two adults (10 animals per plate; $N \geq 7$, $n > 100$) were allowed to lay eggs on seeded plates. Animals were moved every hour, and the progeny number was scored.

## Yolk protein YP170 quantification

Similar numbers of age-synchronized day two adult animals were collected and lysed in SDS sample buffer (92°C for 10 min). Sample (equal volumes) were loaded on 8% SDS-PAGE and separated using gel electrophoresis. Gels were stained using Coomassie brilliant blue and imaged using a ChemiDoc™ MP Imaging System (Bio-Rad Laboratories). The YP170 band was identified by comparing to previous publications (DePina et al., 2011; Plagens et al., 2021), and compared with *glp-1* mutant animals that accumulate YP (Steinbaugh et al., 2015). Images were analyzed using the ImageJ software (NIH).

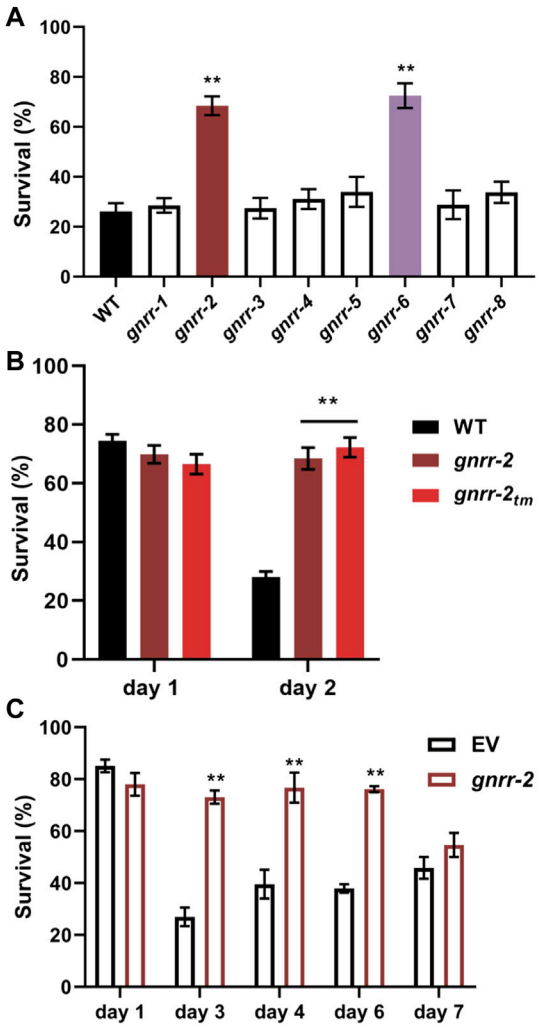


FIGURE 1
Gonadotropin-related hormone receptors *gnrr-2* and *gnrr-6* modulate HS survival in adulthood. **(A)** HS Survival rates of age-synchronized WT or *gnrr-1* to *gnrr-8* mutant animals. Animals were subjected to HS (6 h at 37°C) on day two of adulthood, and survival was assayed ($N \geq 5$). Data are means ±1 standard error of the mean (1 SE). Data were analyzed using one-way ANOVA followed by a Dunnett's *post-hoc* test. (**) denotes $p \leq 0.001$ compared with WT animals. **(B)** HS Survival rates of age-synchronized WT or mutant animals, *gnrr-2* and *gnrr-2*$_{tm}$. Animals were subjected to HS (6 h at 37°C) on day one or two of adulthood, and survival was assayed ($N \geq 5$). Data are means ±1 standard error of the mean (1 SE). Data were analyzed using one-way ANOVA followed by a Tukey's *post-hoc* test. (**) denotes $p \leq 0.001$ compared with same-age WT animals. **(C)** HS Survival rates of age-synchronized WT, fed on empty vector (EV) or *gnrr-2* RNAi-expressing bacteria. Animals were subjected to HS (6 h at 37°C) on days 1–7 of adulthood, as indicated, and survival was assayed ($N \geq 5$). Data are means ±1 standard error of the mean (1 SE). Data were analyzed using one-way ANOVA followed by a Tukey's *post-hoc* test. (**) denotes $p \leq 0.001$ compared with same-age animals fed on EV RNAi.

## Oil-Red-O staining

Animals were fixed and stained as previously described (O'Rourke et al., 2009). Animals were then imaged using a Leica DMIL microscope with a 10x 1.0 objective. Images were analyzed using the ImageJ software (NIH).

## Lifespan analysis

~130 animals were monitored for each strain starting from day one of adulthood (10–15 animals per plate), as previously described (Shemesh et al., 2017a).

## Embryo hatching

Embryos ($N \geq 4$, $n > 100$) were set on a freshly seeded plate, and hatching was examined after 24 or 48 h using a Leica M165 FC stereoscope.

## Developmental timing

Embryos were grown at 20°C, animals' developmental stage was examined daily, and the number of reproductive adults was recorded, as previously described (Dror et al., 2020).

# Results

## Examining the role of GNRR gene family in proteostasis remodeling

To ask whether GNRRs family members play a role in age-dependent proteostasis remodeling, we examine whether mutant animals in each *gnrr* gene (Supplementary Table S1) could rescue the sharp decline in HS survival rates at the onset of reproduction. Survival rates of *gnrr-1*, *gnrr-3*, *gnrr-4*, *gnrr-5*, *gnrr-7*, and *gnrr-8* mutant animals (6 h at 37°C, day two adults) were similar to WT. In contrast, survival rates of *gnrr-2*(*ok3618*) (hereon named *gnrr-2*; Supplementary Figure S1) and *gnrr-6*(*ok3362*) mutant animals were significantly improved (66% ± 3% and 72% + 5%, respectively, ANOVA followed by a Dunnett's post-hoc test, $p \leq 0.001$; Figure 1A). Because GNRR-6 and GNRR-3 are activated by opposing RPamide neuropeptides NLP-22 and NLP-2 and promote sleep and wakefulness, respectively (Van der Auwera et al., 2020), we focused on GNRR-2 and examined the role of this GPCR in proteostasis remodeling.

To validate *gnrr-2* role in HS survival, we tested the thermotolerance of a second *gnrr-2* allele (see *Materials and methods*; Supplementary Figure S1) and used RNA interference (RNAi) to knock down *gnrr-2* expression. We observed increased survival rates for *gnrr-2*(*tm4867*) (hereon named *gnrr-2*$_{tm}$) mutant animals following HS (72% ± 3%, 6 h at 37°C, day two adults, ANOVA followed by a Tukey's post-hoc test, $p \leq 0.001$; Figure 1B). Likewise, HS survival rates of WT animals treated with *gnrr-2*(*RNAi*) were strongly improved compared to animals treated with empty vector (EV) control (6 h at 37°C, day three adults, 73% ± 3% and 28% ± 4%, respectively, ANOVA followed by a Tukey's post-hoc test, $p \leq 0.001$; Figure 1C). Thus, *gnrr-2* dysfunction or downregulation improved thermotolerance in adulthood.

To ask whether *gnrr-2* modulates thermotolerance in general or specifically during adulthood, we compared the thermotolerance of WT and *gnrr-2* mutant animals before the collapse. HS survival rates of *gnrr-2* or *gnrr-2*$_{tm}$ young adults (6 h at 37°C, day one adults) were not significantly different from WT animals (70% ± 3%, 67% ± 3%, and 74% ± 3%, respectively, ANOVA followed by a Tukey's post-hoc test; Figure 1B). We found similar HS survival rates for WT young adults treated with *gnrr-2(RNAi)* or EV (78% ± 5% and 85% + 3%, respectively, ANOVA followed by a Tukey's post-hoc test; Figure 1C). Finally, survival rates of WT animals treated with *gnrr-2*(*RNAi*) remained high during adulthood (73% ± 2% for day six adults; Figure 1C), similar to the activation of gonadal longevity signaling (Shemesh et al., 2013). These data suggest that *gnrr-2* is required for remodeling thermotolerance at the transition to adulthood.

## *gnrr-2* modulates proteostasis during adulthood

WT animals cannot strongly induce the expression of HS genes after the onset of reproduction (Shemesh et al., 2013; Labbadia and Morimoto, 2015). To determine whether the improved thermotolerance of *gnrr-2* mutant animals is associated with HSR activation, we compared the ability of WT and *gnrr-2* mutant animals to mount an effective stress response. For that, we first monitored the expression pattern of a transcriptional reporter in which an *hsp-16.2* promoter regulates the expression of green fluorescent protein ($GFP_{HS}$). We subjected WT and *gnrr-2* mutant animals carrying $GFP_{HS}$ to HS (90 min at 37°C) on day one or three of adulthood and determined the percent of animals expressing $GFP_{HS}$. While WT, *gnrr-2* and *gnrr-2*$_{tm}$ day one adults showed induced $GFP_{HS}$, only *gnrr-2* and *gnrr-2*$_{tm}$ showed strong $GFP_{HS}$ expression on day three of adulthood (Figures 2A,B). We detected expression in various somatic tissues with the most robust $GFP_{HS}$ induction in the intestine (1.5-2-fold; Figures 2A,C). We next compared the expression levels of four HS genes between WT and *gnrr-2* day two adults following HS (90 min at 37°C). The mRNA levels of *hsp-70*, *F44E5.4*, *hsp-16.11*, and *hsp-16.2* were 2-fold higher in *gnrr-2* mutant animals

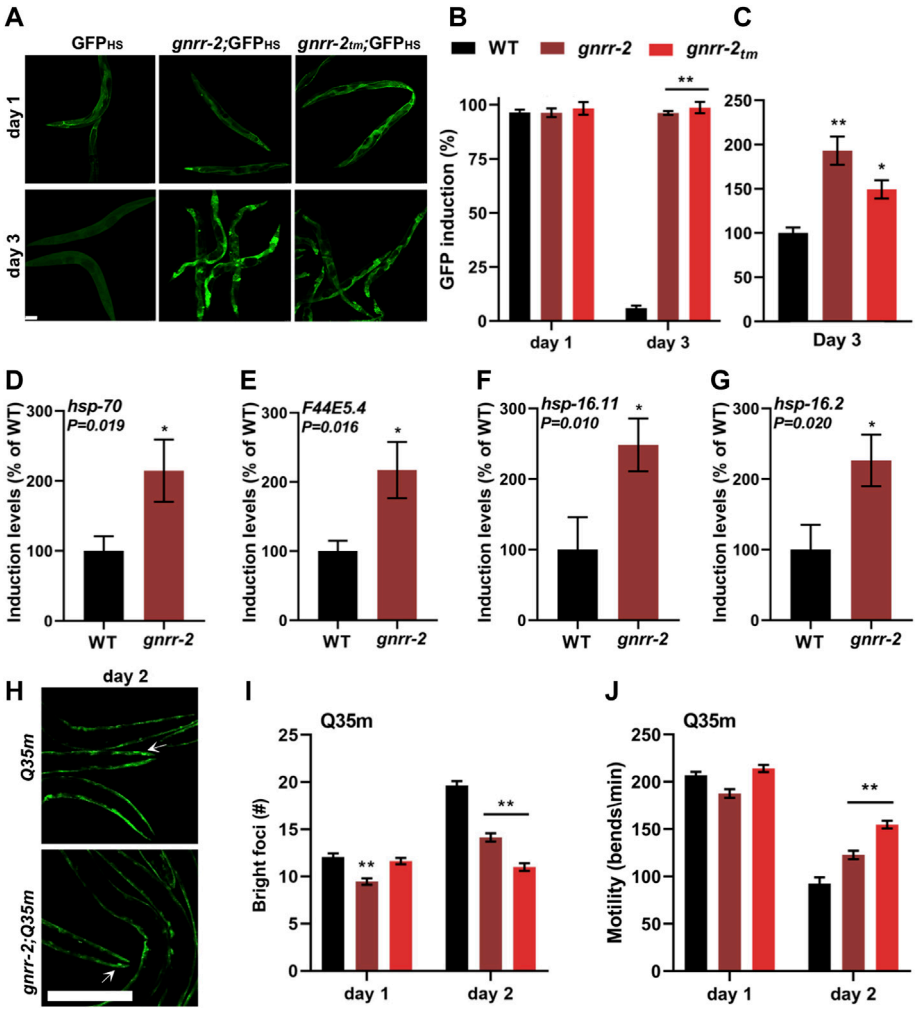


FIGURE 2
*gnrr-2* modulates HS response activation in adulthood. **(A–C)** HS-regulated $GFP_{HS}$ expression. Age-synchronized WT, *gnrr-2*, and *gnrr-2*$_{tm}$ animals expressing $GFP_{HS}$ were imaged following a short HS 90 min at 37°C **(A)**. The percent of animals showing GFP was scored $N \geq 3$ **(B)**, and GFP fluorescence levels (day three adults; $n > 10$) were determined **(C)**. Data are means ±1 standard error of the mean (1 SE). Data were analyzed using one-way ANOVA followed by a Tukey's *post-hoc* test. (**) denotes $p < 0.001$ compared with same-age WT animals. The scale bar is 100 µm. **(D–G)** Expression levels of HS genes. mRNA levels of *hsp-70* **(D)**, *F44E5.4* **(E)**, *hsp-16.11* **(F)**, and *hsp-16.2* **(G)** from age-synchronized WT or *gnrr-2* day two adults subjected to HS (90 min at 37°C; $N \geq 6$). Data are means ±1 standard error of the mean (1 SE). Data were analyzed using the Wilcoxon Mann-Whitney rank sum test ($p \leq 0.020$). **(H–J)** PolyQ foci number and motility in age-synchronized WT, *gnrr-2*, or *gnrr-2*$_{tm}$ animals expressing *Q35m*. Age-synchronized *Q35m* expressing animals were imaged on day two of adulthood **(H)**. The scale bar is 250 µm, and arrows indicate foci. The number of visible foci $n \geq 33$ **(I)** or thrashing rates $n \geq 35$ **(J)** were scored on day one or two of adulthood. Data are means ±1 standard error of the mean (1 SE). Data were analyzed using one-way ANOVA followed by a Tukey's *post-hoc* test. (**) denotes $p < 0.001$ compared with same-age Q35m animals.

than in WT animals (Wilcoxon Mann-Whitney rank sum test, $p \leq 0.02$; Figures 2D–G). Higher levels were not due to improved HSR activation. HS induction of these genes was reduced in WT between day two and day one adults (Wilcoxon Mann-Whitney rank sum test, $p \leq 0.037$; Supplementary Figures S2A–D), as previously demonstrated (Shemesh et al., 2013; Labbadia and Morimoto, 2015). In contrast, their expression was similarly induced in *gnrr-2* day one and two adults (*F44E5.4* expression improved; Supplementary Figures S2E–H). Thus, *gnrr-2* mutant animals maintain the ability to mount an effective HSR after the onset of reproduction rather than modulate HS activation efficacy.

The cell ability to maintain proteostasis in the face of chronic expression of misfolded proteins also declines with age (Ben-Zvi et al., 2009; Shemesh et al., 2013; Huang et al., 2019). To determine whether *gnrr-2* can modulate the accumulation and toxicity of misfolded proteins, we employed two polyQ protein aggregation models. Animals expressing 35 or 40 glutamine-

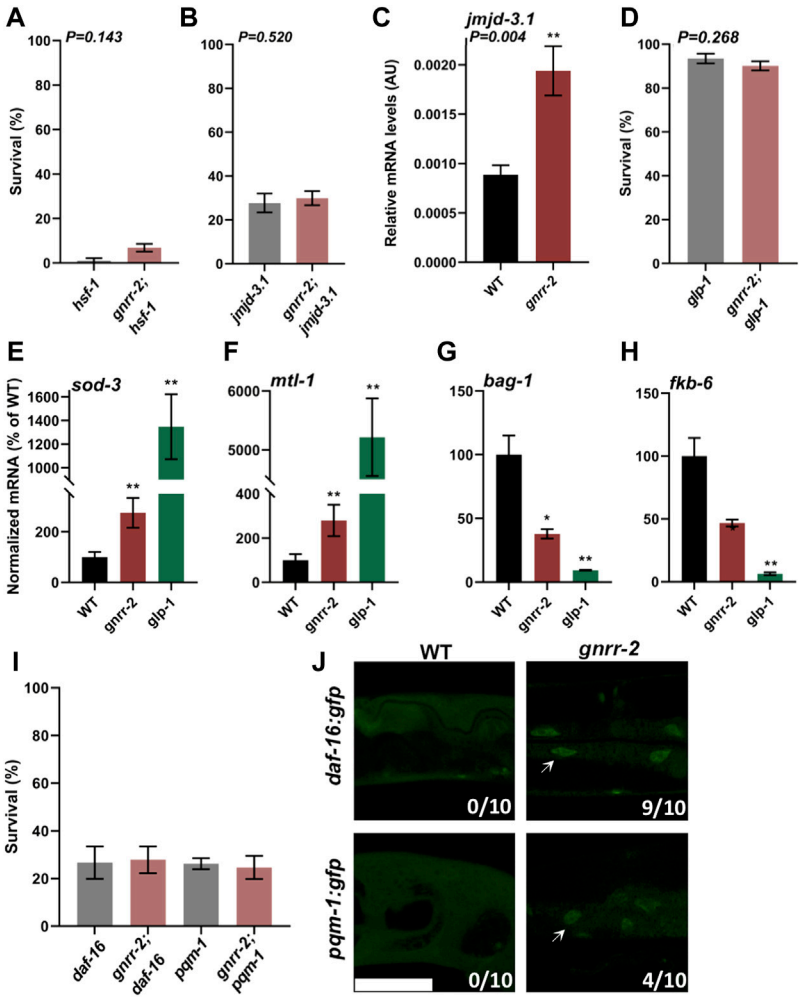


FIGURE 3
*gnrr-2* requires HSF-1, DAF-16, and PQM-1 to modulate somatic proteostasis. **(A,B)** HS Survival rates of age-synchronized *hsf-1(sy441)* and *gnrr-2;hsf-1* **(A)** or *jmjd-3.1(gk384)* and *gnrr-2;jmjd-3.1* **(B)** mutant animals. Animals grown at 15°C **(A)** or 25°C **(B)** were subjected to HS (6 h at 37°C) on day two of adulthood, and survival was assayed ($N \geq 6$). Data are means ±1 standard error of the mean (1 SE). Data were analyzed using the Wilcoxon Mann-Whitney rank sum test ($p = 0.143$ and $p = 0.520$, respectively). **(C)** *jmjd-3.1* expression levels in age-synchronized WT or *gnrr-2* animals. mRNA was extracted from day two adult animals, and *jmjd-3.1* mRNA levels were quantified ($N \geq 5$). Data are means ±1 standard error of the mean (1 SE). Data were analyzed using the Wilcoxon Mann-Whitney rank sum test ($p = 0.004$). **(D)** HS Survival rates of age-synchronized *glp-1(e2144)* or *gnrr-2;glp-1* mutant animals. Animals were subjected to HS (6 h at 37°C) on day two of adulthood, and survival was assayed ($N \geq 5$). Data are means ±1 standard error of the mean (1 SE). Data were analyzed using the Wilcoxon Mann-Whitney rank sum test ($p = 0.268$). **(E–H)** Expression levels of DAF-16 or PQM-1 targets in age-synchronized WT, *gnrr-2*, or *glp-1* animals. mRNA was extracted from day two adult animals, and mRNA levels of *sod-3* **(E)**, *mtl-1* **(F)**, *bag-1* **(G)**, and *fkb-6* **(H)** were quantified ($N \geq 5$). Data are means ±1 standard error of the mean (1 SE). Data were analyzed using the Wilcoxon Mann-Whitney rank-sum test with Bonferroni correction. (*) denotes $p \leq 0.01$ (**) denotes $p \leq 0.003$ compared with same-age WT animals. **(I)** HS Survival rates of age-synchronized *pqm-1(ok485)* or *daf-16(mu86)* mutant animals in a WT or *gnrr-2* background. Animals were subjected to HS (6 h at 37°C), and survival was assayed on day two of adulthood ($N \geq 4$). Data are means ±1 standard error of the mean (1 SE). Data were analyzed using one-way ANOVA followed by a Tukey's *post-hoc* test. **(J)** Representative images of age-synchronized animals expressing DAF-16::GFP or PQM-1::GFP in a WT or *gnrr-2* background. Day two adults were fixed, and the percentage of animals showing nuclear localization (arrows) was scored ($n = 10$ animals). The scale bar is 50 μm.

repeats fused to a fluorescent protein in body-wall muscles (Q35m) or neurons (Q40n), respectively. Animals were crossed with *gnrr-2* or *gnrr-2*$_{tm}$ mutant animals, and foci accumulation or toxicity were monitored. There were fewer bright foci in *gnrr-2*;Q35m and *gnrr-2*$_{tm}$;Q35m compared to same-age Q35m animals (14 ± 1 and 11 ± 1 compared to 21 ± 1, ANOVA followed by a Tukey's post-hoc test, $p \leq 0.001$; Figures 2H,I). In agreement, the motility of *gnrr-2*;Q35m, *gnrr-2*$_{tm}$;Q35m, and *gnrr-2*;Q40n animals, measured as thrashing rates, was more than 1.3-fold improved compared to Q35m and Q40n day two adults, respectively (ANOVA followed by a Tukey's post-hoc test, $p \leq 0.001$; Figure 2J;

Supplementary Figure S2I). We also observed reduced foci number and improved motility rates when Q35m animals were treated with *gnrr-2*(*RNAi*) compared to EV control (ANOVA followed by a Tukey's post-hoc test, $p \leq 0.001$; Supplementary Figures S2J–L). Finally, we examined two well-characterized folding reporters. Temperature-sensitive missense mutations in *unc-45*(*e286ts*) and *unc-52*(*e669*, *su250ts*) destabilize myofilament folding and anchoring, respectively, leading to age-dependent motility defects. Motility of *gnrr-2*; *unc-45*(*ts*) animals, measured as thrashing rate, was more than 2.2-fold improved compared to *unc-45*(*ts*) day two adults. Likewise, motility of animals expressing *unc-52*(*ts*) was 1.8-fold improved in day four adults treated with *gnrr-2*(*RNAi*) compared to EV control (Wilcoxon Mann-Whitney rank sum test; Supplementary Figures S2M–N). Taken together, we find that disrupting *gnrr-2* function or expression led to improved proteostasis during aging.

## *gnrr-2* functions in the gonadal longevity pathway

The decline in stress response activation after the onset of reproduction is linked to a repressed chromatin state at the promoters of HS genes. Specifically, HSF-1 transcriptional activation requires the H3K27 demethylase, JMJD-3.1, and its levels decline in WT animals at the transition to reproductive adulthood (Labbadia and Morimoto, 2015). To ask whether HSF-1 and JMJD-3.1 are required to maintain thermotolerance in *gnrr-2* mutant animals, we crossed *gnrr-2 with hsf-1*(*sy441*) or *jmjd-3.1*(*gk384*) mutant animals and examined their HS survival on day two of adulthood. As expected, we observed reduced survival rates for both *hsf-1* and *gnrr-2;hsf-1* mutant animals (4% ± 3% and 7% ± 2%, respectively, Wilcoxon Mann-Whitney rank sum test; Figure 3A). Likewise, HS survival rates of *gnrr-2;jmjd-3.1* double mutant animals were strongly reduced compared to *gnrr-2* (30% ± 3% compared to 66% ± 3%, respectively) and similar to *jmjd-3.1* single mutant (28% ± 4%, Wilcoxon Mann-Whitney rank sum test; Figure 3B). Activation of the gonadal longevity pathway restores *jmjd-3.1* levels (Labbadia and Morimoto, 2015; Shemesh et al., 2017a), while HS remodeling by dietary restriction does not (Shpigel et al., 2019). In agreement, the levels of *jmjd-3.1* mRNA on day two of adulthood in *gnrr-2* mutant animals were 2-fold higher than in WT animals (Wilcoxon Mann-Whitney rank sum test, $p = 0.004$; Figure 3C). These data suggest that *hsf-1* and *jmjd-3.1* are regulated by *gnrr-2* and support a role for *gnrr-2* in the gonadal longevity pathway.

Inhibition of germline stem cells (GSC) proliferation activates the gonadal longevity pathway and remodels proteostasis (Berman and Kenyon, 2006; Vilchez et al., 2012; Shemesh et al., 2013). To further examine whether *gnrr-2* acts *via* this pathway, we crossed *gnrr-2* mutant animals with *glp-1*(*e2141*), germline proliferation mutant animals, and monitored thermotolerance. The survival rate of the double mutants *gnrr-2;glp-1* was similar to that of *glp-1* mutant animals (6 h at 37°C; day two adults; 90% ± 2% and 93% ± 2%, respectively, Wilcoxon Mann-Whitney rank sum test; Figure 3D) and higher than *gnrr-2* single mutants. We observed similar behavior for *gnrr-2*(*RNAi*) treated animals even in prolonged HS (Supplementary Figure S3A). These data further support a role for *gnrr-2* in the gonadal longevity pathway. However, the lifespan of *gnrr-2* mutant animals was similar to WT (log-rank Mantel-Cox test, $p = 0.066$; Supplementary Figure S3B), as opposed to *glp-1* (Arantes-Oliveira et al., 2002). We, therefore, suggest that disrupting *gnrr-2* modulated some of the transcriptional pathways induced by germline loss.

GSC arrest triggers several transcriptional pathways associated with stress and metabolism, including DAF-16, DAF-12, SKN-1, PHA-4, HLH-30, and NHR-80 that are activated directly or as a result of downstream effectors (Berman and Kenyon, 2006; Gerisch et al., 2007; Goudeau et al., 2011; Lapierre et al., 2011; Tepper et al., 2013; Steinbaugh et al., 2015; Nakamura et al., 2016). To determine which transcription factors in the gonadal signaling pathway *gnrr-2* activates, we monitored the levels of target genes regulated by these downstream transcription factors after the onset of reproduction using qPCR. Of the eleven differentially regulated genes in germline proliferation mutant animals, only mRNA levels regulated by DAF-16 (*sod-1* and *mtl-1*) and PQM-1 (*bag-1* and *fkb-6*) were significantly modulated in *gnrr-2* day two adults (Wilcoxon Mann-Whitney rank-sum test with Bonferroni correction; Figures 3E–H; Supplementary Figures S3C–I). The increase in *sod-1* and *mtl-1* expression and decrease in *bag-1* and *fkb-6* expression in *gnrr-2* compared to WT day two adults were not affected by HS (90 min at 37°C; Supplementary Figures S3J–M). Moreover, crossing *daf-16*(*mu86*) or *pqm-1*(*ok485*) mutants with *gnrr-2* mutant animals abolished their thermotolerance (6 h at 37°C; day two adults; 27% ± 5% and 25% ± 5%, respectively, ANOVA followed by a Tukey's post-hoc test; Figure 3I). Monitoring the localization of DAF-16 or PQM-1 tagged with GFP showed that DAF-16 mainly localized to the nucleus in *gnrr-2* mutant animals, while PQM-1 only partially localized to the nucleus of *gnrr-2* mutant animals (Figure 3J). These data suggest that GNRR-2 regulates DAF-16 and PQM-1.

To ask whether *gnrr-2* regulates DAF-16 and PQM-1 specifically during adulthood, we compared the expression of *sod-1*, *mtl-1*, *bag-1*, and *fkb-6* in WT and *gnrr-2* mutants before the collapse. The expression levels of these four genes were not significantly different between *gnrr-2* and WT young adults (Wilcoxon Mann-Whitney rank sum test; Supplementary Figures S3N–Q). Of note, *gnrr-2* expression is upregulated in DAF-16-dependent manner, and *gnrr-2* promoter has a putative

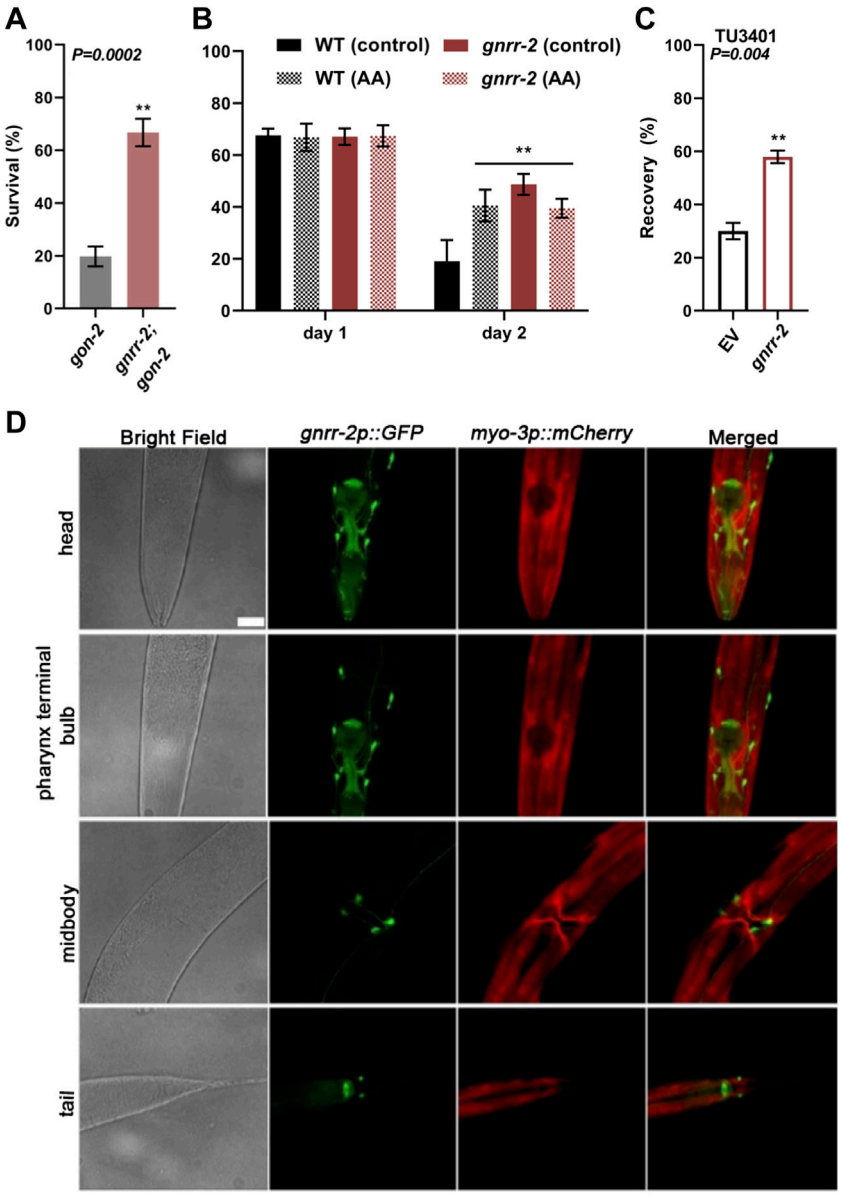


FIGURE 4
*gnrr-2* is expressed in the soma and function downstream of the gonad. **(A)** HS Survival rates of age-synchronized *gon-2* (*q388*) or *gnrr-2;gon-2* mutant animals. Day two adults were subjected to HS (6 h at 37°C), and survival was assayed ($N \geq 7$). Data are means ±1 standard error of the mean (1 SE). Data were analyzed using the Wilcoxon Mann-Whitney rank sum test ($p = 0.0002$). **(B)** HS Survival rates of age-synchronized WT or *gnrr-2* mutant animals grown on control or arachidonic acid (AA) supplemented plates. Animals were subjected to HS (6 h at 37°C) on day one or two of adulthood, and survival was assayed ($N \geq 3$). Data are means ±1 standard error of the mean (1 SE). Data were analyzed using one-way ANOVA followed by a Tukey's *post-hoc* test. (**) denotes $p \leq 0.006$ compared with same-age WT control animals. **(C)** HS recovery rates of age-synchronized neuronal RNAi hypersensitive animals fed on empty vector (EV) or *gnrr-2* RNAi-expressing bacteria. Day three adults were subjected to HS (4 h at 37°C), and recovery was assayed ($N \geq 5$). Data are means ±1 standard error of the mean (1 SE). Data were analyzed using the Wilcoxon Mann-Whitney rank sum test ($p = 0.004$). **(D)** *gnrr-2* expression. Representative confocal Z-stack images of young adults expressing *gnrr-2p::GFP* and marker, *myo-3p::mCherry*. Ventral views of head, pharynx terminal bulb, midbody, and tail. The scale bar is 25 μm.

DAF-16 binding element (Tepper et al., 2013), suggesting that DAF-16 could itself modulate *gnrr-2* expression. Our data, therefore, suggest that GNRR-2 functions in the gonadal longevity pathway and the somatic regulation of DAF-16 and PQM-1.

## *gnrr-2* functions downstream of the gonad

To ask whether *gnrr-2* mediates proteostasis collapse within the reproductive system or in the soma, we next

asked whether mutant *gnrr-2* rescue of HS survival rate required the reproductive system. For that, we crossed *gon-2(q388ts)* mutant animals lacking the entire reproductive system with *gnrr-2* mutant animals and monitored thermotolerance. As shown previously, HS survival rates of *gon-2* mutant animals declined sharply on day two of adulthood (6 h at 37°C, 20% ± 4%), similar to WT (Shemesh et al., 2013). In contrast, the HS survival rate of *gnrr-2;gon-2* mutant animals was higher than *gon-2* (67% ± 5%, Wilcoxon Mann-Whitney rank sum test, $p = 0.002$; Figure 4A), similar to *gnrr-2* (Figure 1B). These data demonstrate that *gnrr-2* impact is downstream of the reproductive system. To further examine whether *gnrr-2* acts in the soma, we monitored the impact of arachidonic acid (AA) supplementation, which remodels somatic proteostasis (Shemesh et al., 2017b), on the thermotolerance of *gnrr-2* mutants. HS survival rate of *gnrr-2* mutant animals treated by AA was not further improved compared to control-treated animals and was similar to AA treated WT animals (day two adults, 6 h at 37°C, 39% ± 4%, 49% ± 4%, and 40% ± 6% respectively, compared to 19% ± 8% for control-treated WT, ANOVA followed by a Tukey's post-hoc test; Figure 4B). Thus, mutant *gnrr-2* behaves similarly to a somatic modulator of the gonadal longevity pathway and does not require the gonad. Notably, *gnrr-2* differs from the embryo-to-mother signaling that requires the gonad and fertilized eggs to remodel somatic proteostasis (Sala et al., 2020). Taken together, our data suggest that *gnrr-2* functions in the soma downstream of the gonadal longevity signals.

We next ask whether GNRR-2 is expressed and functions in the soma (Figures 4C,D). We cloned GFP under the regulation of *gnrr-2* promoter (*gnrr-2p*::*GFP*) and examined the expression pattern of GFP. GFP was detected in the pharynx and specific neurons in the head, vulva, and tail regions (Figure 4D). Apart from the valval expression, GFP was observed throughout larval development (Supplementary Figure S4). Neuronal expression data from individual neurons supports this expression pattern (Taylor et al., 2021). For example, GFP expression was detected in the HSN vulval neurons showing *gnrr-2* expression. Thus, *gnrr-2* is expressed in the soma, mainly in neurons.

To determine whether proteostasis remodeling is associated with *gnrr-2* expression in neurons, we used a neuronal RNAi hypersensitive strain (TU3401) with a neuronal-specific expression of *sid-1* (Calixto et al., 2010). A transmembrane protein that enables passive uptake of dsRNA, and thus required for systemic RNAi. When HS recovery rates (4 h at 37°C, day three adults) were monitored, we observed an increased recovery for TU3401 animals treated with *gnrr-2(RNAi)* compared to EV control (58% ± 2% and 30 ± 3%, respectively, Wilcoxon Mann-Whitney rank-sum test, $p = 0.004$; Figure 4C). Thus, *gnrr-2* neuronal-expression can mediate proteostasis collapse.

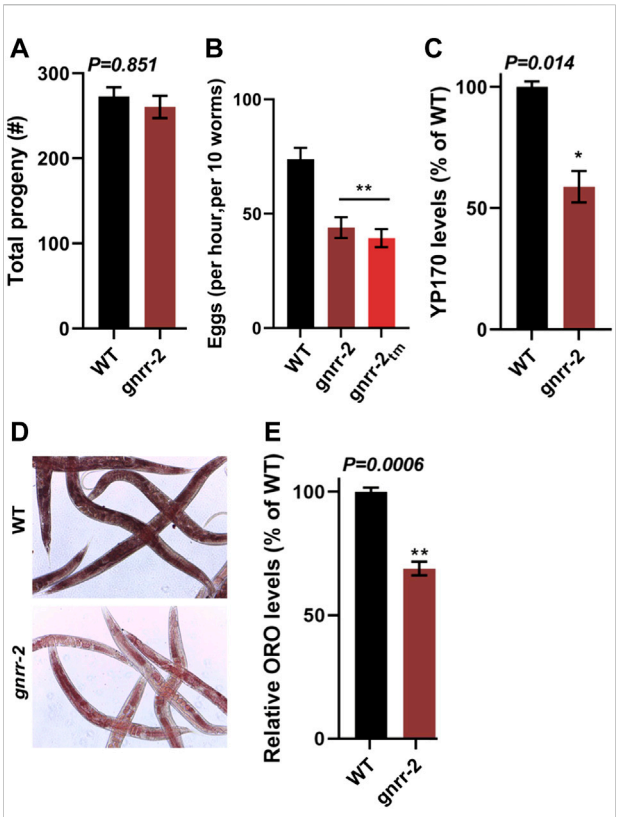


FIGURE 5
*gnrr-2* modulates reproduction. **(A)** Brood size of WT and *gnrr-2* animals. Progeny numbers were scored for age-synchronized fertile animals ($n \geq 18$). Data are means ±1 standard error of the mean (1 SE). Data were analyzed using the Wilcoxon Mann-Whitney rank sum test ($p = 0.851$). **(B)** Egg-laying rates of WT, *gnrr-2*, and *gnrr-2*$_{tm}$ animals. The number of eggs laid by ten age-synchronized day two adult animals per hour ($N \geq 11$). Data are means ±1 standard error of the mean (1 SE). Data were analyzed using one-way ANOVA followed by a Tukey's *post-hoc* test. (**) denotes $p \leq 0.001$ compared with WT animals. **(C)** Vitellogenin levels in age-synchronized WT and *gnrr-2* animals. Extracts of age-synchronized day two adult animals were separated on an SDS-PAGE gel and yolk protein (YP170) levels were quantified ($N = 4$). Data are means ±1 standard error of the mean (1 SE). Data were analyzed using the Wilcoxon Mann-Whitney rank sum test ($p = 0.014$). **(D,E)** Representative images and quantification of total fat stores in WT and *gnrr-2* mutant animals. Total fat stores in age-synchronized day two adult animals were imaged using ORO staining **(D)**, and ORO levels of WT ($n = 60$) or *gnrr-2* ($n = 71$) mutant animals were quantified from the images $N = 3$ **(E)**. Data are means ±1 standard error of the mean (1 SE). Data were analyzed using the Wilcoxon Mann-Whitney rank sum test ($p = 0.006$).

## *gnrr-2* modulates reproduction

GnRH-like signaling in invertebrates regulates various aspects of reproduction and associated reproductive treats (Sakai et al., 2020). Likewise, somatic activation of the gonadal longevity pathway is coupled with reproduction (Shemesh et al., 2017b). Thus, we next focused on the impact of *gnrr-2* on reproduction.

The brood size of *gnrr-2* mutant animals was similar to WT (260 ± 13 and 272 ± 10, respectively, Wilcoxon Mann-Whitney rank sum test; Figure 5A). Likewise, embryo hatching and developmental timing were similar between WT and *gnrr-2* mutant strains (ANOVA followed by a Tukey's post-hoc test; Supplementary Figures S5A–B). However, *gnrr-2* and *gnrr-2*$_{tm}$ mutant animals showed a ~1.7-fold reduction in the egg-laying rate (46 ± 4, 39 ± 4, and 71 ± 5 eggs per ten worms per hour, respectively, ANOVA followed by a Tukey's post-hoc test, $p \leq 0.001$; Figure 5B). In agreement with *gnrr-2* expression in HSN neurons that stimulate egg laying in hermaphrodites (Figure 4D). Moreover, RNAi hypersensitive (TU3401) animals treated with *gnrr-2*(*RNAi*) showed a mild (1.3-fold) reduction in the egg-laying rate compared to EV control, though TU3401 egg laying rate was also reduced (Wilcoxon Mann-Whitney rank-sum test, $p = 0.046$; Supplementary Figure S6A). A reduction in the egg-laying rate was also observed between the *gnrr-2*;*daf-16*, and *daf-16* mutant animals (30 ± 3 and 67 ± 9 eggs per ten worms per hour, respectively, ANOVA followed by a Tukey's post-hoc test. $p \leq 0.001$; Supplementary Figure S6B). In contrast, the egg-laying rates of *gnrr-2*;*pqm-1*, and *pqm-1* mutant animals (48 ± 6 and 45 ± 5 eggs per ten worms per hour, respectively) were similar to *gnrr-2* mutant animals (ANOVA followed by a Tukey's *post-hoc* test; Supplementary Figure S6B). This observation suggests that *gnrr*-2-dependent modulation of PQM-1 function (Figures 3G–J) could impact the animals' egg-laying rate.

GnRH-like signaling in invertebrates modulates vitellogenin (*vit*) gene expression (Gospocic et al., 2017; Nagel et al., 2020). *C. elegans* has six *vit* genes (*vit-1* to *vit-6*), mainly synthesized in the intestine and transported into the germline. Their expression is regulated in the intestine and is modulated by cell-nonautonomous signals from other tissues and in response to environmental cues (Ezcurra et al., 2018; Perez and Lehner, 2019; Sornda et al., 2019; Plagens et al., 2021). We, therefore, next examine the levels of VIT proteins in *gnrr-2* mutant animals. The levels of YP170 (the product of *vit-1* to *vit-5*) in *gnrr-2* mutant animals were reduced compared to WT (65% ± 8%, Wilcoxon Mann-Whitney rank sum test, $p = 0.014$; Figure 5C; Supplementary Figure S6C). Surprisingly, *vit-2* and *vit-3/4/5* mRNA (but not *vit-6*) levels were increased by ~2-fold in *gnrr-2* mutant animals but not in *gnrr-2*;*daf-16* or *gnrr-2*;*pqm-1* mutant animals (ANOVA followed by a Tukey's post-hoc test; Supplementary Figures S6D–F). These changes in expression suggest that disrupting *gnrr-2* dysregulates VIT production with a possible contribution from *daf-16* and *pqm-1*. We next compared fat stores in WT and *gnrr-2* mutant animals to complement this observation. Oil-Red-O (ORO) fatty acids staining in *gnrr-2* mutant animals was also reduced compared to WT (69% ± 3%, Wilcoxon Mann-Whitney rank sum test, $p = 0.006$; Figures 5D,E), further supporting *gnrr-2* impact on VIT production and fat accumulation. Of note, we observe a significant increase in Oil-Red-O staining in *gnrr-2*;*pqm-1* mutant animals (119% ± 3%, ANOVA followed by a Tukey's post-hoc test. $p \leq 0.001$; Supplementary Figure S6G). This increase further links PQM-1 to GNRR-2-dependent *vit* gene regulation.

# Discussion

## GNRR-2 is involved in the decision to commit to reproduction

In *C. elegans*, a decision point at the onset of oogenesis regulates somatic proteostasis robustness in different somatic tissues (Shemesh et al., 2013; Labbadia and Morimoto, 2015). It also directs fat reserve usage to support reproduction by mobilizing fat stores from the intestine to the germline (Wang et al., 2008; Lapierre et al., 2011; Shemesh et al., 2017b; Dowen, 2019; Heimbucher et al., 2020). Here we asked whether GnRH-like signaling, which regulates reproduction and reproductive behaviors in various invertebrates (Zandawala et al., 2018; Sakai et al., 2020), promotes proteostasis remodeling. We identified a GnRH-like GPCR, *gnrr-2*, as a modifier of proteostasis in adulthood (Figures 1–3; Supplementary Figures S2–S3). *gnrr-2* also modulated egg-laying rates and vitellogenesis (Figure 5; Supplementary Figure S6). We determine that *gnrr-2* acts in the soma, specifically neurons (Figures 3, 4). We propose that neuronal *gnrr-2* responds to gonadal signaling and coordinates the somatic response to these signals, inversely modulating proteostasis and reproductive robustness, thus committing the organism to reproduction (Figure 6A). Other activating or repressing signals are likely to contribute to GNRR-2 function, as thermotolerance decline in gonad-less animals depends on GNRR-2 activity (Figure 4A). When GNRR-2 is inactivated or downregulated, gonadal (or other) signals are transmitted. However, they are no longer mediated to the soma, robust proteostasis is maintained, and resource transfer to progeny production is limited due to the modulation of different somatic transcriptional programs (Figure 6B). Our findings, therefore, support the emerging role of the nervous system, specifically neuropeptide signaling, in coordinating proteostasis across somatic tissues (Prahlad et al., 2008; Maman et al., 2013; Frakes et al., 2020; Hoppe and Cohen, 2020; Ozbey et al., 2020; Prahlad, 2020; Boocholez et al., 2022).

## GNRR-2 is required for remodeling proteostasis and reproduction at the onset of oogenesis

The decision to commit the organism to reproduction depends on nutrient availability, germline and embryo reproductive potency, and favorable environmental conditions (Maklakov and Immler, 2016; Aprison et al., 2022; Sala and Morimoto, 2022). This decision thus requires integrating internal and external signals to weigh the chances to reproduce successfully before reallocating metabolic

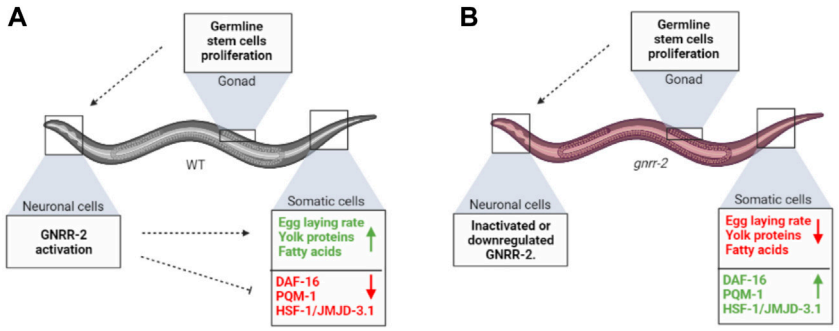


FIGURE 6
*gnrr-2* mediates signals from the reproductive system to the soma. **(A)** At the onset of WT oogenesis, gonadal signaling reports on GSCs' competence to neuronal *gnrr-2*, who coordinately activates or represses various transcriptional programs in the soma, inversely modulating somatic maintenance and reproductive robustness. **(B)** Disrupting GNRR-2 function alters these signals, resulting in inhibition of proteostasis collapse and inhibition of somatic resources reallocation to the reproductive system. The figure was created using BioRender.com.

resources (Antebi, 2013; Baugh and Hu, 2020; Gaddy et al., 2021; Aprison et al., 2022). Several at least partially independent pathways mediate proteostasis remodeling specifically in adulthood; gonadal longevity signaling reports on germline reproductive potency (Berman and Kenyon, 2006; Ermolaeva et al., 2013; Shemesh et al., 2017a; Yunger et al., 2017), an embryo-to-mother pathway reports on embryo integrity (Sala et al., 2020), and dietary signaling reports on nutrient availability (Tepper et al., 2013; Thondamal et al., 2014; Steinbaugh et al., 2015; Nakamura et al., 2016; Matai et al., 2019; Shpigel et al., 2019). The inhibition of proliferation or damage to germ cells results in DAF-16 nuclear localization and activation (Berman and Kenyon, 2006; Shemesh et al., 2017a; Yunger et al., 2017). It upregulates the expression of H3K27 demethylase *jmjd-3.1*, required for chromatin accessibility and HSF-1 transcriptional activation (Labbadia and Morimoto, 2015; Shemesh et al., 2017a). Likewise, disrupting embryo integrity activates DAF-16, albite only in vulval muscle (Sala et al., 2020). In contrast, dietary restriction requires *pqm-1* and modulates HSF-1 activation even late in life, independent from *jmjd-3.1* (Tepper et al., 2013; Shpigel et al., 2019). PQM-1 also mediates transcellular chaperone signaling that regulates inter-tissue proteostasis (O'Brien et al., 2018). Like gonadal signaling, mutations in *gnrr-2* resulted in upregulation of *jmjd-3.1* and required *jmjd-3.1* for HSR activation (Figure 3). Likewise, disrupting *gnrr-2* led to DAF-16 relocation to the nucleus and activation after the onset of reproduction. However, it also resulted in partial nuclear localization and activation of PQM-1 (Figure 3; Supplementary Figure S3). This dual requirement is unexpected because DAF-16 and PQM-1 function and localization are antagonistic (Tepper et al., 2013). However, *daf-16* and *pqm-1* are also required for insulin/IGF-1-like signaling and *ceh-60*-associated longevity (Tepper et al., 2013; Dowen, 2019). Moreover, both can regulate vitellogenesis (DePina et al., 2011; Dowen, 2019; Perez and Lehner, 2019; Heimbucher et al., 2020). Interestingly, DAF-16 could also modulate *gnrr-2* expression (Tepper et al., 2013). GNRR-2 activation may thus fine-tune DAF-16 and PQM-1 function to adjust somatic proteostasis and reproduction to various signals rather than act as an on/off switch.

GNRR-2 is expressed and potentially functions in neurons to regulate proteostasis and reproduction. Disrupting *gnrr-2* expression or function in gonad-less animals or specifically in neurons still remodeled proteostasis in adulthood (Figure 4). Moreover, arachidonic acid, a somatic regulator of the gonadal longevity signaling (Shemesh et al., 2017b), did not further improve *gnrr-2*-dependent HS survival rates. Likewise, the effect of GNRR-2 on egg-laying rate was in agreement with its expression in HSN neurons that stimulate egg-laying in hermaphrodites [and modulated by neuronal-specific *gnrr-2*(*RNAi*)]. Moreover, GNRR-2 modulated vitellogenin production, mainly synthesized in the intestine, and reduced YP170 protein levels and fat stores in *gnrr-2* mutant animals could be linked to DAF-16 and PQM-1 activation in the intestine. Nevertheless, other signaling pathways could also be involved (Wang et al., 2008; Dowen, 2019; Perez and Lehner, 2019; Sornda et al., 2019; Heimbucher et al., 2020). Thus, while GNRR-2 likely functions in neurons, tissue-specific expression of *gnrr-2* in the *gnrr-2* mutant background is needed to determine where GNRR-2 acts and whether proteostasis and reproduction regulation differ.

## GNRR-2 has a GnRH-like role, mediating reproduction-fitness trade-offs

In invertebrates, members of the GnRH superfamily neuropeptide signaling show pleiotropic activities (Zandawala et al., 2018; Sakai et al., 2020). Recently non-reproductive functions were also linked to GnRH and the pituitary gonadotropin, follicle-stimulating hormone, FSH, in vertebrates, including modulating Alzheimer's disease-associated amyloid-β and Tau deposition (Skrapits et al., 2021; Xiong et al., 2022). However, many members regulate

reproductive functions and metabolism, modulating reproduction-fitness trade-offs (Zandawala et al., 2018; Sakai et al., 2020). Specifically, members of the GnRH superfamily regulate brood size, egg-laying rates, vitellogenesis, mating behaviors, and even social reproductive behaviors such as cast identity in insects (Lindemans et al., 2009; Lebreton et al., 2016; Gospocic et al., 2017; Andreatta et al., 2020; Sakai et al., 2020). In *C. elegans*, there are eight members of this family, four of which were deorphanized. However, DAF-38/GNRR-8 functions with DAF-37 to mediate dauer entry in response to ascaroside pheromones (Park et al., 2012), while GNRR-3 and GNRR-6 regulate sleep and wakefulness in response to RPamide neuropeptides NLP-2 and NLP-22 (Van der Auwera et al., 2020). RPamide peptides share sequence similarity with GnRH/AKH peptides (Van der Auwera et al., 2020). However, only GNRR-1 was shown to respond to GnRH/AKH neuropeptide ortholog, NLP-47 (Lindemans et al., 2009). GNRR-1 is expressed in the nucleus of maturing oocytes and sperm cells and delayed egg-laying, supporting a GnRH-like role in modulating reproduction (Vadakkadath Meethal et al., 2006). But *gnrr-1* did not affect HS survival rates at the transition to adulthood (Figure 1). Thus, *gnrr* genes in *C. elegans* diverged both in function and peptide specificity.

The ability of a *C. elegans* peptide library to activate the GNRR-2 receptor was examined using an *in vitro* calcium mobilization assay, but no putative ligands were identified (Van der Auwera et al., 2020). Thus, while we find that GNRR-2 function is linked to GnRH-associated reproductive functions, such as egg-laying rates and vitellogenesis, it remains to be determined whether it responds to a GnRH neuropeptide ortholog. Likewise, the role of GNRR-6 in HSR modulation needs to be further examined, specifically whether this function is associated with sleep and wakefulness regulation by NLP-2 and NLP-22 or by a different neuropeptide. In this regard, it is interesting to note that GNRR-6 also responded to the FRPamide neuropeptide, NLP-23-2, *in vitro,* but *nlp-23* did not impact behavioral quiescence (Van der Auwera et al., 2020). NLP-23 could thus be a modulator of the HSR. Other neuropeptides were shown to modulate proteostasis (Frakes et al., 2020; Hoppe and Cohen, 2020; Ozbey et al., 2020; Prahlad, 2020; Boocholez et al., 2022) and might be linked to *gnrr-2*-depednent proteostasis remolding. Considering the conservation of proteostasis collapse (Sabath et al., 2020), understanding how non-autonomous signaling pathways integrate to modulate somatic proteostasis in *C. elegans* could offer novel approaches for treating age-dependent protein folding diseases. The findings that GnRH and FSH have non-reproductive functions and could modulate Alzheimer's disease (Skrapits et al., 2021; Xiong et al., 2022), further stresses the importance of non-autonomous signaling pathways in regulating proteostasis.

## Data availability statement

The raw data supporting the conclusion of this article will be made available by the authors, without undue reservation.

## Author contributions

Conceptualization, MK, LH, and AB-Z; Experimental design, MK, LH, and AB-Z; Data acquisition, MK, LH, TM, AP, and LM; Data analysis, MK, TM, and AB-Z; Writing and revising the text, MK and AB-Z. All authors read and approved the final manuscript.

## Funding

This study was funded by the Binational Science Foundation (BSF) grant 2017241 to AB-Z. MK was supported by the Ministry of Science and Technology, Levi Eshkol Ph.D. fellowship (3-16593). LM was supported by the Ministry of Science and Technology, Yitzhak Navon Ph.D. fellowship (3-16627), and Kreitman Biotech scholarship.

## Acknowledgments

We thank Prof. Isabel Beets for sharing unpublished data and discussions. Some nematode strains used in this work were provided by the Caenorhabditis Genetics Center, which is funded by the NIH National Center for Research Resources (NCRR).

## Conflict of interest

The authors declare that the research was conducted in the absence of any commercial or financial relationships that could be construed as a potential conflict of interest.

## Publisher's note



## Supplementary material

The Supplementary Material for this article can be found online at: https://www.frontiersin.org/articles/10.3389/fcell.2022.951199/full#supplementary-material

# References


Aman, Y., Schmauck-Medina, T., Hansen, M., Morimoto, R. I., Simon, A. K., Bjedov, I., et al. (2021). Autophagy in healthy aging and disease. *Nat. Aging* 1 (8), 634–650. doi:10.1038/s43587-021-00098-4

Andreatta, G., Broyart, C., Borghgraef, C., Vadiwala, K., Kozin, V., Polo, A., et al. (2020). Corazonin signaling integrates energy homeostasis and lunar phase to regulate aspects of growth and sexual maturation in Platynereis. *Proc. Natl. Acad. Sci. U. S. A.* 117 (2), 1097–1106. doi:10.1073/pnas.1910262116

Antebi, A. (2013). Regulation of longevity by the reproductive system. *Exp. Gerontol.* 48 (7), 596–602. doi:10.1016/j.exger.2012.09.009

Aprison, E. Z., Dzitoyeva, S., Angeles-Albores, D., and Ruvinsky, I. (2022). A male pheromone that improves the quality of the oogenic germline. *Proc. Natl. Acad. Sci. U. S. A.* 119 (21), e2015576119. doi:10.1073/pnas.2015576119

Arantes-Oliveira, N., Apfeld, J., Dillin, A., and Kenyon, C. (2002). Regulation of life-span by germ-line stem cells in *Caenorhabditis elegans*. *Science* 295 (5554), 502–505. doi:10.1126/science.1065768

Baugh, L. R., and Hu, P. J. (2020). Starvation responses throughout the *Caenorhabditis elegans* life cycle. *Genetics* 216 (4), 837–878. doi:10.1534/genetics.120.303565

Ben-Zvi, A., Miller, E. A., and Morimoto, R. I. (2009). Collapse of proteostasis represents an early molecular event in *Caenorhabditis elegans* aging. *Proc. Natl. Acad. Sci. U. S. A.* 106 (35), 14914–14919. doi:10.1073/pnas.0902882106

Berman, J. R., and Kenyon, C. (2006). Germ-cell loss extends *C. elegans* life span through regulation of DAF-16 by kri-1 and lipophilic-hormone signaling. *Cell* 124 (5), 1055–1068. doi:10.1016/j.cell.2006.01.039

Boocholez, H., Marques, F. C., Levine, A., Roitenberg, N., Siddiqui, A. A., Zhu, H., et al. (2022). Neuropeptide signaling and SKN-1 orchestrate differential responses of the proteostasis network to dissimilar proteotoxic insults. *Cell Rep.* 38 (6), 110350. doi:10.1016/j.celrep.2022.110350

Brehme, M., Voisine, C., Rolland, T., Wachi, S., Soper, J. H., Zhu, Y., et al. (2014). A chaperome subnetwork safeguards proteostasis in aging and neurodegenerative disease. *Cell Rep.* 9 (3), 1135–1150. doi:10.1016/j.celrep.2014.09.042

Calixto, A., Chelur, D., Topalidou, I., Chen, X., and Chalfie, M. (2010). Enhanced neuronal RNAi in *C. elegans* using SID-1. *Nat. Methods* 7 (7), 554–559. doi:10.1038/nmeth.1463

Cohen-Berkman, M., Dudkevich, R., Ben-Hamo, S., Fishman, A., Salzberg, Y., Waldman Ben-Asher, H., et al. (2020). Endogenous siRNAs promote proteostasis and longevity in germline-less *Caenorhabditis elegans*. *Elife* 9, e50896. doi:10.7554/eLife.50896

Consortium, C. e. D. M. (2012). large-scale screening for targeted knockouts in the *Caenorhabditis elegans* genome. *G3 (Bethesda)* 2 (11), 1415–1425. doi:10.1534/g3.112.003830

DePina, A. S., Iser, W. B., Park, S. S., Maudsley, S., Wilson, M. A., and Wolkow, C. A. (2011). Regulation of *Caenorhabditis elegans* vitellogenesis by DAF-2/IIS through separable transcriptional and posttranscriptional mechanisms. *BMC Physiol.* 11, 11. doi:10.1186/1472-6793-11-11

Dowen, R. H. (2019). CEH-60/PBX and UNC-62/MEIS coordinate a metabolic switch that supports reproduction in *C. elegans*. *Dev. Cell* 49 (2), 235–250.e7. doi:10.1016/j.devcel.2019.03.002

Dror, S., Meidan, T. D., Karady, I., and Ben-Zvi, A. (2020). Using *Caenorhabditis elegans* to screen for tissue-specific chaperone interactions. *J. Vis. Exp.* 160, e61140. doi:10.3791/61140

Ermolaeva, M. A., Segref, A., Dakhovnik, A., Ou, H. L., Schneider, J. I., Utermohlen, O., et al. (2013). DNA damage in germ cells induces an innate immune response that triggers systemic stress resistance. *Nature* 501 (7467), 416–420. doi:10.1038/nature12452

Ezcurra, M., Benedetto, A., Sornda, T., Gilliat, A. F., Au, C., Zhang, Q., et al. (2018). *C. elegans* eats its own intestine to make yolk leading to multiple senescent pathologies. *Curr. Biol.* 28 (16), 2544–2556.e5. e2545. doi:10.1016/j.cub.2018.06.035

Frakes, A. E., Metcalf, M. G., Tronnes, S. U., Bar-Ziv, R., Durieux, J., Gildea, H. K., et al. (2020). Four glial cells regulate ER stress resistance and longevity via neuropeptide signaling in *C. elegans*. *Science* 367 (6476), 436–440. doi:10.1126/science.aaz6896

Gaddy, M. A., Kuang, S., Alfhili, M. A., and Lee, M. H. (2021). The soma-germline communication: Implications for somatic and reproductive aging. *BMB Rep.* 54 (5), 253–259. doi:10.5483/bmbrep.2021.54.5.198

Gerisch, B., Rottiers, V., Li, D., Motola, D. L., Cummins, C. L., Lehrach, H., et al. (2007). A bile acid-like steroid modulates *Caenorhabditis elegans* lifespan through nuclear receptor signaling. *Proc. Natl. Acad. Sci. U. S. A.* 104 (12), 5014–5019. doi:10.1073/pnas.0700847104

Gospocic, J., Shields, E. J., Glastad, K. M., Lin, Y., Penick, C. A., Yan, H., et al. (2017). The neuropeptide corazonin controls social behavior and caste identity in ants. *Cell* 170 (4), 748–759.e12. e712. doi:10.1016/j.cell.2017.07.014

Goudeau, J., Bellemin, S., Toselli-Mollereau, E., Shamalnasab, M., Chen, Y., and Aguilaniu, H. (2011). Fatty acid desaturation links germ cell loss to longevity through NHR-80/HNF4 in *C. elegans*. *PLoS Biol.* 9 (3), e1000599. doi:10.1371/journal.pbio.1000599

Heimbucher, T., Hog, J., Gupta, P., and Murphy, C. T. (2020). PQM-1 controls hypoxic survival via regulation of lipid metabolism. *Nat. Commun.* 11 (1), 4627. doi:10.1038/s41467-020-18369-w

Hoppe, T., and Cohen, E. (2020). Organismal protein homeostasis mechanisms. *Genetics* 215 (4), 889–901. doi:10.1534/genetics.120.301283

Huang, C., Wagner-Valladolid, S., Stephens, A. D., Jung, R., Poudel, C., Sinnige, T., et al. (2019). Intrinsically aggregation-prone proteins form amyloid-like aggregates and contribute to tissue aging in *Caenorhabditis elegans*. *Elife* 8, e43059. doi:10.7554/eLife.43059

Karady, I., Frumkin, A., Dror, S., Shemesh, N., Shai, N., and Ben-Zvi, A. (2013). Using *Caenorhabditis elegans* as a model system to study protein homeostasis in a multicellular organism. *J. Vis. Exp.* 82, e50840. doi:10.3791/50840

Labbadia, J., Brielmann, R. M., Neto, M. F., Lin, Y. F., Haynes, C. M., and Morimoto, R. I. (2017). Mitochondrial stress restores the heat shock response and prevents proteostasis collapse during aging. *Cell Rep.* 21 (6), 1481–1494. doi:10.1016/j.celrep.2017.10.038

Labbadia, J., and Morimoto, R. I. (2015). Repression of the heat shock response is a programmed event at the onset of reproduction. *Mol. Cell* 59 (4), 639–650. doi:10.1016/j.molcel.2015.06.027

Lapierre, L. R., Gelino, S., Melendez, A., and Hansen, M. (2011). Autophagy and lipid metabolism coordinately modulate life span in germline-less *C. elegans*. *Curr. Biol.* 21 (18), 1507–1514. doi:10.1016/j.cub.2011.07.042

Lebreton, S., Mansourian, S., Bigarreau, J., and Dekker, T. (2016). The adipokinetic hormone receptor modulates sexual behavior, pheromone perception and pheromone production in a sex-specific and starvation-dependent manner in *Drosophila melanogaster*. *Front. Ecol. Evol.* 3. doi:10.3389/fevo.2015.00151

Li, J., Labbadia, J., and Morimoto, R. I. (2017). Rethinking HSF1 in stress, development, and organismal health. *Trends Cell Biol.* 27 (12), 895–905. doi:10.1016/j.tcb.2017.08.002

Lindemans, M., Liu, F., Janssen, T., Husson, S. J., Mertens, I., Gade, G., et al. (2009). Adipokinetic hormone signaling through the gonadotropin-releasing hormone receptor modulates egg-laying in *Caenorhabditis elegans*. *Proc. Natl. Acad. Sci. U. S. A.* 106 (5), 1642–1647. doi:10.1073/pnas.0809881106

Maklakov, A. A., and Immler, S. (2016). The expensive germline and the evolution of ageing. *Curr. Biol.* 26 (13), R577–R586. doi:10.1016/j.cub.2016.04.012

Maman, M., Carvalhal Marques, F., Volovik, Y., Dubnikov, T., Bejerano-Sagie, M., and Cohen, E. (2013). A neuronal GPCR is critical for the induction of the heat shock response in the nematode *C. elegans*. *J. Neurosci.* 33 (14), 6102–6111. doi:10.1523/JNEUROSCI.4023-12.2013

Matai, L., Sarkar, G. C., Chamoli, M., Malik, Y., Kumar, S. S., Rautela, U., et al. (2019). Dietary restriction improves proteostasis and increases life span through endoplasmic reticulum hormesis. *Proc. Natl. Acad. Sci. U. S. A.* 116 (35), 17383–17392. doi:10.1073/pnas.1900055116

Meller, A., and Shalgi, R. (2021). The aging proteostasis decline: From nematode to human. *Exp. Cell Res.* 399 (2), 112474. doi:10.1016/j.yexcr.2021.112474

Meshnik, L., Bar-Yaacov, D., Kasztan, D., Neiger, T., Cohen, T., Kishner, M., et al. (2022). Mutant *C. elegans* mitofusin leads to selective removal of mtDNA heteroplasmic deletions across generations to maintain fitness. *BMC Biol.* 20 (1), 40. doi:10.1186/s12915-022-01241-2

Morimoto, R. I. (2020). Cell-nonautonomous regulation of proteostasis in aging and disease. *Cold Spring Harb. Perspect. Biol.* 12 (4), a034074. doi:10.1101/cshperspect.a034074

Nagel, M., Qiu, B., Brandenborg, L. E., Larsen, R. S., Ning, D., Boomsma, J. J., et al. (2020). The gene expression network regulating queen brain remodeling after insemination and its parallel use in ants with reproductive workers. *Sci. Adv.* 6 (38), eaaz5772. doi:10.1126/sciadv.aaz5772

Nakamura, S., Karalay, O., Jager, P. S., Horikawa, M., Klein, C., Nakamura, K., et al. (2016). Mondo complexes regulate TFEB via TOR inhibition to promote longevity in response to gonadal signals. *Nat. Commun.* 7, 10944. doi:10.1038/ncomms10944

O'Brien, D., Jones, L. M., Good, S., Miles, J., Vijayabaskar, M. S., Aston, R., et al. (2018). A PQM-1-mediated response triggers transcellular chaperone signaling and regulates organismal proteostasis. *Cell Rep.* 23 (13), 3905–3919. doi:10.1016/j.celrep.2018.05.093

O'Rourke, E. J., Soukas, A. A., Carr, C. E., and Ruvkun, G. (2009). *C. elegans* major fats are stored in vesicles distinct from lysosome-related organelles. *Cell Metab.* 10 (5), 430–435. doi:10.1016/j.cmet.2009.10.002

Ozbey, N. P., Imanikia, S., Krueger, C., Hardege, I., Morud, J., Sheng, M., et al. (2020). Tyramine acts downstream of neuronal XBP-1s to coordinate inter-tissue UPR(ER) activation and behavior in *C. elegans*. *Dev. Cell* 55, 754–770.e6. doi:10.1016/j.devcel.2020.10.024

Park, D., O'Doherty, I., Somvanshi, R. K., Bethke, A., Schroeder, F. C., Kumar, U., et al. (2012). Interaction of structure-specific and promiscuous G-protein-coupled receptors mediates small-molecule signaling in *Caenorhabditis elegans*. *Proc. Natl. Acad. Sci. U. S. A.* 109 (25), 9917–9922. doi:10.1073/pnas.1202216109

Perez, M. F., and Lehner, B. (2019). Vitellogenins - yolk gene function and regulation in *Caenorhabditis elegans*. *Front. Physiol.* 10, 1067. doi:10.3389/fphys.2019.01067

Plagens, R. N., Mossiah, I., Kim Guisbert, K. S., and Guisbert, E. (2021). Chronic temperature stress inhibits reproduction and disrupts endocytosis via chaperone titration in *Caenorhabditis elegans*. *BMC Biol.* 19 (1), 75. doi:10.1186/s12915-021-01008-1

Prahlad, V., Cornelius, T., and Morimoto, R. I. (2008). Regulation of the cellular heat shock response in *Caenorhabditis elegans* by thermosensory neurons. *Science* 320 (5877), 811–814. doi:10.1126/science.1156093

Prahlad, V. (2020). The discovery and consequences of the central role of the nervous system in the control of protein homeostasis. *J. Neurogenet.* 34 (3-4), 489–499. doi:10.1080/01677063.2020.1771333

Sabath, N., Levy-Adam, F., Younis, A., Rozales, K., Meller, A., Hadar, S., et al. (2020). Cellular proteostasis decline in human senescence. *Proc. Natl. Acad. Sci. U. S. A.* 117, 31902–31913. doi:10.1073/pnas.2018138117

Sakai, T., Yamamoto, T., Matsubara, S., Kawada, T., and Satake, H. (2020). Invertebrate gonadotropin-releasing hormone receptor signaling and its relevant biological actions. *Int. J. Mol. Sci.* 21 (22), E8544. doi:10.3390/ijms21228544

Sala, A. J., Bott, L. C., Brielmann, R. M., and Morimoto, R. I. (2020). Embryo integrity regulates maternal proteostasis and stress resilience. *Genes Dev.* 34 (9-10), 678–687. doi:10.1101/gad.335422.119

Sala, A. J., and Morimoto, R. I. (2022). Protecting the future: Balancing proteostasis for reproduction. *Trends Cell Biol.* 32 (3), 202–215. doi:10.1016/j.tcb.2021.09.009

Shemesh, N., Meshnik, L., Shpigel, N., and Ben-Zvi, A. (2017a). Dietary-induced signals that activate the gonadal longevity pathway during development regulate a proteostasis switch in *Caenorhabditis elegans* adulthood. *Front. Mol. Neurosci.* 10, 254. doi:10.3389/fnmol.2017.00254

Shai, N., Shemesh, N., and Ben-Zvi, A. (2014). Remodeling of proteostasis upon transition to adulthood is linked to reproduction onset. *Curr. Genomics* 15 (2), 122–129. doi:10.2174/1389202915666140221005023

Shemesh, N., Jubran, J., Dror, S., Simonovsky, E., Basha, O., Argov, C., et al. (2021). The landscape of molecular chaperones across human tissues reveals a layered architecture of core and variable chaperones. *Nat. Commun.* 12 (1), 2180. doi:10.1038/s41467-021-22369-9

Shemesh, N., Shai, N., and Ben-Zvi, A. (2013). Germline stem cell arrest inhibits the collapse of somatic proteostasis early in *Caenorhabditis elegans* adulthood. *Aging Cell* 12 (5), 814–822. doi:10.1111/acel.12110

Shemesh, N., Shai, N., Meshnik, L., Katalan, R., and Ben-Zvi, A. (2017b). Uncoupling the trade-off between somatic proteostasis and reproduction in *Caenorhabditis elegans* models of polyglutamine diseases. *Front. Mol. Neurosci.* 10, 101. doi:10.3389/fnmol.2017.00101

Shpigel, N., Shemesh, N., Kishner, M., and Ben-Zvi, A. (2019). Dietary restriction and gonadal signaling differentially regulate post-development quality control functions in *Caenorhabditis elegans*. *Aging Cell* 18 (2), e12891. doi:10.1111/acel.12891

Skrapits, K., Sarvari, M., Farkas, I., Gocz, B., Takacs, S., Rumpler, E., et al. (2021). The cryptic gonadotropin-releasing hormone neuronal system of human basal ganglia. *Elife* 10, e67714. doi:10.7554/eLife.67714

Sornda, T., Ezcurra, M., Kern, C., Galimov, E. R., Au, C., de la Guardia, Y., et al. (2019). Production of YP170 vitellogenins promotes intestinal senescence in *Caenorhabditis elegans*. *J. Gerontol. A Biol. Sci. Med. Sci.* 74 (8), 1180–1188. doi:10.1093/gerona/glz067

Steinbaugh, M. J., Narasimhan, S. D., Robida-Stubbs, S., Moronetti Mazzeo, L. E., Dreyfuss, J. M., Hourihan, J. M., et al. (2015). Lipid-mediated regulation of SKN-1/Nrf in response to germ cell absence. *Elife* 4, e07836. doi:10.7554/eLife.07836

Taylor, R. C., and Dillin, A. (2013). XBP-1 is a cell-nonautonomous regulator of stress resistance and longevity. *Cell* 153 (7), 1435–1447. doi:10.1016/j.cell.2013.05.042

Taylor, R. C., and Hetz, C. (2020). Mastering organismal aging through the endoplasmic reticulum proteostasis network. *Aging Cell* 19 (11), e13265. doi:10.1111/acel.13265

Taylor, S. R., Santpere, G., Weinreb, A., Barrett, A., Reilly, M. B., Xu, C., et al. (2021). Molecular topography of an entire nervous system. *Cell* 184, 4329–4347.e23. doi:10.1016/j.cell.2021.06.023

Tepper, R. G., Ashraf, J., Kaletsky, R., Kleemann, G., Murphy, C. T., and Bussemaker, H. J. (2013). PQM-1 complements DAF-16 as a key transcriptional regulator of DAF-2-mediated development and longevity. *Cell* 154 (3), 676–690. doi:10.1016/j.cell.2013.07.006

Thondamal, M., Witting, M., Schmitt-Kopplin, P., and Aguilaniu, H. (2014). Steroid hormone signalling links reproduction to lifespan in dietary-restricted *Caenorhabditis elegans*. *Nat. Commun.* 5, 4879. doi:10.1038/ncomms5879

Vadakkadath Meethal, S., Gallego, M. J., Haasl, R. J., Petras, S. J., 3rd, Sgro, J. Y., and Atwood, C. S. (2006). Identification of a gonadotropin-releasing hormone receptor orthologue in *Caenorhabditis elegans*. *BMC Evol. Biol.* 6, 103. doi:10.1186/1471-2148-6-103

Van der Auwera, P., Frooninckx, L., Buscemi, K., Vance, R. T., Watteyne, J., Mirabeau, O., et al. (2020). RPamide neuropeptides NLP-22 and NLP-2 act through GnRH-like receptors to promote sleep and wakefulness in *C. elegans*. *Sci. Rep.* 10 (1), 9929. doi:10.1038/s41598-020-66536-2

Vilchez, D., Morantte, I., Liu, Z., Douglas, P. M., Merkwirth, C., Rodrigues, A. P., et al. (2012). RPN-6 determines *C. elegans* longevity under proteotoxic stress conditions. *Nature* 489 (7415), 263–268. doi:10.1038/nature11315

Vilchez, D., Saez, I., and Dillin, A. (2014). The role of protein clearance mechanisms in organismal ageing and age-related diseases. *Nat. Commun.* 5, 5659. doi:10.1038/ncomms6659

Wang, M. C., O'Rourke, E. J., and Ruvkun, G. (2008). Fat metabolism links germline stem cells and longevity in *C. elegans*. *Science* 322 (5903), 957–960. doi:10.1126/science.1162011

Xiong, J., Kang, S. S., Wang, Z., Liu, X., Kuo, T. C., Korkmaz, F., et al. (2022). FSH blockade improves cognition in mice with Alzheimer's disease. *Nature* 603, 470–476. doi:10.1038/s41586-022-04463-0

Yunger, E., Safra, M., Levi-Ferber, M., Haviv-Chesner, A., and Henis-Korenblit, S. (2017). Innate immunity mediated longevity and longevity induced by germ cell removal converge on the C-type lectin domain protein IRG-7. *PLoS Genet.* 13 (2), e1006577. doi:10.1371/journal.pgen.1006577

Zandawala, M., Tian, S., and Elphick, M. R. (2018). The evolution and nomenclature of GnRH-type and corazonin-type neuropeptide signaling systems. *Gen. Comp. Endocrinol.* 264, 64–77. doi:10.1016/j.ygcen.2017.06.007

Zheleva, A., Gomez-Orte, E., Saenz-Narciso, B., Ezcurra, B., Kassahun, H., de Toro, M., et al. (2019). Reduction of mRNA export unmasks different tissue sensitivities to low mRNA levels during *Caenorhabditis elegans* development. *PLoS Genet.* 15 (9), e1008338. doi:10.1371/journal.pgen.1008338

frontiers | Frontiers in Cell and Developmental Biology

TYPE Original Research
PUBLISHED 13 October 2022
DOI 10.3389/fcell.2022.986997



OPEN ACCESS

EDITED BY
Linda M Hendershot,
St. Jude Children's Research Hospital, United States

REVIEWED BY
Deborah J Andrew,
Johns Hopkins Medicine, United States
Cecilia Alvarez,
National University of Cordoba, Argentina

*CORRESPONDENCE
Tiziana Anelli,
anelli.tiziana@hsr.it

†These authors share first authorship

SPECIALTY SECTION
This article was submitted to Signaling, a section of the journal Frontiers in Cell and Developmental Biology

RECEIVED 05 July 2022
ACCEPTED 20 September 2022
PUBLISHED 13 October 2022

CITATION
Pittari D, Dalla Torre M, Borini E, Hummel B, Sawarkar R, Semino C, van Anken E, Panina-Bordignon P, Sitia R and Anelli T (2022), CREB3L1 and CREB3L2 control Golgi remodelling during decidualization of endometrial stromal cells.
*Front. Cell Dev. Biol.* 10:986997.
doi: 10.3389/fcell.2022.986997



# CREB3L1 and CREB3L2 control Golgi remodelling during decidualization of endometrial stromal cells

Daniele Pittari[1†], Marco Dalla Torre[1,2†], Elena Borini[1], Barbara Hummel[3], Ritwick Sawarkar[3,4], Claudia Semino[2], Eelco van Anken[1,2], Paola Panina-Bordignon[1,5], Roberto Sitia[1,2] and Tiziana Anelli[1,2]*

[1]Faculty of Medicine, Vita-Salute San Raffaele University, Milan, Italy, [2]Division of Genetics and Cell Biology, IRCCS Ospedale San Raffaele, Milan, Italy, [3]Max Planck Institute of Immunobiology and Epigenetics, Freiburg, Germany, [4]Medical Research Council (MRC), University of Cambridge, Cambridge, United Kingdom, [5]Division of Neuroscience, IRCCS Ospedale San Raffaele, Milan, Italy

Upon progesterone stimulation, Endometrial Stromal Cells (EnSCs) undergo a differentiation program into secretory cells (decidualization) to release in abundance factors crucial for embryo implantation. We previously demonstrated that decidualization requires massive reshaping of the secretory pathway and, in particular, of the Golgi complex. To decipher the underlying mechanisms, we performed a time-course transcriptomic analysis of *in vitro* decidualizing EnSC. Pathway analysis shows that Gene Ontology terms associated with vesicular trafficking and early secretory pathway compartments are the most represented among those enriched for upregulated genes. Among these, we identified a cluster of co-regulated genes that share CREB3L1 and CREB3L2 binding elements in their promoter regions. Indeed, both CREB3L1 and CREB3L2 transcription factors are up-regulated during decidualization. Simultaneous downregulation of CREB3L1 and CREB3L2 impairs Golgi enlargement, and causes dramatic changes in decidualizing EnSC, including Golgi fragmentation, collagen accumulation in dilated Endoplasmic Reticulum cisternae, and overall decreased protein secretion. Thus, both CREB3L1 and CREB3L2 are required for Golgi reshaping and efficient protein secretion, and, as such, for successful decidualization.

KEYWORDS

**secretory pathway, vesicular transport, differentiation, transcriptomics analysis, collagen**

## Introduction

With only few exceptions, secretory proteins are cotranslationally translocated into the Endoplasmic Reticulum (ER), where they undergo oxidative folding, N-glycosylation and other posttranslational modifications under the control of devoted chaperones and enzymes (Braakman and Bulleid, 2011). Protein quality control (QC) mechanisms ensure that only native proteins proceed along the secretory pathway (Anelli and Sitia, 2008; Sun

and Brodsky, 2019); proteins that fail to fold are instead destined for degradation *via* cytosolic proteasomes (Ruggiano et al., 2014; Christianson and Carvalho, 2022). Cargo receptors (such as ERGIC-53) are active at ER exit sites (ERES) to accelerate the secretion of folded molecules (Zhang, 2009; Anelli and Panina-Bordignon, 2019). Recruiting cytosolic COPII components, they ensure efficient movement of secretory proteins from the ER to the Golgi. In the Golgi compartment, cargo proteins are further processed and finally get secreted or exposed on the plasma membrane (Schwabl and Teis, 2022). To maintain membrane homeostasis and organelle composition, anterograde traffic is paralleled by COPI-dependent retrograde transport. All these events must be precisely coordinated.

The organelles of the secretory compartment are particularly developed in professional secretors, since these are the sites devoted to the production of almost all proteins destined to be secreted (Federovitch et al., 2005). Indeed, their components are selectively up-regulated in all well-studied differentiation programs towards secretory phenotypes (Harding et al., 2001; Christis et al., 2010). This is the case, for example, of B to plasma cell differentiation: after the encounter with antigens, B lymphocytes first proliferate and then transform into *protein factories*, dramatically enlarging their ER under the control of Ire1, Xbp1 and other Unfolded Protein Response (UPR)-related factors (Reimold et al., 2001; Iwakoshi et al., 2003; Van Anken et al., 2003).

Another example of a secretory differentiation program is the decidualization of Endometrial Stromal Cells (EnSC) (Figure 1) (Gellersen and Brosens, 2014). With each menstrual cycle, human EnSCs undergo a phase of intense proliferation. Then, upon the post-ovulatory increase of progesterone, cells exit the cell cycle, enlarge and differentiate into secretory cells that produce different mediators (IL-6, Tissue Factor, IGFBP1, Matrix metalloproteinases (MMPs), collagens, Prolactin) to anticipate blastocyst implantation, should fertilization occur. We recently demonstrated that decidualization entails massive rearrangements of EnSCs cytoarchitecture, with enlargement of the entire cell, and most prominently of the secretory pathway organelles (Anelli et al., 2021). In contrast to what occurs during B to plasma cell differentiation, however, in decidualizing EnSCs the Golgi complex expands more than the ER (Anelli et al., 2021). This divergence in how the secretory pathway differentiates might be due to the different cargoes produced by either cell type. The more pronounced Golgi enlargement, that is also a hallmark of decidualization, may be required to sustain bulk production of highly O-glycosylated proteins (Noske et al., 2008).

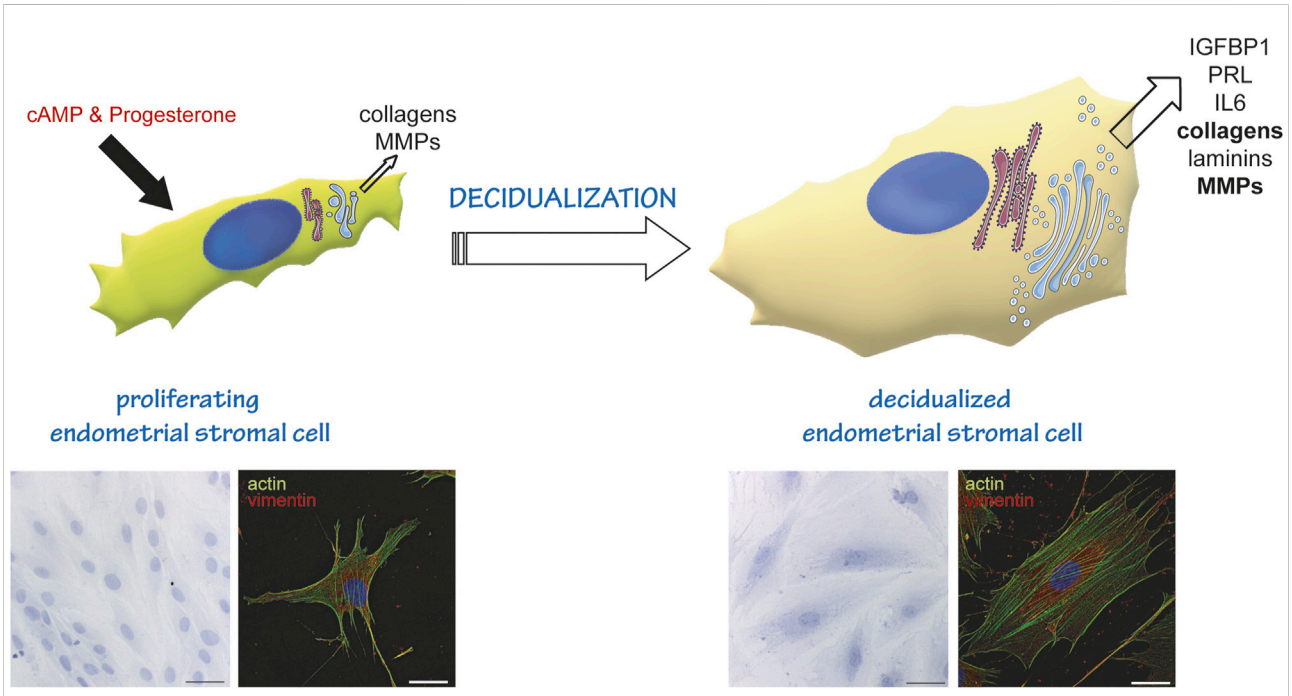


FIGURE 1
Endometrial stromal cells as a model of cell differentiation to a secretory phenotype. In the proliferative state, EnSC show a fibroblastoid shape, and produce and secrete some collagens and metalloproteases (MMPs). Decidualisation (induced *in vitro* by cAMP and Progesterone stimulation) induces a reshaping of the entire cell and of the secretory compartment. Cells stop proliferating and enlarge, acquiring an epithelioid-like shape. They enlarge their ER and Golgi compartment (Anelli et al., 2021) and transform into professional secretors, expressing and secreting decidualization markers (IGFBP1, PRL, IL6), more and different collagens, MMPs and laminins. The lower insets on the left show a Hematoxylin-Eosin staining of cells at day 0 (proliferating, left) and day 6 of decidualization (right). Images were acquired with a ×20 objective; bar: 60 μm. The lower insets on the right show an immunofluorescence of proliferating (left) and decidualized cells (right) stained with fluorescently labelled Phalloidin (actin, green) and anti-vimentin antibody (red). Note the change in cytoskeletal reorganization following stimulation. Images were acquired with a ×60 objective; bar: 20 μm.

How are the above morphological rearrangements orchestrated during decidualization? We previously showed (Anelli et al., 2021) that decidualization entails minimal activation of the UPR pathways that are instead key in plasma cell development. Quiescent B lymphocytes secrete little if any proteins: hence, they need to build up a secretory machinery almost from scratch, which explains the reliance of B to plasma cell differentiation on the UPR. Conversely, EnSCs secrete proteins also before progesterone stimulation. Therefore, they apparently modulate the rates of protein production and transport rather than massively expanding the ER during decidualization.

However, it is not clear whether the morphological changes of decidualizing EnSCs are inherently encoded in the transcriptional program of decidualization itself or, *vice versa*, they are driven by the increased cargo production and secretion.

This study aims to elucidate the mechanisms that orchestrate cellular reshaping during decidualization: we focused on the characterization of the gene expression trends and on the prediction and experimental validation of transcription factors implicated in the enlargement of the Golgi compartment. To this end, we performed unbiased transcriptomic analyses of *in vitro* decidualization of human immortalized endometrial stromal cells (T-HESC) at different time points after progesterone stimulation. A distinct upregulation of the ER, Golgi and lysosomal proteins is evident at the (relative) expense of the cytosolic components. The members of a cluster of upregulated transcripts related to the early secretory compartment share binding sites for CREB3L1 and CREB3L2. Accordingly, both transcription factors are not only upregulated during decidualization, but also necessary for Golgi remodelling. Their ablation has dramatic consequences on protein secretion, with collagen accumulating in dilated ER cisternae, which abrogates the efficient decidualization process. Our results demonstrate that the activation of CREB3L1 and CREB3L2 is key for the reshaping of the early secretory compartment during decidualization and for achieving a secretory phenotype.

# Results

## *In vitro* decidualization of T-HESC entails extensive transcriptomics rearrangements

To characterize the gene expression changes occurring in decidualization, we performed bulk RNA sequencing of human immortalized endometrial stromal cells (T-HESC) under basal conditions (0 h) and at various time points during *in vitro* decidualization (i.e. 6 h, 18 h, day 1, 1.5, 2, 3, and 6 after hormonal stimulation). We focused on short intervals between early time points to better discriminate transcriptional modifications characterizing the first phases of decidualization.

Differential expression analysis (DEA) was performed by pairwise comparisons of samples from each time point with untreated samples. The volcano plots comparing expression patterns at day 3 and day 6 with basal expression (Figure 2A) highlight the upregulation of known markers [Prolactin (PRL), WNT4, IGFBP1 and TFBI], as a positive control of ongoing decidualization. Our results show that *in vitro* decidualization is accompanied by a profound transcriptome rearrangement, featuring up or down-regulation of thousands of genes. As differentiation progresses, the number of differentially expressed genes (DEGs) progressively increases: from 984 at 6 h, their number rises to its maximum of 5,136 DEGs at day 3. At the end of our differentiation protocol (day 6), the number of DEGs is 4,780 (Figure 2B, Supplementary Table S1).

## Transcriptional profile of stimulated T-HESC reflects physiological decidualization program

To get insights into the biological significance of the various DEGs observed at each time point, we performed over-representation analysis (ORA) for the major Gene Ontology annotations: biological processes (BP), cellular component (CC), and molecular function (MF). As expected, ORA reveals significant enrichment at 6 h for terms related to response to hormonal stimulation (cAMP-mediated signalling, glucocorticoid receptor binding, 3′,5′-cyclic-AMP phosphodiesterase activity; Supplementary Table S2A–E, Figure 2C). An enrichment for terms associated with ER-Golgi vesicular trafficking, protein glycosylation and Golgi organization follows at the next time point (18 h). These terms turn out to be predominant at all further time points, suggesting the centrality of secretory pathway reshaping among upregulated DEGs from the early to last stages of our decidualization protocol. In accordance, we found the same trends for terms associated with the main compartments of the early secretory pathway, such as ER lumen and membranes, ER-Golgi intermediate compartment (ERGIC), cis-Golgi and lysosomes (Figure 2C, Supplementary Table S2C).

Conversely, downregulated DEGs show enrichment for terms associated with DNA replication, DNA repair, cell cycle progression, and nuclear compartment (Supplementary Table S2B–D). As observed for upregulated genes, the enrichment for these terms was consistent throughout the decidualization process from 18 h onwards. In addition, an early enrichment for terms related to cytoskeleton, focal adhesion and cell-cell junctions is seen at 6 h (Figure 2C; Supplementary Table S2C).

The expression profile of representative genes of the main compartments or biological processes is shown in Figure 2D. The panel indicates a coordinated upregulation of genes encoding proteins involved in disulfide bond formation in the ER (redox enzymes) and of genes of ER to Golgi vesicular trafficking and of the Golgi complex. As expected, the expression of genes involved in cell cycle progression is downregulated, as well as cytoskeleton genes. The analysis also reflects a shift in the cargo produced during the decidualization process (Carbone et al., 2006; Shi et al., 2020): while proliferating EnSCs produce Collagen type VI, after decidualization they

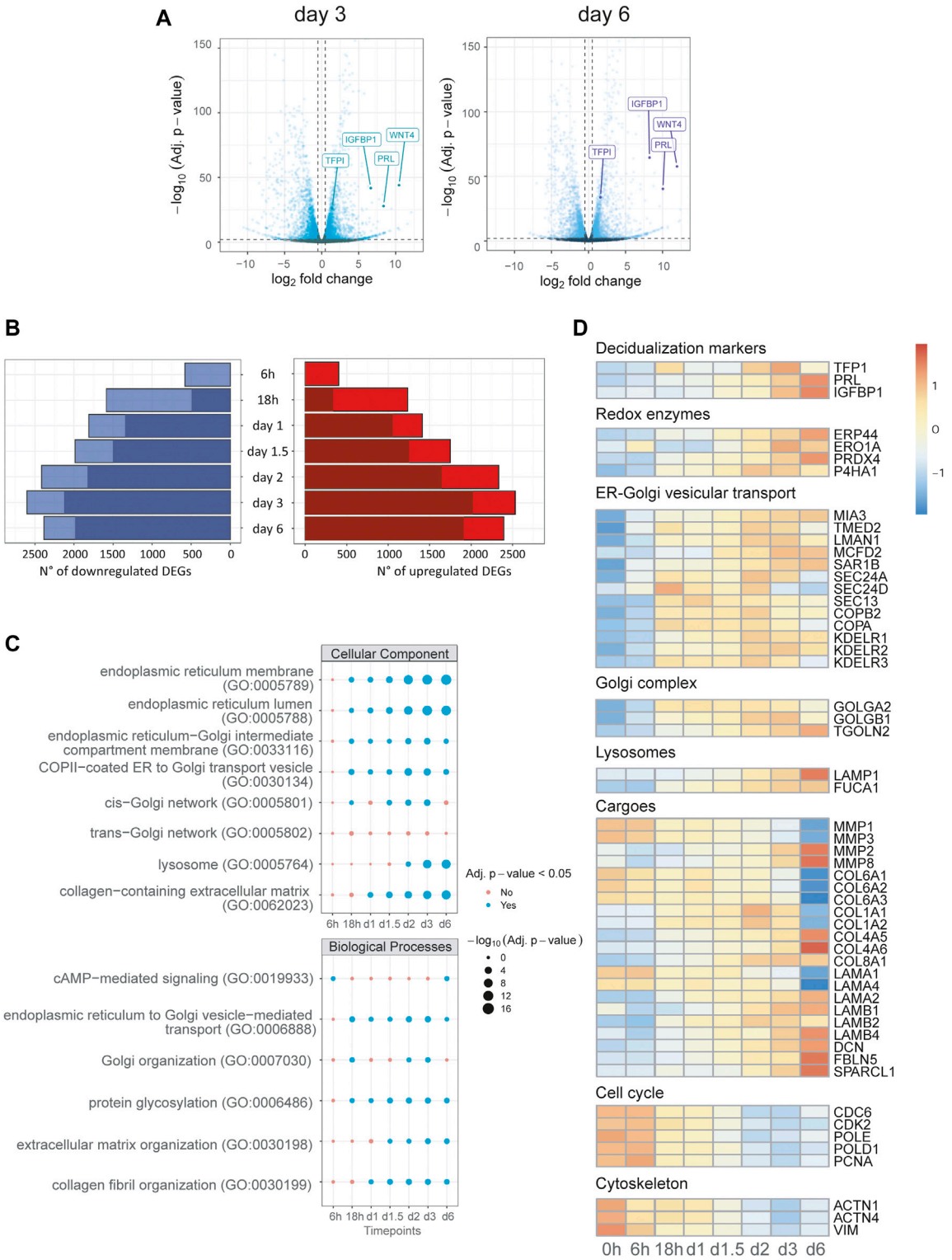


FIGURE 2
Transcriptional reprogramming of the secretory compartment is an early event in decidualization. Differential expression analysis and Over-Representation Analysis (ORA) of time course bulk RNA-seq. **(A)** Volcano plots of day 3 and 6, gene labelling for decidualization markers (PRL, IGFBP1, TFP1), which act as positive controls for our experimental set up. **(B)** Number of DEGs called for each timepoint grouped for upregulation or downregulation: for each bar, the darker shades of colour represent the number of genes called DEGs also at the previous time point. **(C)** ORA of upregulated DEGs for GO terms for each timepoint: early enrichment is observed for pathways related to the compartments and biological processes of the secretory pathway. **(D)** Heatmap of representative DEGs for canonical biological functions involved in decidualization up to day 6 of differentiation. Note the upregulation of genes of the early secretory pathway and the downregulation of genes correlated with cell cycle and DNA repair. The rearrangements of cargos (collagens, laminins) is already evident just a few hours after stimulation.

downregulate collagen type VI and upregulate instead collagen type I, IV, and VIII. Changes occurs also in the types of laminins expressed.

To further corroborate our results, we compared the DEGs identified at the end of the decidualization protocol (day 6) with a list of 115 gene products experimentally validated for showing functional reprogramming upon decidualization of human endometrial stromal cells (Gellersen and Brosens, 2014). Indeed, we found an almost perfect overlap between this list and prominent upregulated DEGs identified by our analysis (Supplementary Table S3), further supporting our choice for *in vitro* differentiation of T-HESC as a model to study the decidualization process.

## Time-series clustering reveals a class of co-regulated genes linked with vesicular transport

To predict shared cis-regulatory elements orchestrating early secretory pathway reshaping and, possibly, Golgi expansion, we used a data-driven approach that takes advantage of our bulk RNA-seq time-course design. First, we created a subset of 626 DEGs by selecting those annotated in GO terms for the cellular component (CC) related to the ER and Golgi apparatus, as well as called differentially expressed in the first 3 days of differentiation. Then, we performed partitional clustering based on their co-expression patterns. In this way, we identified five different clusters, two describing downregulation and three describing upregulation trends (Figure 3A). In cluster 5, one of those describing upregulation trends, we identified the presence of canonical genes involved in vesicular transport, such as COPI and COPII components, and cargo receptors (SEC23A, SEC24A, SEC16A, COPZ1/2, COPA, COPB2, LMAN1, MIA3; Figure 3A; Supplementary Table S4). ORA for biological processes (BP) GO terms also reveals functional enrichment for vesicular transport genes in this cluster (Figure 3B). Next, we predicted common cis-regulatory elements in each cluster using the tool RcisTarget. Interestingly, cluster five scores the highest enrichment values for top putative transcription factors associated with vesicular transport promotion, such as CREB3L2, CREB3L1, CREB3, ATF6, and Xbp1 (Supplementary Table S5).

## CREB3L1 and CREB3L2 are upregulated during decidualization

Since our previous studies identified only a minimal induction of ATF6, and no activation of the Xbp1 pathway during decidualization (Anelli et al., 2021), we focused our attention on CREB3L1 and CREB3L2, two transcription factors (TF) that have been previously linked to collagen secretion and vesicular trafficking in other cell types (Fox et al., 2010; Asada et al., 2011; Chan et al., 2011; Ishikawa et al., 2017; Khetchoumian et al., 2019; Jhonson et al., 2020). These transcription factors are under basal conditions localized in the ER, where they are readily ubiquitinated, extracted from the membrane and degraded (Kondo et al., 2012). Upon activation, CREB3L1 and CREB3L2 translocate to the Golgi complex, where they undergo RIP (Regulated Intramembrane Proteolysis) by the proteases S1P and S2P. This proteolytic cleavage event releases their cytosolic domains that migrate to the nucleus to exert their function as TFs (Kondo et al., 2007; Murakami et al., 2009). qPCR shows that, during *in vitro* decidualization, both CREB3L1 and CREB3L2 are upregulated at the mRNA level, although with slightly different kinetics (Figure 4): the mRNA of CREB3L1 shows a trend with a peak at day 3 (Figure 4A), while CREB3L2 increases steadily throughout the decidualization process, up till day 6 (Figure 4D). At the protein level, CREB3L1 is already upregulated on day 1 of decidualization, and then its levels start to decrease (Figures 4B,C). Cleaved CREB3L1 seems to peak at day 1 and then decreases. On the contrary, we did not detect any induction of CREB3L2 at the protein level (Figures 4E,F), despite its mRNA increases during decidualization. We could hypothesise a fast turnover of this protein, preventing its accumulation, but this phenomenon awaits further clarification.

## CREB3L1 and CREB3L2 are needed for efficient decidualization

To gain insight into the role of CREB3L1 and 2 during decidualization, we used small interfering RNAs targeted to CREB3L1 and 2, individually or in combination. Silencing was started before inducing decidualization (Day -1) so that, when decidualization was induced (Day 0), expression of CREB3L1 and 2 was already suppressed (Supplementary Figures 1A and 4B,E). Silencing was repeated after 3 days, to sustain the downregulation of the transcription factors for the entire experiment (see Material and Methods section and Supplementary Figure 1A). qPCR analysis (Supplementary Figure 1A) indicates that no major compensatory responses (up-regulation of one TF in the absence of the other) are activated during the experiments. Cells responded as expected to hormonal stimulation also upon CREB3L1 and/or 2 silencing, as shown by the increase in PRL mRNA levels (Supplementary Figure 1B). However, suppression of both transcription factors dramatically impaired the expression of ERGIC-53 (LMAN1), SEC24A and SEC24D (involved in ER to Golgi vesicular traffic), and of KDELR2 and 3 (involved in retrieving ER chaperone escapees from the Golgi). Trends suggesting minor effects were

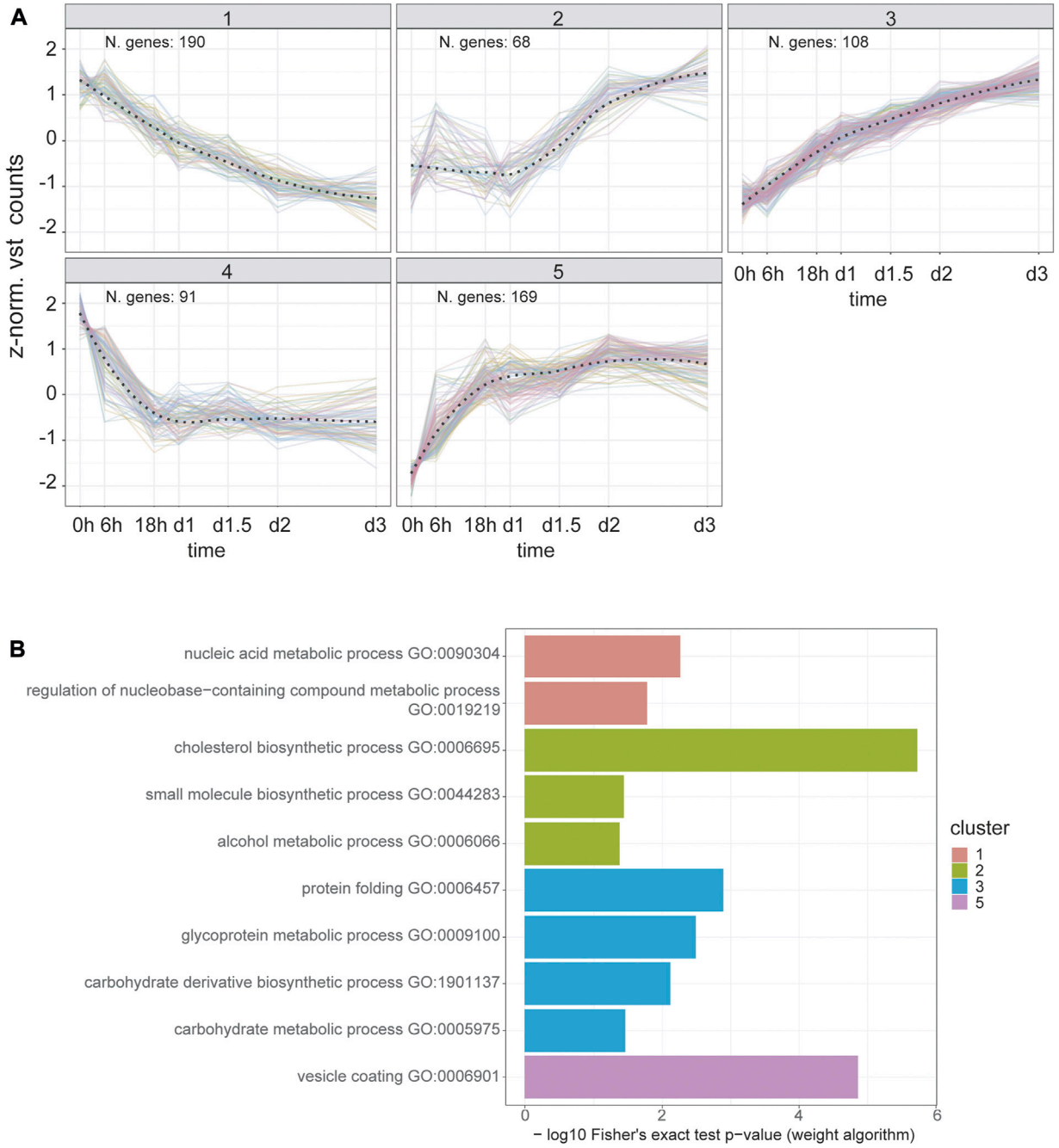


FIGURE 3
Time series clustering dissects the temporal orchestration of ER and Golgi apparatus DEGs. **(A)** Temporal expression trends for DEGs annotated to "Golgi Apparatus" and/or "Endoplasmic Reticulum" GO cellular component terms. *Y*-axis represents the z-normalized, averaged expression value transformed using DESEQ2 variance stabilized transformation. The overall trends for each cluster (dashed line) were estimated using a LOESS fit. **(B)** Over-representation analysis results for biological process GO terms in each cluster. Fisher's exact test was carried out using the weight algorithm proposed in Alexa et al., 2006, implemented in TopGO. Cluster five shows enrichment for vesicular transport terms, reflecting the presence of the main components of COPI, COPII and cargo receptors genes (Supplementary Table 4). Cluster four does not show terms with a significant enrichment (i.e. $p$ value < 0.05).

observed for other Golgi-related genes, such as GOLGA2 (GM130), giantin (GOLGB1) and TGN46 (TGOLN2) (Figure 5A). Moreover, for most of the transcripts analysed, a strong effect of CREB3L1/2 silencing was observed already at day 0, which suggests a major role of the two transcription factors in regulating their expression

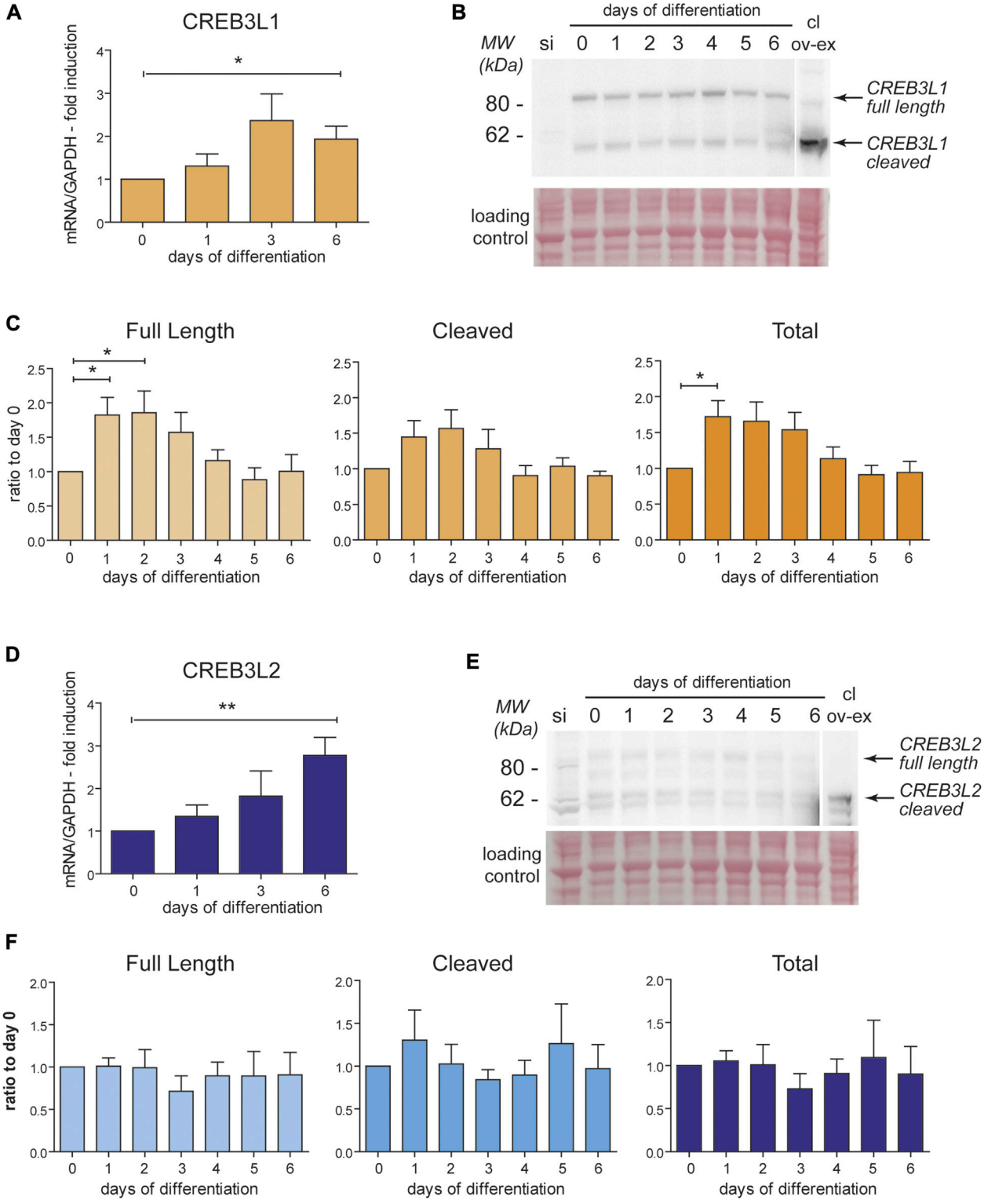


FIGURE 4
CREB3L1 and two are upregulated during decidualization. T-HESC were treated with cAMP and progesterone and samples (RNA and total protein lysates) were collected every day up to day6 after the treatment. **(A)** mRNA levels of CREB3L1 were quantified using qPCR, normalized on GAPDH and expressed as fold induction on day 0. The mRNA increases after stimulation up to day 3 and then start decreasing. Average of samples from six independent experiments ± SEM. *$p < 0.05$, *t*-test vs day0. **(B)** 40 µg of total proteins were analyzed in SDS-PAGE, under reducing conditions on a 4–12% precasted acrylamide gel. As a negative control, a sample of cells subjected to CREB3L1 siRNA the day before were loaded (si).
(*Continued*)

FIGURE 4 (Continued)
As a positive control to discriminate the cleaved form, 40 μg of protein extract of HeLa cells transiently transfected with cleaved CREB3L1 was loaded (cl ov-ex). The full length and the cleaved forms are indicated by arrows on the right. The ponceau staining of the nitrocellulose is shown as a loading control. The lane showing the over-expressed cleaved form comes from a lower exposure image of the same nitrocellulose. **(C)** Densitometric quantification of six independent experiments as the one showed in B (average ± SEM). An increase at the protein levels in the first days parallels the increase in the mRNA level shown in panel A. *$p < 0.05$, *t*-test vs day 0. **(D)** mRNA levels of CREB3L2 were analyzed in qPCR. The mRNA increases after stimulation up to day 6. Average of samples from six independent experiments ± SEM. *$p < 0.05$, *t*-test vs day 0. **(E)** 40 μg of total proteins were analyzed as described in panel B. As a negative control, a sample of cells subjected to CREB3L2 siRNA the day before were loaded (si). As a positive control to visualized the cleaved form, 40ug of protein extract of HeLa cells transiently transfected with cleaved CREB3L2 was loaded (cl ov-ex). The lane showing the over-expressed cleaved form comes from a lower exposure image of the same nitrocellulose. The full length and the cleaved forms are indicated by arrows on the right. The ponceau staining of the nitrocellulose is shown as a loading control. **(F)** Densitometric quantification of five independent experiments as the one showed in B (average ± SEM). Despite the continuous increase of the mRNA of CREB3L2 during decidualization, nothing seems to change at the protein level.

also in resting conditions. We excluded a nonspecific effect of the silencing procedure, since other secretory pathway genes (such as ERp44 and KDELR1) were not affected.

The effects of CREB3L1/2 silencing were confirmed at the protein level (Figure 5B). A reduced induction of both ERGIC-53 and GM130 was observed by western blotting, especially upon silencing of both transcription factors. As expected from the mRNA analysis, no effect on ERp44 induction was observed.

## Ablation of CREB3L1 and CREB3L2 affects Golgi structure

To better understand the structural changes of the secretory pathway following CREB3L1/2 silencing, we performed morphometric analyses of cells at day 0 and day 6 of decidualization, using calreticulin (CRT) as a marker of the ER, giantin as cis-Golgi marker, and golgin 97 as trans-Golgi marker. Cells were also stained with a membrane marker (HLA 1) to calculate the total cell volume. Silencing of either CREB3L1, 2, or both did not impact on the overall increase in cell volume that characterizes decidualization (Supplementary Figure S2). When expressed as a percentage of the total cell volume, ER size was not affected by the silencing, even if some morphological alterations were evident (Figures 6A upper panels, B). The volume of both the cis-Golgi and the trans-Golgi were instead severely affected by CREB3L1 silencing, both before (Supplementary Figure S2) and after 6 days of decidualization (Figures 6A,B).

Moreover, morphological changes of the Golgi complex were detected, both ad day 0 and at day 6 of decidualization under depletion of one or both TFs (Figure 6C and Supplementary Figure S3). While downregulation of CREB3L1 seems to reduce the Golgi dimension (as indicated by morphometry analyses), CREB3L2 KD seems to cause Golgi fragmentation (Supplementary Figure S3). Combined CREB3L1 and CREB3L2 ablation causes a dramatic decrease of the organelle size, as well as fragmentation and scattering of its *cisternae,* both in resting (day 0) and fully decidualized (day 6) conditions (Figure 6C).

## Impaired secretion upon ablation of CREB3L1 and CREB3L2

EnSCs express various types of collagen, and their expression changes during decidualization. Under basal conditions, EnSCs express collagen type VI in large amounts, but in the course of decidualization, collagen VI is downregulated, while collagen type I, IV and VIII are upregulated (Figure 2D). CREB3L1 and 2 have been previously identified as necessary for collagen type I and II secretion in osteoblasts and chondrocytes (Murakami et al., 2009; Saito et al., 2009; Chen et al., 2014). We therefore analysed trafficking of collagen type I (intracellular content and localization, and secretion) in decidualizing T-HESC upon silencing of either CREB3L1, 2, or both (Figure 7). Ablation of CREB3L1/2 dramatically affected the fate of collagen type I in decidualizing T-HESC (Figure 7A), causing the formation of long stacks or enlarged lacunae in the endoplasmic reticulum. The trafficking defect is particular evident in the double KD, with the formation of abnormal structures, filled with ProCol1A1 and positive for calreticulin (not shown), that are reminiscent of aggregated Ig-containing Russell Bodies (Valetti et al., 1991). In accordance, ablation of CREB3L1/2 led to high MW collagen complexes in cell lysates (Figure 7C), which is indicative of the intracellular accumulation of collagen aggregates. Consequently, collagen type I secretion was almost completely abrogated (Figure 7B), in particular upon double silencing. Moreover, ablation of CREB3L1/2 caused an overall reduction in the secreted material of decidualizing T-HESC (Figure 7D). For instance, PRL, which normally is abundantly secreted upon decidualization, was no longer detectable in the supernatants of double CREB3L1 and 2 KD cells (Figure 7E). This suggests a more general effect on total protein trafficking and secretion.

# Discussion

We previously described how decidualization of EnSC goes hand in hand with morphological changes of the entire secretory pathway, which include rearrangements not only of the ER but also of the Golgi compartment (Anelli et al., 2021). Here, by

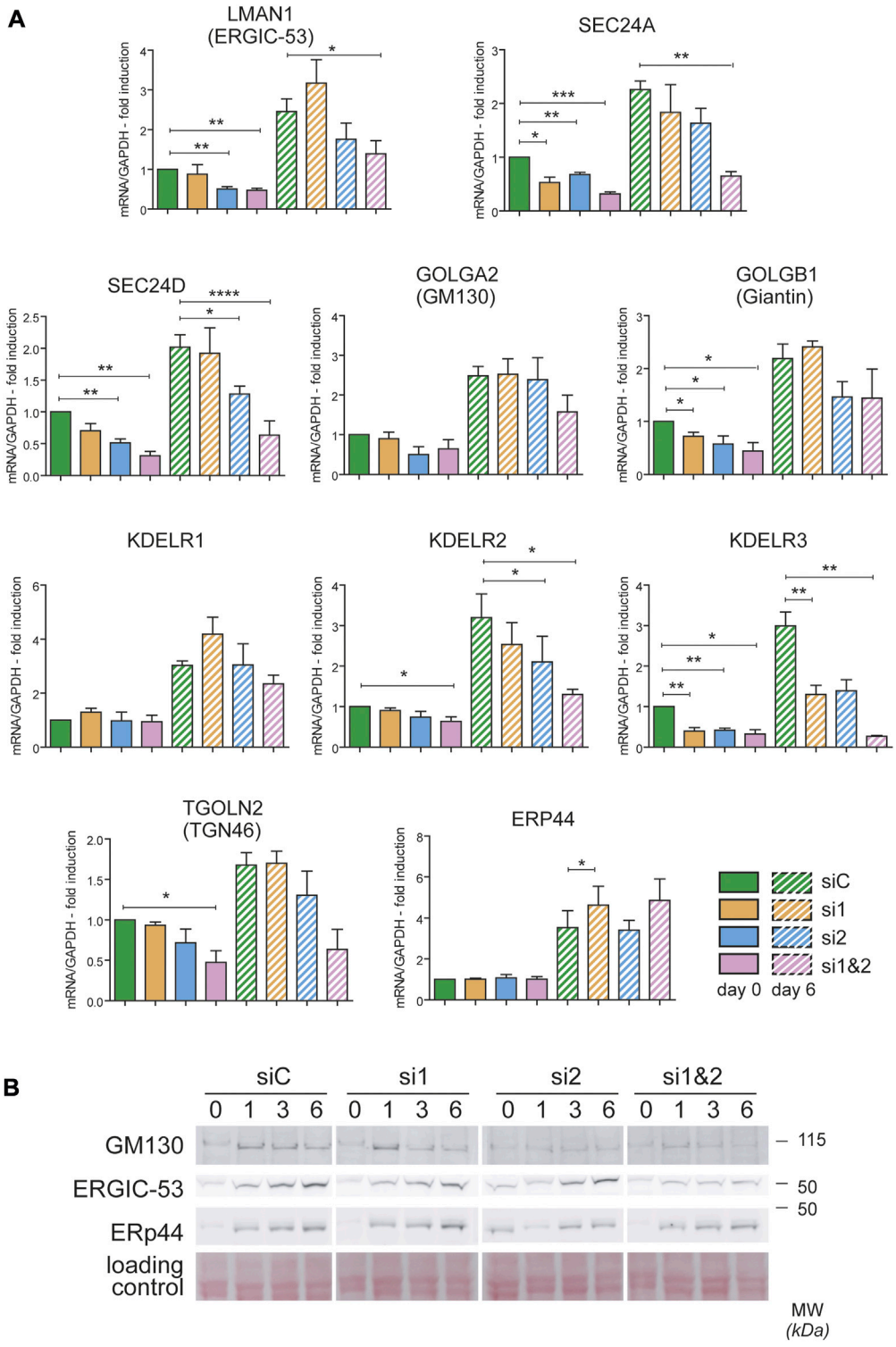


FIGURE 5
CREB3L1 and CREB3L2 drive the upregulation of many genes of the early secretory pathway during decidualization. T-HESC were treated with scramble duplexes (siC, green bars), with duplexes specific for CREB3L1 (si1, orange), CREB3L2 (si2, light blue) or both (si1&2, pink). The day after treatment (day 0) cells were collected or treated with cAMP and progesterone and then collected at day 6 of decidualization. **(A)** mRNA for different genes encoding proteins of the early secretory pathway were analyzed by qPCR and expressed as fold induction to day 0 siC after normalization on GAPDH. Solid bars represent values at day 0, striped bars values at day 6. Average of 3–4 independent experiments ± SEM. *$p < 0.05$; **$p < 0.01$; ***$p < 0.001$; ****$p < 0.0001$, *t*-test vs day 0 siC. The KD of CREB3L1 and/or 2 affects the expression of the majority of the genes analyzed, both at day 0 and after 6 days of decidualization. **(B)** Total protein extracts were loaded on SDS PAGE under reducing conditions (40 µg of proteins/lane). The behavior of GM130, ERGIC-53 and ERp44 are shown. While ERGIC-53 and GM130 suffer from the absence of CREB3L1 and/or 2, the protein levels of ERp44 are unaffected. A part of the ponceau is shown as a loading control.

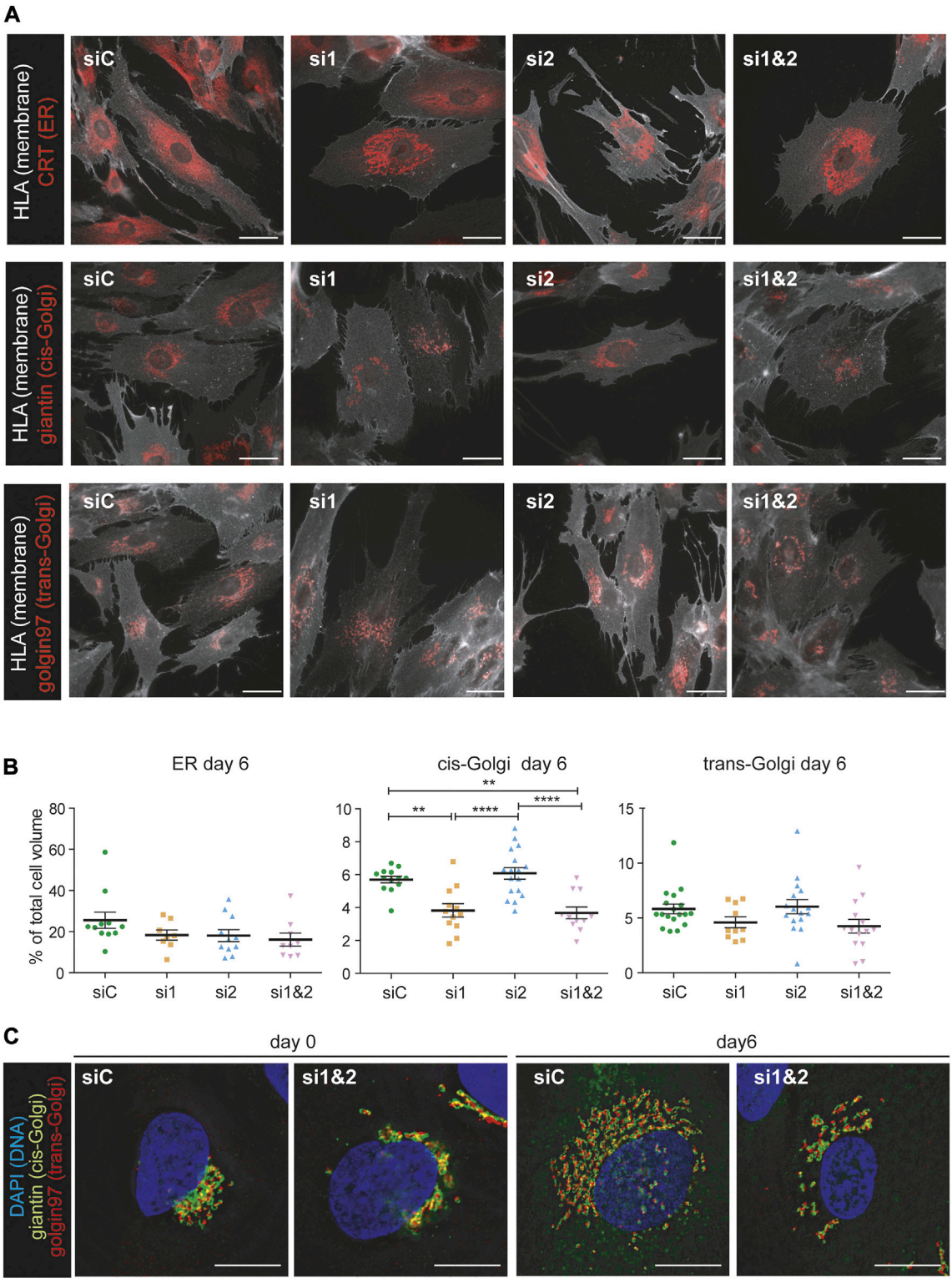


FIGURE 6
CREB3L1 and CREB3L2 drive the decidualization induced rearrangement of the Golgi compartment. **(A)** T-HESC were treated with scramble duplexes (siC), with duplexes specific for CREB3L1 (si1), CREB3L2 (si2) or both (si1&2). The day after treatment (day0) cells were fixed with PFA or treated with cAMP and progesterone and then collected at day 6 of decidualization. Cells were first decorated with anti-HLA1 antibody to stain the membrane, and then permeabilized and stained with antibodies against different compartment of the early secretory pathway (calreticulin CRT

(*Continued*)

FIGURE 6 (Continued)
as a marker of the ER, giantin for the cis-Golgi and golgin97 for the trans-Golgi). Representative images of cells at day 6 of differentiation are shown. Images were acquired with a ×60 objective; bar: 20 μm. **(B)** The volume of the cells and of the intracellular compartments was calculated using morphometric analysis of images as the ones shown in **(A)**. The volume of the intracellular compartments was then expressed as a percentage of the total cell volume. The plots show the volume of the ER, cis-Golgi and trans-Golgi of cells at day 6 of decidualization. Each dot in the plot corresponds to a single cell. The plot shows the population distribution and the value of the mean ± SEM for cells of two independent experiments (green: siC, orange: si1, light blue: si2, pink: si1 and 2). *$p < 0.05$; **$p < 0.01$, ****$p < 0.001$, one-way ANOVA with Turkey correction. **(C)** Morphology of the Golgi compartment of cells treated with scrambled duplexes (siC) of KD for both CREB3L1 and 2 (si1&2) at day 0 or day 6 of decidualization. Markers of the cis-Golgi (giantin, green) and of the trans-Golgi (golgin97, red) were used. The DNA is stained in blue (DAPI). Images were acquired with a ×100 objective; bar: 20 μm. Note the fragmentation and the inhibited enlargement of the Golgi compartment under KD of both CREB3L1 and 2. The scattering effect is visible also at day 0.

transcriptomics analysis of *in vitro* T-HESC differentiation, we employed an "omic" approach to dissect the gene expression changes occurring during decidualization. Our current study confirms in further detail that decidualization entails the upregulation of genes associated with several components of the secretory pathway. Moreover this analysis reveals how decidualization stimuli induce a readjustment of the secretory cargoes, with not only an increase in the amount of cargoes produced, but also a change in the types of collagens and laminins synthesized (Figure 2D). This is in line with previous studies which suggested that a change in the composition of the extracellular matrix is needed to accomodate the incoming embryo (Iwahashi et al., 1996; Shi et al., 2020). Our results furthermore highlight that, even if decidualization intails a dramatic increase in the secretory activity, proliferating EnSC are already active secretors, specifically releasing components of the extracellular matrix. Moreover, activation of cAMP-dependent pathways and the upregulation of genes of the early secretory pathway can be detected early during decidualization, even before the upregulation of secretory cargoes (Figures 2C,D). Evidently, this is due to the activation of a differentiation program and is not a cargo-induced effect: decidualizing EnSCs first adapt and reshape their secretory machinery and later up-regulate their cargoes.

Clustering analysis showed that genes of the early secretory compartment specifically involved in ER to Golgi trafficking and Golgi structure are upregulated with a similar pattern, which suggests shared transcriptional regulation(s). Promoter analyses revealed a potential contribution of ATF6, CREB3L1 and CREB3L2. Having shown previously that UPR branches are not overtly activated during decidualization (Anelli et al., 2021), we focused our attention on CREB3L1 and 2, two transcription factors that are known to regulate collagen secretion (Saito et al., 2009; Chen et al., 2014). These factors are also required in some cell types that do not produce collagens. Indeed, CREB3L1 is upregulated in thyrocytes upon TSH stimulation to sustain Golgi enlargement (Garcia et al., 2017). CREB3L2 instead is needed for hepatic stellate cells differentiation to myoblasts-like cells, a process requiring ER and Golgi enlargement (Tomoishi et al., 2017), as well as for maturation of pituitary cells into hormone producing factories (Khetchoumian et a., 2019). CREB3L2 has been suggested as a master TF for the control of secretory capacity of cells (Khetchoumian et a., 2019). CREB3L1 and CREB3L2 Drosophila Melanogaster homologue, CREB3A, controls the transcriptional activation of many genes encoding the core secretory pathway (Johnson et al., 2020). We show here that, in EnSCs, both CREB3L1 and CREB3L2 sustain the expression of SEC24A and D, GOLGB1 and KDELR2 and 3 even under basal conditions (Figure 5). Moreover, they are needed for organelle remodelling upon progesterone stimulation. Upon CREB3L1 ablation, the Golgi complex does no longer enlarge, while the ablation of CREB3L2 results in Golgi scattering. Thus, CREB3L1 and CREB3L2 jointly regulate both Golgi volume and structure (Figure 6), and, consequently, are key for efficient protein secretion (Figure 7 and Figure 8). The changes in ER morphology upon CREB3L1 and/or 2 KD are also striking (Figure 6 and Figure 8). Whether the anomalous swelling of the ER is a direct consequence of the ablation of the two TFs, or whether it is due to impaired collagen trafficking and accumulation is not clear and cannot be easily addressed, given the high diversity of collagens produced by EnSCs. No canonical UPR activation is observed under condition of CREB3L1 and/or 2 ablation at day 0 (not shown), even if their KD still have consequences both at a transcriptional and at a morphological level.

Up to now, defects of CREB3L1 or CREB3L2 have been linked to skeletal disorders. CREB3L1 mutations are associated with Osteogenesis Imperfecta (Symoens et al., 2013; Keller et al., 2018; Lindahl et al., 2018), while $CREB3L2^{KO}$ mice, instead, display a severe chondrodysplasia (Saito et al., 2009). Differently from osteoblasts or chondrocytes, our results indicate that decidualizing cells rely on both CREB3L1 and 2. We could speculate that this is due to dEnSC producing and secreting different cargoes, including various collagen types. We cannot exclude that in EnSC CREB3L1 and 2 could also heterodimerize, as previously described (Khan and Margulies, 2019).

The mechanism by which CREB3L1 and 2 are activated has been well characterized. Both must exit the ER to be cleaved by S1P and S2P at the Golgi: this process liberates the cytosolic portions that translocate to the nucleus to become

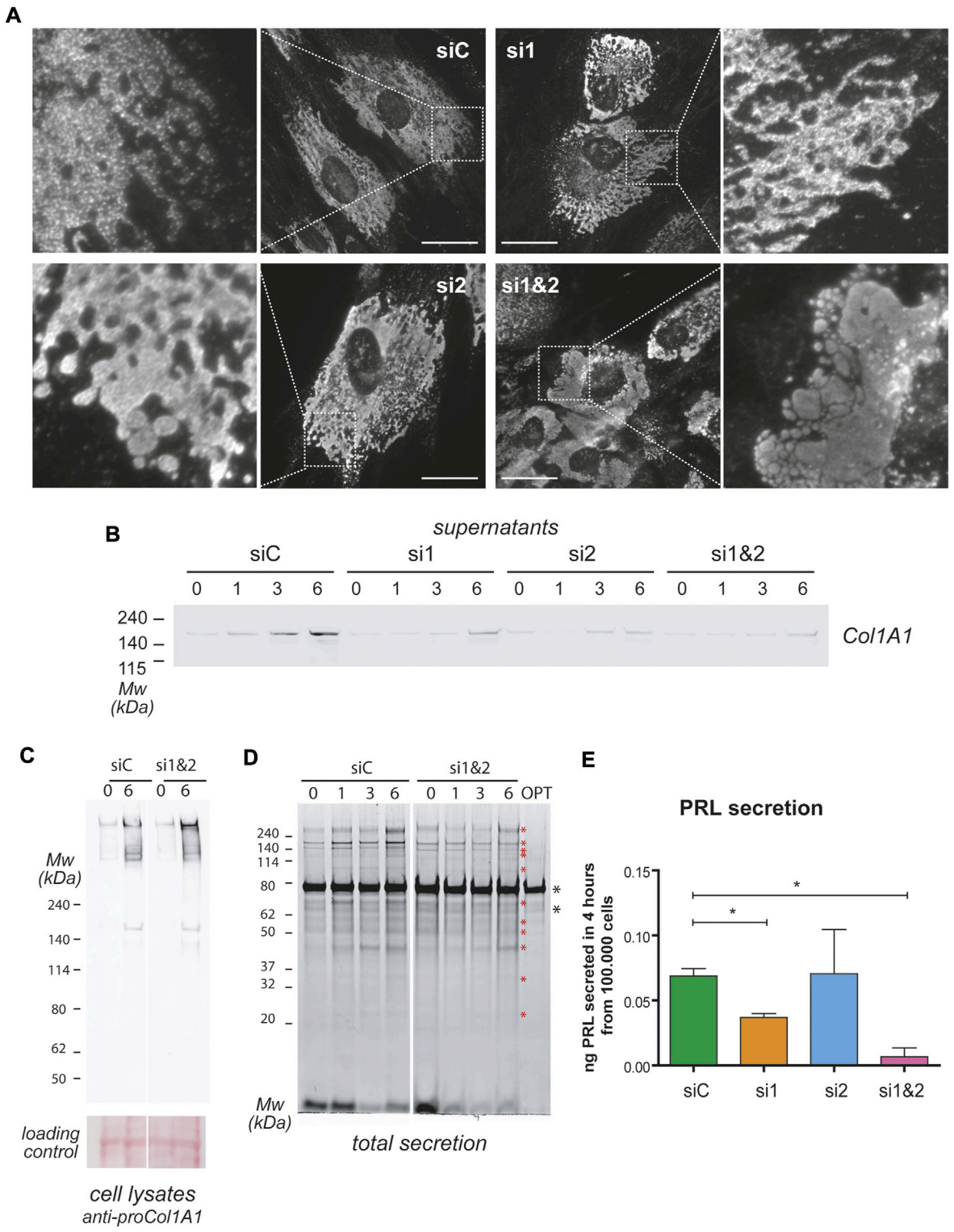


FIGURE 7
CREB3L1 and 2 KD affects general protein secretion. T-HESC were treated with scramble duplexes (siC), with duplexes specific for CREB3L1 (si1), CREB3L2 (si2) or both (si1&2). The day after treatment (day0) cells were treated with cAMP and progesterone and analyzed at different days of the decidualization process as indicated. **(A)** Images of cells at day 6 of differentiation. Cells were fixed with PFA, permeabilized and stained with anti Pro-Collagen1A1 antibody. In control cells, procollagen is present in the ER. The KD of CREB3L1 and/or 2 dramatically increases the amount of intracellular Pro-Collagen1A1, with swelling of the ER, culminating in Russell Bodies-like structures in conditions of double KD. Images were acquired

(*Continued*)

FIGURE 7 (Continued)
with a ×60 objective; bar: 20 μm. **(B)** Cells at the indicated days of differentiation were cultured for 6 h in OPTIMEM. The SN corresponding to 10.000 cells were loaded on SDS-PAGE under reducing conditions and, after transferring to nitrocellulose, stained with antibodies against Collagen1A1. The KD of CREB3L1 and/or 2 affects Collagen1A1 secretion. **(C)** The lysates of control cells or of cells subjected to double KD were loaded under non-reducing conditions on SDS-PAGE (3–8% precasted gradient gel), and nitrocellulose was decorated with anti Pro-Collagen1A1. Note the intracellular accumulation of Pro-Collagen1A1 in high molecular weight complexes in conditions of double KD. The ponceau staining of the nitrocellulose is shown as a loading control. **(D)** The absence of CREB3L1 and two affects total protein secretion. The total SN of 10.000 cells treated as indicated were loaded on a precast 4–12% polyacrylamide gel under reducing conditions (SN volumes were normalized with OPTIMEM). Optimem alone (OPT) was loaded as a control. Gels were stained with SyproRuby to stain total secreted proteins. During the decidualization process, protein secretion increases [as previously described (Anelli et al., 2021)]. Asterisks indicate bands that are less present in the double KD SNs. **(E)** PRL secretion was measured with ELISA test in the 4 h SN of day 6 cells treated as indicated. Data as expressed as ng of PRL secreted in 4 h by 100.000 cells. Average of three independent experiments ± SEM. *$p < 0.05$.

transcriptionally active, analogous to the activation mechanism of ATF6 and SREBP proteins (Kondo et al., 2007; Murakami et al., 2009). What drives the exit of CREB3L1 and 2 from the ER is, however, not completely understood yet. In fibroblasts and HeLa cells, CREB3L1 and 2 are continuously rapidly degraded, such that their up-regulation allows a fraction of the CREB3L1 and 2 pool to escape from the degradation machinery and, hence, exit from the ER to the Golgi, leading to their activation (Kondo et al., 2012). Whether such a scenario holds true for the decidualization process awaits further analysis. While both CREB3L1 and 2 are transcriptionally induced in stimulated EnSC, only CREB3L1 increases also at the protein level, suggesting that different processing mechanisms may apply to either of the two TF. Androgen receptor activates CREB3L2, increasing protein trafficking in prostate cancers (Hu et al., 2021), but the biochemical details remain to be elucidated. It is tempting to speculate that similar mechanisms are shared by progesterone receptor, which will be a topic for further studies.

Altogether, our data shed new light on the molecular mechanisms underlying the reshaping of the secretory pathway during decidualization. With their unique cargo heterogeneity, EnSCs behave differently from other known cell types differentiating towards *protein factories*. Thus, they prove to be an invaluable model to study adaptation of the secretory pathway during differentiation towards a highly secretory phenotype.

# Materials and methods

## Reagents and antibodies

Chemicals and reagents were purchased from Sigma-Aldrich (St Louis, MO), unless otherwise specified. Custom oligonucleotides were purchased from Metabion International AG (Planegg, Germany). The following primary antibodies were used: mouse monoclonal anti-ERp44 36C9, that has been previously described (Anelli et al., 2003; Anelli et al., 2007); mouse monoclonal anti-HLA1 W6/32 (ATCC); mouse monoclonal anti-actin, rabbit anti-CRT, goat anti-Vimentin, rabbit anti-ERGIC-53 and Phallodin-FITC (Sigma, St Louis, MO); mouse monoclonal anti-proCOL1A1 (Developmental Studies Hybridoma Bank [DSHB]); rabbit polyclonal anti-Col1A1 and mouse monoclonal anti-golgin 97 (CDF4) (Invitrogen Molecular Probes [Eugene, OR, United States]); mouse monoclonal anti-GM130 (BD Biosciences, Franklin Lakes, NJ); rabbit polyclonal anti-giantin (19243) (Biolegend, San Diego, CA); Alexa Fluor conjugated secondary antibodies (488, 647 and 700) were from Invitrogen Molecular Probes (Eugene, OR). CREB3L1 and CREB3L2 were detected respectively using the following antibodies: anti-OASIS, clone 10H1, MABE1151 (EMD corp., United States); anti-BBF2H7, clone 28G9, MABE1018 (EMD corp., United States).

## Cell lines

Experiments were performed on the human immortalized EnSC cell line T-HESC, obtained from ATCC (ATCC CRL-4003). Cells were cultured, according to manufacturer's instructions, in a 1:1 mixture of Dulbecco's modified Eagle's medium and Ham's F-12 medium without Phenol Red, containing 3.1 g/L glucose and 1 mM sodium pyruvate, and supplemented with 1.5 g/L sodium bicarbonate, 1% ITS + Premix (Corning), 500 ng/ml puromycin, and 10% charcoal/dextran treated fetal bovine serum. Medium was supplemented every 3–4 days with 50 ug/ml ascorbic acid. Decidualisation was induced by adding in the medium cAMP (8-bromoadenosine 3′, 5′ cyclic monophosphate) 0.5 mM and MPA (medroxyprogesterone) 1uM as previously described (Anelli et al., 2021). HeLa cells were maintained in High Glucose DMEM supplemented with 10% fetal bovine serum and with penicillin/streptomycin (100 U/ml and 100 ug/ml respectively).

## Bulk RNA-seq time course analysis and clustering

Cell samples were collected in duplicate before the stimulus (0 h) and at time 6, 18 h, d1, d1.5, d2, d3, d6 after the start of the decidualization protocol. RNA was harvested using TRIzol (Invitrogen) according to the manufacturer's

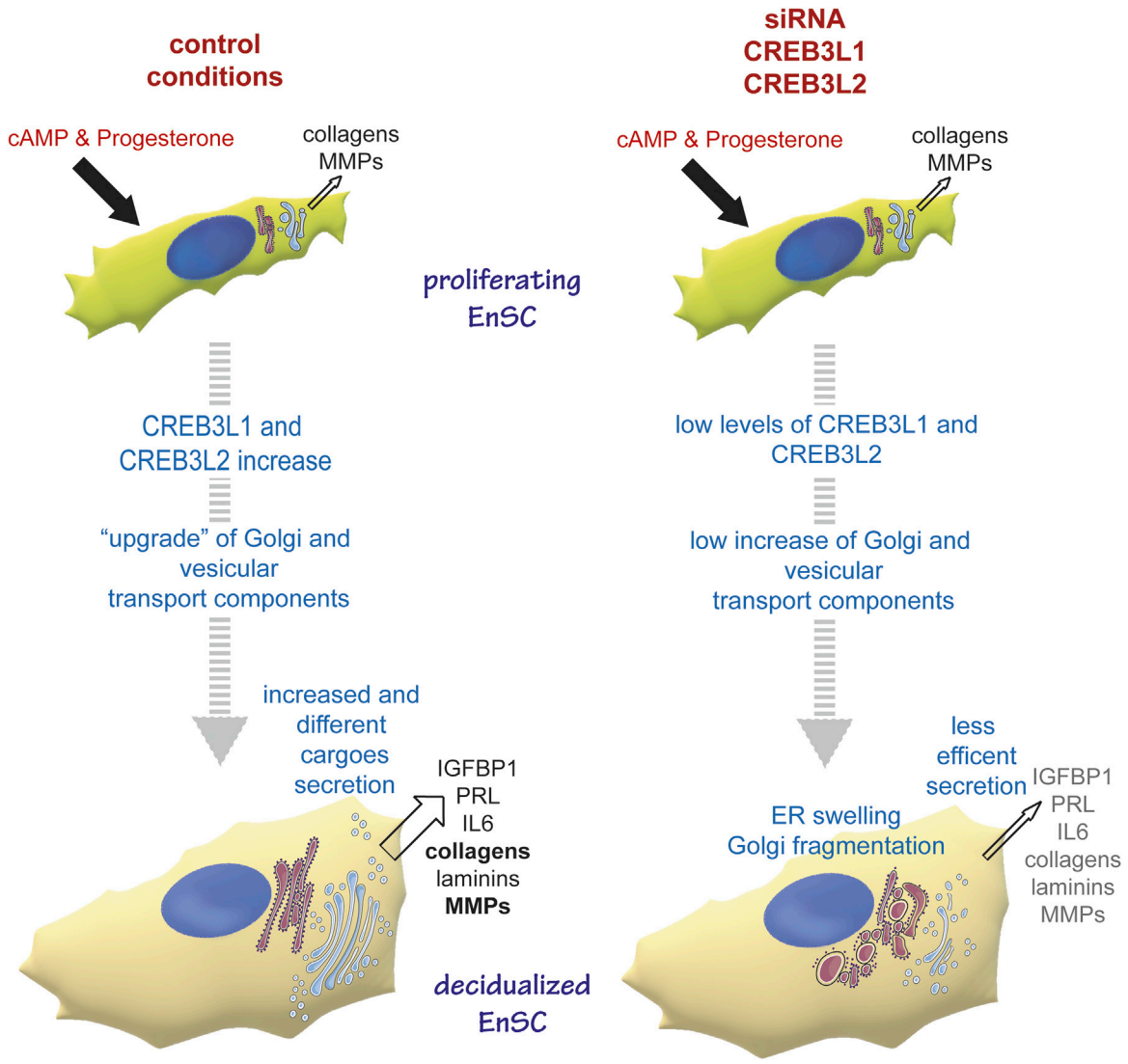


FIGURE 8
CREB3L1 and 2 mediate the reshaping of the early secretory pathway during decidualization. Under proliferating conditions, EnSC produce and secrete some collagens and MMPs. The decidualising stimulus induces upregulation and activation of CREB3L1 and CREB3L2, which have consequences on cell morphology, with a reshaping of the early secretory pathway. Thus Golgi and ER to Golgi vesicular transport components are up-regulated, which ensures more efficient secretion of new and different cargoes. In conditions of CREB3L1 and/or 2 KD, the cells are not able to adjust their secretory machinery to the new cargo load and production. Hence the ER swells, Golgi morphology is profoundly affected (with no enlargement and cisternae fragmentation) and secretion in general is lowered.

instructions. Library preparation was created from 500 ng of total RNA per sample and processed using the TruSeq Stranded mRNA kit, according to the manufacturer's protocol. The sequencing step was carried on an Illumina HiSeq 3,000 platform. Sequencing data were analyzed using snakePipes with standard parameters (Bhardwaj et al., 2019). The pipeline employs STAR aligner to map the reads to the human genome (genome build hg38). FeatureCounts was utilized to count the number of reads per annotated gene using gencode gtf file (release 27). Raw sequencing data and raw counts are available on the Gene Expression Omnibus repository, accession number: GSE200200. Differential expression analysis (DEA), over-representation analysis (ORA), time series clustering and data visualization were performed using the R programming language (v. 4.1.0). Count matrix was prefiltered before DEA by removing all genes showing a total number of counts, across al the samples, less than 30. DEA design consists of a pairwise comparison of each timepoint replicates *versus* untreated ones using the DESEQ2 package (v. 1.32.0) (Love et al., 2014). DEGs were

called based on adjusted $p$-value < 0.01 and absolute $\log_2$ fold change >0.5. ORA of DEA outputs was carried out on the enrichR package (v. 3.0). Enrichment for Gene Ontology (GO) terms was performed based on the database GO molecular function, cellular component, biological pathways, 2021 release. Candidate genes for time series clustering of ER and Golgi apparatus compartments were selected for both of the following criteria: being called differentially expressed at any timepoints ranging from 6 to 72 h and being annotated to GO cellular component terms GO:0005783 Endoplasmic Reticulum and/or GO:0005794 Golgi Apparatus, 2018 release. Annotations were downloaded from AmiGO2, setting "*Homo Sapiens*" and "experimental evidence" as filtering criteria parameters for "organism" and "evidence", respectively. The input matrix for clustering was retrieved by subsetting the time-course expression of the genes of interest from the original expression matrix transformed using DESEQ2 variance stabilizing transformation. Then, expression value information for each time point was obtained by averaging replicates of the same time point. Last, we performed z-normalization to optimize the performance of the distance metric utilized in the clustering. Time-series clustering was performed using the dtwclust package (v. 5.5.10) (Sardà-Espinosa, 2019). The shape-based distance (SBD) proposed by Paparrizos and colleagues (Paparrizos and Gravano, 2015) and partition around medoids (PAM) were chosen as the distance metric and clustering algorithm, respectively. SBD consists of a normalized version of the cross-correlation measure, which allows for determining the similarity of the shape between time signals, even if they are not properly aligned. PAM requires to set a k number of clusters *a priori*. The optimal number of k clusters was determined with a heuristic approach based on the visual inspection of the clusters that maximized the average Silhouette index. The presented clustering output was obtained by choosing k = 5 and the seed set to 23. To polish the clusters from genes showing dramatic out of phase temporal expression, we removed from the clustering output all genes showing, at any time point, an absolute z-score expression value higher or lower than two standard deviations from the mean z-score expression for the considered timepoint. Enrichment for BP GO terms for each cluster was carried out on topGO package (v.2.44.0) (Alexa and Rahnenfuhrer, 2022). ORA was performed by adjusting the gene Universe to the genes contained in the polished version of the clustering output. The weighted algorithm proposed in Alexa et al., 2006 was used to reduce the impact of local dependencies in the GO graph. Enrichment for shared transcription factor binding motif (TFBM) for the genes in each cluster was performed using RcisTarget (v. 1.12.1) (Aibar et al., 2017). The analysis was performed by evaluating the shared motifs found at ± 10 kb from the transcription start site of the genes in the input list. Data visualization was performed using the packages ggplot2 (v. 3.3.6) (Wickham et al., 2016) and pheatmap (v. 1.0.12) (Raivo Kolde, 2019).

## siRNA and transient transfection

Silencing was performed with Lipofectamine RNAiMax reagent (Thermofisher) according to manufacturer's instruction. CREB3L1 was silenced with a custom siRNA oligonucleotide [5′CCACCAAGUACCUGAGUGA (dT)(dT)-3′, sense], while for CREB3L2 a previously described siRNA oligonucleotide was used [5′GAGUCUUGUUCAACUGAGA (dT)(dT)-3′, sense] (Tomoishi et al., 2017). Non-targeting duplexes used as control (SiC) were purchased from Darmachon (Lafayette, Colorado, United States) (catalog number D-001810–01). Silencing of the genes of interest was confirmed by RealTime qPCR, as described below.

HeLa cells were transfected with JetPEI transfection reagent (Euroclone) according to manufacturer's instructions.

## Cloning of cytosolic CREB3L1 and CREB3L2

Cytosolic domains of CREB3L1 and CREB3L2 were cloned from RNA of T-HESC cell line, retrotranscribed with RT Polymerase (Promega) and oligo-dT primers (Promega) according to manufacturer's instructions. To ensure high expression of the transcripts and avoid cross-contamination, RNAs at day 3 of decidualization with silencing of CREB3L2 and CREB3L1 (confirmed by RealTime quantitative PCR) were used to amplify CREB3L1 and CREB3L2 respectively. PCR was performed with Pfu DNA Polymerase (Promega), with the following conditions: 95°C 2 min; 95°C 30 s, 52°C (CREB3L1)/56°C (CREB3L2) 30 s, 72°C 3 min × 35 cycles; 72°C, 5 min (CREB3L1 fw: CTAGCTAGCTAGGGC TGCGATGGACGCCGTC; rev: CCGGATATCTTATTATGGTCC CAGTCTGGGTG; CREB3L2 fw: CTAGCTAGCTAGGGCCCG CACCGCCATG; rev: CCGGATATCTTATTAGCAGGTGCC AGTCTGCGTG). Vector pcDNA3.1 (+) and PCR products were digested with NheI-HF (Biolabs) and EcoRV (Biolabs), run in 1% agarose gel and purified (ZymoClean Gel DNA Recovery Kit, Zymo Research). Ligation was performed with T4 DNA ligase (Promega), with a 3:1 insert/plasmid ratio. Plasmid identity was then confirmed by site-specific enzymatic digestion with NotI (Biolabs) and BstxI (Promega) and by sequencing (Metabion, Planegg/Steinkirchen Germany).

## Western blot analysis

Western Blot assay was performed as previously described (Anelli et al., 2021). Briefly, cells were detached with Trypsin/0.5% EDTA (ThermoFisher) and counted with Neubauer chamber, washed once in ice-cold PBS (Gibco) and once in ice-cold PBS containing 10 mM N-ethylmaleimide (NEM) to block rearrangement of disulfide bonds; lysis was performed in 150 mM NaCl, 1% NP-40, 2% SDS, 50 mM Tris HCl

pH7.4 containing 10 mM NEM, cOmplete EDTA-free protease inhibitor cocktail (Roche) and phosphatase inhibitors, using 10uL of lysis buffer for 100.000 cells. Samples were processed with Benzonase nuclease according to manufacturer's instruction. Samples were then loaded in reducing conditions (50 mM DTT) on SDS-PAGE (4–12% or 3–8% precast gel, Invitrogen), normalizing by protein quantity (40 ug/lane), unless differently specified. Western blot in Figure 6C was instead performed in non-reducing conditions. After transfer on nitrocellulose (0.2 um, Ahmersham), membranes were saturated in 5% milk in PBS 0.1% Tween and then incubated with specific antibodies as indicated (primary antibodies 1:500 in PBS 0.1% tween, 2% milk; secondary antibodies Alexa Fluor conjugated [647 or 546] 1:1,000 in PBS 0.1% Tween; HRP-conjugated secondary antibodies 1:5,000 in PBS-0.1% tween). Signals were detected by fluorescence, with FujiFilm FLA 9000 (FujiFilm Life Science, Tokyo, Japan), or by chemoluminescence, with Uvitec Alliance Mini HD9 (Cambridge, United Kingdom). Densitometric analysis of the images was performed with ImageJ. Signals were normalized on protein loading (ponceau staining).

## Secretion assay and SYPRO Ruby staining

For secretion assays, at the end of the siRNA and decidualization period, the cells were washed three times in PBS and incubated for 6 h in serum free medium (OPTIMEM) (Gibco) containing 50 ug/ml Ascorbic Acid (final concentration). The 6-h culture supernatants were collected and centrifuged once at 1000 g to get rid of detached dead cells; then they were added with 10 mM NEM and cOmplete EDTA-free protease inhibitor cocktail (Roche). Cells were detached, counted and lysed as described above. A volume of the supernatants corresponding to equal cell numbers was loaded on SDS-PAGE (4–12% precast gel, Invitrogen). The gels were then either used for Western Blot analysis (as described above), or stained with SYPRO Ruby Protein Gel Stain (Merck) according to the manufacturers' protocols. For SYPRO Ruby staining, fluorescence signals images were acquired with FujiFilm FLA 9000 (FujiFilm Life Science, Tokyo, Japan) and processed with ImageJ.

## Prolactin measurements

For PRL measurements, cells (control or subjected to siRNA as indicated) at day 6 of decidualization were incubated for 4 h in OPTIMEM. Cell culture supernatants were collected and cells were detached and counted. PRL concentration in the spent medium was measured using a two-steps Sandwich ELISA. Briefly, plate wells were coated with capture antibody (anti-human PRL Goat IgG RD System, 800 ng/ml 100 µL/well) O/N at 4°C. After three washes in 300 µL of wash buffer (WaBu, PBS 0.05% Tween 20), saturation was performed in PBS 1% BSA (300 µL/well). Blocking was discarded and samples (100 µL of 6 h SN in OPTIMEM) were added, O/N at 4°C. Purified human PRL (RD System) diluted in PBS was used as standard curve, in a range from 0.01 ng/100 µL to 5 ng/100 µL. OPTIMEM alone (100 µL/well) was used as a negative control. After three washing in 300 µL of WaBu, wells were treated with a biotinylated detection antibody (Goat anti-human PRL IgG RD System, 400 ng/ml, 100 µL/well, 2 h RT). Wells were washed 3 times with 300 µL of WaBu, and then treated with HRP conjugated Streptavdin (RD System, DY998) (1:200, 100µL/well, 1 h RT). After three washings with 300 µL of WaBu, the HRP substrate (SigmaFast OPD, Sigma) was added (100 µL/well, 20 min RT) and the optical density was measured at 450 nm. The amount of secreted PRL was expressed as a ratio on the cell number.

## Immunofluorescence and morphometric analysis

Cells were plated at a suitable confluence directly on glass slides. After treatments, cells were fixed in 4% PFA for 10 min at RT and washed in PBS. For conventional immunofluorescence, cells were permeabilized with 0.1% Triton X-100 in PBS, incubated with blocking solution (PBS-5% FCS) for 30 min at RT, and then incubated with primary and secondary antibodies (Alexa Fluor conjugated 488 or 647) or with Phalloidin-FITC (Sigma), 1:500 in PBS-5% FCS, for 30 min at RT. For staining with anti-golgin 97 cells were permeabilized in 0.1% saponin, and the detergent was kept for all the subsequent steps of staining. Nuclei were stained with DAPI (Sigma) (1:5,000), and coverslips were mounted using Mowiol mounting medium. For morphometry, cells were first incubated with blocking solution, anti-HLA antibody (W6-32), and fluorescent secondary antibody before permeabilization; immunofluorescence for the intracellular proteins was then performed as described above. Images were acquired with DeltaVision GE healthcare DeltaVision Ultra microscope (ALEMBIC, Milan, Italy), equipped with oil lenses. A ×60 magnification (Olympus ×60/1.42, Plan Apo N, UIS2, 1-U2B933) was used for morphometry, while a ×100 magnification (Olympus ×100/1.40, UPLS Apo, UIS2, 1-U2B836) was used for organelle morphology analysis. For morphometry analyses, images were deconvolved with Huygens Professional version 19.04 (Scientific Volume Imaging, Hilversum, The Netherlands, http://svi.nl), using the CMLE algorithm, with SNR:10 and 40 iterations. Analyses of Golgi, ER and total cell volume were performed with the advanced Object Analyzer plugin of the Huygens Professional software (garbage 1, seed value 10%, and threshold 4%). With this strategy, cell volume, ER or Golgi volume and organelle/cell volume ratio were determined for each cell.

## PCR and quantitative real-time PCR

Semi-quantitative real-time PCR (qRT-PCR) amplification was performed (as described in Sanchez et al., 2016) with the

TABLE 1 Primer list.

| Gene | Primer forward | Primer reverse |
|---|---|---|
| GAPDH | TGAAGGTCGGAGTCAACGGATTT | CATGTAAACCATGTAGTTGAGGT |
| CREB3L1 | ACAATGCGCACTTTCCTGAG | GAGGGCTCTTCTCATCCAGC |
| CREB3L2 | AGAATACATGGACAGCCTGGAG | TCTAGAACCTCTACCTTCTTCCGA |
| ERP44 | CAGCACTCTGACATAGCCCA | CTGATCGCTGACCCCTGTAT |
| LMAN1 | TCAGGAGGAATTTGAGCACTTT | GCTCTCGATCTCCTACACTCTCA |
| GOLGA2 | CAGCCGCCTGCAGTATTC | TGAGGGCGTCTCTCTCTTTG |
| GOLGB1 | AGCATCTCAGACTTCTTTCCCA | GAGCAAGGCTCCCTTTTCAT |
| TGOLN2 | GAGCAGCCACTTCTTTGCAT | TTCCTTCCAGGACAAAAGCA |
| SEC24A | ACACTGGAGGCTGAGGTGG | ACACTGGAGGCTGAGGTGG |
| SEC24D | ACCCCATCAGTTTGGTCAGA | CCACATTGTTGACAGGTGGA |
| PRL | AGCCAGGTTCATCCTGAAA | AGCAGAAAGGCGAGACTCTT |

SYBR PCR Master Mix kit (Applied Biosciences, Waltham, MA) using the Biorad Real Time PCR machine (CFX96 Real Time System). Briefly, 1uL of primers (final concentration 2,5 uM), 4 ng of template DNA in nuclease free water and 5uL of Master Mix were added to each reaction. All the samples were loaded in technical triplicate, and at least in biological duplicate, Cycling was performed with the following conditions: preincubation 10 min 95°, amplification 40 cycles 15″ 95° + 60″ 60°. Melting curves were evaluated for each gene. Relative quantification of gene expression was performed for each condition: GAPDH was chosen as a reference gene, since it is constant during all the days of decidualization. Mock-transfected, undifferentiated cells (D0 siC) were considered as control condition, and the expression of each gene was expressed as an increase (or decrease) relative to the value measured at D0 siC (ΔΔCT). The results were expressed as fold gene expression values (2−ΔΔCT), averaged and plotted in the graphs.

qRT-PCR primers used for KDELRs were obtained from Qiagen (Hilden, Germany): Hs_KDELR1_1_SG QuantiTect Primer Assay (QT00090811) for KDELR1, Hs_KDELR2_1_SG QuantiTect Primer Assay (QT00092715) for KDELR2, Hs_KDELR3_1_SG QuantiTect Primer Assay (QT00097790) for KDELR3. Other primers were purchased from Metabion (Planegg, Germany) and are listed in Table 1.

## Statistical analysis

Statistical analysis for wet biology experiments was performed using a two tails unpaired student's *t* Test with Welch's correction or, in case of multiple comparisons, with one-way Anova with Turkey correction. $p$ values ≤ 0.5 were considered significant. Statistics were obtained using Graph Pad Prism (6.0 version).

## Data availability statement

The datasets presented in this study can be found in online repositories. The names of the repository/repositories and accession number(s) can be found below: GEO accession: GSE200200.

## Author contributions

DP designed and performed the bioinformatics analyses; MDT performed morphometric analyes and replicates of the first wet experiments; EB performed the first wet experiments and morphometric analyses; BH contributed in the processing of bulk RNA-seq data; PP-B supervised the project together with TA; RiS supervised the bioinformatic studies; CS produced the samples for transcriptomics analysis; EA set up the RNAseq experiments; RoS contributed to data discussion; TA started and supervised the project and performed part of the wet experiments. TA, DP and MDT wrote the manuscript, that was discussed and critically reviewed together with all other co-authors.

## Funding

The study was supported by a research grant from AIRC (IG 2019 ID. 23285), Telethon (GGP15059), and Ministero dell'Università e Ricerca (PRIN 2017XA5J5N) to Roberto Sitia. DP is the recipient of a fellowship from Università Statale di Milano.

## Acknowledgments

The authors thank the ALEMBIC staff in particular Valeria Berno for assistance with immunofluorescence analysis and morphometry, and Ioana Olan for help and suggestions for bioinformatics analyses. We also thank all members of our laboratories for fruitful discussions.

## Conflict of interest

The authors declare that the research was conducted in the absence of any commercial or financial relationships that could be construed as a potential conflict of interest.

## Publisher's note



## Supplementary material

The Supplementary Material for this article can be found online at: https://www.frontiersin.org/articles/10.3389/fcell.2022.986997/full#supplementary-material

## References

Aibar, S., Gonzalez-Blas, C. B., Moerman, T., Huynh-Thu, V. A., Imrichova, H., Hulselmans, G., et al. (2017). Scenic: Single-cell regulatory network inference and clustering. *Nat. Methods* 14, 1083–1086. doi:10.1038/nmeth.4463

Alexa, A., Rahnenfuhrer, J., and Lengauer, T. (2006). Improved scoring of functional groups from gene expression data by decorrelating GO graph structure. *Bioinformatics* 22, 1600–1607. doi:10.1093/bioinformatics/btl140

Alexa, A, and Rahnenfuhrer, J (2022). topGO: Enrichment Analysis for Gene Ontology. R package version 2.48.0.

Anelli, T., Dalla Torre, M., Borini, E., Mangini, E., Ulisse, A., Semino, C., et al. (2021). Profound architectural and functional readjustments of the secretory pathway in decidualization of endometrial stromal cells. *Traffic* 23, 4–20. doi:10.1111/tra.12822

Anelli, T., and Panina-Bordignon, P. (2019). How to avoid a No-deal ER exit. *Cells* 8, E1051. doi:10.3390/cells8091051

Anelli, T., and Sitia, R. (2008). Protein quality control in the early secretory pathway. *Embo J.* 27, 315–327. doi:10.1038/sj.emboj.7601974

Asada, R., Kanemoto, S., Kondo, S., Saito, A., and Imaizumi, K. (2011). The signalling from endoplasmic reticulum-resident bZIP transcription factors involved in diverse cellular physiology. *J. Biochem.* 149, 507–518. doi:10.1093/jb/mvr041

Bhardwaj, V., Heyne, S., Sikora, K., Rabbani, L., Rauer, M., Kilpert, F., et al. (2019). snakePipes: facilitating flexible, scalable and integrative epigenomic analysis. *Bioinformatics* 35, 4757–4759. doi:10.1093/bioinformatics/btz436

Braakman, I., and Bulleid, N. J. (2011). Protein folding and modification in the mammalian endoplasmic reticulum. *Annu. Rev. Biochem.* 80, 71–99. doi:10.1146/annurev-biochem-062209-093836

Carbone, K., Pinto, N. M., Abrahamsohn, P. A., and Zorn, T. M. (2006). Arrangement and fine structure of collagen fibrils in the decidualized mouse endometrium. *Microsc. Res. Tech.* 69, 36–45. doi:10.1002/jemt.20265

Chan, C. P., Kok, K. H., and Jin, D. Y. (2011). CREB3 subfamily transcription factors are not created equal: Recent insights from global analyses and animal models. *Cell Biosci.* 1, 6. doi:10.1186/2045-3701-1-6

Chen, Q., Lee, C. E., Denard, B., and Ye, J. (2014). Sustained induction of collagen synthesis by TGF-beta requires regulated intramembrane proteolysis of CREB3L1. *PloS one* 9, e108528. doi:10.1371/journal.pone.0108528

Christianson, J. C., and Carvalho, P. (2022). Order through destruction: How ER-associated protein degradation contributes to organelle homeostasis. *EMBO J.* 41, e109845. doi:10.15252/embj.2021109845

Christis, C., Fullaondo, A., Schildknegt, D., Mkrtchian, S., Heck, A. J., and Braakman, I. (2010). Regulated increase in folding capacity prevents unfolded protein stress in the ER. *J. Cell Sci.* 123, 787–794. doi:10.1242/jcs.041111

Federovitch, C. M., Ron, D., and Hampton, R. Y. (2005). The dynamic ER: Experimental approaches and current questions. *Curr. Opin. Cell Biol.* 17, 409–414. doi:10.1016/j.ceb.2005.06.010

Fox, R. M., Hanlon, C. D., and Andrew, D. J. (2010). The CrebA/Creb3-like transcription factors are major and direct regulators of secretory capacity. *J. Cell Biol.* 191, 479–492. doi:10.1083/jcb.201004062

Garcia, I. A., Torres Demichelis, V., Viale, D. L., Di Giusto, P., Ezhova, Y., Polishchuk, R. S., et al. (2017). CREB3L1-mediated functional and structural adaptation of the secretory pathway in hormone-stimulated thyroid cells. *J. Cell Sci.* 130, 4155–4167. doi:10.1242/jcs.211102

Gellersen, B., and Brosens, J. J. (2014). Cyclic decidualization of the human endometrium in reproductive health and failure. *Endocr. Rev.* 35, 851–905. doi:10.1210/er.2014-1045

Harding, H. P., Zeng, H., Zhang, Y., Jungries, R., Chung, P., Plesken, H., et al. (2001). Diabetes mellitus and exocrine pancreatic dysfunction in perk-/- mice reveals a role for translational control in secretory cell survival. *Mol. Cell* 7, 1153–1163. doi:10.1016/s1097-2765(01)00264-7

Hu, L., Chen, X., Narwade, N., Lim, M. G. L., Chen, Z., Tennakoon, C., et al. (2021). Single-cell analysis reveals androgen receptor regulates the ER-to-Golgi trafficking pathway with CREB3L2 to drive prostate cancer progression. *Oncogene* 40, 6479–6493. doi:10.1038/s41388-021-02026-7

Ishikawa, T., Toyama, T., Nakamura, Y., Tamada, K., Shimizu, H., Ninagawa, S., et al. (2017). UPR transducer BBF2H7 allows export of type II collagen in a cargo- and developmental stage-specific manner. *J. Cell Biol.* 216, 1761–1774. doi:10.1083/jcb.201609100

Iwahashi, M., Muragaki, Y., Ooshima, A., Yamoto, M., and Nakano, R. (1996). Alterations in distribution and composition of the extracellular matrix during decidualization of the human endometrium. *J. Reprod. Fertil.* 108, 147–155. doi:10.1530/jrf.0.1080147

Iwakoshi, N. N., Lee, A. H., Vallabhajosyula, P., Otipoby, K. L., Rajewsky, K., and Glimcher, L. H. (2003). Plasma cell differentiation and the unfolded protein response intersect at the transcription factor XBP-1. *Nat. Immunol.* 4, 321–329. doi:10.1038/ni907

Johnson, D. M., Wells, M. B., Fox, R., Lee, J. S., Loganathan, R., Levings, D., et al. (2020). CrebA increases secretory capacity through direct transcriptional regulation of the secretory machinery, a subset of secretory cargo, and other key regulators. *Traffic* 21 (9), 560–577. doi:10.1111/tra.12753

Keller, R. B., Tran, T. T., Pyott, S. M., Pepin, M. G., Savarirayan, R., Mcgillivray, G., et al. (2018). Monoallelic and biallelic CREB3L1 variant causes mild and severe osteogenesis imperfecta, respectively. *Genet. Med.* 20, 411–419. doi:10.1038/gim.2017.115

Khan, H. A., and Margulies, C. E. (2019). The role of mammalian creb3-like transcription factors in response to nutrients. *Front. Genet.* 10, 591. doi:10.3389/fgene.2019.00591

Khetchoumian, K., Balsalobre, A., Mayran, A., Christian, H., Chénard, V., St-Pierre, J., et al. (2019). Pituitary cell translation and secretory capacities are enhanced cell autonomously by the transcription factor Creb3l2. *Nat. Commun.* 10 (1), 3960. doi:10.1038/s41467-019-11894-3

Kondo, S., Hino, S. I., Saito, A., Kanemoto, S., Kawasaki, N., Asada, R., et al. (2012). Activation of OASIS family, ER stress transducers, is dependent on its stabilization. *Cell Death Differ.* 19, 1939–1949. doi:10.1038/cdd.2012.77

Kondo, S., Saito, A., Hino, S., Murakami, T., Ogata, M., Kanemoto, S., et al. (2007). BBF2H7, a novel transmembrane bZIP transcription factor, is a new type of

endoplasmic reticulum stress transducer. *Mol. Cell. Biol.* 27, 1716–1729. doi:10.1128/MCB.01552-06

Lindahl, K., Astrom, E., Dragomir, A., Symoens, S., Coucke, P., Larsson, S., et al. (2018). Homozygosity for CREB3L1 premature stop codon in first case of recessive osteogenesis imperfecta associated with OASIS-deficiency to survive infancy. *Bone* 114, 268–277. doi:10.1016/j.bone.2018.06.019

Love, M. I., Huber, W., and Anders, S. (2014). Moderated estimation of fold change and dispersion for RNA-seq data with DESeq2. *Genome Biol.* 15, 550. doi:10.1186/s13059-014-0550-8

Murakami, T., Saito, A., Hino, S., Kondo, S., Kanemoto, S., Chihara, K., et al. (2009). Signalling mediated by the endoplasmic reticulum stress transducer OASIS is involved in bone formation. *Nat. Cell Biol.* 11, 1205–1211. doi:10.1038/ncb1963

Noske, A. B., Costin, A. J., Morgan, G. P., and Marsh, B. J. (2008). Expedited approaches to whole cell electron tomography and organelle mark-up *in situ* in high-pressure frozen pancreatic islets. *J. Struct. Biol.* 161, 298–313. doi:10.1016/j.jsb.2007.09.015

Paparrizos, J., and Gravano, L. (2015). "k-Shape: Efficient and accurate clustering of time series," in SIGMOD '15: Proceedings of the 2015 ACM SIGMOD International Conference on Management of Data, Melbourne Victoria Australia, 31 May 2015- 4 June 2015, 1855–1870.

Raivo Kolde (2019). pheatmap: Pretty Heatmaps. R package version 1.0.12.

Reimold, A. M., Iwakoshi, N. N., Manis, J., Vallabhajosyula, P., Szomolanyi-Tsuda, E., Gravallese, E. M., et al. (2001). Plasma cell differentiation requires the transcription factor XBP-1. *Nature* 412, 300–307. doi:10.1038/35085509

Ruggiano, A., Foresti, O., and Carvalho, P. (2014). Quality control: ER-associated degradation: Protein quality control and beyond. *J. Cell Biol.* 204, 869–879. doi:10.1083/jcb.201312042

Saito, A., Hino, S., Murakami, T., Kanemoto, S., Kondo, S., Saitoh, M., et al. (2009). Regulation of endoplasmic reticulum stress response by a BBF2H7-mediated Sec23a pathway is essential for chondrogenesis. *Nat. Cell Biol.* 11, 1197–1204. doi:10.1038/ncb1962

Sanchez, A. M., Cioffi, R., Vigano, P., Candiani, M., Verde, R., Piscitelli, F., et al. (2016). Elevated systemic levels of endocannabinoids and related mediators across the menstrual cycle in women with endometriosis. *Reprod. Sci.* 23, 1071–1079. doi:10.1177/1933719116630414

Sardà-Espinosa, A. (2019). Time-series clustering in R using the dtwclust package. *R J.* 11, 22–43. doi:10.32614/RJ-2019-023

Schwabl, S., and Teis, D. (2022). Protein quality control at the Golgi. *Curr. Opin. Cell Biol.* 75, 102074. doi:10.1016/j.ceb.2022.02.008

Shi, J. W., Lai, Z. Z., Yang, H. L., Yang, S. L., Wang, C. J., Ao, D., et al. (2020). Collagen at the maternal-fetal interface in human pregnancy. *Int. J. Biol. Sci.* 16, 2220–2234. doi:10.7150/ijbs.45586

Sun, Z., and Brodsky, J. L. (2019). Protein quality control in the secretory pathway. *J. Cell Biol.* 218, 3171–3187. doi:10.1083/jcb.201906047

Symoens, S., Malfait, F., D'hondt, S., Callewaert, B., Dheedene, A., Steyaert, W., et al. (2013). Deficiency for the ER-stress transducer OASIS causes severe recessive osteogenesis imperfecta in humans. *Orphanet J. Rare Dis.* 8, 154. doi:10.1186/1750-1172-8-154

Tomoishi, S., Fukushima, S., Shinohara, K., Katada, T., and Saito, K. (2017). CREB3L2-mediated expression of Sec23A/Sec24D is involved in hepatic stellate cell activation through ER-Golgi transport. *Sci. Rep.* 7, 7992. doi:10.1038/s41598-017-08703-6

Valetti, C., Grossi, C. E., Milstein, C., and Sitia, R. (1991). Russell bodies: A general response of secretory cells to synthesis of a mutant immunoglobulin which can neither exit from, nor be degraded in, the endoplasmic reticulum. *J. Cell Biol.* 115, 983–994. doi:10.1083/jcb.115.4.983

Van Anken, E., Romijn, E. P., Maggioni, C., Mezghrani, A., Sitia, R., Braakman, I., et al. (2003). Sequential waves of functionally related proteins are expressed when B cells prepare for antibody secretion. *Immunity* 18, 243–253. doi:10.1016/s1074-7613(03)00024-4

Wickham, H (2016). ggplot2: Elegant Graphics for Data Analysis. Springer-Verlag New York. ISBN 978-3-319-24277-4

Zhang, B. (2009). Recent developments in the understanding of the combined deficiency of FV and FVIII. *Br. J. Haematol.* 145, 15–23. doi:10.1111/j.1365-2141.2008.07559.x

# Frontiers in
# Cell and Developmental Biology

**Explores the fundamental biological processes of life, covering intracellular and extracellular dynamics.**

The world's most cited developmental biology journal, advancing our understanding of the fundamental processes of life. It explores a wide spectrum of cell and developmental biology, covering intracellular and extracellular dynamics.

---

## Discover the latest Research Topics

See more →


**Frontiers**

Avenue du Tribunal-Fédéral 34
1005 Lausanne, Switzerland
frontiersin.org

**Contact us**

+41 (0)21 510 17 00
frontiersin.org/about/contact